

Co-crystallisation with 1,2,3,5-dithiadiazolyl radicals

by

Sean Wade Robinson

*Thesis presented in partial fulfilment of the requirements for
the degree Master of Science in Chemistry at the University
of Stellenbosch*



Supervisor: Dr Delia Ann Haynes
Co-supervisor: Dr Gareth E. Arnott
Faculty of Science
Department of Chemistry & Polymer Science

March 2012

Declaration

By submitting this thesis/dissertation electronically, I declare that the entirety of the work contained therein is my own, original work, that I am the sole author thereof (save to the extent explicitly otherwise stated), that reproduction and publication thereof by Stellenbosch University will not infringe any third party rights and that I have not previously in its entirety or in part submitted it for obtaining any qualification.

March 2012

Abstract

This thesis begins with an overview of supramolecular chemistry, crystal engineering and the field of 1,2,3,5-dithiadiazolyl radical chemistry to provide a context for the work presented.

In the first part of this study, the aims were to characterise the two known co-crystals of 1,2,3,5-dithiadiazolyl radicals using thermal analysis and to investigate alternative methods by which the two known co-crystals could be formed in order for novel co-crystals to be synthesised using these techniques. The co-crystal formers; 4-phenyl-, 4-perfluorophenyl- and 4'-perfluorophenyl-1,2,3,5-dithiadiazolyl radicals, were synthesised using standard techniques. In addition, their sublimation onset temperatures were determined by TGA, and their respective melting and crystallisation temperatures determined by DSC. The two known co-crystals (consisting of phenyl- and perfluorophenyl-, and phenyl- and perfluoropyridyl-dithiadiazolyls) were synthesised and analysed by DSC. During the analysis, a phase transition in the pure 4'-perfluoropyridyl-1,2,3,5-dithiadiazolyl radical was identified and characterised using DSC, hot-stage microscopy and variable temperature powder X-ray diffraction. Co-crystallisation by mechanochemical synthesis, mixing the co-crystal formers in solution, melting a mixture of the co-crystal formers and sublimation of a co-reduced mixture of the dithiadiazolyl radicals was investigated. Analysis by powder X-ray diffraction revealed successful co-crystal formation by all techniques except mechanochemical synthesis. It was determined that co-crystal formation is quantitative by each of these methods.

The second part of this study aimed to investigate steps towards the synthesis of 1,2,3,5-dithiadiazolyl radicals that are functionalised with hydrogen-bonding functional groups such as the hydroxyl-, amino- and carboxyl-moieties. Experiments (using standard procedures) on starting materials which already contained the desired hydrogen-bonding groups showed that it was necessary to protect these moieties before synthesising the dithiadiazolyl heterocycle. Four novel dithiadiazolyl radicals were prepared, namely, the 3'- and 4'-trimethylsiloxyphenyl- and 3'- and 4'-N,N'-bis-*t*-Boc-aminophenyl-1,2,3,5-dithiadiazolyl radicals. Initial attempts at deprotecting these dithiadiazolyl radicals to yield the target radicals were unsuccessful. Synthesis of the 4'-carboxyphenyl-1,2,3,5-dithiadiazolyl radical

was also attempted by lithium halogen exchange with 4'-bromophenyl-1,2,3,5-dithiadiazolyl and subsequent quenching with CO₂, but this was unsuccessful.

The last part of this study aimed to co-crystallise novel combinations of 1,2,3,5-dithiadiazolyl radicals with either the CN \cdots S-S or the NO₂ \cdots halogen interaction as a target synthon in the resulting solid-state structure using techniques developed in the first part of this study. Attempts at co-crystallising 3'-cyanophenyl- with 3'-cyanoperfluorophenyl-, perfluorophenyl- and perfluoropyridyl-1,2,3,5-dithiadiazolyl radicals were unsuccessful. Similarly, combinations between 4'-bromophenyl-, 4'-iodophenyl-, 3'- and 4'-nitrophenyl-1,2,3,5-dithiadiazolyl radicals did not produce co-crystals. However, during this study, novel crystal structures were determined for the 4'-bromophenyl- and 3'- nitrophenyl-1,2,3,5-dithiadiazolyl radicals.

Opsomming

Hierdie tesis verskaf 'n oorsig van supramolekulêre chemie, kristalingenieurswese en die gebied van 1,2,3,5-ditiadiazoliel radikaalchemie om 'n konteks te skep vir die werk wat aangebied word. Die studie bestaan uit drie dele.

Die mikpunte van die eerste deel was om die twee bekende mede-kristalle van 1,2,3,5-ditiadiazoliel radikale deur middel van termiese analise te karakteriseer en om alternatiewe metodes waarmee die twee bekende ditiadiazoliel mede-kristalle gevorm kan word te ondersoek. Hierdie tegnieke is later toegepas om nuwe mede-kristalle te sintetiseer. Die mede-kristalvormers, 4-feniel-, 4-perfluorofeniel- en 4'-perfluoropyridiel-1,2,3,5-ditiadiazoliel radikale, is gesintetiseer met behulp van standaard Schlenk-tegnieke. Daarbenewens is hul sublimasie aanvangstemperature deur middel van TGA bepaal, en hul onderskeie smelt en kristallasie temperature met DSK bepaal. Die twee bekende mede-kristalle (bestaande uit feniel- en perfluorofeniel-, en feniel- en perfluoropyridiel-ditiadiazoliel radikale) is gesintetiseer en ontleed deur DSK. Tydens die analise is 'n fase-oorgang in die suiwer 4'-perfluoropyridiel-1,2,3,5-ditiadiazoliel radikaal geïdentifiseer en gekarakteriseer met behulp van DSK, warmplatform mikroskopie en veranderlike temperatuur poeier X-straaldiffraksie. Ko-kristallasie van 1,2,3,5-ditiadiazoliel radikale is deur meganochemiese sintese, die vermenging van die mede-kristalvormers in oplossing, die smelt van 'n mengsel van die mede-kristalvormers en sublimasie van 'n mede-reduksie mengsel van die ditiadiazoliel radikale ondersoek. Ontleding deur poeier X-straaldiffraksie het die suksesvolle mede-kristalvorming deur al die tegnieke, behalwe meganochemiese sintese, bewys. Daar is bepaal dat mede-kristalvorming kwantitatief is deur elk van hierdie suksesvolle metodes.

Die tweede deel van hierdie studie was daarop gemik om stappe in die rigting van die sintese van 1,2,3,5-ditiadiazoliel radikale, wat met funksionele groepe vir H-binding soos die hidroksiel-, amino- en karboksielgroep-groepe gefunksionaliseer is, te ondersoek. Eksperimente, uitgevoer op die uitgangsreagense wat reeds die gewenste H-binding groepe bevat het, het getoon dat dit nodig was om hierdie groepe te beskerm voordat die sintese van die ditiadiazoliel radikaal mag plaasvind. Vier nuwe ditiadiazoliel radikale is dus gesintetiseer, naamlik die 3'- en 4'-trimetielsiloksyfeniel- en 3'- en 4'-N,N'-bis-*t*-Boc-

aminofeniel-1,2,3,5-ditiadiazoliel radikale. Aanvanklike pogings om die beskermende groepe van die ditiadiazoliel radikale te verwyder, was onsuksesvol. 'n Poging om die 4'-karboksiefeniel-1,2,3,5-ditiadiazoliel radikaal te sintetiseer deur litium-halogen uitruiling met 4'-bromofeniel-1,2,3,5-ditiadiazoliel en die daaropvolgende blus met CO₂ was ook onsuksesvol.

Die doel van die laaste deel van hierdie studie was om nuwe kombinasies van 1,2,3,5-ditiadiazoliel radikale te ko-kristalliseer met óf die CN...S-S óf die NO₂...halogen interaksie as 'n teiken-sinton met behulp van tegnieke wat in die eerste deel van die studie ontwikkel is. Pogings tot mede-kristallisatie met 3'-sianofeniel- en 3'-sianoperfluorofeniel-, perfluorofeniel- of perfluoropyridiel-1,2,3,5-ditiadiazoliel radikale, was onsuksesvol. Kombinasies tussen 4'-bromofeniel-, 4'-iodofeniel-, 3'- en 4'-nitrofeniel-1,2,3,5-ditiadiazoliel radikale het nie mede-kristalle geproduseer nie. Tydens hierdie studie is kristalstrukture vir die 4'-bromofeniel- en 3'-nitrofeniel-1,2,3,5-ditiadiazoliel radikale vir die eerste keer bepaal.

Acknowledgements

I would, firstly, like to express my deepest thanks to my supervisor Dr Delia Haynes for the tremendous support she has been. Thanks for keeping the bigger picture in mind when my imagination began to run away from me and for pointing me in the right direction. I would also like to thank my co-supervisor Dr Gareth Arnott for guiding me with your incomparable synthetic knowledge. I have thoroughly enjoyed working with both of you and I thank you for the time, effort and tireless patience you gave to me.

I would like to acknowledge my friends in the Supramolecular Chemistry Group as well as the Group Of Medicinal and Organic Chemistry. Without each of you, this journey would not have been as enjoyable as it has been. Thank you for picking me up when I was down and for encouraging me to keep pursuing my dreams. Each of you has a very special place in my heart: Laura-Jane van Laeren, Helene Wahl, Leigh Loots, Malcolm Applewhite, Storm Potts, Dr Vincent Smith and Dr Matteo Lusi. I would also like to thank the academic members of these groups Prof Len Barbour, Prof van Otterlo, Dr Esterhuysen, Dr Tanya le Roex and Dr Stephen Pelly for the advice and suggestions you offered me. Thanks also to my friends who have been a part of my university career.

I would like to give a special thanks to Dr Marietjie Stander and Fletcher Hiten at the Mass Spectrometry unit for their analysis of my air sensitive compounds. Your work is truly priceless. I would also like to thank Elsa at the NMR unit for all her assistance with using the NMR spectrometer.

Thanks also to Prof Koch for all his suggestions, advice and faithful support throughout my studies. I really appreciate all you have done for me.

A special thanks to the Harry Crossley Foundation, the NRF, the Agar Hamilton Trust and the University of Stellenbosch for funding my studies.

A heartfelt thank you to my parents, Kay and Ashley, and my grandmother, Drevin. For your support, prayers, love and affection, I am truly grateful. I could not have asked for a better family!

Finally, I would like to thank the Father, the Son and the Holy Spirit for being such an important part of my life and everything that I do. Thank You for all Your blessings. May You be glorified in my life.

List of Abbreviations

ASAP	Atmospheric Solids Analysis Probe
CIF	Crystallographic Information File
CSD	Cambridge Structural Database
DFT	Density Functional Theory
DSC	Differential Scanning Calorimetry
EPR	Electron Paramagnetic Resonance
EI	Electron Impact Ionisation
ESI	Electron Spray Ionisation
GC-MS	Gas Chromatography-Mass Spectrometry
HMDS	1,1,1,3,3,3-Hexamethyldisilylazane
HMPA	Hexamethylphosphoramide
IUPAC	International Union of Pure and Applied Chemistry
IR	Infrared Spectroscopy
LC-MS	Liquid Chromatography-Mass Spectrometry
LiHMDS	Lithium Hexamethyldisilazide
MS	Mass Spectrometry
NMR	Nuclear Magnetic Resonance
SCXRD	Single Crystal X-ray Diffraction
SOMO	Singly-Occupied Molecular Orbital
T	Temperature
TGA	Thermogravimetric Analysis
TLC	Thin Layer Chromatography
TMEDA	Tetramethylethylenediamine
TMS	Trimethylsilyl
TMSCl	Trimethylsilyl Chloride
PXRD	Powder X-ray Diffraction
VT-PXRD	Variable Temperature Powder X-ray Diffraction
Δ_{rxn}	Change in ΔG , ΔH , or ΔS in the reaction
ΔG	Change in Gibbs free energy
ΔG_{rxn}	Change in Gibbs free energy for a reaction
ΔH	Change in enthalpy
ΔS	Change in entropy

Conferences

S. W. Robinson, D. A. Haynes and G. E. Arnott, *Co-crystals of Dithiadiazolyl Radicals*. 20th International Conference on the Chemistry of the Organic Solid State, **2011**, India, poster presentation.

Table of Contents

Declaration.....	i
Abstract.....	ii
Opsomming.....	iv
Acknowledgements.....	vi
List of Abbreviations	vii
Conferences	viii
Table of Contents.....	ix
List of Figures	xiii
List of Tables	xviii
List of Schemes.....	xx
Atom Colours	xxi
Chapter 1: Introduction	1
<hr/>	
1.1) The Molecular Crystal.....	2
1.1.1) van der Waals Interactions	3
1.1.2) Hydrogen Bonds.....	3
1.1.3) Halogen Bonds	4
1.2) X-ray Crystallography & Crystal Engineering.....	5
1.3) Magnetism.....	7
1.3.1) Paramagnetism	9
1.3.2) Ferromagnetism.....	9
1.3.3) Antiferromagnetism.....	9
1.3.4) Ferrimagnetism	10
1.3.5) Weak Ferromagnetism or Canted Antiferromagnetism	10
1.3.6) Applications of Magnetic Materials	10
1.4) Organic Free Radicals	11
1.5) Dithiadiazolyl Radicals	12
1.5.1) Synthesis of 1,2,3,5-Dithiadiazolyl Radicals	12
1.5.2) Reactivity of Dithiadiazolyl Radicals.....	14
1.5.3) Characterisation of 1,2,3,5-Dithiadiazolyl Radicals by Electron Paramagnetic Resonance (EPR) Spectroscopy.....	15
1.5.4) Electronic Structure & Properties	15
1.5.5) Conductivity and Magnetism in 1,2,3,5-Dithiadiazolyl Radicals	16
1.6) Crystal Engineering with Dithiadiazolyl Radicals.....	17
1.7) Project Aims.....	21

1.8)	References.....	21
------	-----------------	----

Chapter 2: Dithiadiazolyl Co-crystal Characterisation & Synthetic Investigation		26
--	--	-----------

2.1)	Definition of a Co-crystal.....	27
2.2)	Co-crystal Growth Methods.....	27
2.3)	Benefits of Co-crystallisation.....	28
2.4)	Known Co-crystals of 1,2,3,5-Dithiadiazolyl Radicals.....	28
2.5)	Synthesis of the Known Co-crystals.....	31
2.6)	Co-crystal Analysis.....	33
2.6.1)	Characterisation by Electron Paramagnetic Resonance (EPR).....	33
2.6.2)	Co-crystal yields by sublimation.....	34
2.6.3)	Mechanochemical Synthesis.....	37
2.6.4)	Melting & Thermal Analysis.....	39
2.6.5)	Mixed Reductions.....	50
2.6.6)	Mixing in Solution.....	53
2.7)	Conclusions & Future Work.....	54
2.8)	Experimental Procedures.....	55
2.8.1)	Synthesis of the Pure Radicals.....	55
2.8.2)	Synthesis of Co-crystals and Synthetic Investigations.....	57
2.9)	References.....	60

Chapter 3: Attempted Synthesis of Novel Dithiadiazolyl Radicals Containing Hydrogen-Bonding Moieties		61
---	--	-----------

3.1)	Supramolecular Synthons.....	62
3.1.1)	Some characteristics of Hydrogen Bonds.....	64
3.2)	Synthetic Considerations.....	65
3.3)	Initial test reactions.....	67
3.4)	An Alternate Synthetic Route.....	71
3.5)	Attempted synthesis with protected hydrogen-bonding groups.....	75
3.5.1)	Protection of 3-hydroxy-benzonitrile.....	76
3.5.2)	Synthesis of 4-(3'-trimethylsiloxyphenyl)-1,2,3,5-dithiadiazolyl.....	79
3.5.3)	Synthesis of 4-(4'-trimethylsiloxyphenyl)-1,2,3,5-dithiadiazolyl.....	81
3.5.4)	Protection of 3-amino-benzonitrile.....	84
3.5.5)	Reaction with 3'-trimethylsilylaza-benzonitrile to form the dithiadiazolyl heterocycle.....	85
3.5.6)	Revision of amino protection.....	86
3.5.7)	Attempted synthesis of 4-(3'-N,N-di-tert-butylcarbamatoxyphenyl)-1,2,3,5-dithiadiazolyl.....	88
3.5.8)	Synthesis of 4-(4'-N,N-di-tert-butylcarbamatoxyphenyl)-1,2,3,5-dithiadiazolyl.....	90

3.6)	Deprotection reactions.....	91
3.7)	Synthesis of 4'-carboxyphenyl-1,2,3,5-dithiadiazolyl by lithium-halogen exchange	92
3.8)	Conclusions.....	93
3.9)	Future Work	95
3.10)	Experimental Procedures	96
3.10.1)	Boeré synthesis without protecting groups.....	96
3.10.2)	Alange synthesis.....	98
3.10.3)	Boeré synthesis with protecting groups	100
3.10.4)	Deprotection reactions	106
3.10.5)	Synthesis of 4'-carboxyphenyl-1,2,3,5-dithiadiazolyl by lithium halogen exchange	107
3.11)	References.....	108
Chapter 4: Novel Crystal Structures & Further Co-crystallisation Experiments		110
4.1)	Introduction.....	111
4.2)	A Supramolecular Strategy.....	111
4.2.1)	The CN...S-S Synthons.....	111
4.2.2)	The Nitro-Halogen Synthons	114
4.3)	Two Novel Crystal Structures	116
4.3.1)	The Crystal Structure of 4-(4'-bromophenyl)-1,2,3,5-dithiadiazolyl, [3]	116
4.3.2)	The Crystal Structure of 4-(3'-nitrophenyl)-1,2,3,5-dithiadiazolyl, [5]	117
4.4)	Co-crystallisation Experiments	119
4.4.1)	[1] & [2] in THF	119
4.4.2)	[1] with other dithiadiazolyls	120
4.4.3)	Nitro-halogen synthon: co-reduction using Ph ₃ Sb.....	121
4.4.4)	[1] & [5]	121
4.5)	Conclusions.....	122
4.6)	Experimental Procedures	123
4.6.1)	1,2,3,5-Dithiadiazolyl Radicals	123
4.6.2)	Co-crystallisation Experiments.....	128
4.7)	References.....	130
Chapter 5: Summary		131
5.1)	Summary.....	132
Appendix A		136
A.1.)	Instrumentation and Chemicals	137
A.1.1.)	Chemicals & Glassware	137

A.1.2.)	Single-Crystal & Powder X-Ray Diffraction	137
A.1.3.)	Electron Paramagnetic Resonance	137
A.1.4.)	Nuclear Magnetic Resonance	138
A.1.5.)	Mass Spectrometry	138
A.1.6.)	Infrared Spectroscopy.....	138
A.1.7.)	Isolation and Purification of the t-Boc-protected amines in Chapter 3.....	138
Appendix B		139
<hr/>		
B.1.)	Molecular Numbering	140
B.1.1)	Chapter 2.....	140
B.1.2)	Chapter 3.....	141
B.1.3)	Chapter 4.....	143
CD Appendix		144
<hr/>		

List of Figures

- Figure 1.1: Generic hydrogen bond representations: a) the linear hydrogen bond with $\theta = 180^\circ$ and b) a diagram of a multifurcated hydrogen bond in which one hydrogen bond donor interacts with two hydrogen bond acceptors thus causing θ to deviate from linearity..... 4
- Figure 1.2: Crystal structure of benzene-hexafluorobenzene: a) shows the stacks of molecular units from above and b) shows the side view of the stacks showing the alternating benzene-hexafluorobenzene units. 6
- Figure 1.3: Diagram showing the quadrupole moments of a) benzene and b) hexafluorobenzene. These complimentary quadrupole moments allow the formation of stacks of alternating molecular units shown in c). 7
- Figure 1.4: Band theory diagram: a) A conduction band would arise from the idealised stacking of π -radicals (indicated by ovals). However, uniform stacks are susceptible to Peierls' distortion which causes b) where dimers form to eliminate the degeneracy of unpaired electrons. Consequently, a band gap is found in the conduction band. 17
- Figure 1.5: Despite the large twist angle of 38.5° in $[\text{C}_6\text{F}_5\text{CN}_2\text{S}_2]_2$, radicals dimerise in the solid state indicating that in order to obtain monomers in the solid state, a large twist angle in conjunction with a structure directing synthon is required. 20
- Figure 1.6: Crystal structure of $[\text{NC}_5\text{F}_4\text{CN}_2\text{S}_2]_2$ showing dimers of the radicals ($\text{S}\cdots\text{S}$ thin black lines) linked by the $\text{N}_{\text{py}}\cdots\text{S}$ -S synthon..... 20
- Figure 1.7: Crystal structures of the homodimers of the co-crystal formers: a) $[\text{PhCN}_2\text{S}_2]_2$ and b) $[\text{C}_6\text{F}_5\text{CN}_2\text{S}_2]_2$, and c) the co-crystal formed by co-sublimation of the these two dithiadiazolyl radicals..... 20
- Figure 2.1: Molecular structures of 4-phenyl-1,2,3,5-dithiadiazolyl, **[1]** (left) and 4-perfluorophenyl-1,2,3,5-dithiadiazolyl, **[2]** (right): the constituents of co-crystal **[1-2]**..... 29
- Figure 2.2: Crystal structure of **[1-2]** showing intermolecular contacts: intradimer $\text{S}\cdots\text{S}$ (purple) and intermolecular $\text{S}\cdots\text{Ar}$ (black), $\text{S}\cdots\text{N}$ (green) and $\text{S}\cdots\text{C}$ (red) contacts inhibit the stacking of the co-crystal formers in the solid state. 29
- Figure 2.3: Molecular structures of 4-phenyl-1,2,3,5-dithiadiazolyl, **[1]** (left) and 4-(4'-perfluoropyridyl)-1,2,3,5-dithiadiazolyl, **[3]** (right): the constituents of co-crystal **[1-3]**. . 30
- Figure 2.4: Crystal structure of **[1-3]** showing in the intermolecular interactions: intramolecular $\text{S}\cdots\text{S}$ (purple) and intermolecular $\text{N}_{\text{py}}\cdots\text{S}$ (green) contacts..... 30
- Figure 2.5: EPR spectra (298 K, CH_2Cl_2) of a) **[1]** ($g = 2.007$, $a_{\text{N}} = 5.0$ G), b) **[2]** ($g = 2.010$, $a_{\text{N}} = 4.9$ G) and c) **[3]** ($g = 2.011$, $a_{\text{N}} = 5.0$ G). 33
- Figure 2.6: EPR spectra (298 K, CH_2Cl_2) of the co-crystals: a) **[1-2]** ($g = 2.010$, $a_{\text{N}} = 5.0$ G) and b) **[1-3]** ($g = 2.010$, $a_{\text{N}} = 4.9$ G)..... 34
- Figure 2.7: Experimental powder patterns (red) of a) **[1]**, b) **[2]** and c) **[3]** compared with the patterns calculated from their respective crystal structures (blue) showing each sample to be phase pure. 35
- Figure 2.8: Powder pattern of the bulk sublimed material (blue) obtained from the sublimation of **[1]** and **[2]** and compared to the calculated patterns of **[1]** (red), the co-crystal **[1-2]** (green) and **[2]** (purple) showing complete conversion of the co-crystal formers to **[1-2]**. 36
- Figure 2.9: Powder pattern of the bulk sublimed material (blue) obtained from the sublimation of **[1]** and **[3]** and compared to the calculated patterns of **[1]** (red), the co-crystal **[1-3]** (green)

- and [3] (purple) showing the majority of peaks corresponding to [1-3] and some trace peaks corresponding to [1] due to a slight excess in the original mixture. No peaks corresponding to [3] are observed. Therefore, conversion to [1-3] is quantitative..... 36
- Figure 2.10: Powder patterns of the grinding experiments: a) Grinding experiment between [1] and [2] where the ground mixture is shown in blue compared to the calculated patterns of [1] (red), the co-crystal [1-2] (green) and [2] (purple). b) Grinding experiment between [1] and [3] where the ground mixture is shown in blue compared to the calculated patterns of [1] (red), the co-crystal [1-3] (green) and [3] (purple). In both cases, grinding resulted in the formation of a physical mixture of the co-crystal formers rather than a co-crystal. . 38
- Figure 2.11: Powder pattern of the physical mixture of radicals comprised of [1] and [2] where the physical mixture is shown in blue compared to the calculated patterns of [1] (red), the co-crystal [1-2] and [2]..... 39
- Figure 2.12: Powder patterns of the melting experiments: a) Melting experiment between [1] and [2] where the melted mixture is shown in blue compared to the calculated patterns of [1] (red), the co-crystal [1-2] (green) and [2] (purple) showing that the residue consisted of [1]. b) Melting experiment between [1] and [3] where the melted mixture is shown in blue compared to the calculated patterns of [1] (red), the co-crystal [1-3] (green) and [3] (purple) showing some peaks corresponding to the co-crystal and some trace peaks corresponding to [1] due to imperfect stoichiometry..... 40
- Figure 2.13: TGA analysis of a) [1], b) [2] and c) [3] yielding sublimation onset temperatures of 98.13 °C, 54.82 °C and 71.18 °C, respectively..... 42
- Figure 2.14: DSC analysis of a) [1], b) [2] and c) [3] showing their melting and recrystallisation temperatures. Furthermore, an additional thermal event is observed in [3]..... 44
- Figure 2.15: DSC analysis of [3] showing the thermal event at 82.97 °C..... 45
- Figure 2.16: DSC analysis of [3] cycled three times showing the thermal event at 81.14 °C in the first cycle only..... 45
- Figure 2.17: Hot-stage photos of [3]: a) at 24.9 °C, b) at 87.1 °C, c) at 88.5 °C and d) at 90 °C showing a phase transition between 88.5 °C and 90 °C..... 46
- Figure 2.18: VT-PXRD of [3] showing a phase transition between 70 °C and 80 °C. The calculated powder pattern from the known crystal structure is shown as the bottommost powder pattern. The powder pattern second from the top (purple) shows the melt as it is amorphous. Another powder pattern was collected after cooling the sample back to 25 °C (topmost pattern - orange) to determine the recrystallised phase. Some degree of preferred orientation is observed in the recrystallised sample. 47
- Figure 2.19: DSC analysis of the co-crystals a) [1-2] and b) [1-3] showing single melting and recrystallisation events..... 48
- Figure 2.20: DSC analysis of the melting experiments: a) the mixture of [1] and [2] and b) the mixture of [1] and [3] showing recrystallisation points corresponding to the co-crystals [1-2] and [1-3], respectively. 49
- Figure 2.21: Powder patterns of the crude reduction mixtures from the concurrent reduction experiments using Ph_3Sb : a) the pattern in blue represents the crude reduction mixture of the precursors of [1] and [2] compared to the patterns calculated from the crystal structures of [1] (red), the co-crystal [1-2] (green) and [2] (purple) and b) the pattern in blue represents the crude reduction mixture of the precursors of [1] and [3] compared to the patterns calculated from the crystal structures of [1] (red), the co-crystal [1-3] (green) and [3] (purple). Both powder patterns of the crude material indicate no formation of a co-crystal..... 51

- Figure 2.22: Powder patterns of the bulk material sublimed from the concurrent reduction experiments using Ph_3Sb : a) the pattern in blue represents the sublimed material compared to the patterns calculated from the crystal structures of [1] (red), the co-crystal [1-2] (green) and [2] (purple) and b) the pattern in blue represents the sublimed material compared to the patterns calculated from the crystal structures of [1] (red), the co-crystal [1-3] (green) and [3] (purple). In both sublimation experiments, conversion to the co-crystal is quantitative..... 52
- Figure 2.23: Powder patterns of the solvent mixing experiments: a) the residue after mixing [1] and [2] is shown in blue and is compared to the patterns calculated from the crystal structures of [1] (red), the co-crystal [1-2] (green) and [2] (purple), b) the residue after mixing [1] and [3] is shown in blue and is compared to the patterns calculated from the crystal structures of [1] (red), the co-crystal [1-3] (green) and [3] (purple). The co-crystals are formed in both solvent mixing experiments. A small amount of [1] is observed in the experimental pattern in a) due to imperfect stoichiometry..... 53
- Figure 3.1: Summary of target 1,2,3,5-dithiadiazolyl radicals containing either a hydroxy-, amino- or carboxy- functional group in either the 2-, 3-, or 4- position. 65
- Figure 3.2: ESI Mass spectra of a) [1] in positive mode and b) [1] in negative mode..... 68
- Figure 3.3: ESI Mass spectra of a) [2] in positive mode and b) [2] in negative mode..... 69
- Figure 3.4: Mass spectrum of the synthesis of [3] using HMPA as an additive to improve the nucleophilicity of LiHMDS. 70
- Figure 3.5: Mass spectrum of the 4-phenyl-1,3,2,4-dithiadiazolylum chloride salt, [4], formed using NH_4Cl and SCl_2 in nitrobenzene..... 72
- Figure 3.6: MS of the product of the reaction of 4-carboxy-benzonitrile with NH_4Cl and SCl_2 in nitrobenzene yielding [5] 72
- Figure 3.7: A possible side product that could form in the reaction using NH_4Cl and SCl_2 . Other possible thiazyl compounds may account for the peaks at $m/z = 205$ and 338 73
- Figure 3.8: MS of the product mixture of the reaction of 4-hydroxy-benzonitrile with NH_4Cl and SCl_2 in nitrobenzene yielding [6]. The peaks at $m/z = 205$ and 211 are attributed to thiazyl side products formed between NH_4Cl and SCl_2 73
- Figure 3.9: Mass spectrum of the product of the reaction between 4-amino-benzonitrile, NH_4Cl and SCl_2 in nitrobenzene to yield [8]. Loss of a proton from [8] would yield the peak at $m/z = 195.2$ and loss of the amine would yield the peak at $m/z = 177.2$. A possible structure for the base peak at $m/z = 153$ is shown..... 75
- Figure 3.10: ^1H -NMR spectrum of the oil obtained after drying benzene extract in vacuo. The insert is an expansion of the aromatic region showing proton assignments. The peak at 0.30 ppm corresponds to the TMS methyl protons..... 77
- Figure 3.11: ^1H -NMR spectrum of the oil obtained after drying hexane extract in vacuo. The insert is an expansion of the aromatic region showing proton assignments. The peak at 0.29 ppm corresponds to the TMS methyl protons. Again, the solvent residual peak coincides with one of the aromatic protons in the 3-trimethylsiloxy-benzonitrile..... 78
- Figure 3.12: ^1H -NMR spectrum of [9] purified by hexane extraction. The insert is an expansion of the aromatic protons: assignments are shown. In addition, the peak at 0.28 ppm corresponds to the TMS methyl protons..... 79
- Figure 3.13: ^{13}C -NMR spectrum of [9] purified by hexane extraction. Assignments are shown..... 79
- Figure 3.14: Mass spectrum showing the molecular ion of the desired salt: 4-(3'-trimethylsiloxyphenyl)-1,2,3,5-dithiadiazolylum chloride, [10]..... 80

Figure 3.15: Mass spectrum showing the fragmentation pattern of the 4-(3'-trimethylsiloxyphenyl)-1,2,3,5-dithiadiazolyl radical, [11]	81
Figure 3.16: EPR spectrum of the radical: 4-(3'-trimethylsiloxyphenyl)-1,2,3,5-dithiadiazolyl, [11] (CH ₂ Cl ₂ : g = 2.010, a _N = 5.1 G).	81
Figure 3.17: ¹ H-NMR of the hexane extract showing [12] with some hexane impurity. The insert is an expansion of the aromatic region to clarify the proton assignments.	82
Figure 3.18: Mass spectrum of the desired salt: 4-(4'-trimethylsiloxyphenyl)-1,2,3,5-dithiadiazolium chloride, [13]	83
Figure 3.19: Mass spectrum of the 4-(4'-trimethylsiloxyphenyl)-1,2,3,5-dithiadiazolyl, [14] showing the molecular ion at <i>m/z</i> = 270 and the loss of SSN at <i>m/z</i> = 192.	83
Figure 3.20: EPR spectrum of the desired radical: 4-(4'-trimethylsiloxyphenyl)-1,2,3,5-dithiadiazolyl, [14] . (CH ₂ Cl ₂ , g = 2.010, a _N = 5.2 G)	84
Figure 3.21: ¹ H-NMR spectrum of [15] . The insert is an expansion of the aromatic region.....	85
Figure 3.22: ¹³ C-NMR spectrum of the silylated amine, [15] . Some impurities are observed in the spectrum corresponding to hexane. In addition, the small peaks in the aromatic region could correspond to the degradation of [15] to the unprotected nitrile due to the slight acidity of CDCl ₃	85
Figure 3.23: Mass spectrum of the crude powder resulting from the reaction to form the dithiadiazolyl heterocycle, [15]	86
Figure 3.24: ¹ H-NMR spectrum of the column fraction containing the protected 3'-aminobenzonitrile, [17] . The tBoc-groups appear to be chemically inequivalent resulting in a doublet at 1.45 ppm. Furthermore, this affects the aromatic protons: these could not be assigned to specific peaks in the aromatic region as they overlap forming a multiplet. .	88
Figure 3.25: ¹ H-NMR spectrum of the column fraction containing the protected 4'-aminobenzonitrile, [18]	88
Figure 3.26: MS spectrum of the purple powder containing [19]	89
Figure 3.27: EPR spectrum of 4-(3'-N,N-di- <i>tert</i> -butylcarbamatoxyphenyl)-1,2,3,5-dithiadiazolyl, [19] (CH ₂ Cl ₂ : g = 2.010, a _N = 5.0 G)	89
Figure 3.28: MS spectrum of the crude reaction mixture to form [20]	90
Figure 3.29: EPR spectrum of 4-(4'-N,N-di- <i>tert</i> -butylcarbamatoxyphenyl)-1,2,3,5-dithiadiazolyl, [20] (CH ₂ Cl ₂ : g = 2.010, a _N = 5.1 G)	91
Figure 3.30: EPR spectrum of the residue after the attempted lithium-halogen exchange reaction and CO ₂ quench. The pentet is indicative of a dithiadiazolyl radical. Thus, the radical species survived the lithium-halogen exchange and did not react with the <i>n</i> -BuLi. (298 K, CH ₂ Cl ₂ : g = 2.010, a _N = 5.2)	93
Figure 3.31: Mass spectrum of the product of the attempted lithium halogen exchange reaction with [22] and quench with CO ₂ to form 4'-carboxyphenyl-1,2,3,5-dithiadiazolyl. The spectrum shows peaks corresponding to [22] and none corresponding to the desired product indicating that the reaction was unsuccessful.....	93
Figure 4.1: Diagram of the asymmetric unit of [1] in the solid state. Molecules dimerise in a <i>cis</i> -oid fashion through intermolecular S··S contacts. Non-hydrogen atoms in [1] are depicted as ellipsoids (50%).	112
Figure 4.2: Crystal packing diagram of [1] viewed in the <i>b-c</i> plane. Dimers of radicals stack in columns normal to this plane. The radicals are shown to pack in antiparallel chains (shown in green for example) stabilised by CN··S-S interactions.....	112

- Figure 4.3: Crystal packing diagram of **[1]** showing interchain S \cdots N contacts (red dashed lines).... 112
- Figure 4.4: Asymmetric unit of **[2]**. Atoms are depicted as ellipsoids (50%). 113
- Figure 4.5: Crystal structure diagram showing intradimer S \cdots S contacts in **[2]** (3.115(1) Å) as blue dashed lines and bifurcated interdimer CN \cdots S-S contacts (3.037(3) – 3.101(2) Å) as red dashed lines. 113
- Figure 4.6: Comparison of the crystal structures of β -**[1]** and **[2]**: a) packing diagram of β -**[1]** viewed down the *b* axis, b) packing diagram of **[2]** viewed down the *b* axis, c) structural overlay of **[1]** (red) and **[2]** (blue) calculated in Mercury showing the isostructurality of **[1]** and **[2]** (intermolecular contacts are shown as black lines) and d) structural overlay of **[1]** and **[2]** showing the 15° out-of-plane tilt angle of the dithiadiazolyl heterocycle in **[2]** (blue) in comparison to the co-planar **[1]** (red). 114
- Figure 4.7: Molecular structures of the target molecules: **[3]** - *para*-bromophenyl-dithiadiazolyl, **[4]** - *para*-iodophenyl-dithiadiazolyl, **[5]** - *meta*-nitrophenyl-dithiadiazolyl and **[6]** - *para*-nitrophenyl-dithiadiazolyl 115
- Figure 4.8: Asymmetric unit of the 4-(4'-bromophenyl)-1,2,3,5-dithiadiazolyl radical, **[3]**. *Cis*-oid dimers form in the solid state with intermolecular S \cdots S contacts (3.056(1) and 3.132(1) Å) shown as red dashed lines. Non-hydrogen atoms are modelled as ellipsoids (50%). 116
- Figure 4.9: Crystal packing diagram of the *b*-*c* plane of **[3]** showing interdimer contacts as dashed lines: green - Br \cdots S-S, dark blue - Br \cdots Ar, red - Br \cdots S and light blue - S-S \cdots Ar. Intradimer S \cdots S contacts are shown as dashed orange lines. 116
- Figure 4.10: Crystal packing diagram **[3]** showing inter-dimer S \cdots N contacts (3.065(3) – 3.166(3) Å) (red dashed lines) between herring-bone sheets of dimers..... 117
- Figure 4.11: Asymmetric unit of 4-(3'-nitrophenyl)-1,2,3,5-dithiadiazolyl, **[5]**, showing *cis*-oid dimerisation through strong intermolecular S \cdots S contacts (3.066(2) – 3.089(2) Å). Non-hydrogen atoms are modelled as ellipsoids (50%). 117
- Figure 4.12: Crystal packing diagram of **[5]** viewing the *b*-*c* plane in which radical dimers form chains stabilised by interdimer NO₂ \cdots S-S (2.865(4) – 3.222(4) Å) interactions and interchain S \cdots N contacts (3.192(4) – 3.269(4) Å). 117
- Figure 4.13: Crystal packing diagram showing layers of staggered dimers of **[5]** forming chains linked by NO₂ \cdots S interactions. Chains of dimers are coloured differently. 118
- Figure 4.14: Crystal packing diagram showing different layers of **[5]** distinguished by their chain-forming interactions: the blue layers contain molecules of **[5]** in chains linked by a NO₂ \cdots S-S interaction (or two O \cdots S interactions) whereas the green layers contain molecules of **[5]** in chains linked by a single NO₂ \cdots S (or O \cdots S) interaction. 118
- Figure 4.15: Structure overlay showing the isostructurality of **[1]** and **[5]** (calculated in Mercury). Short contacts are omitted for clarity. A small difference in the out-of-plane twist angles, 1-5°, of the heterocycles with respect to the plane of the aryl rings is noticeable. 119
- Figure 4.16: Powder patterns of **[1]** and **[2]** calculated from their crystal structures showing that PXRD would be able to show if a new phase had been formed between these two radicals. 120

List of Tables

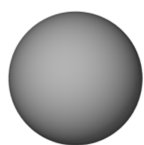
Table 1.1: Diagrammatic representation of magnetic ordering of unpaired spins resulting in the net magnetic behaviour of materials	8
Table 1.2: Comparison of the crystal structures of 3'-cyanophenyl- and 4'-cyanophenyl-1,2,3,5-dithiadiazolyl radicals showing chains (green) of radicals and CN...S interactions (red dashed lines)	18
Table 1.3: Crystal structures for the α - and β -phases of 4'-NCC ₆ F ₄ CN ₂ S ₂ ' showing the out-of-plane twist angles (prepared in Mercury), the CN...S interactions and the crystal packing diagram (prepared using POV-Ray).	19
Table 2.1: Thermodynamic Parameters for [PhCN ₂ S ₂] ₂ , [C ₆ F ₅ CN ₂ S ₂] ₂ and [PhCN ₂ S ₂][C ₆ F ₅ CN ₂ S ₂]	32
Table 2.2: Summary of the Melting and Recrystallisation Points observed in the DSC analysis of the pure radicals.....	43
Table 2.3: Quantities of reagents used to form the salt of [1]	56
Table 2.4: Quantities of reagents used to form [1]	56
Table 2.5: Quantities of reagents used to form the salt of [2]	56
Table 2.6: Quantities of reagents used to form [2]	56
Table 2.7: Quantities of reagents used to form the salt of [3]	57
Table 2.8: Quantities of reagents used to form [3]	57
Table 2.9: Quantities of reagents used to synthesise [1-2] and [1-3] and for percentage conversion experiments	57
Table 2.10: Quantities of reagents used to synthesise [1-2] and [1-3] by melting.....	58
Table 2.11: Quantities of reagents used to synthesise [1-2] and [1-3] from the melt while monitored by DSC	58
Table 2.12: Quantities of reagents used to synthesise [1-2] and [1-3] by the co-reduction of the parent salts with Zn-Cu couple in THF	59
Table 2.13: Quantities of reagents used to synthesise [1-2] and [1-3] by the co-reduction of the parent salts from the melt of Ph ₃ Sb.....	59
Table 2.14: Quantities of reagents used to synthesise [1-2] and [1-3] by mixing in solution	59
Table 3.1: Quantities of reagents used to form [1]	96
Table 3.2: Quantities of reagents used to form [2]	97
Table 3.3: Quantities of reagents used to form [3]	97
Table 3.4: Quantities of reagents used to form [4]	98
Table 3.5: Quantities of reagents used to form [5]	98
Table 3.6: Quantities of reagents used to form [6]	99
Table 3.7: Quantities of reagents used to form [7]	99
Table 3.8: Quantities of reagents used to form [8]	100
Table 4.1: Quantities of reagents used to form the salt of [1]	124
Table 4.2: Quantities of reagents used to form the radical [1]	124

Table 4.3: Quantities of reagents used to form the salt of [2]	124
Table 4.4: Quantities of reagents used to form the radical [2]	124
Table 4.5: Quantities of reagents used to form the salt of [3]	125
Table 4.6: Quantities of reagents used to form the radical [3]	125
Table 4.7: Quantities of reagents used to form the salt of [4]	125
Table 4.8: Quantities of reagents used to form the radical [4]	125
Table 4.9: Quantities of reagents used to form the salt of [5]	126
Table 4.10: Quantities of reagents used to form the radical [5]	126
Table 4.11: Quantities of reagents used to form the salt of [6]	126
Table 4.12: Quantities of reagents used to form the radical [6]	126
Table 4.13: Quantities of reagents used to form the salt of [7]	127
Table 4.14: Quantities of reagents used to form the radical [7]	127
Table 4.15: Quantities of reagents used to form the salt of [8]	127
Table 4.16: Quantities of reagents used to form the radical [8]	127
Table 4.17: Reduced cell parameters of the blue blocks obtained by sublimation shown to be [8] when compared the literature.....	128
Table 4.18: Unit cell parameters of the red blocks show them to consist of [4] when compared to the literature	129
Table 4.19: Unit cell parameters of the red blocks show them to consist of [4] when compared to the literature	129

List of Schemes

Scheme 1.1: Geometric isomers of the dithiadiazolyl radicals. The two top isomers are the only two which have been isolated to date.....	12
Scheme 1.2: Simple synthetic procedure to prepare 1,2,3,5-dithiadiazolyl radicals from their 1,3,2,4-dithiadiazolyl isomers	13
Scheme 1.3: General synthetic procedure to form 1,2,3,5-dithiadiazolyl radicals using LiHMDS and SCl ₂ to form the parent salts and reduction to form the radical.	13
Scheme 1.4: Solid state 1,2,3,5-dithiadiazolyl radical dimer configurations: a) twisted, b) <i>cis</i> -oid, c) <i>trans</i> -oid (<i>trans</i> -antarafacial), d) <i>trans</i> -cofacial and e) orthogonal. Heteroatoms are not shown for clarity.	16
Scheme 3.1: Some representative supramolecular synthons: a) a carboxyl dimer, b) a carboxyl chain, c) a hydroxyl ring, d) an OH...NH chain, e) a nitro...amine synthon, f) a Cl...Cl synthon, g) an I...I synthon and h) a nitro...iodo synthon.....	63
Scheme 3.2: General synthetic procedure to form 1,2,3,5-dithiadiazolyl radicals using LHMDS to form a silylated amidinate. Quenching with SCl ₂ yields the dithiadiazolylium chloride salt which can be reduced to the radical using Zn-Cu in THF or Ph ₃ Sb.....	65
Scheme 3.3: Possible side products observed in the mass spectrum (Figure 3.4) from the attempted synthesis of [3] using HMPA as an additive.	70
Scheme 3.4: General dithiadiazolyl heterocycle synthesis to form dithiadiazolyl radicals using NH ₄ Cl and SCl ₂ in nitrobenzene.....	71

Atom Colours



Hydrogen



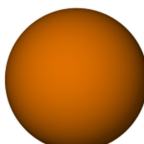
Carbon



Nitrogen



Oxygen



Sulphur



Fluorine



Bromine

Chapter 1: Introduction

1.1) The Molecular Crystal

The manner in which atoms associate with one another is a fundamental concept in chemistry. One of the early definitions of the molecule is that it is a “group of atoms held together with interactions that are so strong that it remains relatively stable under many variations in temperature and pressure.”¹ Thus, a molecule is a chemical substance, comprised of a discrete group of atoms, whose form exists in the gas, liquid and solid phases of that compound. Furthermore, the energy required to disrupt the interactions between the atoms forming the molecule is much greater than the energy required to convert one phase into another. In the 1930s, Linus Pauling defined these very strong interatomic interactions, which group and hold the atoms in the form of a molecule, as a *bond* in his book, *The Nature of the Chemical Bond*.² These bonds, specifically covalent bonds in which electrons are shared between the bonding atoms, hold the atoms in a particular arrangement, thus forming the molecule.³

This definition has been greatly refined and the IUPAC Gold Book now defines a molecule as “An electrically neutral entity consisting of more than one atom ($n > 1$) ... in which $n > 1$ must correspond to a depression on the potential energy surface that is deep enough to confine at least one vibrational state.”³ Therefore, a molecule is distinguished from an ion by its neutral electrical charge and a gain in energy is observed from the covalent bonding of two or more atoms together.

The solid crystalline form of a molecule is known as a molecular crystal: a crystal comprised of molecules.¹ Perhaps, a better definition would be that “within a molecular crystal, it is possible to identify groups of atoms such that for every atom in a group, at least one interatomic distance within this group is significantly shorter than the smallest interatomic distance to an atom in another group.”⁴ Thus, the interatomic distance between atoms that are bonded to one another to form a molecule must be significantly shorter than the interatomic distance between two non-bonded atoms in adjacent molecules. This is because when two atoms bond, sharing electrons between them, they are able to approach one another closer than if they were not bonded: closer than the sum of the van der Waals radii of the two bonding atoms. The van der Waals radius is one way to define the size of an atom.⁵

In addition to these bonding interactions which hold atoms together to form molecules, there are several weaker intermolecular interactions which allow molecules to associate with one another in the solid state. Although these interactions are weak, they can help to stabilise the molecular crystal.⁶ When molecules orientate and arrange themselves with respect to one another such that attractive interactions are maximised while repulsive interactions are minimised, a molecular crystal is formed.⁷ This usually coincides with the most efficient utilisation of space,⁸ known as close packing: where any particular molecule is surrounded by the maximum number of neighbouring molecules. The aforementioned weaker interactions that help to control this include van der Waals interactions, hydrogen and halogen bonds.

1.1.1) van der Waals Interactions

The van der Waals interaction is the sum of the attractive and repulsive forces between two or more molecules excluding covalent bonds and ionic interactions.³ Polarisation of covalent bonds, due to electronegativity differences between the bonding atoms, causes dipoles to form in the molecule. These dipoles are then able to interact with dipoles in nearby molecules either attractively or repulsively. Attractive interactions will cause molecules to associate with one another. Van der Waals interactions include London forces (induced dipole to induced dipole), permanent dipole interactions and permanent dipole to induced dipole interactions. These forces are quite weak. However, they are numerous and a net attractive force will enable molecules to associate with one another to form a molecular crystal. They also contribute towards the solubility, density and melting point characteristics, amongst others, of organic compounds.¹

1.1.2) Hydrogen Bonds

Hydrogen bonds were first mentioned by Moore and Winmill in 1912.⁹ Since then, they have been widely studied for their structural and functional importance in organic and biological systems.¹⁰ IUPAC defines a hydrogen bond as:

“A form of association between an electronegative atom and a hydrogen atom attached to a second, relatively electronegative atom. It is best considered as an electrostatic interaction, heightened by the small size of hydrogen, which permits proximity of the interacting dipoles or charges. Both electronegative atoms are usually (but not necessarily) from

the first row of the Periodic Table, i.e. N, O or F. Hydrogen bonds may be inter-molecular or intramolecular. With a few exceptions, usually involving fluorine, the associated energies are less than 20 - 25 kJ mol⁻¹ (5 - 6 kcal mol⁻¹).³

In fact, hydrogen bond strengths vary over quite a wide range: 0.2 – 40 kJ mol⁻¹,^{11, 12} and are generally much stronger than van der Waals interactions (<5 kJ mol⁻¹).¹³ In addition, they are directional in nature, where the bond angle from the hydrogen donor (X) to the hydrogen atom (H) to the hydrogen acceptor (Y), denoted X-H...Y, is predominantly linear ($\theta = 180^\circ$) (Figure 1.1a).¹ However, the average value of θ observed in crystal structures is around 165° due to the possibility of forming multifurcated hydrogen bonds (Figure 1.1b), which are hydrogen bonds that are formed between a single hydrogen bond donor (X-H) and more than one hydrogen bond acceptor (Y).¹ Indeed, the converse is also true: a single hydrogen bond acceptor may form contacts with more than one hydrogen bond donor. Due to this near linear geometry of hydrogen bonds, they are able to direct the packing arrangement of molecules within the crystal lattice.⁶

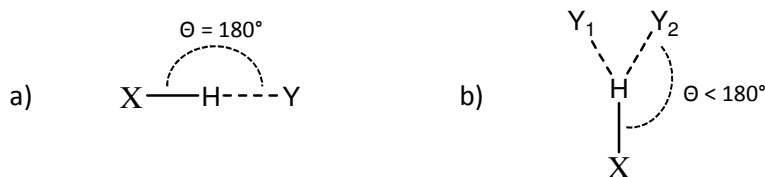


Figure 1.1: Generic hydrogen bond representations: a) the linear hydrogen bond with $\theta = 180^\circ$ and b) a diagram of a multifurcated hydrogen bond in which one hydrogen bond donor interacts with two hydrogen bond acceptors thus causing θ to deviate from linearity.

1.1.3) Halogen Bonds

The first halogen bond was reported in 1863;¹⁴ however it was only termed a halogen bond by Dumas *et al.* in 1983.¹⁵ Halogen bonds form as a result of the polarisation of a halogen atom.^{16, 17} In the case where a halogen is bonded to a carbon atom, the halogen is positively polarised in the area of the halogen diametrically opposite to the carbon atom. The so-called equatorial region is negatively polarised. Thus, an electrostatic interaction is able to form between a halogen and a negatively polarised or electronegative species. Halogen bonds can form between two halogens of the same type (X...X, symmetrical) or between one halogen and an electronegative atom (X...Y, unsymmetrical where Y is a different halogen or a non-halogen atom).¹ Halogen bonds were first shown to be useful as structure directing interactions in molecular crystals by Hassel *et al.*¹⁸

1.2) X-ray Crystallography & Crystal Engineering

The study of crystals is known as crystallography. Since the discovery of X-rays in 1895 by Röntgen¹⁹ and their diffraction by crystals in 1912 by von Laue *et al.*,²⁰ the analysis of crystal structures and their properties has become a popular field of research in the development of new materials with specific properties.⁷ Crystal structures may also be analysed by their diffraction of electrons and neutrons. However, for the purposes of this study, focus will be placed on the diffraction of X-rays in the context of crystal structure analysis. The diffraction of X-rays by the electron clouds surrounding the atoms in molecules in the solid state gives information regarding the relative atomic positions within a molecular crystal. Analysis of this data then allows the visualisation of the crystal structure.

The study of crystal structures has advanced our understanding of the properties that a crystal exhibits as these can often be directly related to the crystal structure or, in other words, the packing arrangement of the molecules.²¹ Chemical properties of a crystal include its reactivity while the physical properties that it exhibits include electric, magnetic, optical, solubility, melting point, etc. characteristics.²¹ The ability to visualise the three-dimensional packing arrangement of molecules in a crystal lattice allows the identification of the key interactions (such as van der Waals interactions, hydrogen bonds and halogen bonds) by which the molecules associate with one another and stabilise the structure. The study of these intermolecular interactions which allow molecules to recognise one another and hold them together is known as supramolecular chemistry: chemistry beyond the molecule.³ Supramolecular chemistry is not limited to the solid state: it can also be used to describe intermolecular interactions in solution.²²

The understanding of supramolecular interactions and the application of that knowledge in the design of molecular entities which, when crystallised, will hopefully confer a pre-determined property to the molecular crystal, is the basis of crystal engineering.⁶ The purpose of crystal engineering is to synthesise crystals that have specific properties and functions. To do this, the manner in which molecules assemble to form a crystal must be controlled and manipulated.

Desiraju proposed the term supramolecular synthon to describe the “structural units within supermolecules which can be formed and/or assembled by known or conceivable synthetic operations involving intermolecular interactions.”²³ Corey introduced the term “synthon” in 1967 when describing the strategy by which complex molecules could be

synthesised: by identifying “structural units within molecules which can be formed and/or assembled by known or conceivable synthetic operations.”²⁴ In other words, a synthon in a crystal engineering context refers to the interactions between functional groups of the molecules which make up the molecular crystal. Thus, synthon comprises a molecular (a functional group) and a supramolecular component (an intermolecular interaction).

An example of a supramolecular synthon is the structure of the aryl-perfluoroaryl co-crystal.^{25, 26} In Figure 1.2 the crystal structure of benzene-hexafluorobenzene is shown to contain uniform stacks of alternating units of benzene and hexafluorobenzene.

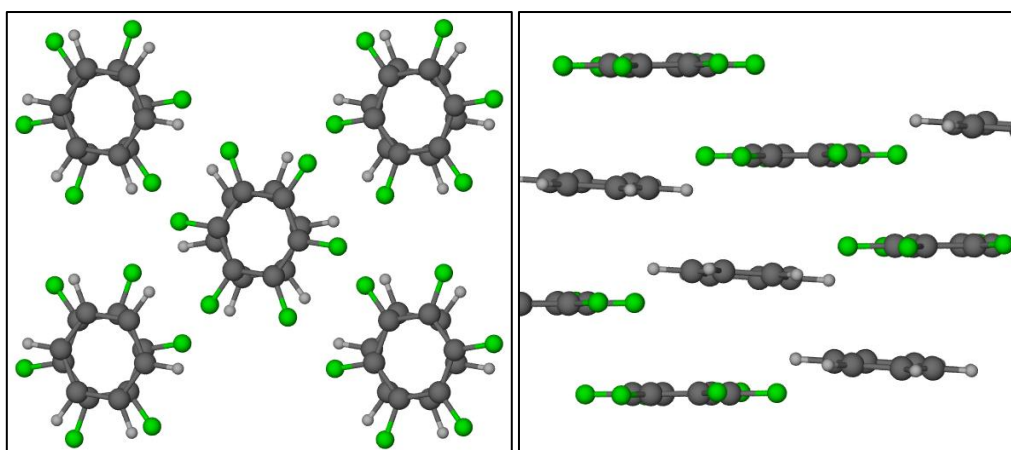


Figure 1.2: Crystal structure of benzene-hexafluorobenzene: a) shows the stacks of molecular units from above and b) shows the side view of the stacks showing the alternating benzene-hexafluorobenzene units.²⁵

Due to the aromatic nature of benzene, the reorganisation of the electronic charge distribution results in the formation of a quadrupole moment as the electrons in the C-H bonds are drawn towards the aromatic ring.²⁷ Consequently, the C-H bond is slightly polarised to $(\delta^+)H-C(\delta^-)$ leading to the formation of the quadrupole moment where the molecule is δ^+ in the plane of the benzene ring and δ^- above and below the ring (Figure 1.3a). In contrast, this quadrupole moment is inverted in hexafluorobenzene due to the electronegativity of the fluorine atoms drawing electron density from the aromatic ring towards themselves resulting in δ^- in the plane of the aromatic ring and δ^+ above and below the ring (Figure 1.3b). The complimentary electrostatic nature of these quadrupole moments allows the propagation of stacks of alternating units in the solid state with a cohesive energy of $\sim 20\text{-}25 \text{ kJ mol}^{-1}$.²⁶

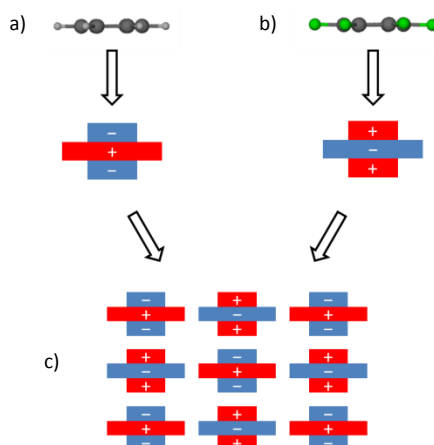


Figure 1.3: Diagram showing the quadrupole moments of a) benzene and b) hexafluorobenzene. These complimentary quadrupole moments allow the formation of stacks of alternating molecular units shown in c).²⁸

Studying crystal structures enables the identification of patterns in the way that functional groups interact with one another and consequently, the prediction of interactions in the design of new crystal structures. Furthermore, similar interactions may be observed in molecular crystals comprised of molecules containing comparable functional groups. When these interactions are observed regularly in a wide variety of crystal structures, they can be considered to represent supramolecular synthons and can be used to design interesting and useful crystal structures.²³ Specifically, strong directional synthons are of interest in crystal engineering because strong interactions are more likely to form over weak ones and directionality in a synthon provides control over the orientation of the molecules in order to form the synthon. Thus, the assembly of molecules in the solid state can be controlled to a certain extent.

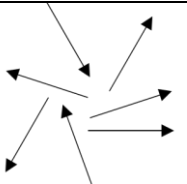
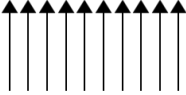
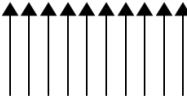

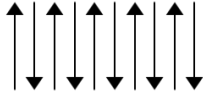
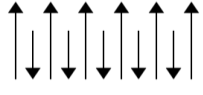



This control over crystal structure now allows the manipulation of interesting properties such as thermal and optical properties, conductivity and magnetism and many others. This study is interested in materials which exhibit magnetic properties.

1.3) Magnetism

For a material to be considered magnetic, it must exhibit magnetic ordering of unpaired electron spins. Materials that do not contain unpaired electrons are called diamagnetic and are repelled by a magnetic field. Therefore, they cannot be used in applications where a magnetic moment is required. Examples of such materials include copper, silver, gold, bismuth, beryllium and most organic molecules.²⁹

Magnetic ordering can present itself in a number of ways due to the manner of interaction between individual magnetic moments within the material. These interactions contribute towards the net magnetic behaviour of the material, namely, paramagnetism, ferromagnetism, antiferromagnetism, ferrimagnetism or weak ferromagnetism (Table 1.1).

Table 1.1: Diagrammatic representation of magnetic ordering of unpaired spins resulting in the net magnetic behaviour of materials

Interaction	Spin representation		Magnetisation
Paramagnetism	Absence of a magnetic field	Presence of an external magnetic field	No net moment unless in the presence of an external magnetic field
			
Ferromagnetism			Net moment 
Antiferromagnetism			No net moment
Ferrimagnetism			Net moment: less than ferromagnetism 
Weak Ferromagnetism / Canted Antiferromagnetism			Net moment: less than ferromagnetism 

1.3.1) Paramagnetism

A paramagnetic material is one in which the magnetic moments are randomly oriented in the absence of an external magnetic field due to no interaction between the magnetic moments. Consequently, no net magnetic moment is observed.³⁰ However, the application of an external magnetic field results in the alignment of the magnetic moments parallel to the field.³¹ Removal of the external magnetic field results in the loss of the net magnetic moment as spins are once again randomly oriented. This response of the material to an external magnetic field is known as permeability.

1.3.2) Ferromagnetism

A material is considered ferromagnetic when the magnetic moments are aligned parallel throughout the solid. The application of an external magnetic field will cause the individual magnetic moments to align parallel to the field. This reorientation of magnetic moments requires energy causing an observable delay in the alignment of the magnetic moments in the direction of the external magnetic field. This phenomenon is known as hysteresis and can be quantified by measuring the magnetisation of the material with varying external magnetic field strengths. If the external magnetic field is switched off, the magnetic moments of the ferromagnetic material will remain aligned in the direction of the external magnetic field (retentivity) and the strength of this magnetisation is known as remanence or remanent magnetisation. The magnetisation of a ferromagnetic material can be reduced to zero by applying a magnetic field in the opposite direction. The magnitude of this magnetic field is unique for each magnetic material and is known as the coercivity of that material.²⁹

Above a certain temperature known as the Curie temperature (T_c),³¹ the material behaves as a paramagnet due to increased thermal energy which overcomes the aligning effect of the interaction energy between magnetic moments.²⁹

1.3.3) Antiferromagnetism

A material in which the magnetic moments are aligned antiparallel throughout the solid resulting in no net magnetic moment is known as an antiferromagnet. It is important to note here that although no net magnetic moment is observed, the spins are ordered unlike in paramagnetism where the spins are randomly oriented. Furthermore, spins are not paired as in diamagnetism. Above a certain temperature known as the Néel temperature (T_N), the material behaves as a paramagnet, again due to increased thermal energy.²⁹

1.3.4) Ferrimagnetism

Because ferrimagnets behave similarly to ferromagnets, for a long time it was believed that no distinction existed between the two. However, ferrimagnetism is much more closely related to antiferromagnetism. This phenomenon arises when the antiparallel magnetic moments are different in magnitude.²⁹ In other words, all the magnetic moments aligned in one direction exhibit a bulk magnetic moment of a different magnitude to the bulk magnetic moment of all the magnetic moments aligned in the opposite direction.³¹ Consequently, a net magnetic moment is observed as the difference between the two bulk magnetic moments. This net magnetic moment is thus smaller than would be expected from a ferromagnetic material. Ferrimagnetic materials behave as paramagnets above the Curie temperature.

1.3.5) Weak Ferromagnetism or Canted Antiferromagnetism

Weak ferromagnetism arises when small canting occurs between antiparallel magnetic moments. Thus, the angle between alternating moments is not equal to 180°. Consequently, a net spontaneous magnetic moment is formed. However, although the magnetic behaviour is very similar to a ferromagnet, the magnitude of its magnetic moment is much less.

1.3.6) Applications of Magnetic Materials

For a magnetic material to find an application in data storage, for instance, it needs to exhibit a spontaneous magnetic moment, *i.e.* exhibit ferro-, ferri- or weak ferromagnetism. This magnetic moment must exist at a reasonable temperature, ideally at or above room temperature, for the material to be generally useful. In addition, the material must exhibit retentivity:²⁹ the memory of magnetisation when the external magnetic field is removed.

Molecular solids formed from a combination of free radicals, transition metal ions, rare earth ions and diamagnetic ligands are capable of exhibiting a spontaneous magnetic moment.³²

In 2000, Miller and Epstein reviewed the applications and attributes of molecular magnets stating that:

“Molecule-based magnets are a broad, emerging class of magnetic materials that expand the materials properties typically associated with magnets to include low density, transparency, electrical insulation, and low-temperature

fabrication, as well as combine magnetic ordering with other properties such as photoresponsiveness."³³

Industrially, organic magnets have potential benefits regarding their processability, optical properties and biocompatibility.³⁴ In terms of processability, the production of organic magnets could be less energy demanding than conventional magnets due to their plasticity, flexibility and solubility in common organic solvents.³² Due to the transparency of organic magnetic materials, interesting optical properties can be expected, leading to applications of the materials as photomagnetic switches or in the manipulation of polarised light in integrated optical devices.³⁴ The biocompatibility could permit the use of organic magnets as selective contrasting agents in nuclear magnetic resonance imaging or as transducers for medical implants.^{32, 34} For this reason people are interested in the synthesis of magnetic materials from organic materials, of which organic free radicals are suitable building blocks.

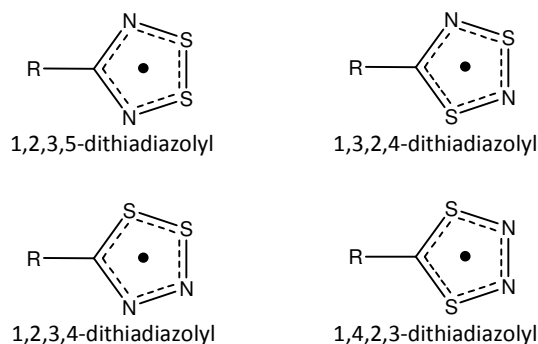
1.4) Organic Free Radicals

Due to their significance in biological systems, organic free radicals are widely known.^{35, 36} The first organic radical to be synthetically prepared was the triphenylmethyl radical.³⁷ Since then, a variety of organic free radicals have been prepared as interest has grown in the potential applications of such materials.³⁸ In particular, organic free radicals have the potential to exhibit conducting and/or magnetic properties, traditionally only found in metal containing compounds. For bulk magnetic ordering to be observed in a molecular material, it must have unpaired electrons (radicals) and the spins of these unpaired electrons must be able to communicate with one another. This is known as a magnetic exchange pathway and is dependent on the solid state arrangement of the molecules comprising the molecular crystal.¹

Although it is not a radical, poly(sulphur-nitride) or SN_x ,³⁹ is a good example of a material that exhibits super-conducting⁴⁰ properties while containing no metallic elements.⁴¹ Studies aiming to modify and improve the properties of SN_x resulted in the synthesis of novel S-N-containing compounds.⁴² Included among these are several heterocyclic sulphur-nitrogen derivatives.⁴³ The family of dithiadiazolyl radicals are of particular interest due to their potential as building blocks for molecular magnets and conductors.⁴⁴

1.5) Dithiadiazolyl Radicals

Dithiadiazolyls originate from a class of five-membered heterocyclic sulphur-nitrogen free radicals. The first radical of this class, $[S_3N_2^{+}]Cl^{-}$, was prepared in 1880.⁴⁵ However, it was nearly a century later when its crystal structure was obtained in 1974.⁴⁶ The family of dithiadiazolyl radicals are related to this molecule by the substitution of S^{+} with R-C resulting in neutral isoelectronic 7π heterocycles.⁴⁴ Dithiadiazolyl heterocycles may exist in one of four geometric isomers (Scheme 1.1), however, only the 1,2,3,5-dithiadiazolyl and the 1,3,2,4-dithiadiazolyl radicals have been observed to date.⁴⁴ Molecular orbital calculations have been performed on the parent cations of the other two isomers showing that it may be possible for them to exist. However, due to the possible loss of dinitrogen from these isomers, they may be unstable.⁴⁴ In addition, these calculations indicate that the 1,2,3,5-dithiadiazolyl heterocycles may be the most stable of these isomers.



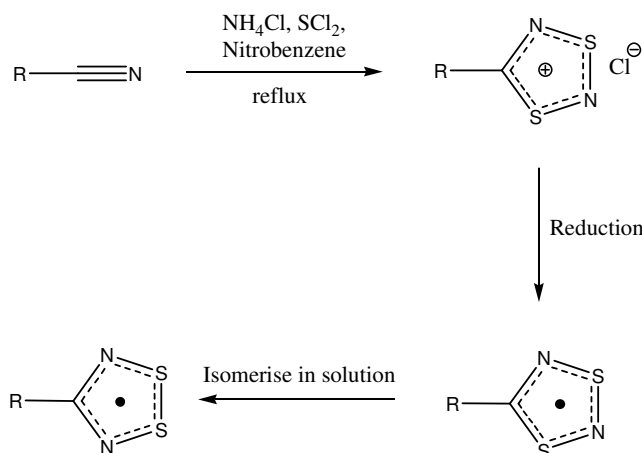
Scheme 1.1: Geometric isomers of the dithiadiazolyl radicals.⁴⁴ The two top isomers are the only two which have been isolated to date.

The 1,2,3,5-dithiadiazolyl radicals are of particular interest in this study. It should be noted that their isoelectronic selenium analogues (1,2,3,5-diselenadiazolyl radicals) are known. The first diselenadiazolyl radical was characterised structurally in 1989.⁴⁷ Since then, several derivatives have been synthesised and characterised for their potential as magnetic and/or conducting materials.⁴⁸⁻⁵⁴ However, the diselenadiazolyl radicals will not be discussed further in this study.

1.5.1) Synthesis of 1,2,3,5-Dithiadiazolyl Radicals

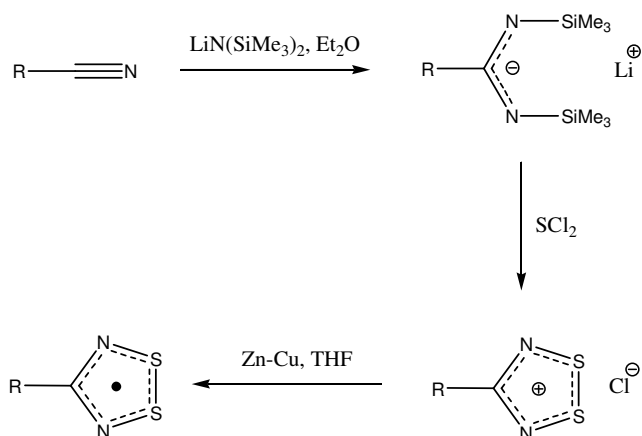
A number of procedures exist by which to form the dithiadiazolyl heterocycle. The first dithiadiazolyl cation was prepared as a chloride salt in 1977⁵⁵ from the reaction of an organic nitrile with thiazyl chloride, $(NSCl)_3$. Soon afterwards, it was discovered that dithiadiazolyl salts could be synthesised from cheap, commercially available starting materials, namely, the parent nitrile, sulphur dichloride and ammonium chloride under an

atmosphere of chlorine (Scheme 1.2).^{56, 57} Consequently, the reactivity of amidines with SCl_2 was investigated as a condensation reaction between N-H and S-Cl bonds was observed.⁴⁴



Scheme 1.2: Simple synthetic procedure to prepare 1,2,3,5-dithiadiazolyl radicals from their 1,3,2,4-dithiadiazolyl isomers

The first synthesis of dithiadiazolyl cations from the reaction between an amidine and SCl_2 involved the hydrochloride salt of benzamidine.⁵⁶ Since then, the dithiadiazolyl cations have been routinely prepared from the condensation reaction between a persilylated amidine and SCl_2 . In this method, the persilylated amidine is prepared by the reaction of the parent nitrile with $\text{Li}[\text{N}(\text{SiMe}_3)_2]$ or LiHMDS in diethyl ether (Scheme 1.3). This method is limited to starting nitriles which do not have protons α to the nitrile as side reactions are likely to occur due to the strong basicity of LiHMDS . At this point, Me_3SiCl (TMSCl) may be added to the N-lithio salt in order to isolate and purify the persilylated amidine.⁵⁸ Often, the intermediate N-lithio salt is condensed with SCl_2 or S_2Cl_2 to form the parent dithiadiazolyl cation as a chloride salt in a one-pot synthesis.⁴⁴ This crude salt can be purified by Soxhlet extraction with acetonitrile if desired.



Scheme 1.3: General synthetic procedure to form 1,2,3,5-dithiadiazolyl radicals using LiHMDS and SCl_2 to form the parent salts and reduction to form the radical.⁵⁸

The first dithiadiazolyl radical, 4-phenyl-1,2,3,5-dithiadiazolyl, $[\text{PhCN}_2\text{S}_2]_2$, was prepared from the anion metathesis of the 4-phenyl-1,2,3,5-dithiadiazolylum chloride salt to the thiocyanate salt and the subsequent disproportionation reaction of the 4-phenyl-1,2,3,5-dithiadiazolylum thiocyanate salt.⁵⁹ Soon afterwards, it was reported that dithiadiazolyl radicals could be prepared by the reduction of the parent salt using sodium dust, triphenylverdazyl radical or tetramethyl-*p*-phenylene diamine.⁶⁰ Since then, a wide variety of reducing agents have been employed to form the radicals, particularly zinc-copper (Zn-Cu) couple,⁵⁷ silver (Ag) powder⁶¹ and Ph_3Sb .⁶²⁻⁶⁴ Generally, dithiadiazolyl radicals are purified by vacuum sublimation.

1,2,3,5-Dithiadiazolyl radicals have also been prepared by the rearrangement of 1,3,2,4-dithiadiazolyl radicals in solution.⁴⁴ However, due to the relative ease by which 1,2,3,5-dithiadiazolyl radicals can be prepared by the reduction of their parent salts, this method is not commonly used.

1.5.2) Reactivity of Dithiadiazolyl Radicals

Dithiadiazolylum salts are able to undergo anion metathesis and react with Lewis acids.⁴⁴ Reaction with water hydrolyses the dithiadiazolylum salt to the corresponding amidinium salt, elemental sulphur and SO_2 .⁴⁴ Aryl-substituted dithiadiazolylum salts containing softer anions such as bromide, iodide or cyanide, can react with a cool direct current nitrogen plasma. This results in the reduction of the cation and subsequent insertion of a nitrogen atom into the disulphide bond.⁶⁵ Salts containing harder anions do not undergo this insertion reaction. Similar to their parent salts, dithiadiazolyl radicals react with cool direct current nitrogen plasma to form dithiatriazines.⁴⁴

Dithiadiazolyl radicals are thermally stable, however they have been shown to be air and moisture sensitive.⁶⁶ Considering that the radicals are synthesised by the reduction of their corresponding cationic salts, the reverse is also true: the radicals are readily oxidised back to their parent salts.⁵⁷ Furthermore, $[\text{PhCN}_2\text{S}_2]_2$ has been shown to behave as a dehalogenating agent in radical coupling reactions. Although the mechanism is not yet known, it has been suggested⁴⁴ that the dithiadiazolyl radical homolytically cleaves E-X type bonds (E = B, P, Si and activated C; X = Cl, Br) with the simultaneous formation of new E-E bonds.⁶⁷ In addition, while investigating these dehalogenation properties, it was discovered that $[\text{PhCN}_2\text{S}_2]_2$ is able to trap some radical intermediates.^{68, 69}

Transition metal complexes may also be formed using dithiadiazolyl radicals through the expansion of the disulphide bond to give two μ_2 bridging sulphur atoms.⁴⁴

1.5.3) Characterisation of 1,2,3,5-Dithiadiazolyl Radicals by Electron Paramagnetic Resonance (EPR) Spectroscopy

In the solution state, an equilibrium between dimers and monomers of 1,2,3,5-dithiadiazolyl radicals exists.⁴⁴ At room temperature, the equilibrium favours the dissociation of dimers into monomeric units^{64, 65} allowing the radicals to be observed using EPR. EPR spectra of 1,2,3,5-dithiadiazolyl radicals typically show a characteristic 1:2:3:2:1 quintet arising from the coupling of the unpaired electron to the two equivalent nitrogen nuclei in the heterocycle.⁴⁴ Nitrogen nuclei have a nuclear spin quantum number of $I = 1$ which, when using the $2nI + 1$ rule to calculate multiplets, yields a quintet.⁷⁰ The coupling constant typically observed between the unpaired electron and nitrogen nuclei (a_N) is in the range of 5.0 G. Coupling to sulphur is usually not observed due to the low natural abundance of ^{33}S .⁴⁴ The quintet is usually observed at an isotropic g -value near to 2.01, comparable to that of the free electron (2.00232).^{44, 71}

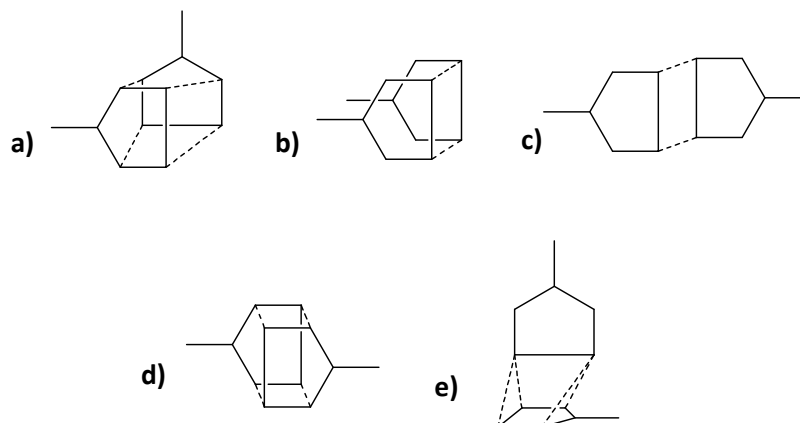
1.5.4) Electronic Structure & Properties

The 1,2,3,5-dithiadiazolyl radical exists due to the partial occupancy of the π^* orbital of the parent salt.⁴⁴ This anti-bonding orbital is known as the singly occupied molecular orbital (SOMO) and is of $2a_2$ symmetry. The SOMO is nodal at the carbon atom⁷² in the heterocycle. Solution-state EPR studies have shown that the unpaired spin density is largely localised to the sulphur and nitrogen atoms in the heterocycle.^{73, 74} In addition, redox potential studies on a number of 1,2,3,5-dithiadiazolyl derivatives have shown a nearly negligible dependence on substituent effects.^{75, 76} Therefore, crystal engineers have become interested in these materials due to the possibility of varying the R-group by incorporating supramolecular synthons without significantly affecting the electronic properties of the dithiadiazolyl heterocycle. Because dithiadiazolyl radicals associate in the solid state forming dimers, which renders their potential conducting and magnetic properties negligible,^{*} the possibility of varying the R-group is useful as the introduction of supramolecular synthons may be able

* Spin pairing of the radicals occurs through a $\pi^*-\pi^*$ bonding interaction between the SOMOs of the radicals.

to overcome the dimerisation of the radicals to yield a material that could exhibit magnetic properties.⁶⁶

X-ray diffraction studies on the solid phases of 1,2,3,5-dithiadiazolyl radicals have revealed a number preferred dimer configurations (Scheme 1.4), all of which contain the same $\pi^*-\pi^*$ bonding interaction.⁶⁶ The enthalpy of dimerisation in dithiadiazolyl radicals has been estimated⁷³ at $\sim 35 \text{ kJ mol}^{-1}$ and minor energy differences of about $\sim 5 \text{ kJ mol}^{-1}$ between the dimer configurations have been calculated.⁷⁷



Scheme 1.4: Solid state 1,2,3,5-dithiadiazolyl radical dimer configurations: a) twisted, b) *cis-oid*, c) *trans-oid* (*trans-antarafacial*), d) *trans-cofacial* and e) *orthogonal*. Heteroatoms are not shown for clarity.⁶⁶

Although dithiadiazolyl radicals tend to be diamagnetic in the solid state due to dimerisation, some derivatives have been shown to possess a few paramagnetic sites. This appears to depend on the degree of crystallinity of the sample as well as the strength of the association between monomeric units. EPR studies have shown strongly associated derivatives such as $[\text{C}_6\text{F}_5\text{CN}_2\text{S}_2]_2$ to be EPR-inactive⁷⁴ whereas weakly associated samples such as $[\text{PhCN}_2\text{S}_2]_2$ are EPR-active⁷³ in the solid state. Heating the samples causes the radicals to dissociate increasing the number of paramagnetic sites and thus magnetic susceptibility. On melting, the radicals are strongly paramagnetic forming part of a rare class of liquids known as “paramagnetic liquids”.^{44, 78} Solutions of dithiadiazolyl radicals tend to exhibit paramagnetism due to the dissociation of dimers.⁴⁴

1.5.5) Conductivity and Magnetism in 1,2,3,5-Dithiadiazolyl Radicals

Before the synthesis of the first 1,2,3,5-dithiadiazolyl radical (R = phenyl) in 1980,⁵⁹ Haddon proposed⁷³ that neutral organic π -radicals would be suitable for the design of molecular conductors.⁷⁹ This is because a molecular material must have mobile, unpaired electrons for it to behave as an electrical conductor.⁶⁶ Uniform stacks of neutral organic π -

radicals would result in a half-filled energy band capable of conduction (Figure 1.4a). However, due to dimerisation the radical units, Peierls' distortion often causes these stacks to deviate from uniformity, thus causing a band gap (Figure 1.4b).⁸⁰ Therefore, in order to overcome the distortion observed in organic molecular conductors and to control the arrangement of potential molecular magnets in the solid state, crystal engineering strategies could be employed.⁸¹

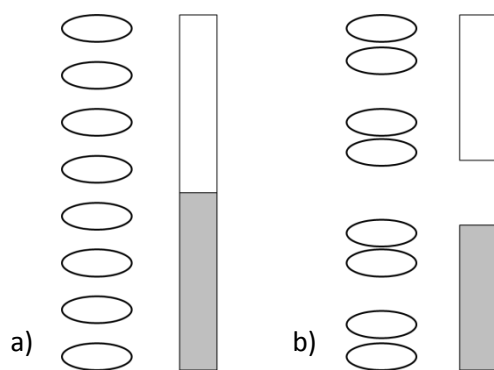


Figure 1.4: Band theory diagram: a) A conduction band would arise from the idealised stacking of π -radicals (indicated by ovals). However, uniform stacks are susceptible to Peierls' distortion which causes b) where dimers form to eliminate the degeneracy of unpaired electrons. Consequently, a band gap is found in the conduction band.⁶⁶

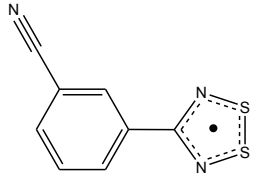
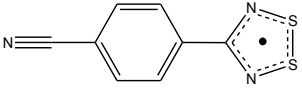
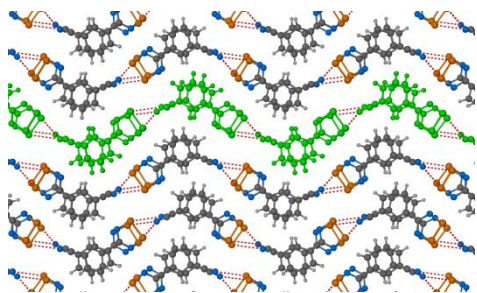
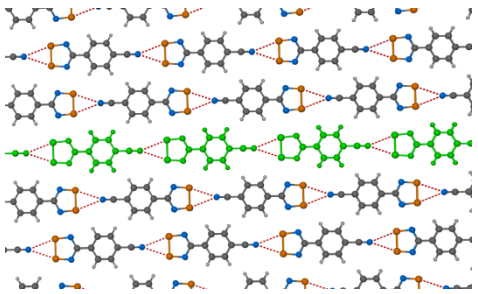
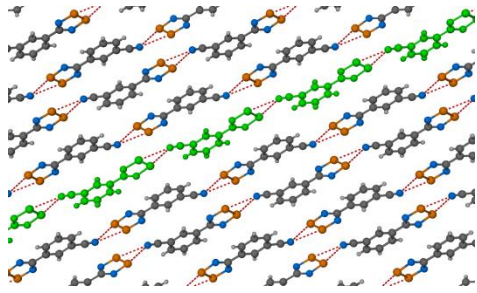
1.6) Crystal Engineering with Dithiadiazolyl Radicals

In a recent article, Haynes reviewed the past and current strategies employed in the design of crystal structures comprised of dithiadiazolyl radicals.⁶⁶ Due to the dimerisation of the radicals in the solid state, it is clear that careful modification of the molecular structure of the dithiadiazolyl radicals is required in order to obtain desired supramolecular structures. To that end, the use of large bulky R-substituents such as adamantyl⁸² to prevent the dimerisation of the radicals was investigated. However, twisted dimers were observed in the solid state structure of 4-adamantyl-1,2,3,5-dithiadiazolyl.

Furthermore, functional groups that could act as structure-directing groups (or synthons) were introduced into the molecular structure. Two of the first examples of this were shown in the synthesis and crystal structure determination of 3'- and 4'-cyanophenyl-1,2,3,5-dithiadiazolyl radicals (Table 1.2).⁵⁰ The cyano functionality is known to be able to form chains of molecules through the $CN\cdots X$ synthon observed in *p*-iodobenzonitrile⁸³ and cyanogen halides.⁸⁴ As predicted, the molecules formed chains in the crystal structure through the $CN\cdots S-S$ synthon. However, neither conductivity nor magnetism was observed in these derivatives as the radicals dimerised. 3'-Cyanophenyl-1,2,3,5-dithiadiazolyl was

found to be polymorphic displaying *cis*-oid and *trans*-antarafacial dimers in the α - and β -phases, respectively. *Cis*-oid dimers were also observed in the 4'-cyanophenyl-1,2,3,5-dithiadiazolyl radical.

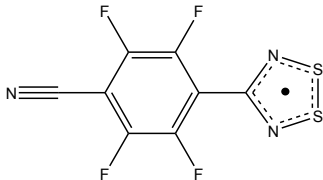
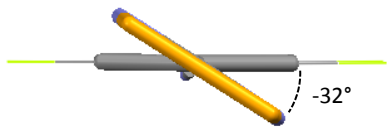
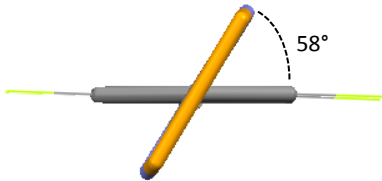
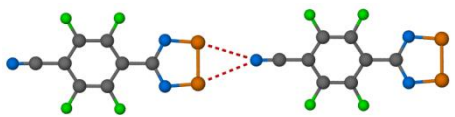
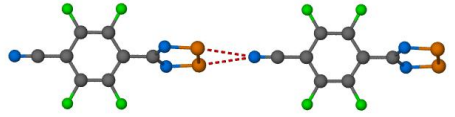
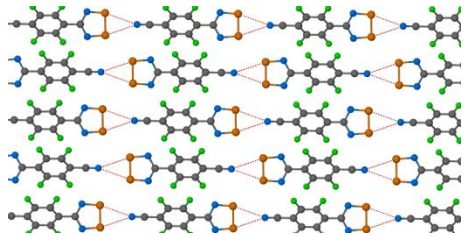
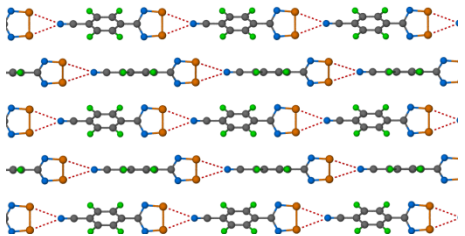
Table 1.2: Comparison of the crystal structures of 3'-cyanophenyl- and 4'-cyanophenyl-1,2,3,5-dithiadiazolyl radicals showing chains (green) of radicals and the CN \cdots S synthon (red dashed lines)

	3'-cyanophenyl-	4'-cyanophenyl-
Molecular Structure		
Crystal Structure	 α -phase	
	 β -phase	

Investigating the CN \cdots S-S synthon further resulted in the isolation of 4'-NCC₆F₄CN₂S₂[•] (Table 1.3).⁸⁵ This polymorphic dithiadiazolyl radical was the first of this class of materials to remain paramagnetic in the solid state. Two factors were identified to which this result is attributed. Firstly, the out-of-plane twist angle of the dithiadiazolyl heterocycle relative to the phenyl ring due to the fluorination of the aryl ring inhibits dimerisation. The α -phase exhibits a torsion angle of -32° while the corresponding angle in the β -phase is 58° . The second factor is the CN \cdots S-S synthon which forms chains of radicals in the solid state. In the α -phase, monomeric radicals pack in antiparallel chains linked by CN \cdots S-S synthons. However, the β -phase exhibits monomeric radicals packing in parallel chains. In addition,

close intermolecular S...N contacts between heterocycles establish an extended three-dimensional network. Consequently, the β -phase exhibits weak ferromagnetism at 36K.⁸⁵

Table 1.3: Crystal structures for the α - and β -phases of 4'-NCC₆F₄CN₂S₂' showing the out-of-plane twist angles (prepared in Mercury⁸⁶⁻⁸⁹), the CN...S synthon and the crystal packing diagram (prepared using POV-Ray).

	α -phase	β -phase
Molecular Structure		
Out-of-plane Twist Angle		
CN...S Synthon		
Packing Diagram		

The successful combination of the dithiadiazolyl twist angle and a favourable structure-directing interaction prompted further study into compounds of the type p -RC₆F₄CN₂S₂, of which some derivatives exhibited magnetic properties.^{90, 91} However, it appears that the combination of these two factors (twist angle and structure-directing interaction) is needed to yield monomeric radicals in the solid state capable of magnetic susceptibility: the absence of either of these factors will be insufficient to overcome the tendency towards dimerisation. Evidence for this is seen in the crystal structure of [C₆F₅CN₂S₂]₂ (Figure 1.5) which was first reported⁹² in 2009 (although the synthesis of the radical was reported as early as 1993).⁹³ Here, the radicals form *cis*-oid dimers despite the large twist angle of 38.5°. Increasing the bulk of the aryl substituent through the incorporation of CF₃ groups in the *ortho*-positions produced monomeric radicals in the solid state.⁹⁴

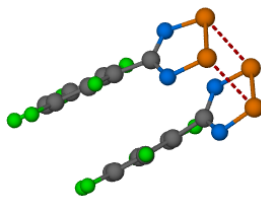


Figure 1.5: Despite the large twist angle of 38.5° in $[\text{C}_6\text{F}_5\text{CN}_2\text{S}_2]_2$, radicals dimerise in the solid state indicating that in order to obtain monomers in the solid state, a large twist angle in conjunction with a structure directing synthon is required.

Another structure-directing interaction observed in the crystal structures of the pyridyl-derived 1,2,3,5-dithiadiazolyl radicals is the $\text{N}_{\text{py}}\cdots\text{S-S}$ synthon (Figure 1.6). Although $[\text{NC}_5\text{F}_4\text{CN}_2\text{S}_2]_2$ forms chains with this synthon, its combination with the fluorine-induced twist was insufficient to inhibit the formation of *cis*-oid dimers in the crystal structure.⁹⁵ The *ortho*-pyridyl-1,2,3,5-dithiadiazolyl radical also shows this synthon.⁹⁶

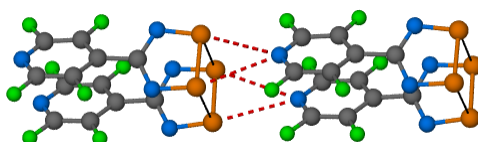


Figure 1.6: Crystal structure of $[\text{NC}_5\text{F}_4\text{CN}_2\text{S}_2]_2$ showing dimers of the radicals ($\text{S}\cdots\text{S}$ thin black lines) linked by the $\text{N}_{\text{py}}\cdots\text{S-S}$ synthon.

The use of co-crystallisation with dithiadiazolyl radicals has recently been investigated as a means to engineer a desirable crystal structure through the introduction of structure-directing synthons on the co-crystal former. The first co-crystal was synthesised by Allen *et al.* in 2009.⁹² The co-crystal, $[\text{C}_6\text{H}_5\text{CN}_2\text{S}_2][\text{C}_6\text{F}_5\text{CN}_2\text{S}_2]$, is prepared by the 1:1 co-sublimation of $[\text{C}_6\text{H}_5\text{CN}_2\text{S}_2]_2$ and $[\text{C}_6\text{F}_5\text{CN}_2\text{S}_2]_2$ and exhibits heterodimers: dimers containing one type of each radical associated together.

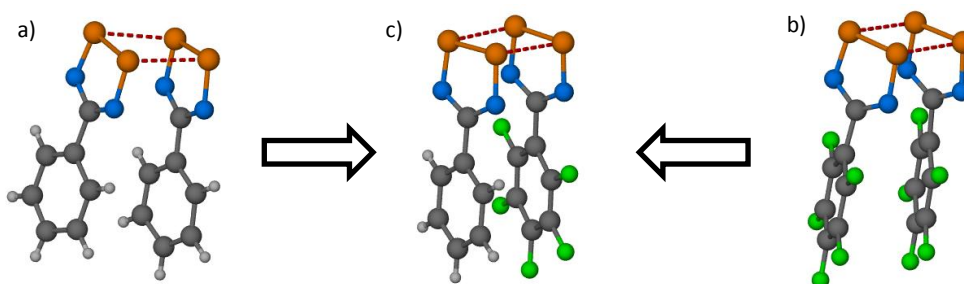


Figure 1.7: Crystal structures of the homodimers of the co-crystal formers: a) $[\text{PhCN}_2\text{S}_2]_2$ and b) $[\text{C}_6\text{F}_5\text{CN}_2\text{S}_2]_2$, and c) the co-crystal formed by co-sublimation of the these two dithiadiazolyl radicals.

Subsequent co-crystallisation experiments yielded $[\text{C}_6\text{H}_5\text{CN}_2\text{S}_2][\text{NC}_5\text{F}_4\text{CN}_2\text{S}_2]$.²⁸ Heterodimers are also observed in this structure. Nonetheless, the $\text{N}_{\text{py}}\cdots\text{S-S}$ synthon is

retained in this structure indicating that co-crystallisation could yield promising results through the incorporation of supramolecular synthons on the co-crystal formers.

1.7) Project Aims

This project aimed to investigate co-crystal formation with dithiadiazolyl radicals. Since the discovery of the two dithiadiazolyl co-crystals, co-crystallisation experiments with many combinations of 1,2,3,5-dithiadiazolyl radicals have been attempted. However, novel co-crystals remain elusive. This study aimed to characterise the two known co-crystals completely using differential scanning calorimetry (DSC) and thermogravimetric analysis (TGA). In addition, using the co-crystal formers of the two known co-crystals, alternative synthetic routes (other than sublimation) to prepare co-crystals of 1,2,3,5-dithiadiazolyl radicals were to be investigated. These were to include mechanochemical, melt and solution-state synthetic techniques.

Steps towards synthesising novel 1,2,3,5-dithiadiazolyl radicals containing hydrogen-bonding functional groups were to be investigated in order that they could later be used in co-crystallisation experiments. This would include the attempted synthesis of phenyl-substituted dithiadiazolyl radicals containing one hydroxyl, amino or carboxyl functional group in the *ortho*-, *meta*- or *para*- position of the phenyl ring relative to the dithiadiazolyl heterocycle. Synthetic procedures by Boéré *et al.* and Alange *et al.* were to be investigated on starting nitriles which already contained the desired hydrogen bonding group. The use of protecting groups for the hydrogen bonding moieties was also to be investigated in the synthesis of 1,2,3,5-dithiadiazolyl radicals.

Co-crystallisation with combinations of dithiadiazolyl radicals that have not yet been attempted were to be investigated using sublimation and any alternate synthetic routes resulting from the characterisation of the two known co-crystals.

1.8) References

1. G. R. Desiraju, J. J. Vittal and A. Ramanan, *Crystal Engineering: A Textbook*, World Scientific Publishing, Singapore, 2011.
2. L. Pauling, *The nature of the chemical bond and the structure of molecules and crystals: an introduction to modern structural chemistry*, Cornell University Press, Ithaca, NY, 1960.
3. IUPAC Compendium of Chemical Terminology, 2nd ed. (the "Gold Book"). Compiled by A. D. McNaught and A. Wilkinson. Blackwell Scientific Publications, Oxford (1997). XML on-line corrected version: <http://goldbook.iupac.org> (2006-) created by M. Nic, J. Jirat, B. Kosata;

- updates compiled by A. Jenkins. ISBN 0-9678550-9-8. doi:10.1351/goldbook. Last update: 2011-10-11; version: 2.3.
4. A. I. Kitaigorodskii, *Molecular crystals and molecules*, Academic Press, 1973.
 5. V. Z. Yu and P. M. Zorkii, *Russian Chemical Reviews*, 1989, **58**, 421-440.
 6. C. B. Aakeroy, *Acta Crystallographica Section B-Structural Science*, 1997, **53**, 569-586.
 7. C. Giacovazzo, *Fundamentals of crystallography*, International Union of Crystallography, Oxford University Press, Oxford, 1992.
 8. D. Braga, L. Brammer and N. R. Champness, *CrystEngComm*, 2005, **7**, 1-19.
 9. T. S. Moore and T. F. Winmill, *Journal of the Chemical Society, Transactions*, 1912, **101**, 1635-1676.
 10. G. A. Jeffrey and W. Saenger, *Hydrogen bonding in biological structures*, Springer-Verlag, New York, 1994.
 11. T. Steiner, *Angewandte Chemie International Edition*, 2002, **41**, 48-76.
 12. G. R. Desiraju, *Angewandte Chemie International Edition*, 2011, **50**, 52-59.
 13. J. W. Steed and J. L. Atwood, *Supramolecular chemistry*, Wiley, New York, 2000.
 14. F. Guthrie, *Journal of the Chemical Society*, 1863, **16**, 239-244.
 15. J.-M. Dumas, L. Gomel and M. Guerin, in *The Chemistry of Functional Groups, Supplement D*, Wiley, New York, 1983, 985-1020.
 16. P. Metrangolo, H. Neukirch, T. Pilati and G. Resnati, *Accounts of Chemical Research*, 2005, **38**, 386-395.
 17. B. K. Saha, A. Nangia and M. Jaskolski, *CrystEngComm*, 2005, **7**, 355-358.
 18. O. Hassel, *Science*, 1970, 497-502.
 19. R. F. Mould, *British Journal of Radiology*, 1995, **68**, 1145-1176.
 20. W. Friedrich, P. Knipping and M. von Laue, *Abhandlungen der Bayerische Akademie der Wissenschaften, Mathematisch-Physikalische Klasse*, 1912, 303.
 21. J. Bernstein, *Journal of Physics D: Applied Physics*, 1993, **26**, B66.
 22. J. W. Steed, D. R. Turner and K. J. Wallace, *Core concepts in supramolecular chemistry and nanochemistry*, John Wiley, Chichester, 2007.
 23. G. R. Desiraju, *Angewandte Chemie International Edition in English*, 1995, **34**, 2311-2327.
 24. E. J. Corey, *Pure and Applied Chemistry*, 1967, **14**, 19-38.
 25. J. H. Williams, J. K. Cockcroft and A. N. Fitch, *Angewandte Chemie International Edition in English*, 1992, **31**, 1655-1657.
 26. S. Bacchi, M. Benaglia, F. Cozzi, F. Demartin, G. Filippini and A. Gavezzotti, *Chemistry – A European Journal*, 2006, **12**, 3538-3546.
 27. J. Vrbancich and G. L. D. Ritchie, *Journal of the Chemical Society, Faraday Transactions 2: Molecular and Chemical Physics*, 1980, **76**, 648-659.
 28. D. A. Haynes, *Unpublished results*, 2010.
 29. D. Jiles, *Introduction to magnetism and magnetic materials*, Chapman and Hall, London, 1991.
 30. P. Curie, *Comptes rendus hebdomadaires des séances de l'Académie des Sciences*, 1906, **143**, 1136.
 31. D. J. Craik, *Magnetism: principles and applications*, Wiley, Chichester, 1995.
 32. E. Coronado, *Molecular magnetism: from molecular assemblies to the devices*, Kluwer Academic, Dordrecht, 1996.
 33. J. S. Miller and A. J. Epstein, *MRS Bulletin*, 2000, **25**, 21-30.
 34. J. A. Crayston, J. N. Devine and J. C. Walton, *Tetrahedron*, 2000, **56**, 7829-7857.
 35. I. Yamazaki, *Free Radical Biology and Medicine*, 1987, **3**, 397-404.
 36. B. Halliwell and J. M. C. Gutteridge, *Free radicals in biology and medicine*, Clarendon Press, 1989.
 37. M. Gomberg, *Journal of the American Chemical Society*, 1900, **22**, 752-757.
 38. J. S. Miller, *Advanced Materials*, 1994, **6**, 322-324.

39. A. J. Banister and I. B. Gorrell, *Advanced Materials*, 1998, **10**, 1415-1429.
40. M. M. Labes, P. Love and L. F. Nichols, *Chemical Reviews*, 1979, **79**, 1-15.
41. J. E. Huheey, E. A. Keiter and R. L. Keiter, *Inorganic chemistry: principles of structure and reactivity*, Pearson Education, New York, 2000.
42. R. T. Oakley, in *Progress in Inorganic Chemistry*, John Wiley & Sons, Inc., 2007, Hoboken, NJ, 299-391.
43. T. Chivers and I. Manners, *Inorganic rings and polymers of the p-block elements: from fundamentals to applications*, Royal Society of Chemistry, Cambridge, 2009.
44. J. M. Rawson, A. J. Banister and I. Lavender, *Advances in Heterocyclic Chemistry*, Vol 62, 1995, **62**, 137-247.
45. E. Demarcay, *Comptes rendus hebdomadaires des séances de l'Académie des Sciences*, 1880, **91**, 854.
46. A. J. Banister, H. G. Clarke, I. Rayment and H. M. M. Shearer, *Inorganic and Nuclear Chemistry Letters*, 1974, **10**, 647-654.
47. P. D. B. Belluz, A. W. Cordes, E. M. Kristof, P. V. Kristof, S. W. Liblong and R. T. Oakley, *Journal of the American Chemical Society*, 1989, **111**, 9276-9278.
48. M. P. Andrews, A. W. Cordes, D. C. Douglass, R. M. Fleming, S. H. Glarum, R. C. Haddon, P. Marsh, R. T. Oakley and T. T. M. Palstra, *Journal of the American Chemical Society*, 1991, **113**, 3559-3568.
49. A. W. Cordes, R. C. Haddon, R. T. Oakley, L. F. Schneemeyer, J. V. Waszczak, K. M. Young and N. M. Zimmerman, *Journal of the American Chemical Society*, 1991, **113**, 582-588.
50. A. W. Cordes, R. C. Haddon, R. G. Hicks, R. T. Oakley and T. T. M. Palstra, *Inorganic Chemistry*, 1992, **31**, 1802-1808.
51. A. W. Cordes, C. D. Bryan, W. M. Davis, R. H. de Laat, S. H. Glarum, J. D. Goddard, R. C. Haddon, R. G. Hicks and D. K. Kennepohl, *Journal of the American Chemical Society*, 1993, **115**, 7232-7239.
52. A. W. Cordes, R. C. Haddon, R. G. Hicks, D. K. Kennepohl, R. T. Oakley, T. T. M. Palstra, L. F. Schneemeyer, S. R. Scott and J. V. Waszczak, *Chemistry of Materials*, 1993, **5**, 820-825.
53. N. Feeder, R. J. Less, J. M. Rawson, P. Oliete and F. Palacio, *Chemical Communications*, 2000, 2449-2450.
54. J. F. Britten, O. P. Clements, A. W. Cordes, R. C. Haddon, R. T. Oakley and J. F. Richardson, *Inorganic Chemistry*, 2001, **40**, 6820-6824.
55. G. G. Alange, A. J. Banister, B. Bell and P. W. Millen, *Inorganic and Nuclear Chemistry Letters*, 1977, **13**, 143-144.
56. G. G. Alange, A. J. Banister, B. Bell and P. W. Millen, *Journal of the Chemical Society, Perkin Transactions 1*, 1979, 1192-1194.
57. A. J. Banister, N. R. M. Smith and R. G. Hey, *Journal of the Chemical Society, Perkin Transactions 1*, 1983, 1181-1186.
58. R. T. Boéré, R. T. Oakley and R. W. Reed, *Journal of Organometallic Chemistry*, 1987, **331**, 161-167.
59. A. Vegas, A. Perez-Salazar, A. J. Banister and R. G. Hey, *Journal of the Chemical Society, Dalton Transactions*, 1980, 1812-1815.
60. L. N. Markovski, O. M. Polumbrik, V. S. Talanov and Y. G. Shermolovich, *Tetrahedron Letters*, 1982, **23**, 761-762.
61. G. K. MacLean, J. Passmore, M. N. S. Rao, M. J. Schriver, P. S. White, D. Bethell, R. S. Pilkington and L. H. Sutcliffe, *Journal of the Chemical Society, Dalton Transactions*, 1985, 1405-1416.
62. R. T. Boere, R. T. Oakley, R. W. Reed and N. P. C. Westwood, *Journal of the American Chemical Society*, 1989, **111**, 1180-1185.
63. A. W. Cordes, C. M. Chamchoumis, R. G. Hicks, R. T. Oakley, K. M. Young and R. C. Haddon, *Canadian Journal of Chemistry*, 1992, **70**, 919-925.

-
64. A. W. Cordes, R. C. Haddon, R. G. Hicks, R. T. Oakley and T. T. M. Palstra, *Inorganic Chemistry*, 1992, **31**, 1802-1808.
 65. A. J. Banister, M. I. Hansford, Z. V. Hauptman, S. T. Wait and W. Clegg, *Journal of the Chemical Society, Dalton Transactions*, 1989, 1705-1713.
 66. D. A. Haynes, *CrystEngComm*, 2011, **13**, 4793-4805.
 67. N. Adamson, A. J. Banister, I. B. Gorrell, A. W. Luke and J. M. Rawson, *Journal of the Chemical Society, Chemical Communications*, 1993, 919-921.
 68. A. J. Banister, W. Clegg, Z. V. Hauptman, A. W. Luke and S. T. Wait, *Journal of the Chemical Society, Chemical Communications*, 1989, 351-352.
 69. A. J. Banister, M. I. Hansford, Z. V. Hauptman, A. W. Luke, S. T. Wait, W. Clegg and K. A. Jorgensen, *Journal of the Chemical Society, Dalton Transactions*, 1990, 2793-2802.
 70. D. L. Pavia, G. M. Lampman, G. S. Kriz and J. R. Vyvyan, *Introduction to Spectroscopy*, 4th edn., Brooks/Cole, 2009.
 71. M. C. R. Symons, *Electron Spin Resonance*, Royal Society of Chemistry, London, 1988.
 72. K. F. Preston, J. P. Charland and L. H. Sutcliffe, *Canadian Journal of Chemistry*, 1988, **66**, 1299-1303.
 73. S. A. Fairhurst, K. M. Johnson, L. H. Sutcliffe, K. F. Preston, A. J. Banister, Z. V. Hauptman and J. Passmore, *Journal of the Chemical Society, Dalton Transactions*, 1986, 1465-1472.
 74. S. A. Fairhurst, L. H. Sutcliffe, K. F. Preston, A. J. Banister, A. S. Partington, J. M. Rawson, J. Passmore and M. J. Schriver, *Magnetic Resonance in Chemistry*, 1993, **31**, 1027-1030.
 75. R. T. Boéré and K. H. Mook, *Journal of the American Chemical Society*, 1995, **117**, 4755-4760.
 76. R. T. Boéré and T. L. Roemmele, *Coordination Chemistry Reviews*, 2000, **210**, 369-445.
 77. H.-U. Hofs, J. W. Bats, R. Gleiter, G. Hartmann, R. Mews, M. Eckertmaksic, H. Oberhammer and G. M. Sheldrick, *Chemische Berichte-Recueil*, 1985, **118**, 3781-3804.
 78. W. V. F. Brooks, N. Burford, J. Passmore, M. J. Schriver and L. H. Sutcliffe, *Journal of the Chemical Society, Chemical Communications*, 1987, 69-71.
 79. R. C. Haddon, *Nature*, 1975, **256**, 394-396.
 80. R. E. Peierls, *Quantum theory of solids*, Clarendon Press, Oxford, 1955.
 81. A. W. Cordes, R. C. Haddon and R. T. Oakley, in *The Chemistry of Inorganic Ring Systems*, ed. R. Steudel, Elsevier, Amsterdam, 1992, vol. 14, p. 295.
 82. J. N. Bridson, S. B. Copp, M. J. Schriver, S. G. Zhu and M. J. Zaworotko, *Canadian Journal of Chemistry*, 1994, **72**, 1143-1153.
 83. E. O. Schlemper and D. Britton, *Acta Crystallographica*, 1965, **18**, 419-424.
 84. R. B. Heiart and G. B. Carpenter, *Acta Crystallographica*, 1956, **9**, 889-895.
 85. A. J. Banister, N. Bricklebank, I. Lavender, J. M. Rawson, C. I. Gregory, B. K. Tanner, W. Clegg, M. R. J. Elsegood and F. Palacio, *Angewandte Chemie International Edition in English*, 1996, **35**, 2533-2535.
 86. R. Taylor and C. F. Macrae, *Acta Crystallographica Section B*, 2001, **57**, 815-827.
 87. I. J. Bruno, J. C. Cole, P. R. Edgington, M. Kessler, C. F. Macrae, P. McCabe, J. Pearson and R. Taylor, *Acta Crystallographica Section B*, 2002, **58**, 389-397.
 88. C. F. Macrae, P. R. Edgington, P. McCabe, E. Pidcock, G. P. Shields, R. Taylor, M. Towler and J. van de Streek, *Journal of Applied Crystallography*, 2006, **39**, 453-457.
 89. C. F. Macrae, I. J. Bruno, J. A. Chisholm, P. R. Edgington, P. McCabe, E. Pidcock, L. Rodriguez-Monge, R. Taylor, J. van de Streek and P. A. Wood, *Journal of Applied Crystallography*, 2008, **41**, 466-470.
 90. G. Antorrena, J. E. Davies, M. Hartley, F. Palacio, J. M. Rawson, J. N. B. Smith and A. Steiner, *Chemical Communications*, 1999, 1393-1394.
 91. A. Alberola, R. J. Less, C. M. Pask, J. M. Rawson, F. Palacio, P. Oliete, C. Paulsen, A. Yamaguchi, R. D. Farley and D. M. Murphy, *Angewandte Chemie International Edition in English*, 2003, **42**, 4782-4785.
-

92. C. Allen, D. A. Haynes, C. M. Pask and J. M. Rawson, *CrystEngComm*, 2009, **11**, 2048-2050.
93. C. M. Aherne, A. J. Banister, I. B. Gorrell, M. I. Hansford, Z. V. Hauptman, A. W. Luke and J. M. Rawson, *Journal of the Chemical Society, Dalton Transactions*, 1993, 967-972.
94. A. Alberola, C. S. Clarke, D. A. Haynes, S. I. Pascu and J. M. Rawson, *Chemical Communications*, 2005, 4726-4728.
95. A. J. Banister, N. Bricklebank, W. Clegg, M. R. J. Elsegood, C. I. Gregory, I. Lavender, J. M. Rawson and B. K. Tanner, 1995, CSD refcode ZADVAB.
96. N. G. R. Hearn, K. E. Preuss, J. F. Richardson and S. Bin-Salamon, *Journal of the American Chemical Society*, 2004, **126**, 9942-9943.

Chapter 2: Dithiadiazolyl Co-crystal Characterisation & Synthetic Investigation

2.1) Definition of a Co-crystal

A co-crystal can be defined as “a multi-component molecular crystal.”¹ However, the molecular components of a co-crystal must be electrically neutral otherwise the crystal is considered a salt.

In general, the preparation of co-crystals is not necessarily straightforward. For a multi-component system to form, the intermolecular interactions between its constituent parts need to be stronger and more thermodynamically favourable than the interactions found in the pure compounds (co-crystal formers).² Furthermore, considering the different sizes and shapes of molecules, it is understandable that similar molecules would prefer to associate together in a three-dimensional solid rather than forming structures with dissimilarly shaped molecules.² Therefore, the design of co-crystals considers the “structural fit” of the co-crystal formers as well as the use of supramolecular synthons to stabilise the structure.^{3,4}

In this study, the synthesis of co-crystals with molecules containing 1,2,3,5-dithiadiazolyl radical moieties is of interest. Co-crystallisation may provide a means to overcome the dimerisation of the radicals in the solid state, leading to the potential application of these materials as organic conductors or magnets. In addition, alternative methods by which co-crystals with 1,2,3,5-dithiadiazolyl radicals can be prepared are of interest for the synthesis of novel co-crystals with 1,2,3,5-dithiadiazolyl radicals.

2.2) Co-crystal Growth Methods

Co-crystals, originally called binary compounds or complexes, were first identified in the late 1800s by melt crystallisation.^{5, 6} Currently, common methods of co-crystal preparation include solution crystallisation: single crystal growth *via* the evaporation of a solution containing the co-crystal formers,^{3, 7-9} and mechanochemical synthesis: co-crystal preparation *via* the solid-state or “solvent-drop” mechanical grinding of a mixture of the co-crystal formers.¹⁰⁻¹² Solution crystallisation is the preferred method to grow single crystals for structure analysis, although the co-crystal formers must have similar solubilities in the solvent used, otherwise the least soluble component will precipitate out of solution.^{2, 13} However, the use of layered solvent systems could provide a means to overcome this limitation.¹⁴ Mechanochemical grinding to produce co-crystals offers the benefits that it is “green” due to the use of little to no solvent, and provides nearly quantitative yields of

similarly-sized particles suitable for powder X-ray diffraction (PXRD).¹² Furthermore, it has been shown to be effective in screening the potential of co-crystal formation between different combinations of co-crystal formers.¹¹

2.3) Benefits of Co-crystallisation

The benefit of co-crystallisation is that it offers the means to refine the properties of the crystal through the use of one or more co-crystal formers.^{2, 15} Good examples of this come from the pharmaceutical industry where the solubility, and consequently the release, of a drug into a biological system can be controlled and optimised for the best efficacy.^{16, 17} In the case of 1,2,3,5-dithiadiazolyl radicals, polymorphs may exhibit the desired magnetic properties that are not present in the other phases of the same material. For example, the β -phase of [*p*-(CN)C₆F₄CN₂S₂] exhibits paramagnetism whilst the α -phase does not.^{18, 19}

2.4) Known Co-crystals of 1,2,3,5-Dithiadiazolyl Radicals

The co-crystallisation of dithiadiazolyl radicals has recently been investigated as a possible method to prepare purely organic molecular magnets.²⁰ By introducing suitable supramolecular synthons *via* a co-crystal former that could overcome the dimerisation of these radicals in the solid state, one might be able to engineer a crystal structure with the potential to exhibit magnetic properties.

The first known co-crystal with a 1,2,3,5-dithiadiazolyl radical was published in 1989 by Banister *et al.*²¹ after investigating the dehalogenation properties of 4-phenyl-1,2,3,5-dithiadiazolyl, [**1**].* This co-crystal was formed by the reductive ring contraction of [S₄N₃]Cl with [**1**]. Thus, the co-crystal is comprised of heterodimers of [**1**] and isoelectronic [S₃N₂]Cl. However, due to the fact that it forms mixed charge dimers in the solid state, its magnetic and conducting properties are limited.

The first co-crystal comprising only 1,2,3,5-dithiadiazolyl radicals was reported in 2009 by Allen *et al.*²⁰ This co-crystal consists of heterodimers of the phenyl-, [**1**], and 4-perfluorophenyl-1,2,3,5-dithiadiazolyl, [**2**], radicals (Figure 2.1). The co-crystal of these two radicals will be denoted as [**1-2**].

* A note on numbering of compounds in this chapter: the pure phenyl-, perfluorophenyl- and 4'-perfluoropyridyl-1,2,3,5-dithiadiazolyl radicals are denoted as [**1**], [**2**] and [**3**]. The co-crystals formed between [**1**] and [**2**], and [**1**] and [**3**] are denoted as [**1-2**] and [**1-3**], respectively. For a list of compounds and their numbers see Appendix B, Section B.1.

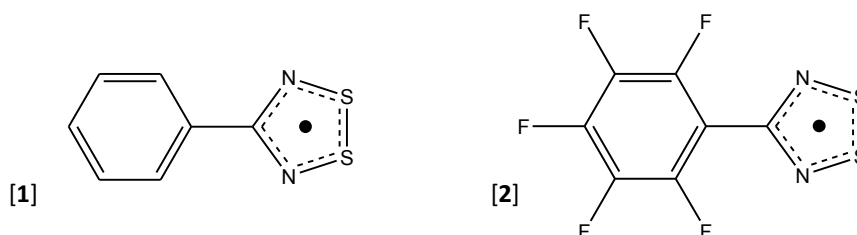


Figure 2.1: Molecular structures of 4-phenyl-1,2,3,5-dithiadiazolyl, [1] (left) and 4-perfluorophenyl-1,2,3,5-dithiadiazolyl, [2] (right): the constituents of co-crystal [1-2].

The design of co-crystal [1-2] arose from a hypothesis that using a supramolecular synthon²² such as the aryl-perfluoroaryl interaction[†] would cause stacking of the dithiadiazolyl radicals in the crystal structure. Uniform stacking of 1,2,3,5-dithiadiazolyl radicals would lead to a half-filled band gap, thus allowing conduction. For bulk magnetic ordering to be exhibited in a molecular material such as [1-2], it needs to have both unpaired electrons and a magnetic exchange pathway.²³ Therefore, in addition to stacking, it was hoped that the large fluorine atoms in the positions *ortho*- to the dithiadiazolyl moiety would force the dithiadiazolyl heterocycle to twist out-of-plane with the phenyl ring and thus inhibit dimerisation of the radicals. Bulk magnetic ordering could be observed if the radicals exist as monomers in the solid state and a magnetic exchange pathway is present through close intermolecular contacts. However, in the crystal structure of [1-2], the radicals dimerised through S...S contacts (Figure 2.2).²⁰ A number of important interdimer contacts were identified that prevented the stacking of radicals. These contacts include interdimer S...N, S...C and S...Ar interactions.

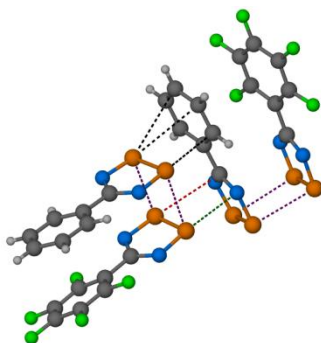


Figure 2.2: Crystal structure of [1-2]²⁰ showing intermolecular contacts: intradimer S...S (purple) and intermolecular S...Ar (black), S...N (green) and S...C (red) contacts inhibit the stacking of the co-crystal formers in the solid state.

[†] This supramolecular synthon was discussed in Chapter 1, Section 1.2.

Further research into co-crystallisation of dithiadiazolyl radicals yielded co-crystal [1-3] comprising heterodimers of the phenyl-, [1], and 4-(4'-perfluoropyridyl)-1,2,3,5-dithiadiazolyl, [3], radicals (Figure 2.3).²⁴

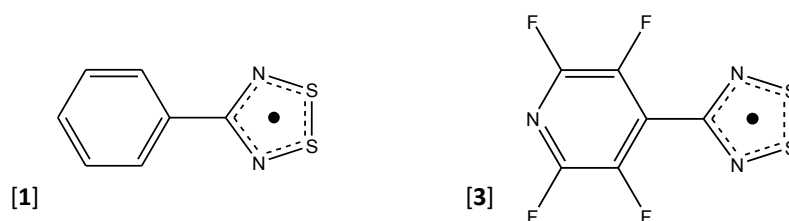


Figure 2.3: Molecular structures of 4-phenyl-1,2,3,5-dithiadiazolyl, [1] (left) and 4-(4'-perfluoropyridyl)-1,2,3,5-dithiadiazolyl, [3] (right): the constituents of co-crystal [1-3].

The design concept of [1-3] was similar to that of [1-2]: of a perfluoroaryl-substituted dithiadiazolyl radical was used as a co-crystal former with [1], to induce stacking of the radicals and inhibit dimerisation through the substituent-induced out-of-plane twist of the dithiadiazolyl and perfluoroaryl rings. In addition, it was hoped that using the perfluoropyridyl substituent would introduce a useful supramolecular synthon ($N_{py}\cdots S-S$) that would cause the radicals to form chains in the structure.

Despite this design strategy, the radicals dimerised in the crystal structure (Figure 2.4)²⁴ but the $N_{py}\cdots S-S$ synthon was robust enough to be present in the co-crystal structure.

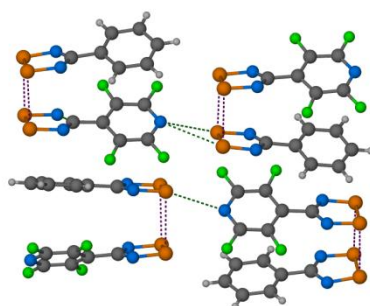


Figure 2.4: Crystal structure of [1-3]²⁴ showing in the intermolecular interactions: intramolecular S...S (purple) and intermolecular $N_{py}\cdots S$ (green) contacts.

From these results, it appears that the introduction of a structure directing supramolecular synthon on a co-crystal former is able to cause a change in the crystal structure. This can be likened to the use of supramolecular synthons in homomeric crystals of 1,2,3,5-dithiadiazolyls where structure directing synthons have caused interesting crystal structures to form: for example, the cyanophenyl-substituted derivatives which show dimeric (3'- and 4'-cyanophenyl)-²⁵ and monomeric (4'-cyanoperfluorophenyl)-¹⁹ 1,2,3,5-

dithiadiazolyl radicals in the solid state. Therefore, co-crystallisation has potential as a strategy to create a molecular magnet with dithiadiazolyl radicals.

However, despite the success of preparing these two co-crystals, the design of co-crystals using 1,2,3,5-dithiadiazolyl radicals is not straightforward. It appears that these radicals co-crystallise very selectively. Thus far, **[1-2]** and **[1-3]** are the only known co-crystals, despite attempts using many other combinations of 1,2,3,5-dithiadiazolyl radicals.²⁴ This research aimed to characterise these two co-crystals using differential scanning calorimetry (DSC) and thermogravimetric analysis (TGA) in order to determine whether any polymorphs of these co-crystals exist. In addition, alternate synthetic routes to prepare co-crystals of 1,2,3,5-dithiadiazolyl radicals using **[1]**, **[2]** and **[3]** as positive test materials to form **[1-2]** and **[1-3]** were to be investigated. This included the investigation of mechanochemical, melt and solution-state crystallisation techniques.

2.5) Synthesis of the Known Co-crystals

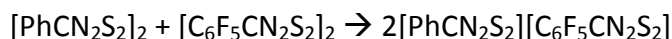
The two co-crystals, **[1-2]** and **[1-3]**, are both synthesised by subliming a 1:1 mixture of the pure radicals together under reduced pressure.^{20, 24} Sublimation is a method often used to purify low molecular weight organic compounds and organometallic complexes which have a sufficiently high vapour pressure,²⁶ but, growing co-crystals by sublimation for crystallographic purposes is quite rare.

In the case of 1,2,3,5-dithiadiazolyl radical co-crystals, the association mechanism of the two pure radicals to form the heterodimer is unknown. However, in order to form heterodimers, the homodimers must be dissociated in the vapour phase and a favourable interaction must occur between the co-crystal formers just before or at the moment of nucleation.

It is quite possible that in the case of **[1-2]** and **[1-3]**, that the aryl-perfluoroaryl interaction (discussed in Chapter 1) was sufficient to cause a favourable interaction between the co-crystal formers. However, this interaction was not strong enough to form uniform stacks of the radicals in the crystal structure. Thus, many other combinations (not necessarily using only 1,2,3,5-dithiadiazolyl radicals) were attempted using the same intermolecular interaction.²⁴ However, co-crystallisation using the aryl-perfluoroaryl interaction and 1,2,3,5-dithiadiazolyl radicals appears to be much more selective than first anticipated.

The temperature of sublimation to form the co-crystals was considered as a means to explain why the combinations of [1-2] and [1-3] had worked and others had not. Did a difference in the sublimation temperatures of the pure radicals affect whether a co-crystal was formed or not? The sublimation temperatures of [1], [2] and [3] are approximately 90 °C, 40 °C and 100 °C at a pressure of 10^{-1} Torr. Here we see a large difference between the sublimation temperatures of [1] and [2], whereas there is a much smaller difference between [1] and [3]. Thus, from this data, it would seem that the differing sublimation temperatures do not affect the growth of the co-crystal. In other words, neither a large, nor a small, difference in sublimation temperatures affects the formation of a co-crystal.

In order to explain the observation that heterodimers form in the solid state, Rawson performed some single point energy calculations on the dimer structures determined by X-ray diffraction of the pure co-crystal formers, [1] and [2], and the co-crystal [1-2].²⁷ The B3LYP/6-31G*+ level of theory was used with a closed shell singlet configuration within Jaguar.²⁸ The thermodynamic calculations were zero point energy corrected and determined at 298.15 K. For the reaction:



the thermodynamic parameters are shown in Table 2.1 showing that the forward reaction is favoured, albeit by a small $\Delta G_{\text{rxn}}(298 \text{ K}) = -24 \text{ kJ mol}^{-1}$. Because the enthalpy is negative and the entropy is positive, the forward reaction should be favoured for a broad range of temperatures assuming the enthalpies and entropies are not significantly temperature dependent. In addition, the entropy term appears to be the dominant term (although not by much), implying that the forward reaction is driven by entropy and not enthalpy.

Table 2.1: Thermodynamic Parameters for $[\text{PhCN}_2\text{S}_2]_2$, $[\text{C}_6\text{F}_5\text{CN}_2\text{S}_2]_2$ and $[\text{PhCN}_2\text{S}_2][\text{C}_6\text{F}_5\text{CN}_2\text{S}_2]$

Compound	ΔH (Hartree)	ΔG (Hartree)	$T\Delta S$ (Hartree)
$[\text{PhCN}_2\text{S}_2]_2$	-2350.819891	-2350.883403	0.063512
$[\text{C}_6\text{F}_5\text{CN}_2\text{S}_2]_2$	-3343.365223	-3343.449343	0.084120
$[\text{PhCN}_2\text{S}_2][\text{C}_6\text{F}_5\text{CN}_2\text{S}_2]$	-2847.094468	-2847.170952	0.076484
Δ_{rxn} (Hartree)	-0.0038222	-0.009158	0.005336
Δ_{rxn} (kJ/mol)	-10.0347	-24.0443	14.00967

Despite these interesting results, it is not known whether this favourable association of radical co-crystal formers in the gas phase is due to the aryl-perfluoroaryl interaction or a strong spin-pairing interaction. However, it does offer a possible explanation for the preferential formation of heterodimers over homodimers of 1,2,3,5-dithiadiazolyl radicals in the solid state.

2.6) Co-crystal Analysis

2.6.1) Characterisation by Electron Paramagnetic Resonance (EPR)

1,2,3,5-Dithiadiazolyl radicals are characterised by a quintet in the EPR spectrum near a g -value of 2.01.²⁹ The EPR spectra of [1], [2] and [3] are shown in Figure 2.5.

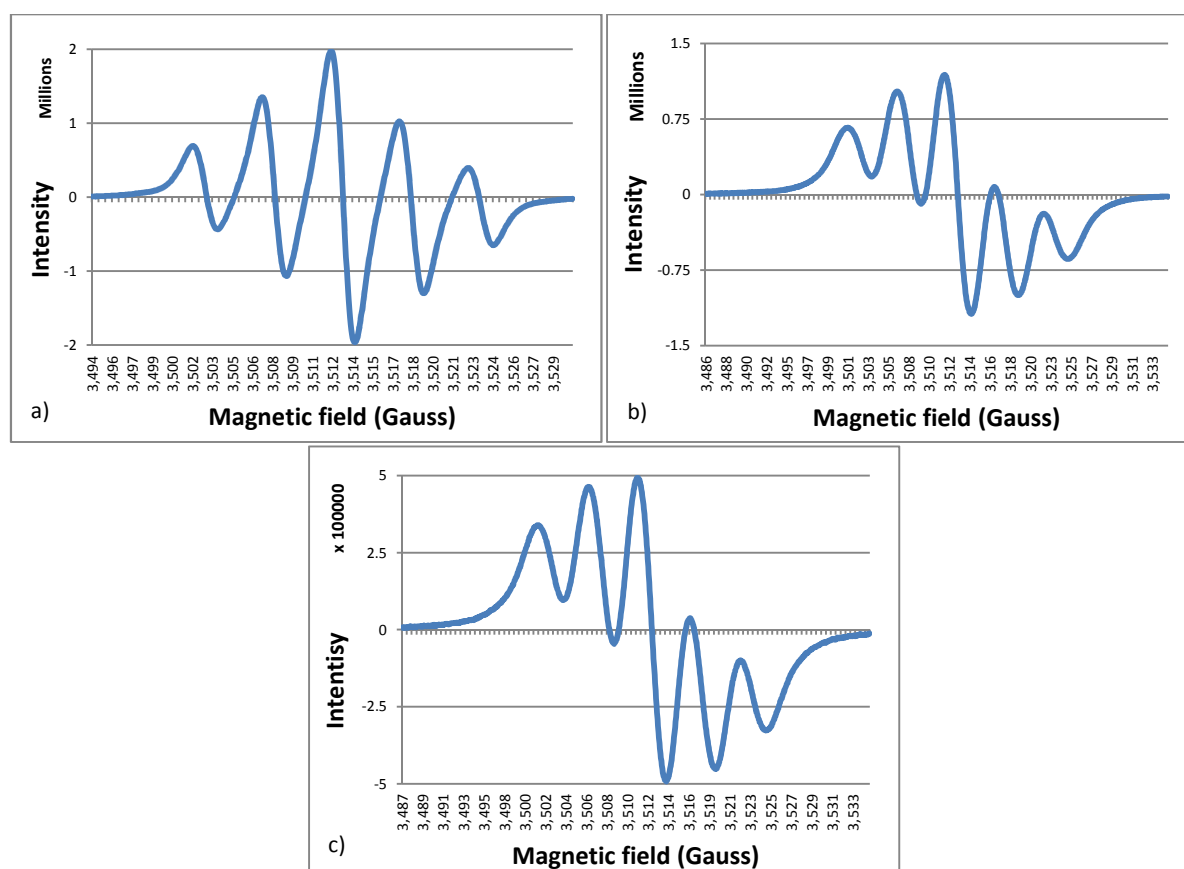


Figure 2.5: EPR spectra (298 K, CH_2Cl_2) of a) [1] ($g = 2.007$, $a_N = 5.0$ G), b) [2] ($g = 2.010$, $a_N = 4.9$ G) and c) [3] ($g = 2.011$, $a_N = 5.0$ G).

The lop-sidedness of the spectra of [2] and [3] is attributed to a high concentration of the radicals in solution. In addition, if the power of the instrument's microwave frequency during acquisition is too high, the radical electrons do not have enough time to return to their ground state configuration before being excited again. Therefore, the Boltzmann distribution of the electrons is not representative resulting in the skewed spectra.

Nonetheless, the characteristic quintuplet may be seen confirming the presence of the radical species.

The EPR spectra of the two co-crystals in solution are shown in Figure 2.6.

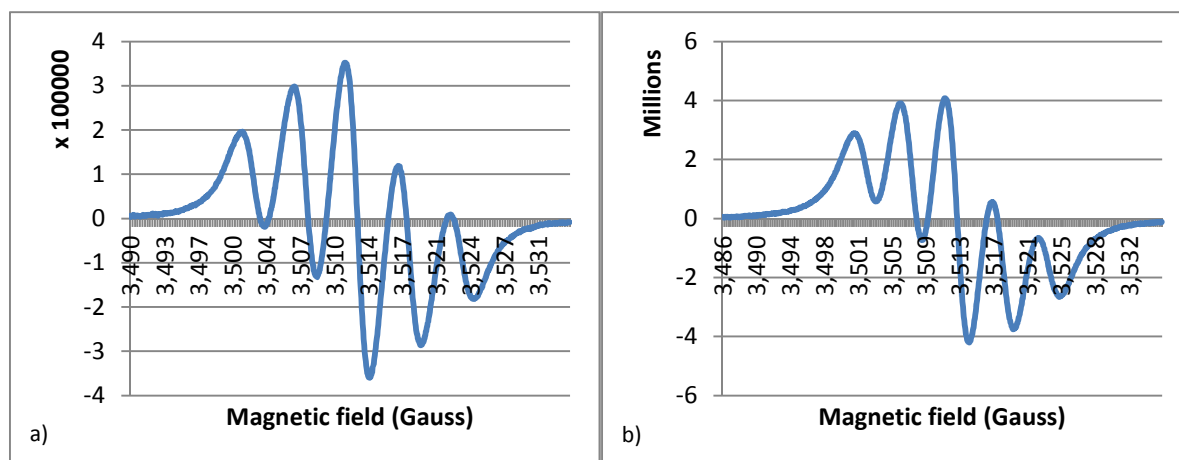


Figure 2.6: EPR spectra (298 K, CH_2Cl_2) of the co-crystals: a) [1-2] ($g = 2.010$, $a_N = 5.0$ G) and b) [1-3] ($g = 2.010$, $a_N = 4.9$ G)

Due to the co-crystals containing two different radical species, one might expect some splitting to occur in the quintuplet. However, considering that one may vary the group attached to the dithiadiazolyl ring without affecting its electronic structure substantially, it is not surprising that their EPR signals lie on top of one another. Therefore, each co-crystal is represented by one quintuplet which confirms that the dithiadiazolyl radicals exist as monomers in solution.

2.6.2) Co-crystal yields by sublimation

Due to the difficulty of forming co-crystals with dithiadiazolyl radicals by sublimation, the question of how much co-crystal actually forms when subliming a physical mixture of the co-crystal formers arose. Powder X-ray diffraction (PXRD) was used to determine the phase purity of the co-crystal formers ([1], [2] and [3]) as well as the bulk sublimed material from the respective sublimation experiments to form co-crystals [1-2] and [1-3]. If the conversion to the co-crystal is quantitative, no reflections in the powder pattern would correspond to the pure co-crystal formers. However, if the conversion is less than quantitative, reflections corresponding to both co-crystal formers would be present in addition to the co-crystal.

2.6.2.1) Phase purity of the co-crystal formers

The powder patterns of each of the co-crystal formers [1], [2] and [3] (Figure 2.7) were compared to their respective calculated powder patterns. In each case, the sample of

sublimed crystals compares well with the calculated pattern indicating that the radicals are phase pure.

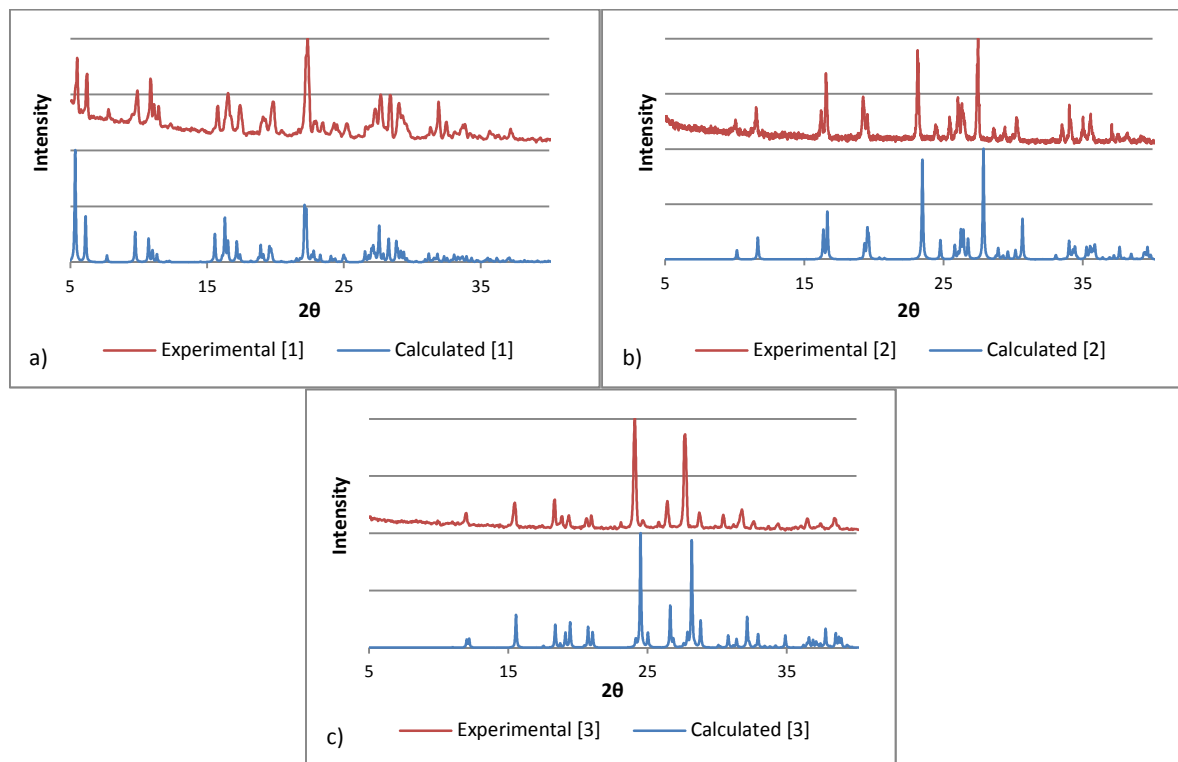


Figure 2.7: Experimental powder patterns (red) of a) [1], b) [2] and c) [3] compared with the patterns calculated from their respective crystal structures (blue) showing each sample to be phase pure.

2.6.2.2) Percentage conversion

To test the percentage of conversion to co-crystal [1-2] by sublimation, a 1:1 stoichiometric ratio of [1] and [2] was placed in a Schlenk, the bottom of which was placed in an oil bath at 70 °C under reduced pressure. After a few minutes, crystals began to grow on the sides of the Schlenk. Once there was no remaining residue of the radicals in the bottom of the Schlenk, the crystalline material on the sides of the Schlenk was scraped out as quantitatively as possible and ground using a dry glass mortar and pestle. This “bulk” sample was then analysed by PXRD using a zero-background holder. The powder pattern obtained is shown in Figure 2.8 and is compared with the powder patterns of the pure materials calculated from their crystal structures.

The reflections in the powder pattern for the bulk sublimed material correspond to the reflections seen in the calculated co-crystal powder pattern. None of the reflections observed in the sublimed material correspond to those of the pure co-crystal formers. This indicates that the conversion to the co-crystal by sublimation is quantitative.

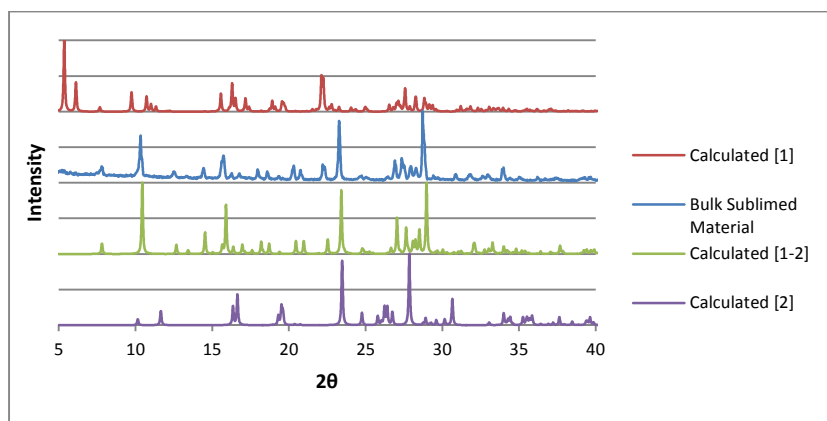


Figure 2.8: Powder pattern of the bulk sublimed material (blue) obtained from the sublimation of [1] and [2] and compared to the calculated patterns of [1] (red), the co-crystal [1-2] (green) and [2] (purple) showing complete conversion of the co-crystal formers to [1-2].

Although the conversion to [1-2] is quantitative, the same may not necessarily be true for [1-3]. Therefore, to test the conversion to [1-3], [1] and [3] were placed in a Schlenk, the bottom of which was placed in a large oil bath under reduced pressure at 80 °C. This sublimation was performed at a higher temperature as the radicals have similar sublimation temperatures near to 100 °C. Similarly, once no residue of the pure co-crystal formers remained in the bottom of the Schlenk, the sublimed residue was scraped out quantitatively and ground using a dry glass mortar and pestle. A powder pattern of this mixture was collected using a zero-background holder. Figure 2.9 shows the collected pattern compared with the calculated patterns of the pure co-crystal formers and the co-crystal for clarity.

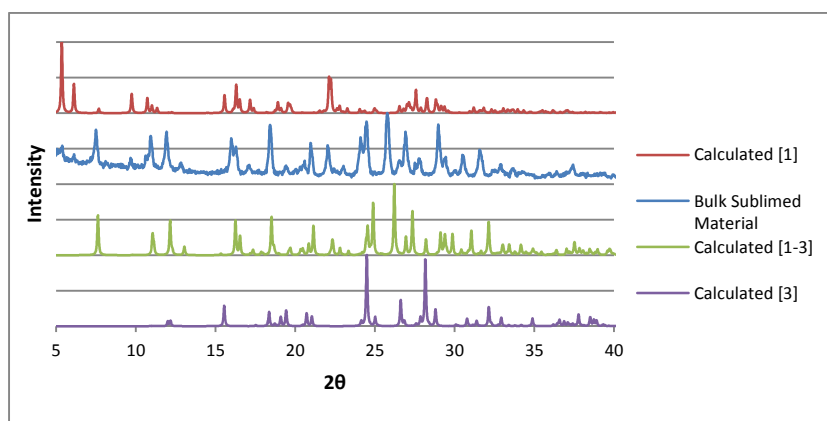


Figure 2.9: Powder pattern of the bulk sublimed material (blue) obtained from the sublimation of [1] and [3] and compared to the calculated patterns of [1] (red), the co-crystal [1-3] (green) and [3] (purple) showing the majority of peaks corresponding to [1-3] and some trace peaks corresponding to [1] due to a slight excess in the original mixture. No peaks corresponding to [3] are observed. Therefore, conversion to [1-3] is quantitative.

It can be seen that the majority of the more intense reflections in the powder pattern of the sublimed material compare quite well with the calculated pattern of co-crystal [1-3]. The

slight shift of these reflections in the collected pattern in comparison to the calculated co-crystal pattern is due to temperature differences: the pattern was collected at room temperature while the calculated pattern was calculated from the crystal structure collected at 180 K. This difference in temperature causes a slight, yet discernible, difference in the unit cell dimensions resulting in a shift of reflections in the powder pattern. In addition, the collected spectrum shows that the stoichiometry of the experiment was imperfect due to the presence of reflections corresponding to [1]. However, we can still conclude that there is a complete conversion of the co-crystal formers to the co-crystal due to the absence of reflections corresponding to [3].

These results beg the question why sublimation did not yield co-crystals for any of the other combinations of dithiadiazolyls that were tried. Therefore, it was considered whether it might be possible to make a co-crystal with 1,2,3,5-dithiadiazolyl radicals by other methods.

2.6.3) Mechanochemical Synthesis

Mechanochemical synthesis or grinding is a method quite commonly used to make co-crystals,^{7, 10} and it offers a simple, solvent-free method by which to create co-crystals that are difficult to synthesise by other means.³⁰ However, it is often difficult to solve the crystal structure of the resulting product as the crystals are often too small or of insufficient quality for single-crystal X-ray diffraction analysis. Nonetheless, a powder pattern of the ground mixture can be used to determine its phase purity and whether or not a co-crystal has, indeed, been made. In some cases, it is possible to solve the crystal structure from PXRD data.

Should grinding result in a novel crystal structure, PXRD would show reflections that do not correspond to either of the co-crystal formers and depending on the quality of the data, it would be possible to determine the crystal structure of this novel co-crystal.

To test whether a co-crystal could be formed by mechanochemical synthesis, a mixture of the two pure co-crystal formers was ground together using a dry glass mortar and pestle. Due to the sensitivity of dithiadiazolyl radicals towards air and moisture, the mixture was ground for about a minute after which the powder pattern was collected using a zero-background holder. Any further grinding resulted in decomposition of the radicals and, in

the case of the co-crystal formers of [1-2], a paste was formed which could not be analysed by PXRD.

Figure 2.10 shows the powder patterns obtained from the grinding experiments of [1] and [2], and [1] and [3]. Products are compared to the calculated patterns of the pure co-crystal formers.

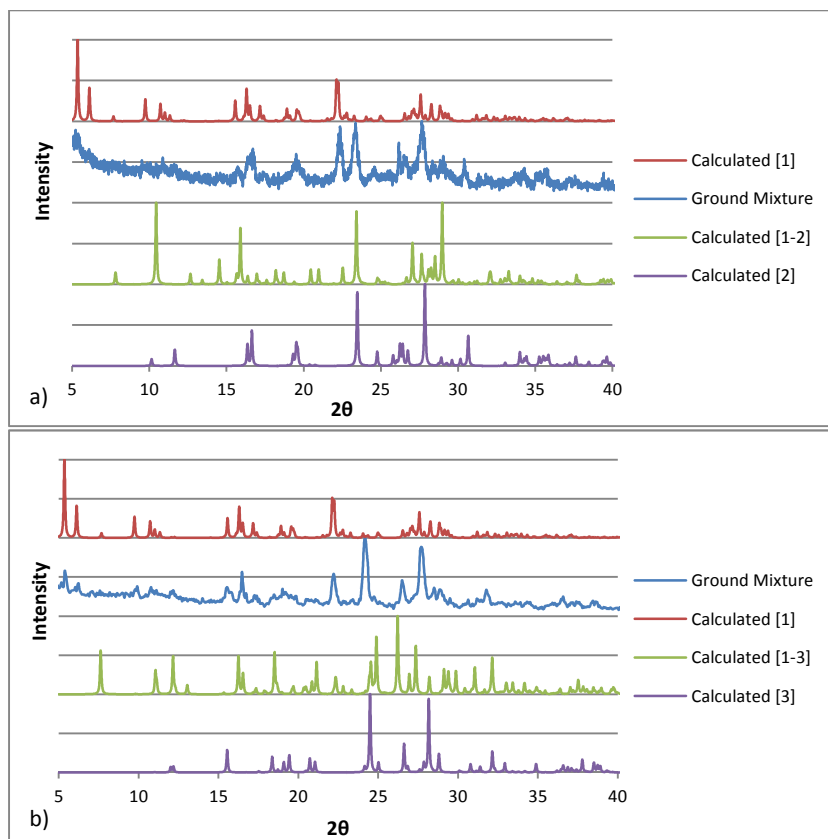


Figure 2.10: Powder patterns of the grinding experiments: a) Grinding experiment between [1] and [2] where the ground mixture is shown in blue compared to the calculated patterns of [1] (red), the co-crystal [1-2] (green) and [2] (purple). b) Grinding experiment between [1] and [3] where the ground mixture is shown in blue compared to the calculated patterns of [1] (red), the co-crystal [1-3] (green) and [3] (purple). In both cases, grinding resulted in the formation of a physical mixture of the co-crystal formers rather than a co-crystal.

These powder patterns show only reflections belonging to the pure radical crystals: peaks corresponding to the co-crystal are absent. Therefore, the co-crystal cannot be formed by the solid-state grinding the pure radicals together in ambient atmosphere. To support this, a powder pattern was obtained of a physical mixture of individually ground [1] and [2] that had been mixed together (Figure 2.11).

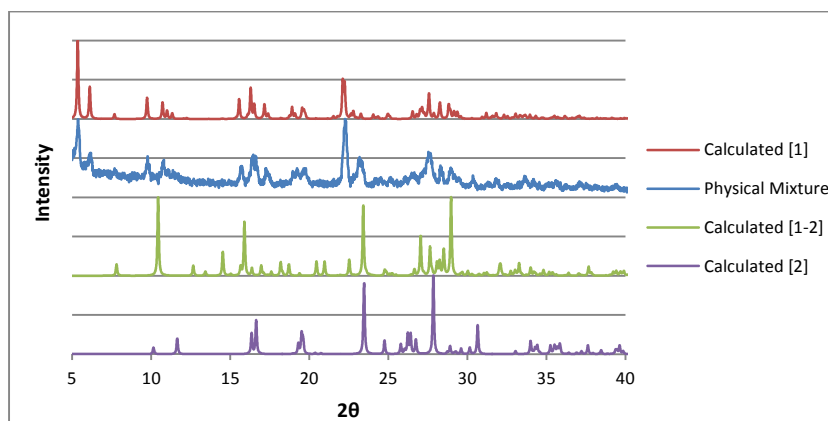


Figure 2.11: Powder pattern of the physical mixture of radicals comprised of [1] and [2] where the physical mixture is shown in blue compared to the calculated patterns of [1] (red), the co-crystal [1-2] and [2].

The powder pattern obtained from the physical mixture appears nearly identical to the mixture of the co-crystal formers after the grinding experiment. Thus, it can be deduced that the grinding of the two pure radicals resulted in a physical mixture being formed.

Although solid-state grinding of radicals was unsuccessful in forming the co-crystals, there are other types of grinding experiments that can be used to form co-crystals such as solvent-drop grinding. This technique, however, was not tested due to the sensitivity of the radicals towards air and moisture. The sample must be ground until the solvent evaporates, which leaves the sample exposed to air and moisture for too long a time. Future work should investigate solvent-drop and solid state grinding of 1,2,3,5-dithiadiazolyl radicals under an inert atmosphere in a glove box because longer grinding times might yield a co-crystal.

2.6.4) Melting & Thermal Analysis

The technique of melting to form co-crystals has been used for more than a century. In fact, the first co-crystal to be identified was formed from the melt.⁵ Currently, melting is commonly used to form crystals of organic solids which have a melting point below 200 °C provided that the solid does not decompose on heating and melting.^{26, 31} As the melted material cools it can recrystallise. Therefore, this technique was investigated as a possible means to form co-crystals of 1,2,3,5-dithiadiazolyl radicals.

Melting experiments to form [1-2] and [1-3] involved placing a 1:1 stoichiometric ratio of the co-crystal formers in a Schlenk under an atmosphere of nitrogen. The mixtures of [1] and [2], and [1] and [3] were then heated in an oil bath to 70 °C and 120 °C, respectively,

until melting had occurred. Once the mixture had cooled to room temperature, the solid mixture at the bottom of the Schlenk was analysed by PXRD (Figure 2.12).

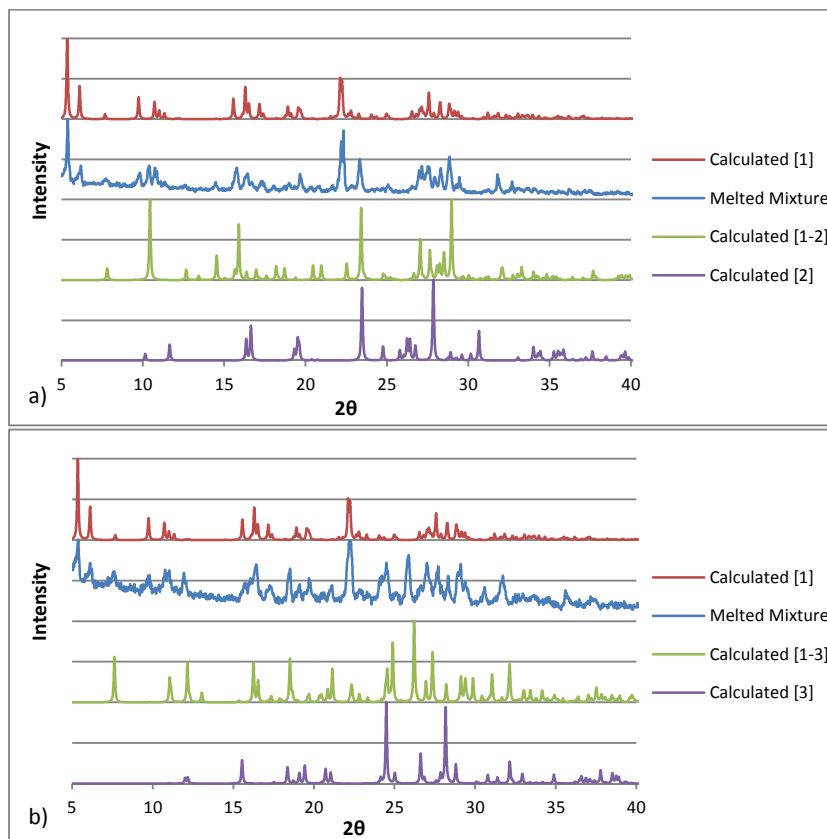


Figure 2.12: Powder patterns of the melting experiments: a) Melting experiment between [1] and [2] where the melted mixture is shown in blue compared to the calculated patterns of [1] (red), the co-crystal [1-2] (green) and [2] (purple) showing that the residue consisted of [1]. b) Melting experiment between [1] and [3] where the melted mixture is shown in blue compared to the calculated patterns of [1] (red), the co-crystal [1-3] (green) and [3] (purple) showing some peaks corresponding to the co-crystal and some trace peaks corresponding to [1] due to imperfect stoichiometry.

The melt experiment between the co-crystal formers [1] and [2] provided quite an interesting result. Even under an atmosphere of nitrogen, at a temperature of 90 °C, it was evident that sublimation of the radicals was occurring in the Schlenk by the formation of a red-purple film on the cooler surfaces higher up in the Schlenk. The powder pattern shows that the melted residue that remained at the bottom of the Schlenk consisted mostly of [1]. There are, however, some peaks indicating a trace amount of co-crystal [1-2]. An explanation of this would be that while [2] was subliming, a small portion was able to form the heterodimers with [1], provided that the temperature is high enough to overcome the activation energy for the recombination of the radicals.

Examining the results of the melt experiment between [1] and [3] showed more significant peaks in the powder pattern corresponding to co-crystal [1-3]. Many of the smaller peaks correspond to pure crystals of [1], however this is attributed to a small excess of [1] in the original mixture.

These preliminary results show that the co-crystals can be made from the melt; however, these results are not conclusive. Thus, the co-crystals and their constituent parts were analysed by thermal gravimetric analysis (TGA) and differential scanning calorimetry (DSC) as the melting points for the pure components and their corresponding co-crystals would be different. Furthermore, DSC would be able to show whether any polymorphs exist in any of the materials.

2.6.4.1) Thermogravimetric Analysis

Thermogravimetric analysis (TGA) measures the weight loss of a sample as a function of temperature. In this way, TGA is able to indicate sublimation and decomposition temperatures of materials. The results of the thermal analysis of compounds [1], [2] and [3] are shown in Figure 2.13. The sublimation onset temperatures of radicals [1], [2] and [3] are 98.13 °C, 54.82 °C and 71.18 °C, respectively. As a result of the sublimation properties of the dithiadiazolyl radicals, there is quite a rapid mass loss with an increase in temperature. Decomposition of the [1] and [2] radicals may be seen in their TGA data above 200 °C and 150 °C, respectively. The compound [3] appears to sublime completely before decomposition.

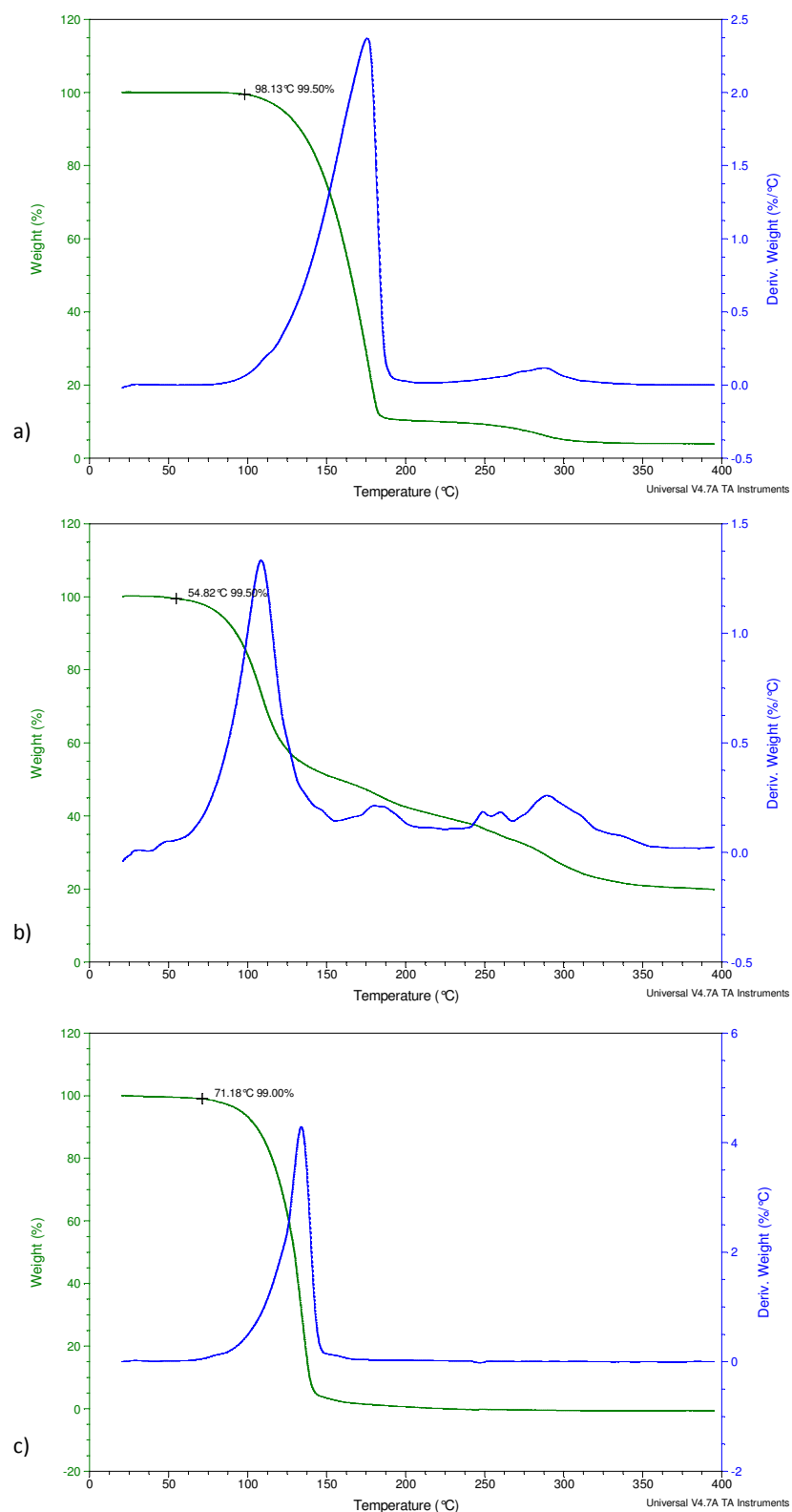


Figure 2.13: TGA analysis of a) [1], b) [2] and c) [3] yielding sublimation onset temperatures of 98.13 °C, 54.82 °C and 71.18 °C, respectively.

2.6.4.2) Differential Scanning Calorimetry of the Pure Dithiadiazolyl Radicals

Differential scanning calorimetry measures the amount of energy required to increase or decrease the temperature of a sample relative to a reference as a function of temperature. In this way, DSC is able to indicate melting points and phase transitions of solid materials. DSC analysis was performed in closed pans to prevent damage to the instrument due to sublimation of the radicals.

The DSC analyses were conducted in the temperature range from $-80\text{ }^{\circ}\text{C}$ to $150\text{ }^{\circ}\text{C}$.[‡] Samples were first cooled and then heated and finally cooled again to room temperature. The DSC results of the pure co-crystal formers are shown in Figure 2.14.

Melting and recrystallisation points for the pure dithiadiazolyl radicals obtained from the DSC data are given in Table 2.2.

Table 2.2: Summary of the Melting and Recrystallisation Points observed in the DSC analysis of the pure radicals

Dithiadiazolyl Radical	Melting Point ($^{\circ}\text{C}$)	Recrystallisation point ($^{\circ}\text{C}$)
[1]	119.66	87.91
[2]	45.03	Not observed
[3]	136.01	125.11

[‡] DSC heating and cooling rates used in these analyses and all subsequent analyses were $10.0\text{ }^{\circ}\text{C min}^{-1}$ and $5.0\text{ }^{\circ}\text{C min}^{-1}$, respectively.

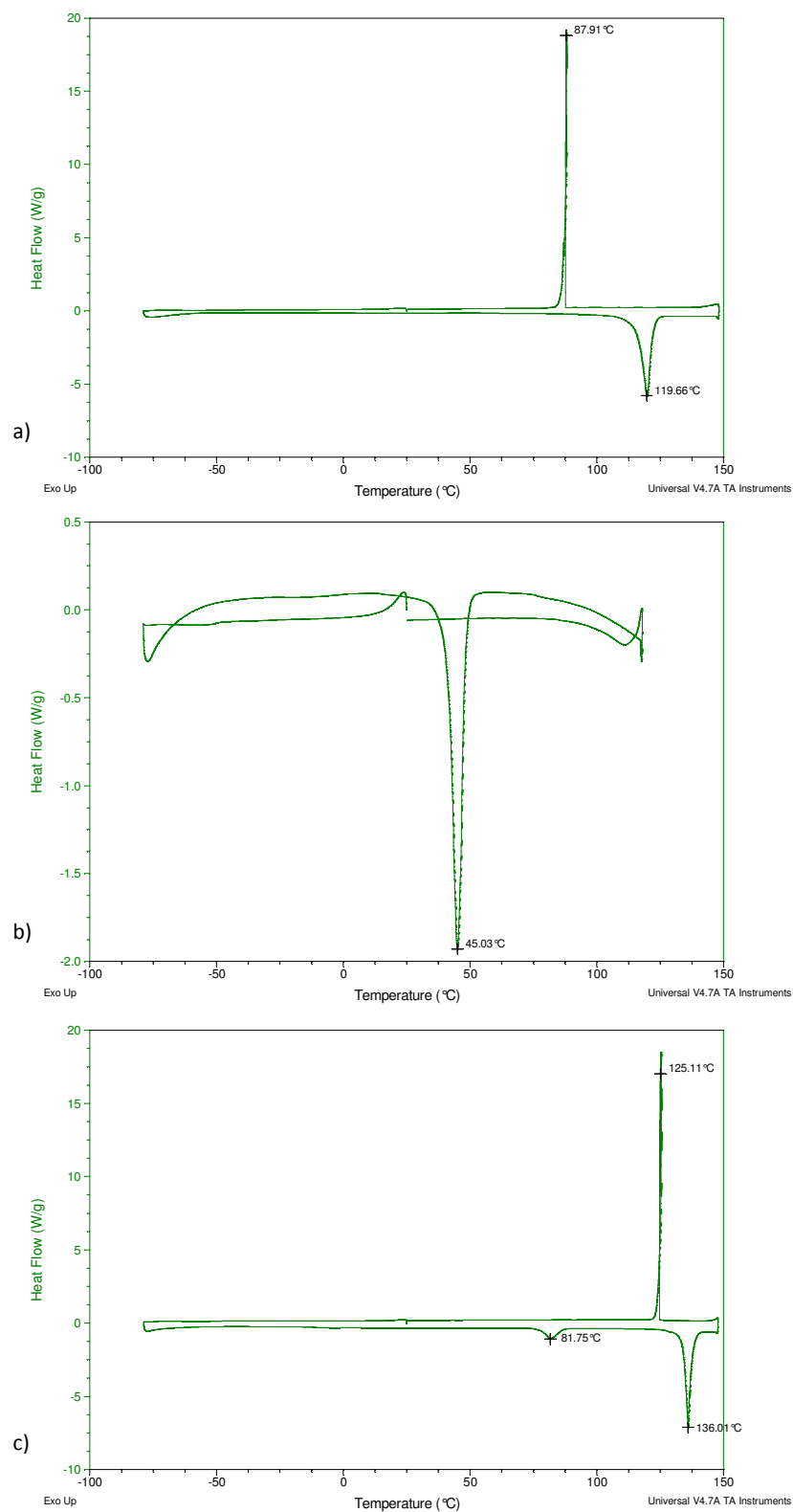


Figure 2.14: DSC analysis of a) [1], b) [2] and c) [3] showing their melting and recrystallisation temperatures. Furthermore, an additional thermal event is observed in [3].

Each of the pure dithiadiazolyl radicals shows quite characteristic melting and recrystallisation points. In the case of **[3]**, there is quite a small additional endotherm at 81.75 °C. To determine what this event represents, another DSC was performed in which a sample of **[3]** was heated from 0 °C to 110 °C and then cooled back down 0 °C (Figure 2.15). The DSC shows the same endothermic event at 82.97 °C but there is no exothermic event during the cooling after this point. This indicates that this event is not a melting point of the radical but rather a possible phase transition.

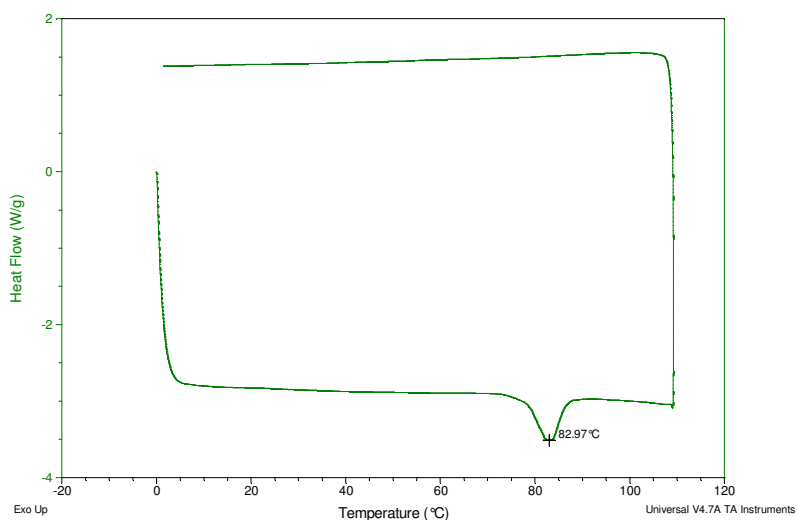


Figure 2.15: DSC analysis of [3] showing the thermal event at 82.97 °C.

A sample of **[3]** was cycled through the heating and cooling process three times. The event at 82 °C was only present in the first pass, indicating an irreversible phase change under the conditions investigated (Figure 2.16).

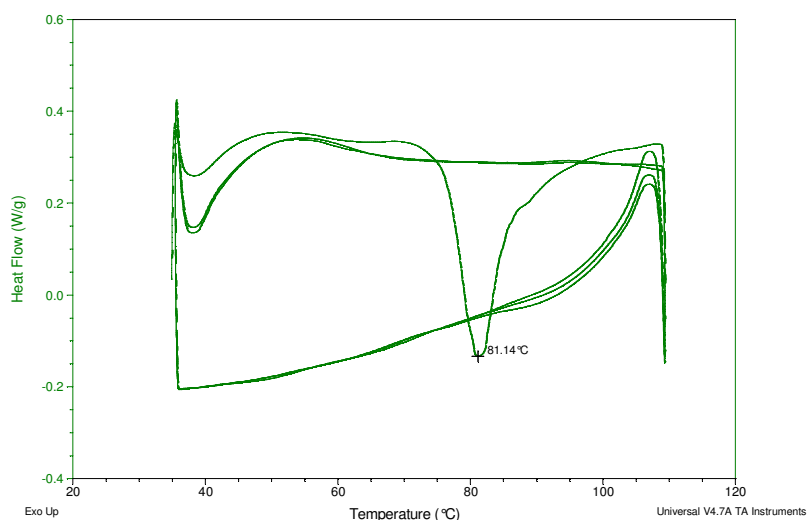


Figure 2.16: DSC analysis of [3] cycled three times showing the thermal event at 81.14 °C in the first cycle only.

In order to investigate this observation further, hot-stage microscopy was used. In this technique, the sample was heated up to 90 °C and the crystals were monitored visually by microscope. A photograph of the sample was taken every 18 seconds. As the sample reached 90 °C, the crystals of [3] changed from a blue colour to black (Figure 2.17). Once the crystals had cooled sufficiently, they were analysed visually by microscope using a light polarising filter and it appeared that they were no longer single crystals. Therefore, the crystals of the new phase of [3] were unsuitable for SCXRD as a powder had formed and it could not be determined if, in fact, a phase change had occurred by structural analysis.

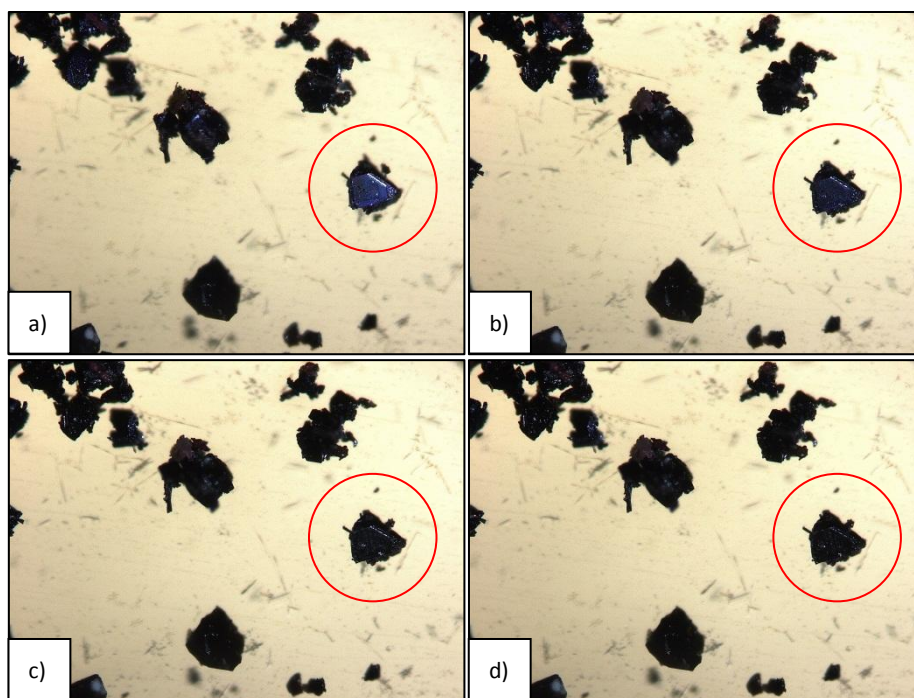


Figure 2.17: Hot-stage photos of [3]: a) at 24.9 °C, b) at 87.1 °C, c) at 88.5 °C and d) at 90 °C showing a phase transition between 88.5 °C and 90 °C.

In an attempt to characterise this new phase further, a sample of [3] was analysed by variable temperature powder X-ray diffraction (VT-PXRD). The results of this analysis are shown in Figure 2.18.

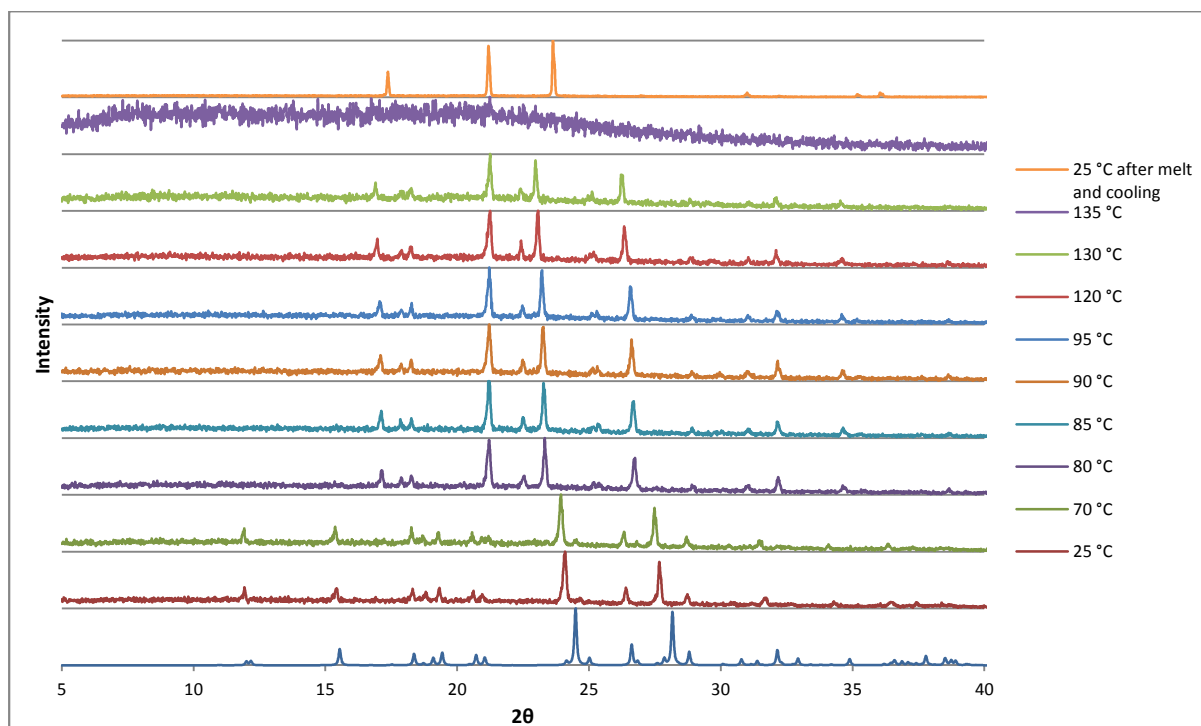


Figure 2.18: VT-PXRD of [3] showing a phase transition between 70 °C and 80 °C. The calculated powder pattern from the known crystal structure is shown as the bottommost powder pattern. The powder pattern second from the top (purple) shows the melt as it is amorphous. Another powder pattern was collected after cooling the sample back to 25 °C (topmost pattern - orange) to determine the recrystallised phase. Some degree of preferred orientation is observed in the recrystallised sample.

Comparison of the powder patterns at 25 °C and 70 °C with the calculated pattern of [3] shows that the sample used for analysis was phase pure. It is evident that a phase change occurs between 70 °C and 80 °C however, a number of the peaks observed in the new phase are reminiscent of peaks in the original phase. This may indicate that the new phase of [3] is quite similar to its original phase. Heating the sample above 130 °C causes it to melt evidenced by the amorphous pattern obtained at 135 °C. After melting [3], the sample was allowed to cool to room temperature to allow the recrystallisation of [3]. A powder pattern was collected in order to determine which phase of [3] recrystallises and although it resembles the new phase, the pattern shows preferred orientation.

2.6.4.3) Differential Scanning Calorimetry of the Co-Crystals [1-2] and [1-3]

The two known co-crystals, [1-2] and [1-3], were characterised by DSC to determine if how their melting points differ from the pure materials. The analysis followed the same procedure used for the pure radicals: cool to -80 °C, heat to 150 °C and finally cool to room temperature again. The results of these experiments are shown in Figure 2.19 below.

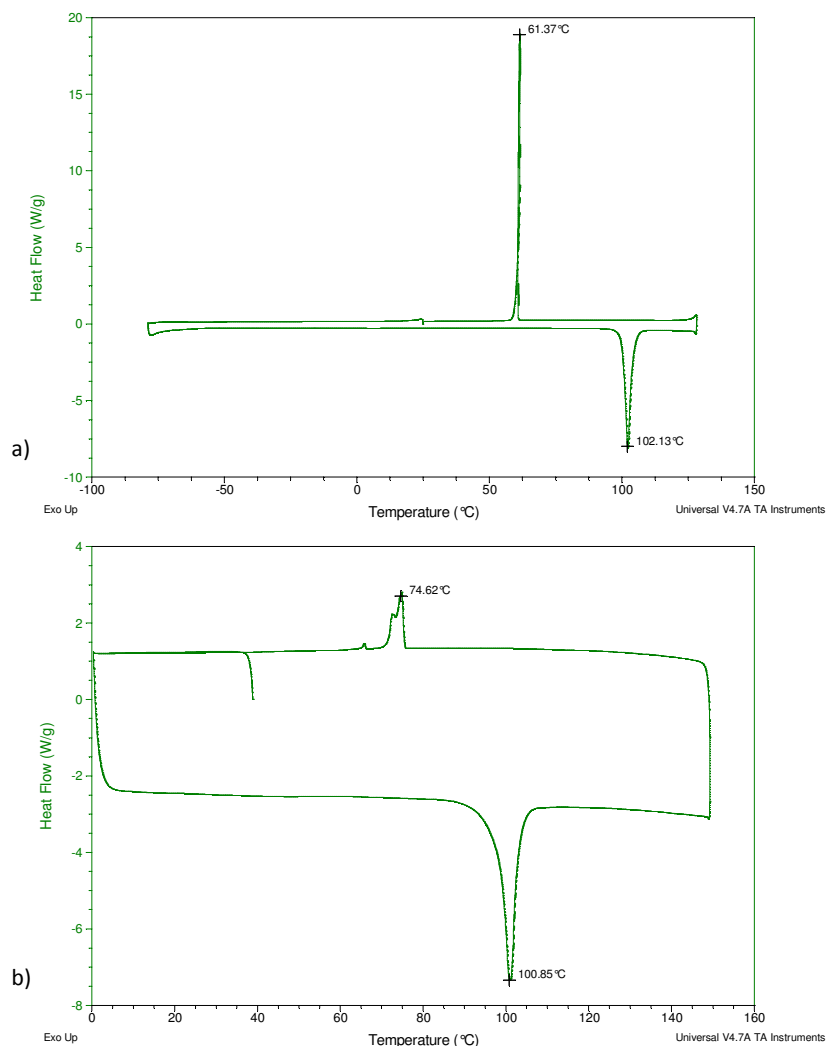


Figure 2.19: DSC analysis of the co-crystals a) [1-2] and b) [1-3] showing single melting and recrystallisation events

Both co-crystals show only one melting point and one recrystallisation point each. Surprisingly, the melting points for [1-2] and [1-3] are quite similar at 102.13 °C and 100.85 °C, respectively. However, their melting points are sufficiently different from their co-crystal formers. Therefore, melting point could be used as a means to differentiate the co-crystal from its pure constituents.

2.6.4.4) DSC Melting Experiments

These melt experiments were performed in the DSC instrument. A 1:1 stoichiometric ratio of the co-crystal formers were placed together in closed pans to prevent the sublimation of the radicals into the instrument. The analysis followed the same heating and cooling profile as the pure radicals: cool to -80 °C, heat to 150 °C and then cool to room temperature again (Figure 2.20).

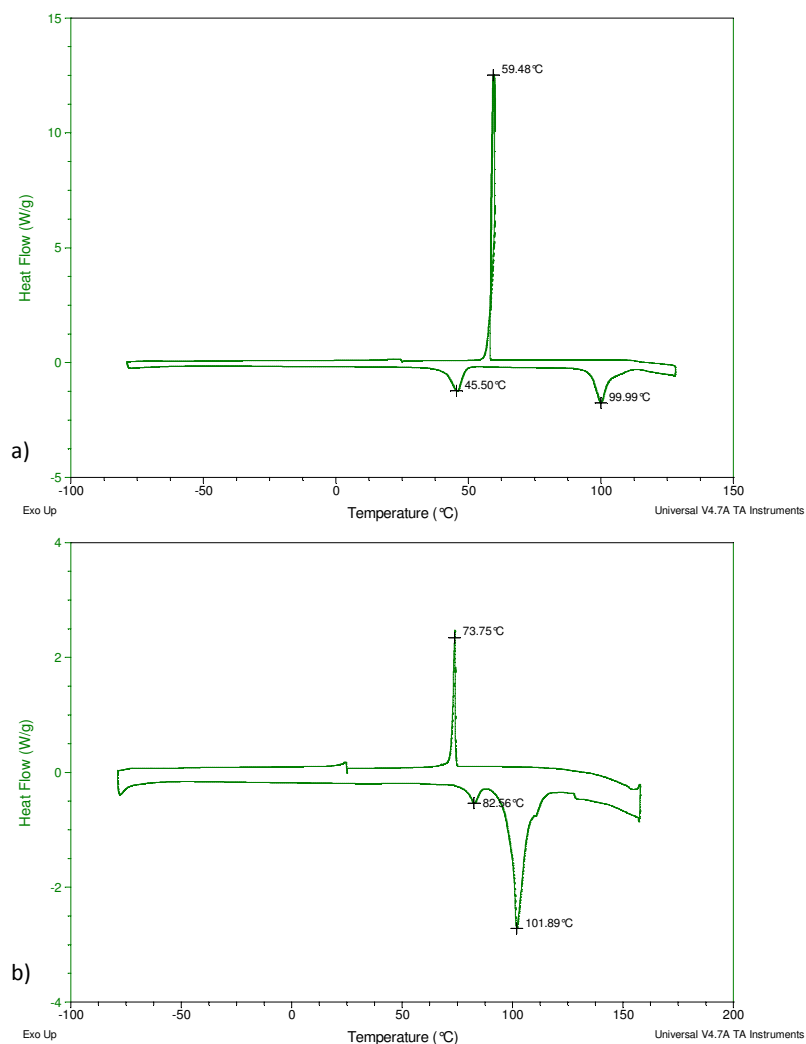


Figure 2.20: DSC analysis of the melting experiments: a) the mixture of [1] and [2] and b) the mixture of [1] and [3] showing recrystallisation points corresponding to the co-crystals [1-2] and [1-3], respectively.

Analysing the results for co-crystal [1-2] reveals that [2] melts first at 45.50 °C. Thereafter, a second melt is observed at 99.99 °C which is interesting as it could be attributed to the co-crystal melting, although the corresponding crystallisation event is not observed between 45.5 °C and 99.99 °C. This result requires further investigation to determine what the endotherm at 99.99 °C represents. Finally, on cooling to room temperature, the sample recrystallises at 59.68 °C which is very close to the recrystallisation temperature of the pure co-crystal at 61.37 °C, possibly indicating the formation of the co-crystal [1-2].

Similarly, the results for co-crystal [1-3] show that [3] undergoes the phase transition at 82.56 °C, before melting occurs at 101.89 °C. Again, this melt event can either be attributed to the co-crystal melting or the assisted melting of the co-crystal former, [1]. Cooling the

sample results in a recrystallisation event at 73.75 °C, comparable to the pure recrystallisation event at 74.62 °C of the co-crystal.

These results indicate that co-crystals with 1,2,3,5-dithiadiazolyl radicals can be formed from the melt supporting data obtained from the powder patterns of the melt experiments at the beginning of section 2.6.4. In addition, the formation of these co-crystals can be monitored using DSC. Indeed, DSC analysis could possibly be used as a screening method to indicate the potential of two 1,2,3,5-dithiadiazolyl co-crystal formers to produce a co-crystal from the melt. However, this technique needs to be investigated further.

2.6.5) Mixed Reductions

Although reduction of the dithiadiazolylum chloride salts to their respective radicals can be achieved using a wide variety of reducing agents, two methods in particular are commonly used in our laboratory. The first uses Zinc-Copper (Zn-Cu) couple in tetrahydrofuran (THF), while the second takes place from the melt of triphenylantimony (Ph₃Sb).²⁹ Until this point, the co-crystals of 1,2,3,5-dithiadiazolyl radicals had been made from the pure co-crystal formers that had been individually reduced to the radicals from their respective dithiadiazolylum chloride salts. However, the possibility existed that the parent salts of the two co-crystal formers could be reduced concurrently and thus form the co-crystal. Consequently, the co-reduction of mixtures of [1] and [2], and [1] and [3] was attempted using Zn-Cu couple in THF and from the melt of Ph₃Sb.

2.6.5.1) Mixed Reduction using Zn-Cu/THF

In this reaction, a 1:1 stoichiometric ratio of the dithiadiazolylum chloride salts (the precursors to the co-crystal formers) were placed together in a Schlenk. THF was then added to the mixture to form a yellow-orange suspension of the two salts. Half an equivalent of Zn-Cu was added to the solution, which was stirred overnight. The reaction was determined to be complete when no orange particulates could be seen in the now brown to purple coloured solution. The solution was filtered off into a second Schlenk and the THF removed by vacuum.

In both cases of mixtures of [1-2] and [1-3], the reactions resulted in a sticky residue. Consequently, these could not be analysed by PXRD.

2.6.5.2) Mixed Reduction using Ph₃Sb

The reduction reaction with Ph₃Sb is intriguing as it is performed from the melt of Ph₃Sb. The dithiadiazolylum chloride salt and half an equivalent of Ph₃Sb are mixed together in a Schlenk under nitrogen. The mixture is then heated to 60 °C, at which temperature the Ph₃Sb melts. It then reduces the salt forming the desired radical which can then be purified by sublimation from the by-product, Ph₃SbCl₂. The reaction can be followed visually by the colour change that occurs: from a yellow-orange powder to a dark purple residue.

The procedure for testing the mixed reduction with Ph₃Sb involved mixing a 1:1 stoichiometric ratio of the two dithiadiazolylum chloride salts in a Schlenk filled with nitrogen. The Ph₃Sb was then added to the mixture which was heated to 60 °C in an oil bath. As the Ph₃Sb melted and reduced the salts the mixture became a dark purple colour.

The mixture was allowed to cool and was analysed by PXRD to determine whether the co-crystal had formed (Figure 2.21).

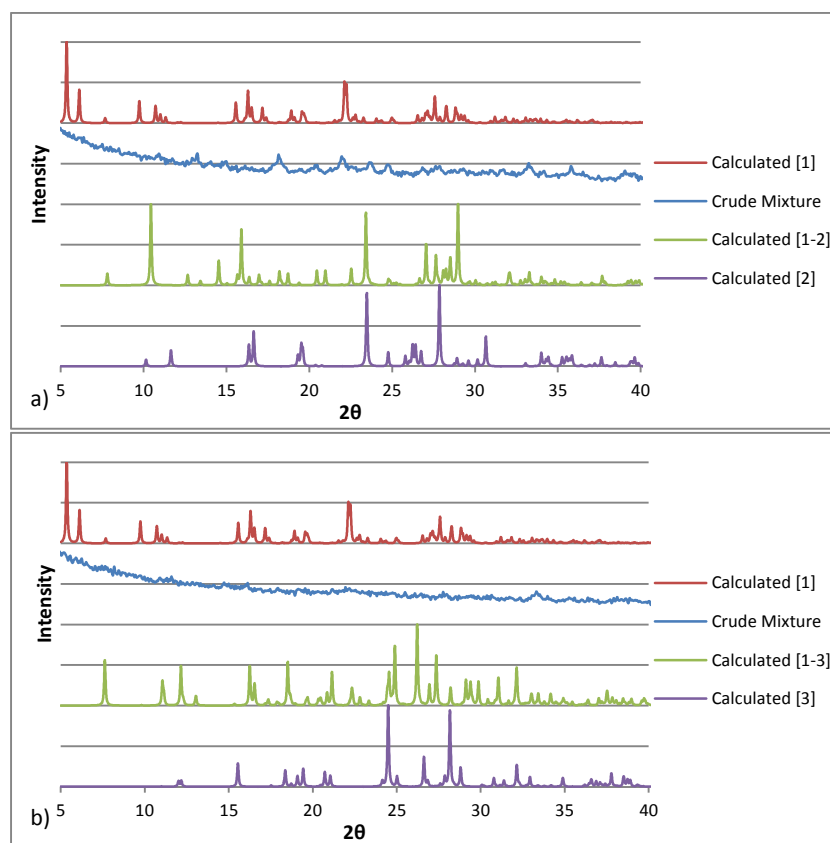


Figure 2.21: Powder patterns of the crude reduction mixtures from the concurrent reduction experiments using Ph₃Sb: a) the pattern in blue represents the crude reduction mixture of the precursors of [1] and [2] compared to the patterns calculated from the crystal structures of [1] (red), the co-crystal [1-2] (green) and [2] (purple) and b) the pattern in blue represents the crude reduction mixture of the precursors of [1] and [3] compared to the patterns calculated from the crystal structures of [1] (red), the co-crystal [1-3] (green) and [3] (purple). Both powder patterns of the crude materials indicate no formation of a co-crystal

The powder pattern of the crude reduction mixtures showed no significant peaks and thus it could not be determined whether or not the co-crystals had formed from the powder pattern.

Consequently, the crude reduction mixtures were sublimed and the bulk products analysed by PXRD to determine whether the co-crystals had formed and whether the conversion was quantitative (Figure 2.22).

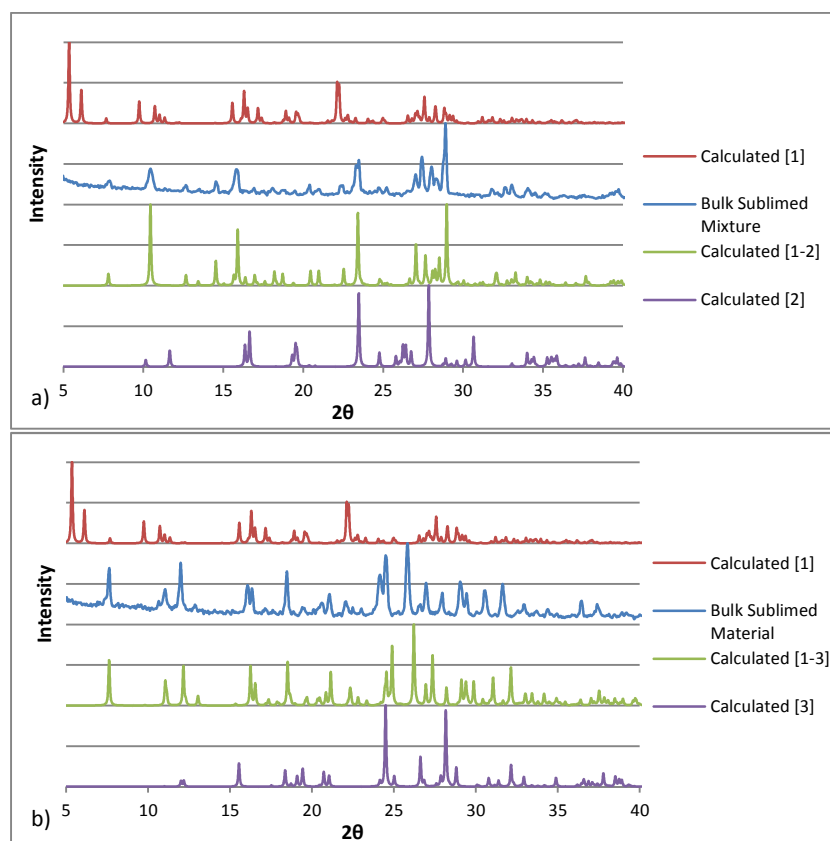


Figure 2.22: Powder patterns of the bulk material sublimed from the concurrent reduction experiments using Ph_3Sb : a) the pattern in blue represents the sublimed material compared to the patterns calculated from the crystal structures of [1] (red), the co-crystal [1-2] (green) and [2] (purple) and b) the pattern in blue represents the sublimed material compared to the patterns calculated from the crystal structures of [1] (red), the co-crystal [1-3] (green) and [3] (purple). In both sublimation experiments, conversion to the co-crystal is quantitative.

In both cases of the co-crystals [1-2] and [1-3], their respective powder patterns show that the co-crystals formed after subliming the mixed reduction mixture. Furthermore, none of the reflections observed in the experimental powder patterns correspond to the pure co-crystal formers, indicating complete conversion of the starting materials to the co-crystal through sublimation.

Therefore, it can be concluded that these known co-crystals are formed quantitatively through the sublimation of the co-crystal formers, either pure or in a concurrent reduction reaction.

2.6.6) Mixing in Solution

The final method that was tested as a means to form the co-crystals was that of mixing in solution. In these experiments, a 1:1 stoichiometric ratio of the pure radicals was dissolved in THF and stirred for half an hour. Thereafter, the solvent was removed *in vacuo* to yield a crystalline material that was analysed by PXRD (Figure 2.23). It is known that the dimers of the 1,2,3,5-dithiadiazolyl radicals dissociate in dilute solutions.²⁹ Thus, solvent mixing provided a means for the homodimers to dissociate and the heterodimers to form.

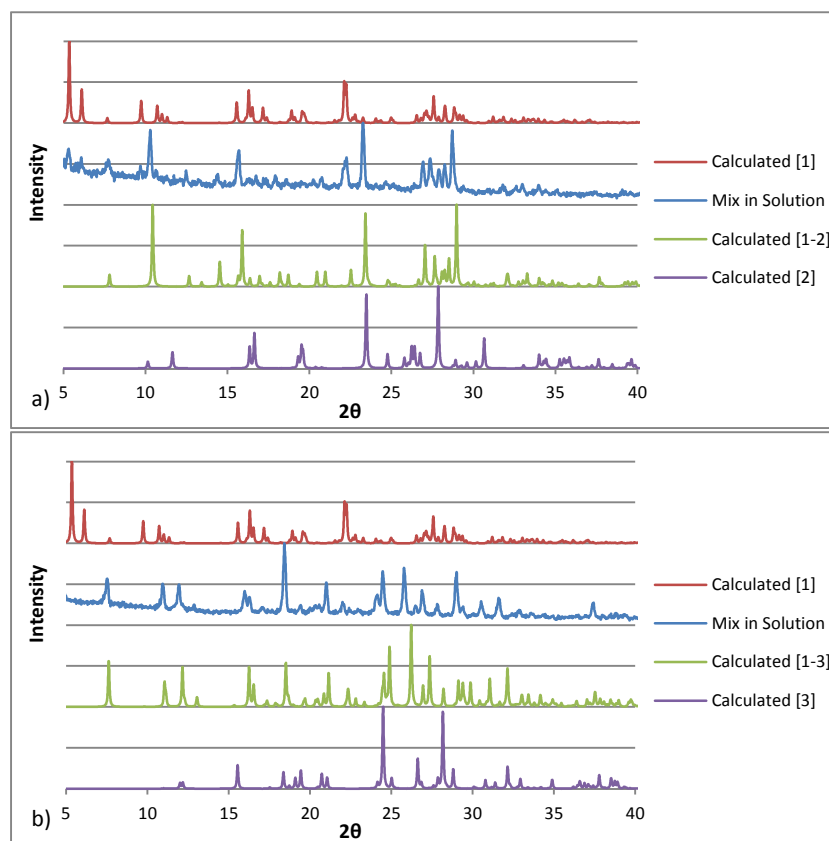


Figure 2.23: Powder patterns of the solvent mixing experiments: a) the residue after mixing [1]₂ and [2] is shown in blue and is compared to the patterns calculated from the crystal structures of [1] (red), the co-crystal [1-2] (green) and [2] (purple), b) the residue after mixing [1] and [3] is shown in blue and is compared to the patterns calculated from the crystal structures of [1] (red), the co-crystal [1-3] (green) and [3] (purple). The co-crystals are formed in both solvent mixing experiments. A small amount of [1] is observed in the experimental pattern in a) due to imperfect stoichiometry.

The powder patterns for the mixing experiments show that the co-crystals, [1-2] and [1-3], were formed by mixing in THF. Some residual peaks in the pattern of [1-3] correspond to

the co-crystal former [1] which was in slight excess in the experiment. The experiment to form co-crystal [1-3] shows only peaks corresponding to the co-crystal.

From this data, it can be concluded that the co-crystal forms quantitatively when the two pure radicals are mixed in a solvent such as THF.

2.7) Conclusions & Future Work

The analysis of the co-crystals, [1-2] and [1-3], showed that they are formed quantitatively by sublimation.

Several other techniques were investigated as methods to synthesise co-crystals including: grinding, melting, concurrent reduction and mixing in solution. Mechanochemical synthesis proved to be unsuccessful while the other techniques yielded positive results for the formation of co-crystals. Furthermore, DSC could provide a means to screen potential co-crystal combinations practically using very small sample sizes.

An important conclusion that should be drawn from these results is that it appears that the homodimers in the co-crystal formers need to be broken down into their monomers before any kind of favourable interaction can occur to form the co-crystal. These two factors are critical to co-crystal formation. For example, although the co-crystal formers of [1-2] and [1-3] possessed a favourable interaction, the co-crystals could not form due to the homodimers not being separated during a grinding experiment (although grinding for longer times may yield the co-crystals). Whereas, the use of sublimation in the concurrent reduction with Ph_3Sb , the solvent mixing in THF and melting of the radicals provided the means for the homodimers to separate either in the gas phase, by dissolution or in the melt. This allowed the association of the co-crystal formers and consequently, the formation of the co-crystal.

Melting is quite interesting as there must be sufficient energy to dissociate the homodimers before the co-crystal can form. As before, the presence of a favourable interaction causing a gain in energy would facilitate the recombination of the co-crystal formers.

The methods of melting, concurrent reduction and solvent mixing now provide new means by which to make co-crystals of 1,2,3,5-dithiadiazolyl radicals. Furthermore, the results show that melting, concurrent reduction and solvent mixing all appear to be quantitative in co-crystal formation. Therefore, these methods now need to be tested with

combinations of radicals and other co-crystal formers. Should co-crystal formation be successful by any of these means, the results of these experiments may provide insight into other supramolecular synthons that may be used in the crystal engineering of 1,2,3,5-dithiadiazolyl radicals. Furthermore, deeper insight into the interactions between the radicals in the solid state may be explored.

Solvent-drop grinding should be investigated as a possible method to form co-crystals if it can be done in a fast and inert manner. Furthermore, grinding a radical with a liquid co-crystal former may be sufficient to generate novel co-crystals. Solid-state grinding experiments should be performed in a glove box to determine whether this has an effect on the formation of the co-crystal.

During the course of this investigation into co-crystal formation, a variety of techniques (DSC, Hot-stage microscopy and VT-PXRD) showed that [3] has a polymorph. This new phase of [3] should be characterised structurally by either solving the crystal structure from the powder pattern or by producing single-crystal diffraction quality crystals.

2.8) Experimental Procedures

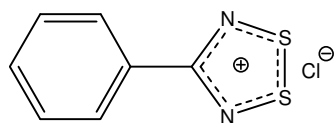
Please consult Appendix A for Instrumentation and Chemicals used.

2.8.1) Synthesis of the Pure Radicals

Salt formation: In a typical experiment,[§] diethyl ether was added to a Schlenk tube filled with nitrogen and containing a magnetic stirrer bar and cooled to $-78\text{ }^{\circ}\text{C}$. 1,1,1,3,3,3-Hexamethyldisilazane (HMDS) was added, followed by *n*-Butyllithium (*n*-BuLi). The solution was allowed to warm to room temperature resulting in a clear solution. The corresponding nitrile was added to the mixture which was stirred overnight, resulting in a pale yellow solution. The mixture was cooled to $0\text{ }^{\circ}\text{C}$ and a slight excess of SCl_2 was added dropwise causing the immediate precipitation of a bright yellow or orange solid. The solution was allowed to warm to room temperature and stirred for a further hour. Thereafter, the mother liquor was filtered off and the bright yellow or orange solid was washed with diethyl ether. The solid was dried *in vacuo* to yield the parent 1,2,3,5-dithiadiazolylum chloride salt as a bright yellow or orange powder.

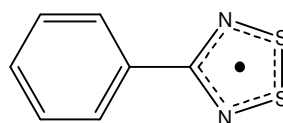
Salt reduction: A portion of the parent salt was placed in a dry Schlenk tube filled with nitrogen. Half an equivalent of Ph_3Sb was added and the Schlenk was heated at $60\text{ }^{\circ}\text{C}$ in an oil bath until the bright yellow salt had changed colour from bright yellow to dark purple. Vacuum was applied to the Schlenk and the temperature set at $90\text{ }^{\circ}\text{C}$ ([1]), $40\text{ }^{\circ}\text{C}$ ([2]) or $100\text{ }^{\circ}\text{C}$ ([3]) to sublime the radicals.

[§] The specific quantities used to synthesise [1], [2] and [3] are shown with their characterisation data below.

4-PHENYL-1,2,3,5-DITHIADIAZOLYL, [1]**Table 2.3: Quantities of reagents used to form the salt of [1]**

Reagent	Volume (ml)	Number of moles (mmol)
HMDS	4.1	20
<i>n</i> -BuLi	13.0	20
Benzonitrile	2.0	20
SCl ₂	3.0	47
Et ₂ O	100	-
Et ₂ O wash	2 x 20	-

(+)-ESI-MS: m/z 182.0 (M^+ , 100%)

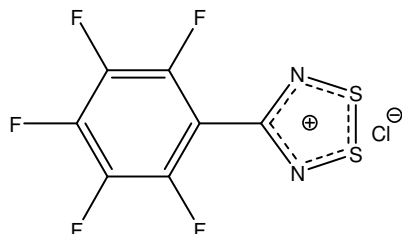
**Table 2.4: Quantities of reagents used to form [1]**

Reagent	Mass (g)	Number of moles (mmol)
Salt	1.071	4.9
Ph ₃ Sb	0.870	2.5

Crystals of [1] appeared as green-black needles.

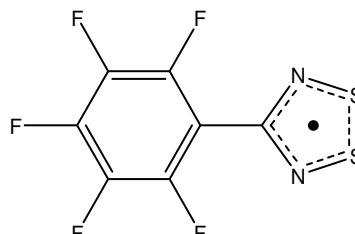
(+)-ESI-MS: m/z 180.9 (M^+ , 85%), 135.0 (38), 77.9 (100)

EPR (298 K, CH₂Cl₂): quintet ($g = 2.007$, $a_N = 5.0$ G)

4-PERFLUOROPHENYL-1,2,3,5-DITHIADIAZOLYL, [2]**Table 2.5: Quantities of reagents used to form the salt of [2]**

Reagent	Volume (ml)	Number of moles (mmol)
HMDS	1.7	8.1
<i>n</i> -BuLi	5.5	8.1
Pentafluorobenzonitrile	1.0	8.1
SCl ₂	1.4	22
Et ₂ O	50	-
Et ₂ O wash	2 x 20	-

(+)-ESI-MS: m/z 270.9 (M^+ , 100%), 257.2 (5), 253.1 (2), 240.9 (3)

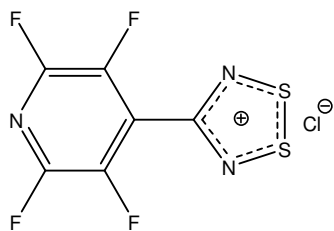
**Table 2.6: Quantities of reagents used to form [2]**

Reagent	Mass (g)	Number of moles (mmol)
Salt	0.344	1.1
Ph ₃ Sb	0.158	0.45

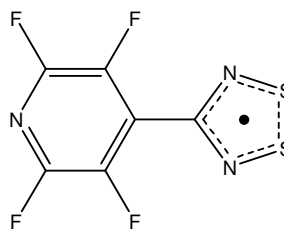
Crystals of [2] appeared as red blocks.

(+)-ESI-MS: m/z 270.9 (M^+ , 100%)

EPR (298 K, CH₂Cl₂): quintet ($g = 2.010$, $a_N = 4.9$ G).

4-(4'-PERFLUOROPYRIDYL)-1,2,3,5-DITHIADIAZOLYL, [3]**Table 2.7: Quantities of reagents used to form the salt of [3]**

Reagent	Mass (g)	Volume (ml)	Number of moles (mmol)
HMDS	-	1.2	5.7
<i>n</i> -BuLi	-	3.8	5.7
Tetrafluoro-4-pyridinenitrile	1.0	-	5.7
SCl ₂	-	1.0	15.7
Et ₂ O	-	40	
Et ₂ O wash	-	2 x 20	

**Table 2.8: Quantities of reagents used to form [3]**

Reagent	Mass (g)	Number of moles (mmol)
Salt	0.149	0.5
Ph ₃ Sb	0.073	0.21

Crystals of [3] appeared as blue blocks.
 (+)-ESI-MS: *m/z* 253.9 (M⁺, 30%), 221.1 (16), 194.0 (100)
 EPR (298 K, CH₂Cl₂): quintet (*g* = 2.011, *a_N* = 5.0 G).

2.8.2) Synthesis of Co-crystals and Synthetic Investigations**2.8.2.1) Synthesis of [1-2] and [1-3] and Percentage Conversion Experiments**

A 1:1 ratio of the co-crystal formers was placed in a Schlenk filled with nitrogen. Vacuum was then applied to the Schlenk and the mixture was then heated to either 65 °C (for [1] and [2]) or 80 °C (for [1] and [3]) in an oil bath allowing the radicals to sublime. The sublimation experiment was stopped when the entire radical mixture had sublimed. The co-crystals, [1-2] and [1-3], both formed as red blocks.

Table 2.9: Quantities of reagents used to synthesise [1-2] and [1-3] and for percentage conversion experiments

Reagent	Mass (g)	Number of moles (mmol)
[1]	0.015	0.08
[2]	0.023	0.08
[1]	0.015	0.08
[3]	0.023	0.08

2.8.2.2) Mechanochemical Synthesis Experiments

A non-stoichiometric ratio of the co-crystal formers (either [1] and [2] or [1] and [3]) was ground in a dry glass mortar and pestle for 1 minute. The ground mixtures were then analysed by PXRD. In both

cases, due to the absence of peaks corresponding to the co-crystal, the yield of co-crystal was determined to be 0%.

2.8.2.3) Melting Experiments

A 1:1 ratio of the co-crystal formers was placed in a Schlenk filled with nitrogen. The mixture was heated to either 80 °C ([1] and [2]) or 120 °C ([1] and [3]) in an oil bath. Once the mixture had cooled, the residue at the bottom of the Schlenk was ground using a dry glass mortar and pestle and analysed by PXRD. For [1] and [2], it was observed that a red film had condensed on the cooler upper areas of the Schlenk during the melting experiment while the distinctive needles of [1] remained intact at the bottom of the Schlenk. The residue was shown to consist of [1]. For [1] and [3], the residue was shown to be a mixture of [1] and co-crystal [1-3].

Table 2.10: Quantities of reagents used to synthesise [1-2] and [1-3] by melting

Reagent	Mass (g)	Number of moles (mmol)
[1]	0.012	0.07
[2]	0.021	0.08
[1]	0.015	0.08
[3]	0.016	0.06

2.8.2.4) DSC Monitored Melting Experiments

Samples were prepared by placing a 1:1 ratio of the co-crystal formers in a standard aluminium DSC pan. The pan was then sealed with a lid. No hole was made in the lid as the sample would sublime out. The sample was then cooled to -80 °C, heated to 150 °C and then cooled to room temperature again.

Table 2.11: Quantities of reagents used to synthesise [1-2] and [1-3] from the melt while monitored by DSC

Reagent	Mass (mg)	Number of moles (mmol)
[1]	2.55	0.01
[2]	3.02	0.01
[1]	1.49	0.01
[3]	2.19	0.01

2.8.2.5) Mixed Reduction: Zn-Cu/THF

A 1:1 ratio of parent salts of the co-crystal formers was placed in a Schlenk containing a magnetic stirrer bar and filled with nitrogen. A portion of THF (20 ml) was then added to the mixture to form a suspension to which a slight excess of the Zn-Cu couple. The solution changed from a yellow-orange colour to a brown colour. The solution was filtered, the THF removed *in vacuo* and the sample dried *in vacuo*.

Table 2.12: Quantities of reagents used to synthesise [1-2] and [1-3] by the co-reduction of the parent salts with Zn-Cu couple in THF

Reagent	Mass (g)	Number of moles (mmol)
Parent salt of [1]	0.100	0.6
Parent salt of [2]	0.111	0.4
Parent salt of [1]	0.120	0.7
Parent salt of [3]	0.197	0.8

2.8.2.6) Mixed Reduction: Ph₃Sb

A 1:1 ratio of the parent salts of the co-crystal formers was placed in a Schlenk filled with nitrogen. A slight deficit of Ph₃Sb was then added to the mixture. The mixture was heated to 60 °C in an oil bath at which temperature the Ph₃Sb melted and reduced the salts to the radicals. A colour change from yellow-orange to dark purple was observed. Once the colour change was complete, the mixture was allowed to cool to room temperature. A sample of this crude reduction mixture was analysed by PXRD at this point which indicated no co-crystal formation. Vacuum was then applied to the Schlenk and it was heated to either 70 °C ([1] and [2]) or 100 °C ([1] and [3]) allowing the radicals to sublime, forming both co-crystals, [1-2] and [1-3], as red and blue blocks, respectively, on the cooler sides of the Schlenk. The conversion was almost quantitative as evidenced by PXRD analysis of the bulk sublimed material.

Table 2.13: Quantities of reagents used to synthesise [1-2] and [1-3] by the co-reduction of the parent salts from the melt of Ph₃Sb

Reagent	Mass (g)	Number of moles (mmol)
Parent salt of [1]	0.495	2.28
Parent salt of [2]	0.757	2.47
Parent salt of [1]	0.138	0.64
Parent salt of [3]	0.190	0.66

2.8.2.7) Mixing in Solution

A 1:1 ratio of the co-crystal formers was placed in a Schlenk containing a magnetic stirrer bar and filled with nitrogen. A portion of THF (5 ml) was added to the mixture forming a yellow solution which was then stirred for 30 minutes. The THF was then removed *in vacuo* and the dry residue was analysed by PXRD showing that both co-crystals, [1-2] and [1-3], had formed. In the case of [1] and [2], some trace peaks of [1] are observed due to the small excess in the reaction.

Table 2.14: Quantities of reagents used to synthesise [1-2] and [1-3] by mixing in solution

Reagent	Mass (g)	Number of moles (mmol)
[1]	0.016	0.09
[2]	0.015	0.06
[1]	0.012	0.07
[3]	0.017	0.07

2.9) References

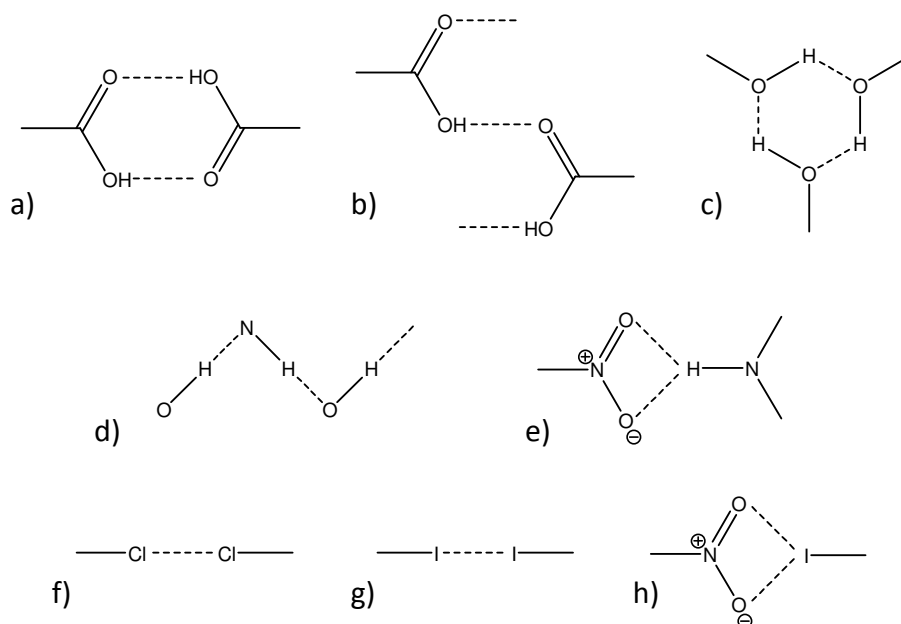
1. A. D. Bond, *CrystEngComm*, 2007, **9**, 833-834.
2. C. B. Aakeroy, *Acta Crystallographica Section B-Structural Science*, 1997, **53**, 569-586.
3. J. A. Bis, P. Vishweshwar, R. A. Middleton and M. J. Zaworotko, *Crystal Growth & Design*, 2006, **6**, 1048-1053.
4. N. Blagden, D. J. Berry, A. Parkin, H. Javed, A. Ibrahim, P. T. Gavan, L. L. De Matos and C. C. Seaton, *New Journal of Chemistry*, 2008, **32**, 1659-1672.
5. A. Miolati, *Zeitschrift für Physikalische Chemie*, 1892, **9**, 649-655.
6. J. C. Philip, *Journal of the Chemical Society, Transactions*, 1903, **83**, 814-834.
7. M. C. Etter and D. A. Adsmond, *Journal of the Chemical Society, Chemical Communications*, 1990, 589-591.
8. V. R. Pedireddi, W. Jones, A. P. Chorlton and R. Docherty, *Chemical Communications*, 1996, 997-1002.
9. S. G. Fleischman, S. S. Kuduva, J. A. McMahon, B. Moulton, R. D. Bailey Walsh, N. Rodríguez-Hornedo and M. J. Zaworotko, *Crystal Growth & Design*, 2003, **3**, 909-919.
10. N. Shan, F. Toda and W. Jones, *Chemical Communications*, 2002, 2372-2373.
11. A. V. Trask, D. A. Haynes, W. D. S. Motherwell and W. Jones, *Chemical Communications*, 2006, 51-53.
12. A. V. Trask, W. D. S. Motherwell and W. Jones, *Chemical Communications*, 2004, 890-891.
13. R. A. Chiarella, R. J. Davey and M. L. Peterson, *Crystal Growth & Design*, 2007, **7**, 1223-1226.
14. P. G. Jones, *Chemistry in Britain*, 1981, **17**, 222-225.
15. G. P. Stahly, *Crystal Growth & Design*, 2007, **7**, 1007-1026.
16. S. R. Byrn, R. R. Pfeiffer and J. G. Stowell, *Solid-state chemistry of drugs*, SSCI, Inc., 1999.
17. L.-F. Huang and W.-Q. Tong, *Advanced Drug Delivery Reviews*, 2004, **56**, 321-334.
18. A. J. Banister, N. Bricklebank, W. Clegg, M. R. J. Elsegood, C. I. Gregory, I. Lavender, J. M. Rawson and B. K. Tanner, *Journal of the Chemical Society, Chemical Communications*, 1995, 679-680.
19. A. J. Banister, N. Bricklebank, I. Lavender, J. M. Rawson, C. I. Gregory, B. K. Tanner, W. Clegg, M. R. J. Elsegood and F. Palacio, *Angewandte Chemie International Edition in English*, 1996, **35**, 2533-2535.
20. C. Allen, D. A. Haynes, C. M. Pask and J. M. Rawson, *CrystEngComm*, 2009, **11**, 2048-2050.
21. A. J. Banister, W. Clegg, Z. V. Hauptman, A. W. Luke and S. T. Wait, *Journal of the Chemical Society, Chemical Communications*, 1989, 351-352.
22. G. R. Desiraju, *Angewandte Chemie International Edition in English*, 1995, **34**, 2311-2327.
23. D. A. Haynes, *CrystEngComm*, 2011, **13**, 4793-4805.
24. D. A. Haynes, *Unpublished results*, 2010.
25. A. W. Cordes, R. C. Haddon, R. G. Hicks, R. T. Oakley and T. T. M. Palstra, *Inorganic Chemistry*, 1992, **31**, 1802-1808.
26. G. R. Desiraju, J. J. Vittal and A. Ramanan, *Crystal Engineering: A Textbook*, World Scientific Publishing, Singapore, 2011.
27. J. M. Rawson, *Unpublished Results*, 2011.
28. Jaguar, version 7.8, Schrödinger, LLC, New York, NY, 2011.
29. J. M. Rawson, A. J. Banister and I. Lavender, *Advances in Heterocyclic Chemistry, Vol 62*, 1995, **62**, 137-247.
30. C. V. K. Sharma, *Crystal Growth & Design*, 2002, **2**, 465-474.
31. R. J. Kirkpatrick, *American Mineralogist*, 1975, **60**, 798-814.

Chapter 3: Attempted Synthesis of Novel Dithiadiazolyl Radicals Containing Hydrogen-Bonding Moieties

3.1) Supramolecular Synthons

When Lehn defined supramolecular chemistry in 1988, he proposed the analogy that “supermolecules are to molecules and the intermolecular bond what molecules are to atoms and the covalent bond”.^{1, 2} In addition, Desiraju described crystal engineering as “the new organic synthesis” when he defined the term “supramolecular synthon”.³ From this perspective, the synthesis or design of a crystal structure can be likened to the synthesis of an organic molecule. Traditionally, the term “synthon” was used to describe “key structural features in a target [organic] molecule”.³ Similarly, on the supramolecular level, “synthon” is now used to describe those key structural features that make up a supermolecule or molecular crystal. In addition, these structural features can be “formed and/or assembled by known or conceivable synthetic operations”.^{3, 4} Therefore, a crystal structure can be analysed retrosynthetically in the same way that a target organic molecule often is when designing its synthesis. However, instead of forming covalent bonds, the molecular crystal is built up using combinations of intermolecular interactions between functional groups in the molecular units: supramolecular synthons. In order to design new materials, these synthons should be robust enough to be exchanged between crystal structures predictably.

A selection of some supramolecular synthons is shown in Scheme 3.1,^{3, 5} where **a)-e)** show hydrogen-bonding motifs that form between different functional groups. Furthermore, **a)** and **b)** contain the same functional groups and hydrogen bonding interaction but the geometry and connectivity of the interaction is different. Thus, they are unique synthons. Different types of synthons containing halogen...halogen interactions are shown in **f)** and **g)** and the NO₂...I synthon is shown in **h)**.



Scheme 3.1: Some representative supramolecular synthons: a) a carboxyl dimer, b) a carboxyl chain, c) a hydroxyl ring, d) an OH...NH chain, e) a nitro...amine synthon, f) a Cl...Cl synthon, g) an I...I synthon and h) a nitro...iodo synthon.

This chapter is concerned with the incorporation of hydrogen-bonding moieties onto molecular scaffolds containing a dithiadiazolyl radical functional group that would form suitable supramolecular synthons in the solid state such as **a)-e)** in Scheme 3.1. The incorporation of strong structure-directing synthons such as these could overcome the dimerisation of the dithiadiazolyl radicals in the solid state leading to a molecular crystal capable of exhibiting interesting magnetic properties.

Hydrogen bonds were first mentioned in 1912 by Moore and Winmill in their study of trimethylammonium hydroxide.⁶ Later, Pauling showed, using quantum mechanical theory, that ionic forces must be responsible for the attraction of two atoms involved in a hydrogen bond.⁷ This is because an hydrogen atom only has a 1s orbital and can therefore, only have “one pure covalent bond”.⁸

Pimentel and McClellan provided an early definition of the hydrogen bond:

“...a hydrogen bond exists if 1) there is evidence of a bond, and 2) there is evidence that this bond sterically involves a hydrogen atom already bonded to another atom.”⁹

In a recent review article, Steiner argues that this definition is inadequate as it is too broad: the components of the hydrogen bond are undefined in terms of their chemical nature, polarity and net charge.¹⁰ In addition, the second part of the definition does not

limit the geometry of the interaction except to say that a hydrogen atom must be involved in the interaction. Consequently, some van der Waals contacts such as dipole-dipole interactions could be considered hydrogen bonds, which is incorrect. Instead, Steiner proposes a modified definition:

“An X-H...A interaction is called a “hydrogen bond”, if 1) it constitutes a local bond, and 2) X-H acts as proton donor to A.”

This definition now describes the chemical nature of the participants as those having acid/base characteristics. Furthermore, it excludes pure van der Waals contacts.*

3.1.1) Some characteristics of Hydrogen Bonds

Hydrogen bonds are some of the strongest intermolecular interactions that can be used to engineer a particular crystal structure. Typically, hydrogen bond energies are in the range of 0.2 – 40 kJ mol⁻¹.^{10, 11} Furthermore, hydrogen bonds are directional, meaning that they can provide geometric specificity in the solid state by holding molecules in a particular arrangement. Because the hydrogen bond provides strong and directional intermolecular interactions, its usefulness is vast allowing an element of predictability in the solid state arrangement of molecules.¹⁰

Due to the strength of hydrogen bonds, their incorporation onto scaffolds containing dithiadiazolyl radical functional groups could provide the means to engineer a crystal structure with the potential to exhibit magnetic properties. The directionality of hydrogen bonds could help to orient the molecules in a desired fashion (such as head-to-tail) by forming energetically favourable interactions. Furthermore, the use of planar molecular building blocks could cause the molecules to stack on top of one another and the strength of hydrogen bonds could be sufficient to overcome the dimerisation of the radicals, which has been estimated¹² at -35 kJ mol⁻¹. This could result in bulk magnetic ordering and an extended magnetic exchange pathway through the stacked columns of radicals.

For these reasons, the synthesis of 1,2,3,5-dithiadiazolyl radicals containing functional groups capable of forming hydrogen bonds, specifically hydroxy-, amino- and carboxy-groups in different geometric isomers (Figure 3.1), was attempted. These hydrogen bonding groups were chosen because the supramolecular synthons formed by these moieties with themselves or one another are well known in the literature,¹³ for example, the carboxyl

* This definition is similar to the IUPAC accepted definition quoted in Chapter 1, section 1.1.2.

dimer and chain shown in Scheme 3.1a and b). A supramolecular synthon like the carboxyl dimer could cause a head-to-tail packing arrangement in the solid-state structure of dithiadiazolyl radicals. Considering that radicals containing these functional groups have never been made before, it was decided that synthesising monofunctionalised dithiadiazolyl radicals with the hydrogen-bonding moiety in various geometric isomers (2-, 3- and 4-positions) on a phenyl ring was an appropriate starting point.

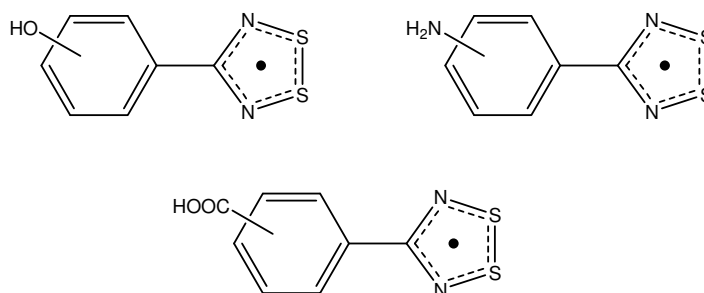
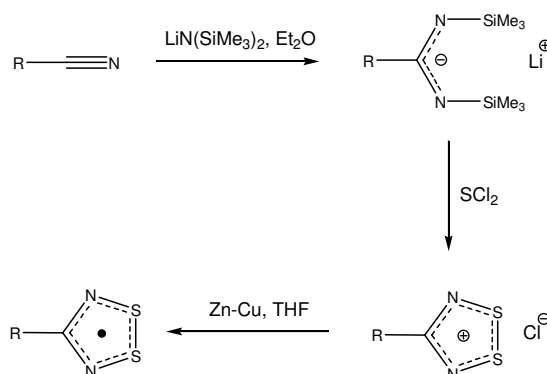


Figure 3.1: Summary of target 1,2,3,5-dithiadiazolyl radicals containing either a hydroxy-, amino- or carboxy- functional group in either the 2-, 3-, or 4- position.

3.2) Synthetic Considerations

The synthesis of 1,2,3,5-dithiadiazolyl radicals containing hydrogen-bonding moieties or functional groups presents some major challenges including the sensitivity of the dithiadiazolyl heterocycle towards air and water,¹⁴ a limited understanding of the reactivity of dithiadiazolyl radicals, and finally, the presence of acidic protons in hydrogen-bonding functional groups. These acidic protons may react with the dithiadiazolyl heterocycle causing its dissociation. Although the general one-pot synthetic procedure to form 1,2,3,5-dithiadiazolyl radicals was discussed in Chapter 1, the reaction steps are briefly shown in Scheme 3.2.



Scheme 3.2: General synthetic procedure to form 1,2,3,5-dithiadiazolyl radicals using LHMDS to form a silylated amidinate. Quenching with SCl₂ yields the dithiadiazolium chloride salt which can be reduced to the radical using Zn-Cu in THF or Ph₃Sb.¹⁵

Despite the simplicity of this procedure, it poses some synthetic challenges that must be considered. Firstly, although HMDS⁻ is used as a nucleophile in this reaction, it is still a very strong base with a pK_a of 26 in THF.^{16, 17} Consequently, only starting nitriles which lack protons in the α -position, relative to the nitrile, can be used to form the silylated amidinate.¹⁴ Thus, aryl-functionalised starting nitriles are suitable for the synthesis of dithiadiazolyl radicals. From a crystal engineering perspective, the phenyl backbone is planar which could allow molecules to stack in the solid state and it contains several positions which can be substituted with various functional groups capable of forming synthons.

Thus, the choice of starting nitrile is quite important: nitriles which already contain the desired hydrogen bonding functional groups are commercially available. However the option to functionalise the phenyl ring after forming the dithiadiazolylum chloride salt, or even the radical, exists, although it is problematic. The reactivity of dithiadiazolyls with various functionalisation agents is largely untested and their sensitivity to water and air must be considered. Therefore, common synthetic routes such as electrophilic aromatic substitution cannot be used due to harsh reaction conditions that would probably destroy the heterocycle. For instance, nitration and sulphonation,¹⁸ using a mixture of concentrated acids, would certainly destroy the dithiadiazolyl heterocycle. In addition, the aluminium trichloride used in Friedel-Crafts¹⁸ alkylation and acylation reactions would possibly cause undesired side reactions to occur. Furthermore, in a nucleophilic aromatic substitution reaction, the nucleophile would probably react with the dithiadiazolylum cation as anion metathesis is known in the salts.¹⁴ The 1,2,3,5-dithiadiazolyl radicals are also readily oxidised to their parent salts¹⁹ which could be induced by the addition of a nucleophile. Lithium-halogen exchange could provide another means to functionalise the phenyl ring provided that a suitable halogen is present on the phenyl ring once the dithiadiazolyl radical is formed. Therefore, the reaction would require a starting nitrile which already contains a suitable halogen on the phenyl ring. The radicals formed from these nitriles are known in the literature and are routinely synthesised using the procedure shown in Scheme 3.2. Nonetheless, a lithium-halogen exchange poses the complication of the stability of the radical species in the presence of such a strong base as butyllithium.

Considering all these factors, it was decided that the synthesis of the target compounds would be attempted on starting nitriles which already contained the desired hydrogen-bonding moiety on the phenyl ring. This would eliminate the difficulty of functionalising the

phenyl ring after forming the salt or radical. Moreover, should the reaction not work initially, the hydrogen-bonding groups could be protected before radical formation and then deprotected once the dithiadiazolyl radical had been formed.

3.3) Initial test reactions

With the above synthetic plan in mind, initial reactions were tested in tandem on a small scale using 4-hydroxy-benzonitrile and 4-carboxy-benzonitrile. Standard reactions using simple starting nitriles usually produce a clear pale yellow to bright orange solution on addition of the nitrile to the LiHMDS solution to form their corresponding amidinates. However, the difficulty with using starting nitriles with unprotected hydrogen-bonding moieties, such as those used in this procedure is that they possess acidic protons which could react with the LiHMDS. Thus, two equivalents of LiHMDS were reacted with the starting nitriles: one equivalent to deprotonate first and a second equivalent to form the amidinate. The solutions were allowed to stir overnight in order to allow time for dissolution and reaction with the LiHMDS. After this time, the solutions appeared pale yellow and milky.

Nonetheless, S₂Cl₂ was added dropwise to the reactions in an attempt to form the dithiadiazolylum chloride salts. TLC could not be used to monitor the reactions as the silylated amidines would probably decompose on the silica plate. S₂Cl₂ was used rather than SCl₂ because it is less harsh than SCl₂. Addition of S₂Cl₂ cause the solutions to modulate through several colour changes before precipitating peach and mustard coloured solids for the reactions with 4-hydroxy- and 4-carboxy-benzonitriles, respectively. LC-MS (ESI) revealed that the dithiadiazolylum chloride salts of 4-hydroxy- and 4-carboxy-benzonitrile were formed (*m/z* = 197 and 225 respectively) but not as the major product.

The positive ion mass spectrum for 4-(4'-hydroxyphenyl)-1,2,3,5-dithiadiazolylum chloride, [1],[†] is shown in Figure 3.2 a) where the dithiadiazolylum ion corresponds to *m/z* = 197: The chlorine counterion is not observed in the spectrum. Loss of a hydroxyl fragment yields *m/z* = 179. The base peak at *m/z* = 137 corresponds to the amidine by the loss of disulphide. The negative ion mass spectrum for [1] is shown in Figure 3.2 b) where the dithiadiazolyl radical is formed in the ionisation chamber and the hydroxyl group is deprotonated resulting in a negatively charged ion corresponding to *m/z* = 196. The base

[†] The numbering of compounds in this chapter is independent of the other chapters. For a list of compounds and their numbers see Appendix B, Section B.2.

peak in the negative spectrum corresponds to the deprotonated starting material, 4-hydroxy-benzonitrile.

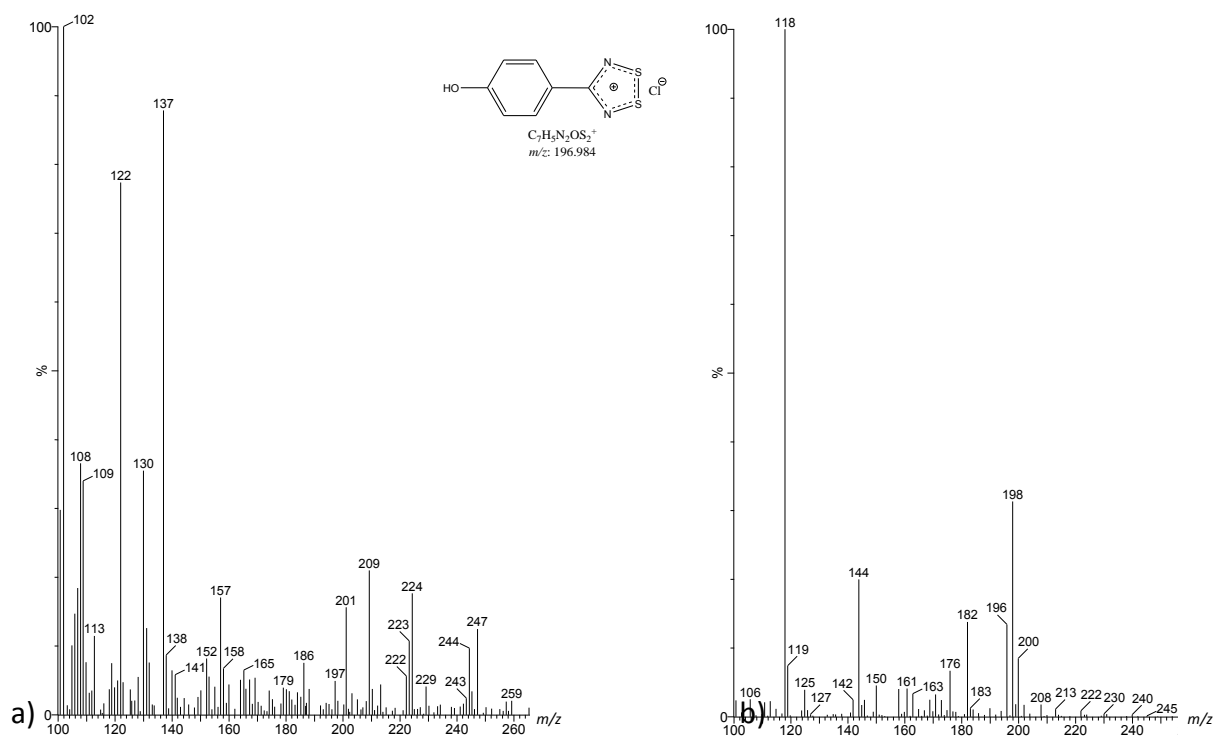


Figure 3.2: ESI Mass spectra of a) [1] in positive mode and b) [1] in negative mode.

The positive ion mass spectrum for 4-(4'-carboxyphenyl)-1,2,3,5-dithiadiazolylium chloride, [2], is shown in Figure 3.3 a) where the dithiadiazolylium ion corresponds to m/z = 224. The base peak at m/z = 165 corresponds to the amidine by the loss of disulphide. The negative ion mass spectrum for [2] is shown in Figure 3.3 b) where the base peak at m/z = 146 corresponds to the starting material, 4-carboxy-benzonitrile. The peak at m/z = 178 corresponds to the loss of the carboxyl group from [2].

It should be noted that the mass spectra for [1] and [2] show numerous unidentifiable peaks and thus, it was assumed that the salts had formed in very low quantities.

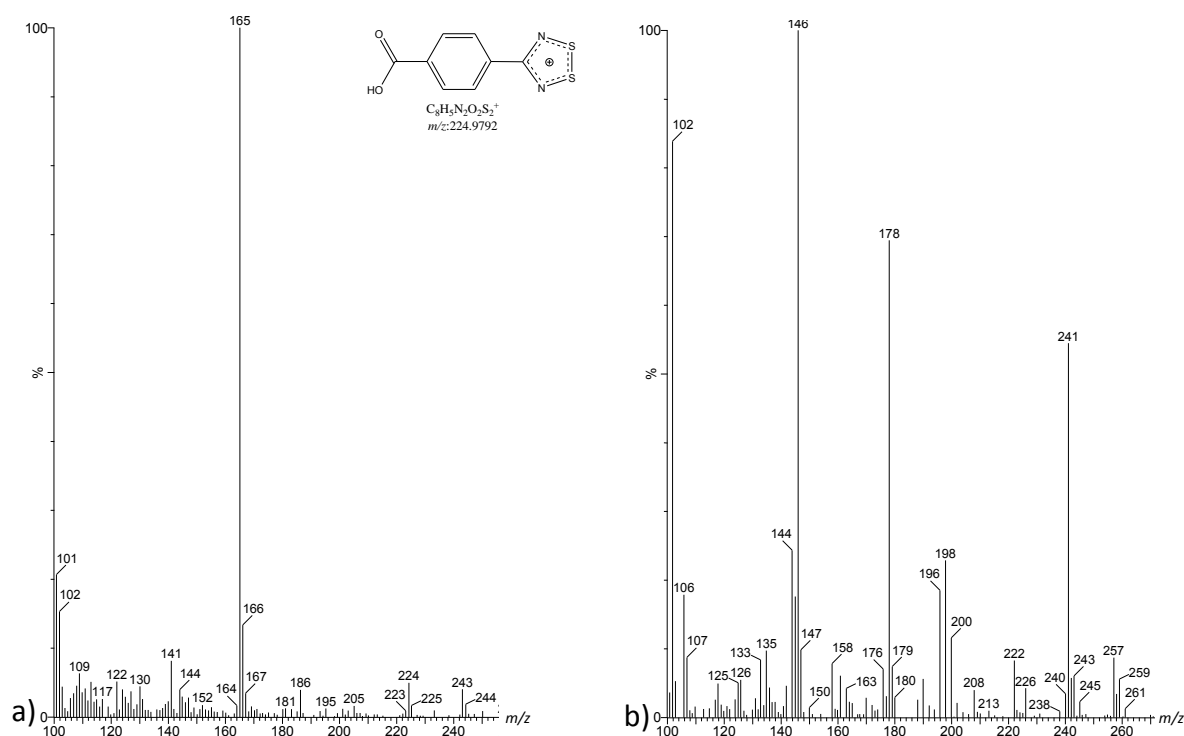


Figure 3.3: ESI Mass spectra of a) [2] in positive mode and b) [2] in negative mode.

In order to optimise the reaction, it was thought that using an additive would improve the yield. Such an additive should either make the nitrile more electrophilic or make the LiHMDS a better nucleophile, therefore making nucleophilic attack on the nitrile more likely. Thus, it was decided that a Lewis base such as hexamethylphosphoramide (HMPA) or tetramethylethylenediamine (TMEDA) could be used to complex to the lithium ion in LiHMDS, consequently making the $(\text{Me}_3\text{Si})_2\text{N}^-$ a better nucleophile.

The reaction with 4-carboxy-benzonitrile was thus repeated using HMPA as an additive. HMPA is able to act as a Lewis base and complex to metal ions in solution. This property is useful as HMPA can coordinate to lithium ions in solution, thus increasing the nucleophilicity of $(\text{Me}_3\text{Si})_2\text{N}^-$. It was observed that the starting nitrile dissolved much more easily in the LiHMDS-HMPA solution. This is attributed to the fact that HMPA is also an aprotic polar solvent which is often used to help polar molecules dissolve in non-polar solvents. The solution was stirred overnight producing a clear pale yellow solution. The dropwise addition of S_2Cl_2 to this solution caused a series of vivid colour changes, ultimately precipitating a yellow-green solid. In addition, a liquid which was immiscible with diethyl ether was observed. The solution was filtered and the solid was dried *in vacuo* yielding a sticky orange residue. The residue was analysed by LC-MS (ESI) which showed that the desired dithiadiazolylum chloride salt, [3] had been formed (Figure 3.4). The dithiadiazolylum ion

can be seen at $m/z = 225.3$ with the loss of sulphur yielding $m/z = 193.2$. The base peak corresponds to the loss of a carboxyl group from [3] ($m/z = 180.2$). The peaks from $m/z = 359.3$ upwards may correspond to the possible side products shown in Scheme 3.3.

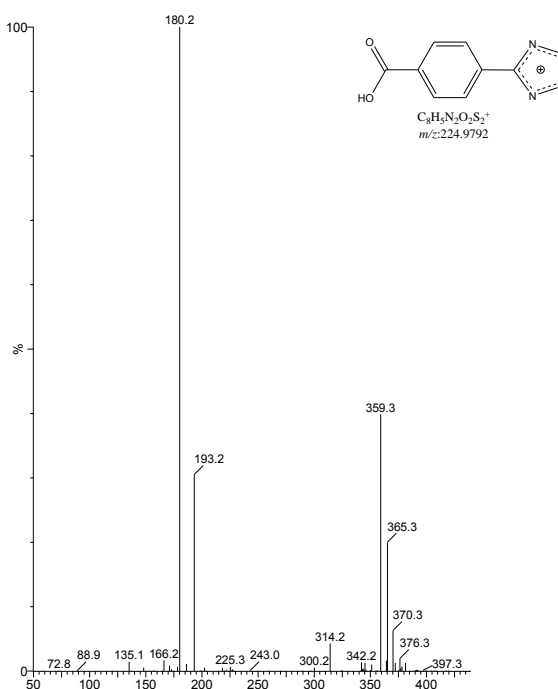
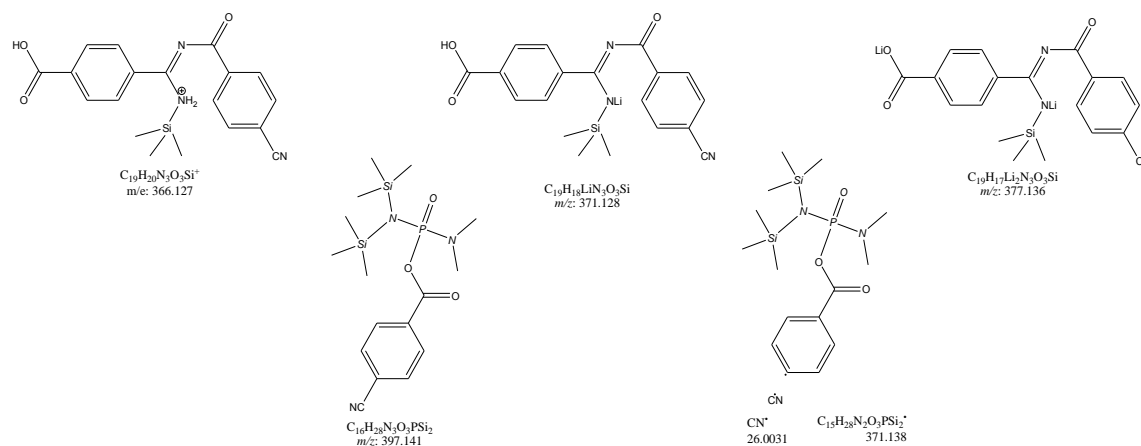


Figure 3.4: Mass spectrum of the product of the reaction to form [3] using HMPA as an additive to improve the nucleophilicity of LiHMDS.

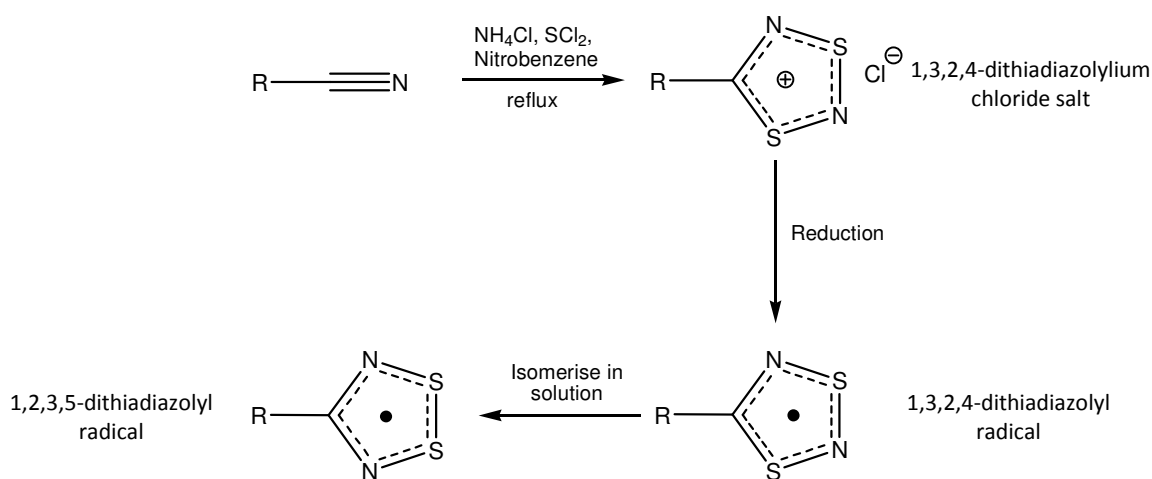


Scheme 3.3: Possible side products observed in the mass spectrum (Figure 3.4) from the attempted synthesis of [3] using HMPA as an additive.

As expected, the synthesis of dithiadiazolyl radicals on starting nitriles containing hydrogen-bonding moieties was not trivial. Thus, it was decided that an alternate route to form these dithiadiazolyl radicals needed to be investigated.

3.4) An Alternate Synthetic Route

In a 1979 paper, Alange *et al.* describe the synthesis of a number of 1,2,3,5-dithiadiazolylum chloride salts by refluxing the appropriate starting nitrile in a suspension of ammonium chloride (NH_4Cl) in sulphur dichloride (SCl_2) and nitrobenzene (Scheme 3.4).²⁰ Mechanistically, Alange *et al.* propose that thiazyl chloride (NSCl) is formed *in situ* which then reacts with excess sulphur in the solution to form dithiazyl chloride (SNSCl). It is this which then adds to the nitrile via a cycloaddition mechanism to form the 1,3,2,4-dithiadiazolylum chloride salt. 1,3,2,4-dithiadiazolylum chloride salts are then reduced to their corresponding radicals which readily isomerise to the 1,2,3,5-dithiadiazolyl radical isomers in solution.²¹⁻²³



Scheme 3.4: General dithiadiazolyl heterocycle synthetic procedure to form dithiadiazolyl radicals using NH_4Cl and SCl_2 in nitrobenzene.²⁰

This procedure appeared to be quite promising as the ammonium chloride would prevent the deprotonation of the hydrogen bonding moieties. This is advantageous as neither the solubility nor the electronic properties of the starting nitriles ought to be affected. Therefore, this procedure offers a potential simple, single step method to form the dithiadiazolylum chloride salts, although product yields are reported to be quite low.

A scaled-down test reaction was performed using benzonitrile as a starting material. The crude sample of the 4-phenyl-dithiadiazolylum chloride salt was analysed by mass spectrometry,[‡] which revealed the positively charged dithiadiazolylum ion at $m/z = 182$

[‡] The sample was analysed using electron spray ionisation (ESI) in the positive ion mode using the ASAP probe which allows the sample to be inserted directly into the ionisation chamber in a solvent-free manner.

indicating that the reaction was successful in synthesising 4-phenyl-1,3,2,4-dithiadiazolium chloride, [4] (Figure 3.5).

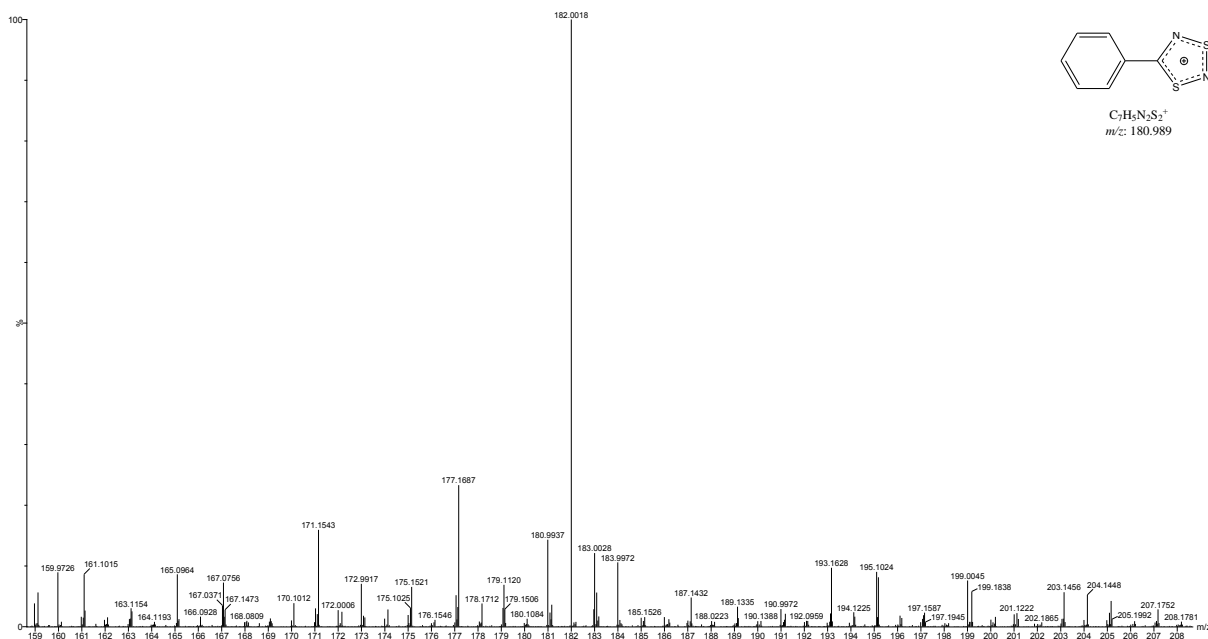


Figure 3.5: Mass spectrum of the 4-phenyl-1,3,2,4-dithiadiazolium chloride salt, [4], formed using NH_4Cl and SCl_2 in nitrobenzene.

This reaction procedure was attempted using several starting nitriles containing hydrogen-bonding groups. The first of these was the reaction with 4-carboxy-benzonitrile. The reaction mixture was refluxed for 7 hours, after which it was cooled resulting in the formation of an orange solid. The orange solid was analysed by MS (Figure 3.6) to determine the nature of the product. Interpretation of the analysis revealed that the desired salt, 4-(4'-carboxyphenyl)-1,2,3,5-dithiadiazolium chloride, [5], had formed but in a very low yield. The dithiadiazolium ion can be seen at $m/z = 224$. Loss of the carboxyl group yields the peak at $m/z = 179$. In addition, the peak at $m/z = 164$ corresponds to the amidine. However, the two major peaks in the MS are $m/z = 124$ and 338. The $m/z = 124$ peak corresponds to two possible analytes, nitrobenzene and $[S_3N_2]^+$, which forms as a by-product.

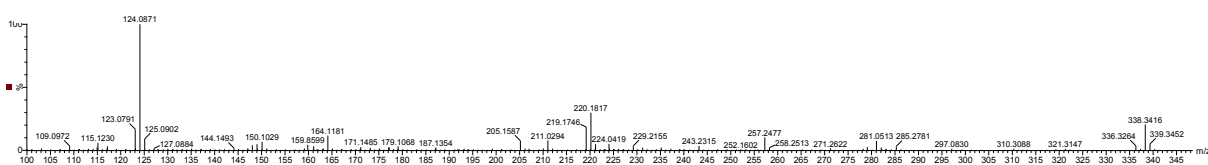


Figure 3.6: MS of the product of the reaction of 4-carboxy-benzonitrile with NH_4Cl and SCl_2 in nitrobenzene yielding [5]

Several peaks, including $m/z = 205$, 211 and 338 are observed in this spectrum and the spectra of subsequent reactions. These peaks are attributed to possible sulphur-nitrogen

side products that could form during the reaction between NH_4Cl and SCl_2 such as the one shown in Figure 3.7.

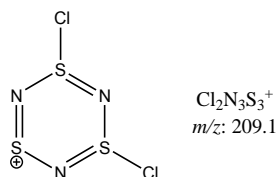


Figure 3.7: A possible side product that could form in the reaction using NH_4Cl and SCl_2 . Other possible thiazyl compounds may account for the peaks at $m/z = 205$ and 338 .

The reaction using NH_4Cl and SCl_2 was attempted with the 4-hydroxy-benzonitrile. The mixture was refluxed for 5 hours after which it was cooled, precipitating a dark purple powder which was dried *in vacuo*. The sample was analysed by MS (Figure 3.8) which revealed the formation of the protonated dithiadiazolyl heterocycle [6] by the presence of the molecular ion peak at $m/z = 198$. However, $^1\text{H-NMR}$ analysis showed an unidentifiable and intractable impurity which obscured the aromatic region of the spectrum. Consequently, the product of this could not be identified by $^1\text{H-NMR}$ analysis.

Sublimation of the powder produced no crystals and reduction reactions with Ph_3Sb were unsuccessful. EPR analysis of the product showed no unpaired electrons indicating that a radical had not formed.

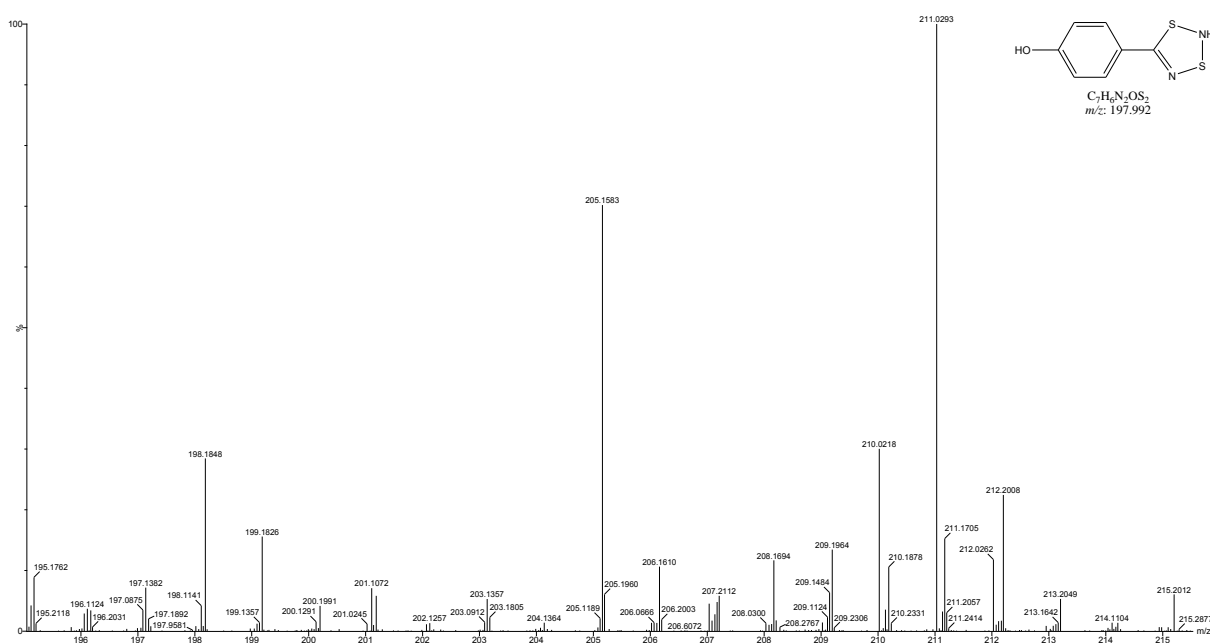


Figure 3.8: MS of the product mixture of the reaction of 4-hydroxy-benzonitrile with NH_4Cl and SCl_2 in nitrobenzene yielding [6]. The peaks at $m/z = 205$ and 211 are attributed to thiazyl side products formed between NH_4Cl and SCl_2 .

In addition, the procedure using NH_4Cl and SCl_2 in nitrobenzene was attempted with the 4- and 2-amino-benzonitrile starting materials. The reaction with the 2-amino-benzonitrile gave a similar result to the 4-hydroxy-derivative. The product obtained was also a dark purple powder. $^1\text{H-NMR}$ analysis yielded a similar result to the reaction with 4-hydroxy-benzonitrile: the presence of an unidentifiable and intractable impurity obscuring the aromatic region preventing the identification of the product. Sublimation and reduction reactions were unsuccessful in producing crystals or radicals, respectively.

In contrast to the previous reactions using NH_4Cl and SCl_2 , the experiment with 4-amino-benzonitrile yielded a bright orange powder reminiscent of the dithiadiazolylum chloride salts. MS (Figure 3.9) showed the molecular ion peak of the dithiadiazolyl heterocycle, [**8**], at $m/z = 195$ (M-H)⁺. Furthermore, loss of the amine yields the peak at $m/z = 178$. Fragmentation resulting in the loss of a sulphur or disulphide yields peaks at $m/z = 164$ and 133 , respectively. The peak at $m/z = 153$ may correspond to some sulphur-nitrogen side product such as HN_4S_3^+ shown adjacent to the peak. Reduction reactions proceeded similarly to known reductions by a colour change from orange to purple. However, crystals of this purple product could not be grown by sublimation. $^1\text{H-NMR}$ analysis was performed on this product yielding the same results as before: an intractable impurity in the aromatic region. Consequently, $^1\text{H-NMR}$ and MS disagreed regarding the formation of the dithiadiazolyl from the reaction of NH_4Cl and SCl_2 with 4-amino-benzonitrile in nitrobenzene.

All these reactions using NH_4Cl and SCl_2 in nitrobenzene to form dithiadiazolyl radicals essentially produced intractable products with spectra that are difficult to interpret. Moreover, it is unlikely that the radical had formed in any of these cases as the EPR spectrum for the 4-hydroxy- derivative showed no signal corresponding to an unpaired electron.

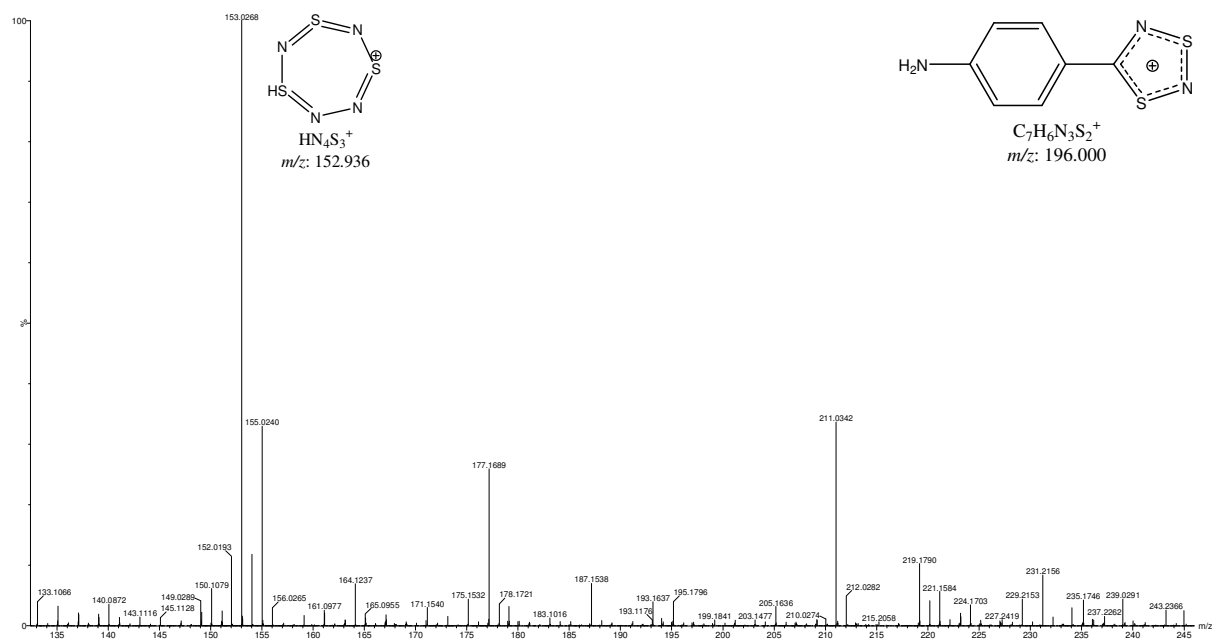


Figure 3.9: Mass spectrum of the product of the reaction between 4-amino-benzonitrile, NH_4Cl and SCl_2 in nitrobenzene to yield [8]. Loss of a proton from [8] would yield the peak at $m/z = 195.2$ and loss of the amine would yield the peak at $m/z = 177.2$. A possible structure for the base peak at $m/z = 153$ is shown.

3.5) Attempted synthesis with protected hydrogen-bonding groups

Earlier, it was mentioned that the hydrogen-bonding groups could be protected before the synthesis of the dithiadiazolyl heterocycle. Thereafter, they could be deprotected affording the desired product. The possibility of forming dithiadiazolyl radicals with protected hydrogen bonding groups was investigated as a means towards forming the target compounds.

The protection of hydrogen-bonding functional groups is well known and regularly used synthetically.²⁴ However, the choice of which protecting group to use, considering the sensitivity of dithiadiazolyl radicals, is a difficult one as the protecting group needs to be removed to obtain the final product. While researching various protecting groups for alcohols, amines and carboxylic acids, a paper by DiLauro *et al.*²⁵ was found which described the cleavage of oxygen-silicon bonds under inert conditions using a catalytic amount of cesium fluoride. Alcohols are regularly protected in the literature by using various silicon protecting groups but in order to deprotect them, aqueous conditions are often required.²⁶ Therefore, this method of inertly deprotecting hydroxyl groups provided a possible means to synthesise the desired products.

Amines can sometimes be protected using silicon protecting groups although the nitrogen-silicon bond is quite labile and the protecting group often dissociates during the work-up of the reaction. Furthermore, primary amines have two protons and thus, need to be protected twice for complete protection. However, using silicon protecting groups often results in the protection of the amine only once, which in most cases is sufficient. Therefore, the protection of hydrogen-bonding moieties, specifically amines and alcohols using trimethylsilyl chloride (TMSCl), was investigated.

Carboxylic acids are not usually protected by silylation, however, an alternate method was envisioned for the synthesis of 4'-carboxyphenyl-1,2,3,5-dithiadiazolyl, namely, a lithium halogen exchange with 4'-bromophenyl-1,2,3,5-dithiadiazolyl and subsequent quench with CO₂ to form the carboxylate salt (Section 3.7).

Up until this point, the 3- derivatives of the starting nitriles had been avoided due to their differing electronic properties in comparison to the 2- and 4- derivatives: resonance of electrons between the hydrogen-bonding moieties and the nitrile cannot occur in the 3- derivatives. Consequently, it was decided that protection of the 3- isomers of the hydroxy- and amino-benzonitrile starting nitriles should be investigated.

3.5.1) Protection of 3-hydroxy-benzonitrile

The protection of 3-hydroxy-benzonitrile was performed by refluxing it with triethylamine (Et₃N) and trimethylsilyl chloride (TMSCl) in dichloromethane (DCM) overnight. The DCM was then removed *in vacuo* and the crude residue analysed by ¹H-NMR[§] to determine the completeness of the reaction and the purity of the product, 3-trimethylsiloxy-benzonitrile, [9]. The spectrum showed Et₃N and silicon grease impurities. However, the reaction appeared complete by NMR due to the trimethylsilyl protons integrating for 9.58 protons relative to four aromatic protons. Consequently, liquid extraction was investigated as a means to purify [9].

Benzene and hexane were compared as extraction solvents by ¹H-NMR. Non-polar solvents were chosen as the Et₃N·HCl salt would be insoluble in them and silylation generally decreases the polarity of a molecule,²⁴ theoretically allowing it to be soluble in non-polar solvents. After mixing the crude product mixture with the applicable organic solvent, the white crystalline material that remained behind was filtered from the mother liquor. The

[§] Samples were dissolved in CDCl₃ for ¹H-NMR analysis.

organic extract was dried *in vacuo* yielding a clear oil. Both the oil and the crystalline material were analysed by $^1\text{H-NMR}$ to determine the efficacy of the extraction and the location of the product. The white crystalline material remaining after extraction with benzene or hexane was shown to be $\text{Et}_3\text{N}\cdot\text{HCl}$. In addition, the 3-trimethylsilyloxy-benzonitrile appeared to have been extracted entirely from the solid material by both benzene and hexane.

Figure 3.10 shows the $^1\text{H-NMR}$ spectrum of the oil, [9], obtained from the benzene extract after drying *in vacuo*. The spectrum shows complete separation of the silylated starting nitrile from the Et_3N . However, some unidentifiable impurities can also be seen in the spectrum. These are assumed to originate from the benzene used for the extraction as they are present in all the spectra where benzene was used for extraction whereas they are absent in the hexane extracts and the white solid remaining after hexane extraction. The integration of the spectrum is difficult as the CDCl_3 signal appears amongst the aromatic protons. Nonetheless, the integration of the peaks was referenced to an identifiable triplet in the aromatic region corresponding to the proton in the 3-position relative to both the trimethylsilyloxy- and cyano-groups. Despite this, the trimethylsilyloxy-protons integrate for less than the expected nine protons. This could indicate some degradation of the desired product.

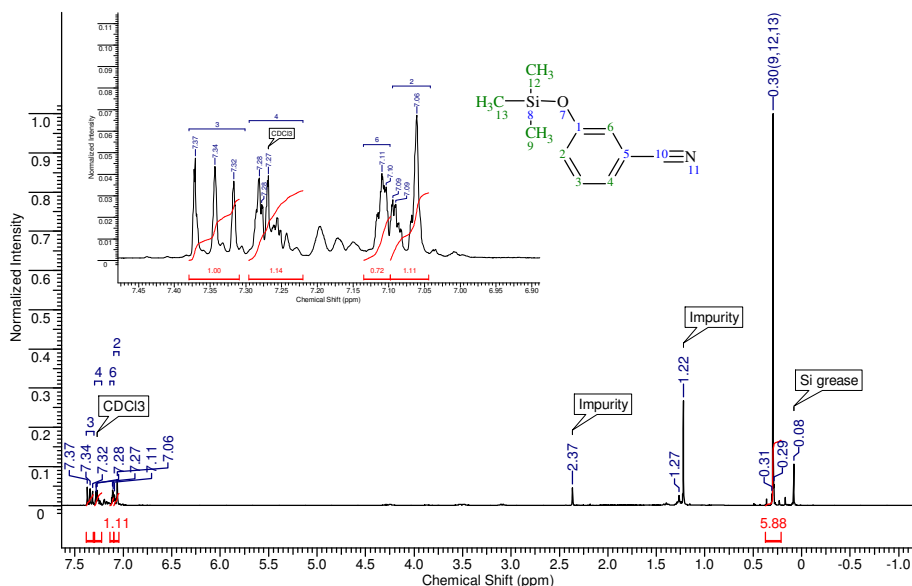


Figure 3.10: $^1\text{H-NMR}$ spectrum of the oil obtained after drying benzene extract *in vacuo*. The insert is an expansion of the aromatic region showing proton assignments. The peak at 0.30 ppm corresponds to the TMS methyl protons.

In comparison, the $^1\text{H-NMR}$ spectrum of the hexane extract is shown in Figure 3.11 revealing the product [9] with only a single impurity of silicon grease. The integration of this spectrum was referenced to two protons in the aromatic region whose signal does not overlap with the CDCl_3 signal. The aromatic signal corresponding to aromatic protons and the CDCl_3 integrates, in total, for 2.25 protons. In addition, the trimethylsiloxy-proton signal integrates for 9.58 protons corresponding quite well with the expected nine protons. Consequently, it was decided that hexane extraction was the most effective in purifying the product, [9].

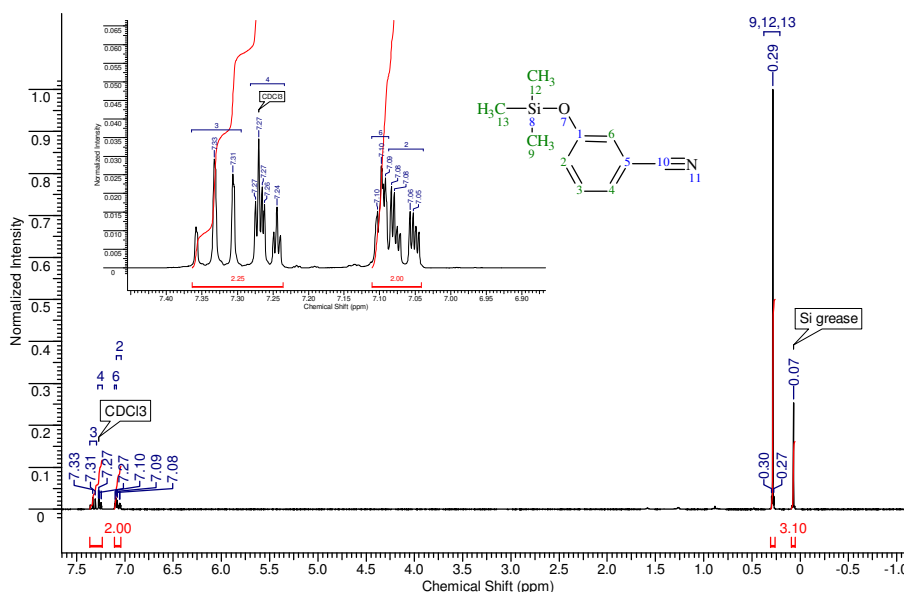


Figure 3.11: $^1\text{H-NMR}$ spectrum of the oil obtained after drying hexane extract *in vacuo*. The insert is an expansion of the aromatic region showing proton assignments. The peak at 0.29 ppm corresponds to the TMS methyl protons. Again, the solvent residual peak coincides with one of the aromatic protons in the 3-trimethylsiloxy-benzotrile.

The extraction was then repeated on the bulk crude material using hexane and the purity of the oil, [9], was confirmed by $^1\text{H-}$ and $^{13}\text{C-NMR}$ (Figure 3.12 and Figure 3.13). The $^1\text{H-NMR}$ spectrum shows a small amount of impurity upfield corresponding to silicon grease. In addition, the $^{13}\text{C-NMR}$ spectrum shows some degradation of [9] to the starting nitrile by the presence of some small peaks in the aromatic region. It is possible that [9] degraded during the acquisition of the $^{13}\text{C-NMR}$ spectrum due to the slight acidity of CDCl_3 .

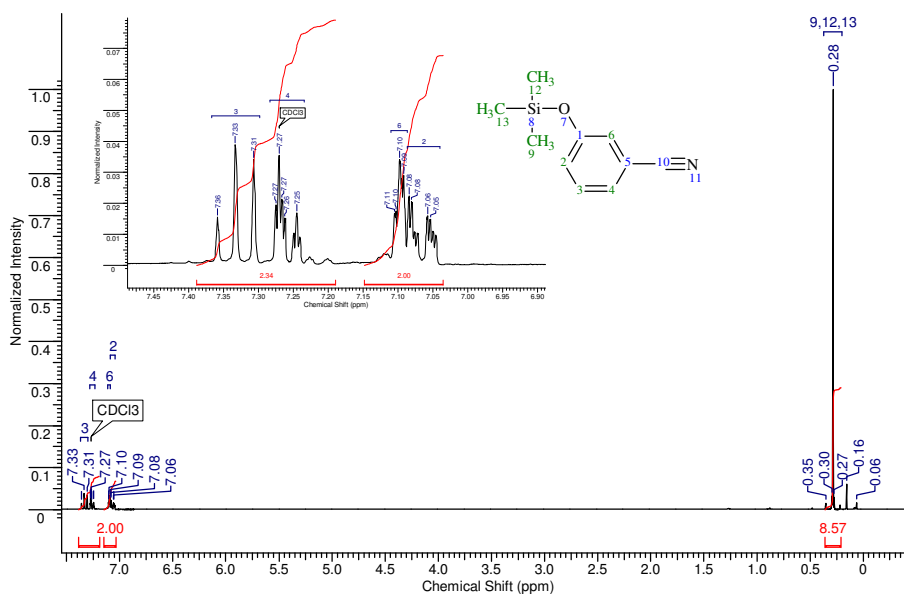


Figure 3.12: $^1\text{H-NMR}$ spectrum of [9] purified by hexane extraction. The insert is an expansion of the aromatic protons: assignments are shown. In addition, the peak at 0.28 ppm corresponds to the TMS methyl protons.

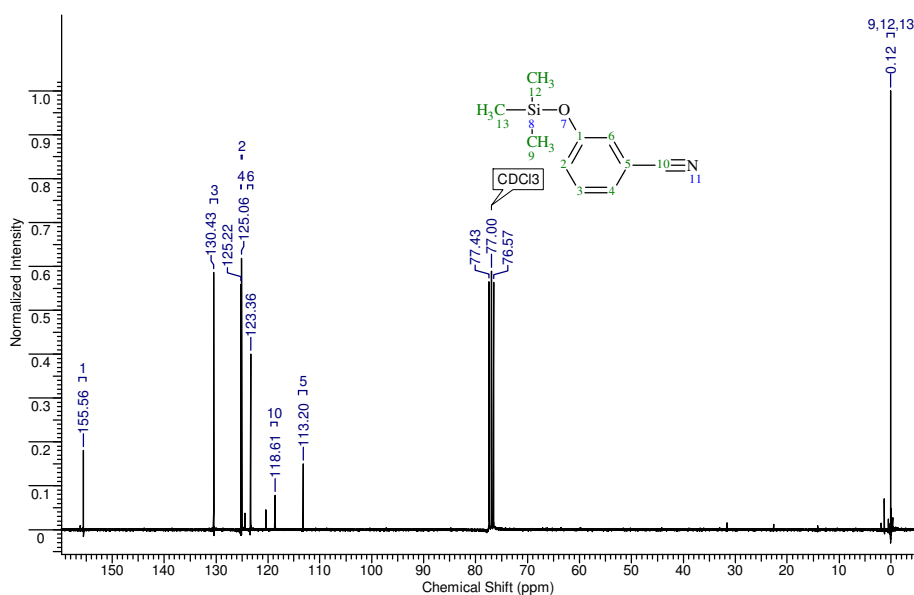


Figure 3.13: $^{13}\text{C-NMR}$ spectrum of [9] purified by hexane extraction. Assignments are shown.

3.5.2) Synthesis of 4-(3'-trimethylsilyloxyphenyl)-1,2,3,5-dithiadiazolyl

A solution of LiHMDS-TMEDA, made *in situ* from HMDS and *n*-butyllithium, was added to a solution of the clear oil [9] in diethyl ether. Immediately, a white precipitate was formed resulting in a milky solution. In order to aid solubility, an equivalent of TMSCl was added to form the persilylated amidine and the solution was stirred overnight. Quenching with SCl_2 resulted in a bright orange precipitate forming from the milky off-white solution. The precipitate was then filtered and washed with diethyl ether. Drying *in vacuo* yielded a light

orange-yellow powder which was shown by mass spectrometry (Figure 3.14) to be the desired dithiadiazolylum chloride salt, [10]. Reduction reactions with Ph_3Sb proceeded similarly to standard reactions as the colour changed from orange-yellow to purple. However, crystals could not be grown by sublimation as a sticky residue was obtained. Due to the silylation of the product, it was theorised that 4-(3'-trimethylsilyloxyphenyl)-1,2,3,5-dithiadiazolyl, [11], was, in fact, an oil at room temperature. Therefore, the reduction was attempted with Zn-Cu couple in THF on a larger scale. The red-purple solution was filtered off and dried *in vacuo* to yield a viscous red-purple oil which was shown by mass spectrometry (Figure 3.15) and electron paramagnetic resonance (Figure 3.16) analysis to be the desired radical, [11].

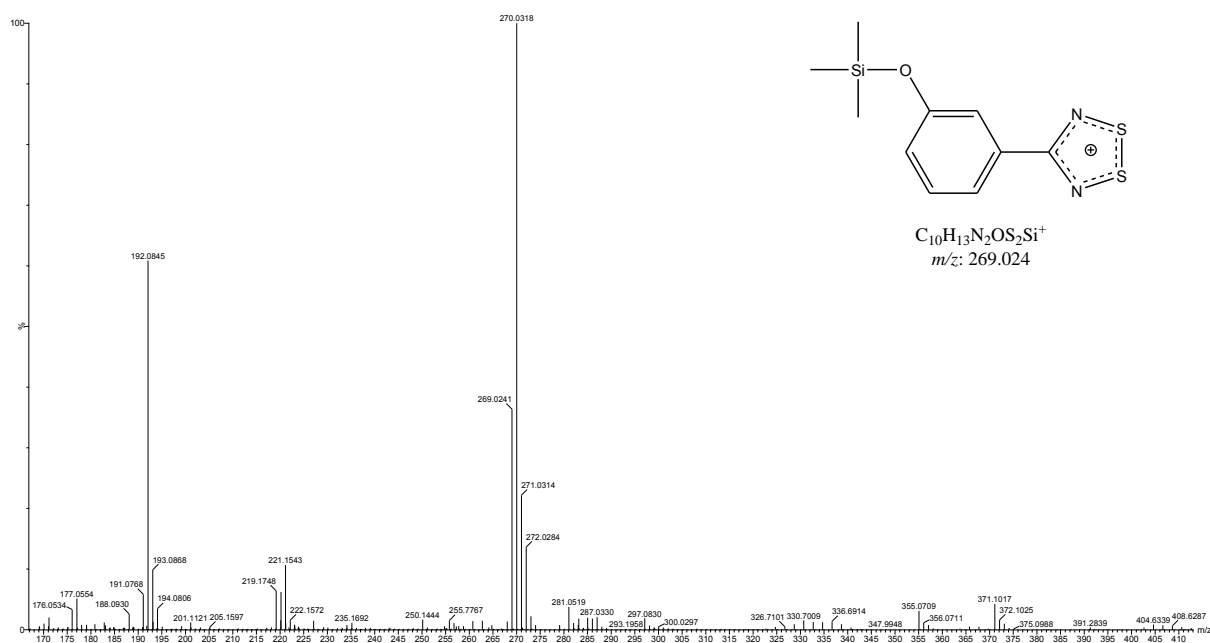


Figure 3.14: Mass spectrum showing the dithiadiazolylum ion of the desired salt: 4-(3'-trimethylsilyloxyphenyl)-1,2,3,5-dithiadiazolylum chloride, [10].

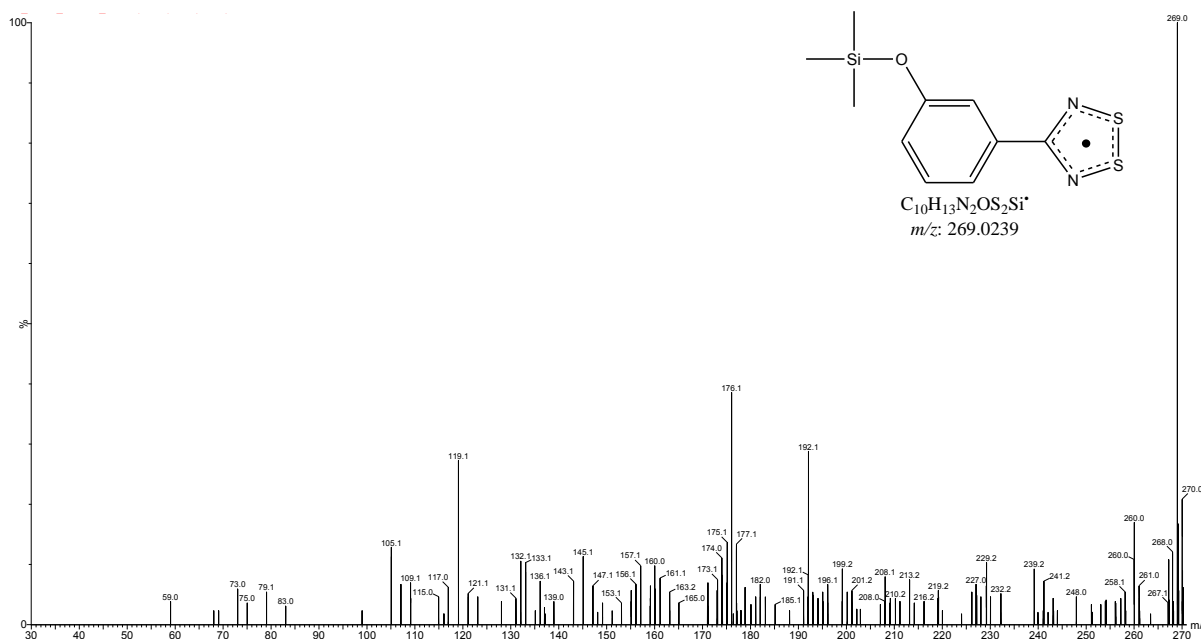


Figure 3.15: Mass spectrum showing the fragmentation pattern of the 4-(3'-trimethylsilyloxyphenyl)-1,2,3,5-dithiadiazolyl radical, [11].

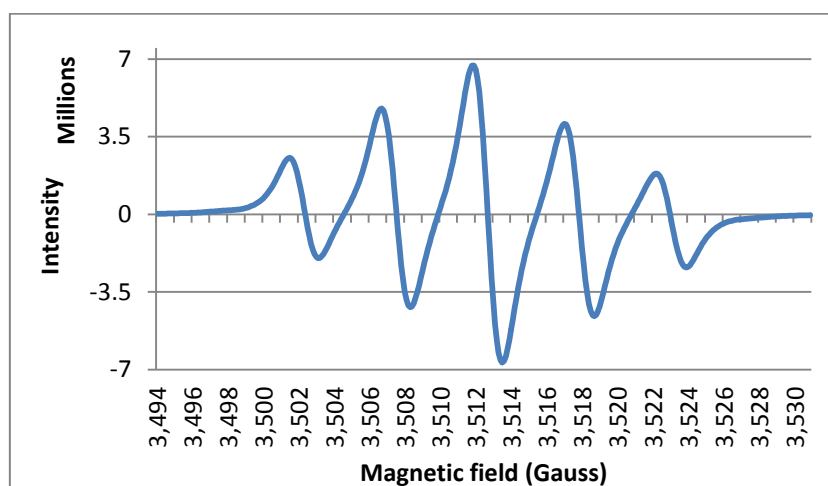


Figure 3.16: EPR spectrum of the radical: 4-(3'-trimethylsilyloxyphenyl)-1,2,3,5-dithiadiazolyl, [11] (CH_2Cl_2 : $g = 2.010$, $a_N = 5.1$ G).

3.5.3) Synthesis of 4-(4'-trimethylsilyloxyphenyl)-1,2,3,5-dithiadiazolyl

Due to the success of forming the radical on the protected 3- derivative, a similar procedure was followed using the 4-hydroxy-benzonitrile starting material. The starting nitrile was silylated using TMSCl and imidazole (instead of Et_3N) in DCM. Thereafter, the silylated product was purified by hexane extraction. The hexane extract was filtered from a white solid which was shown by 1H -NMR analysis to contain imidazole. Drying the hexane extract *in vacuo* yielded a clear oil which 1H -NMR analysis showed to be 4-trimethylsilyloxy-

benzonitrile, [12], (Figure 3.17) with some hexane. This product was then used in the subsequent synthetic steps.

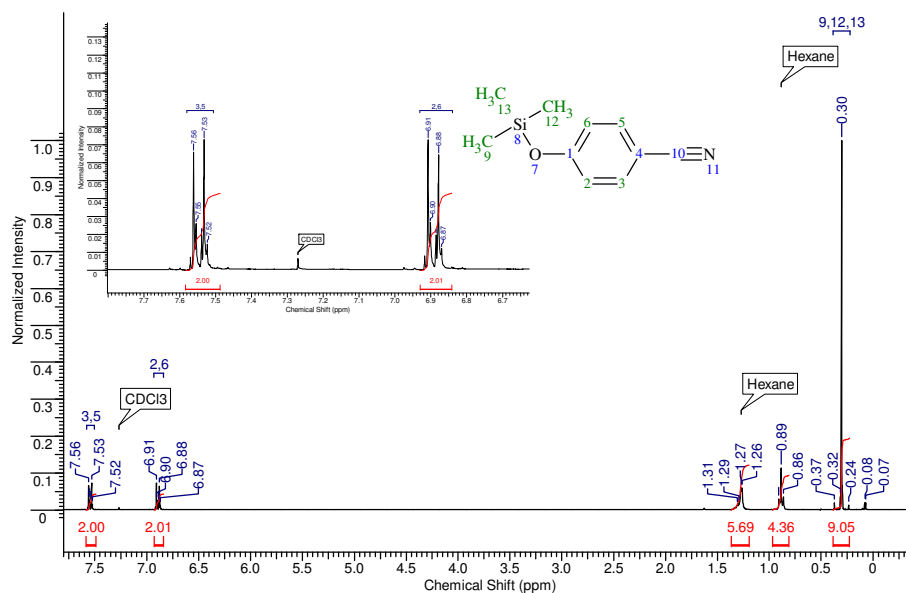


Figure 3.17: $^1\text{H-NMR}$ of the hexane extract showing [12] with some hexane impurity. The insert is an expansion of the aromatic region to clarify the proton assignments.

In order to form the dithiadiazolylum chloride salt of [12], it was reacted with a solution of LiHMDS, TMEDA and TMSCl. A milky white solution was observed by the immediate formation of a white precipitate. Quenching the reaction with SCl_2 resulted in a bright orange precipitate. This solid was worked up as before yielding a light orange-pink powder which was confirmed by MS (Figure 3.18) to be the desired dithiadiazolylum chloride salt, [13]. The dithiadiazolylum ion is clearly seen at $m/z = 270$. The peaks at $m/z = 192$ and 176 correspond to the loss of SSN and NSSN, respectively.

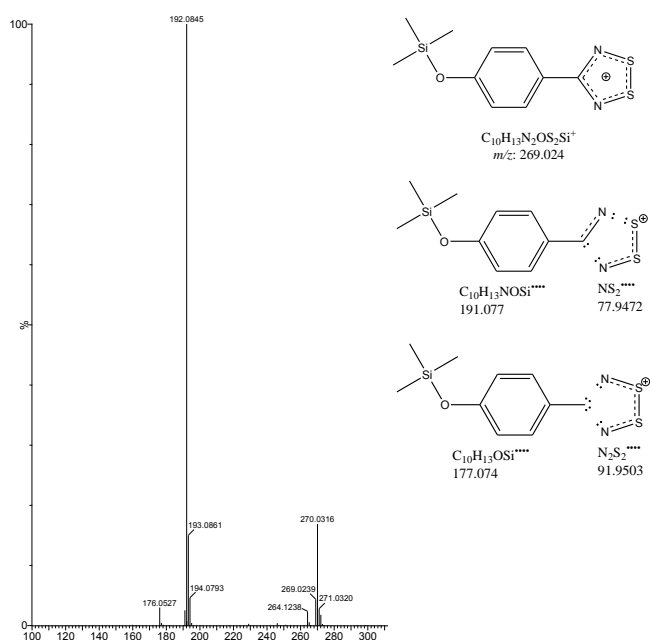


Figure 3.18: Mass spectrum of the desired salt: 4-(4'-trimethylsilyloxyphenyl)-1,2,3,5-dithiadiazolium chloride, [13].

Reduction of the salt was performed using Zn-Cu couple in THF yielding a dark red-purple oil. Mass spectrometry (Figure 3.19) and electron paramagnetic resonance (Figure 3.20) revealed the oil to be the desired 4-(4'-trimethylsilyloxyphenyl)-1,2,3,5-dithiadiazolyl radical, [14]. The dithiadiazolium ion is barely visible at $m/z = 270$ and the base peak at $m/z = 192$ corresponds to the loss of SSN.

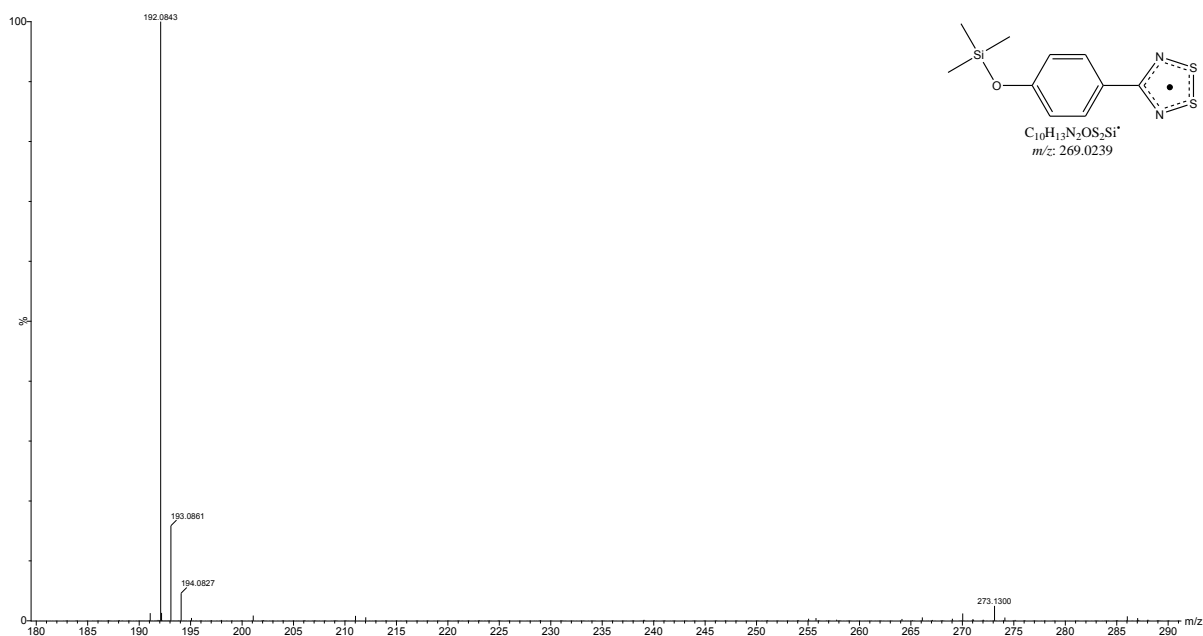


Figure 3.19: Mass spectrum of the 4-(4'-trimethylsilyloxyphenyl)-1,2,3,5-dithiadiazolyl, [14] showing the molecular ion at $m/z = 270$ and the loss of SSN at $m/z = 192$.

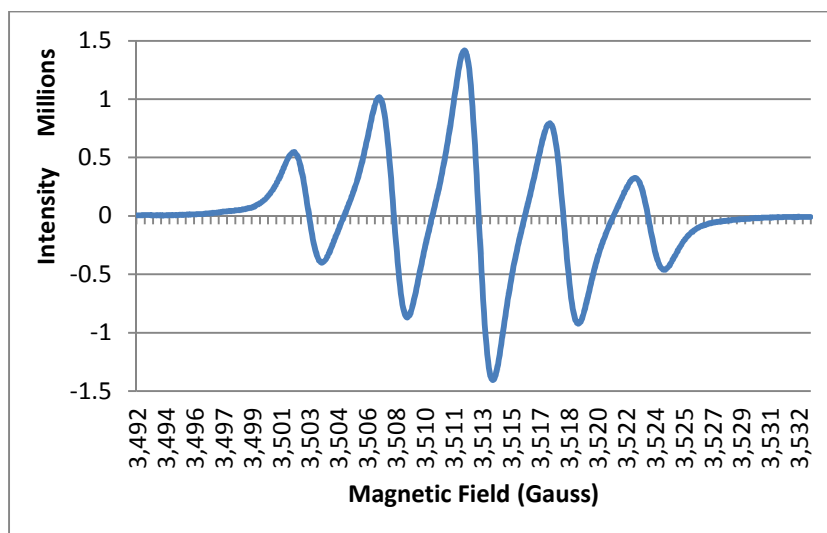


Figure 3.20: EPR spectrum of the desired radical: 4-(4'-trimethylsilyloxyphenyl)-1,2,3,5-dithiadiazolyl, [14]. (CH_2Cl_2 , $g = 2.010$, $a_N = 5.2 \text{ G}$)

3.5.4) Protection of 3-amino-benzonitrile

Although the use of silyl derivatives to protect amines is not very common due to the sensitivity of the silicon-nitrogen bond towards moisture, they are stable when synthesised and used under anhydrous conditions.^{27, 28} In addition, silyl-amines are readily deprotected in the presence of silyl ethers.²⁹ Therefore, protection of the amine with the trimethylsilyl (TMS) group was a good starting point.

3-Amino-benzonitrile was protected by refluxing it in a solution of Et_3N and TMSCl in DCM overnight. $^1\text{H-NMR}$ of the crude product revealed that the amine was only protected once forming 3'-trimethylsilaza-benzonitrile, [15]. This was not surprising due to the bulky size of the TMS group.

The product, [15], was extracted with hexane from the crude reaction mixture. The clear oil obtained was analysed by $^1\text{H-}$ (Figure 3.21) and $^{13}\text{C-NMR}$ (Figure 3.22) to determine its purity before continuing to form the dithiadiazolyl heterocycle. The $^1\text{H-NMR}$ spectrum shows some trace impurities including some silicon grease. The $^{13}\text{C-NMR}$ spectrum shows some peaks corresponding to hexane and some trace peaks in the aromatic region which could have arisen from the degradation of [15] (due to the slight acidity of CDCl_3) to the unprotected nitrile.

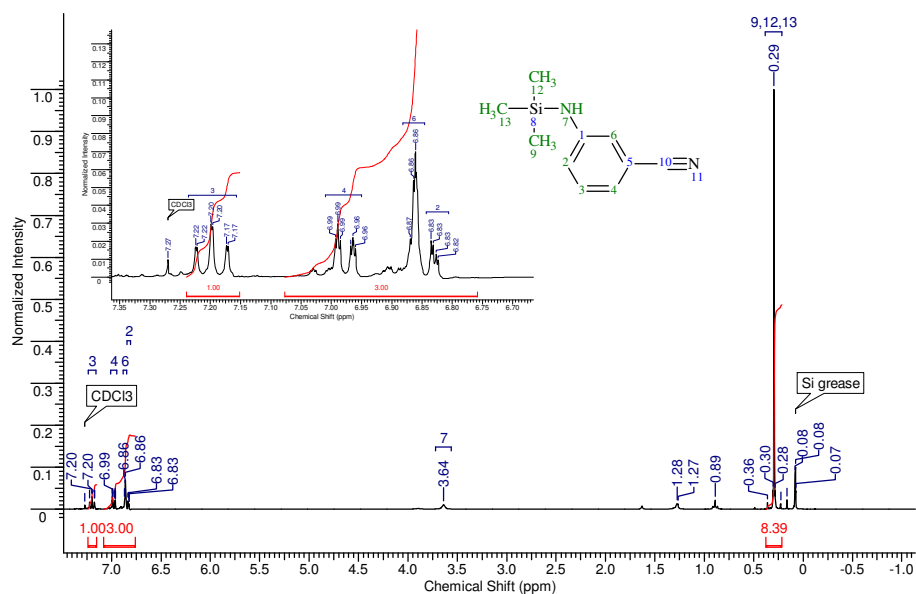


Figure 3.21: ¹H-NMR spectrum of [15]. The insert is an expansion of the aromatic region.

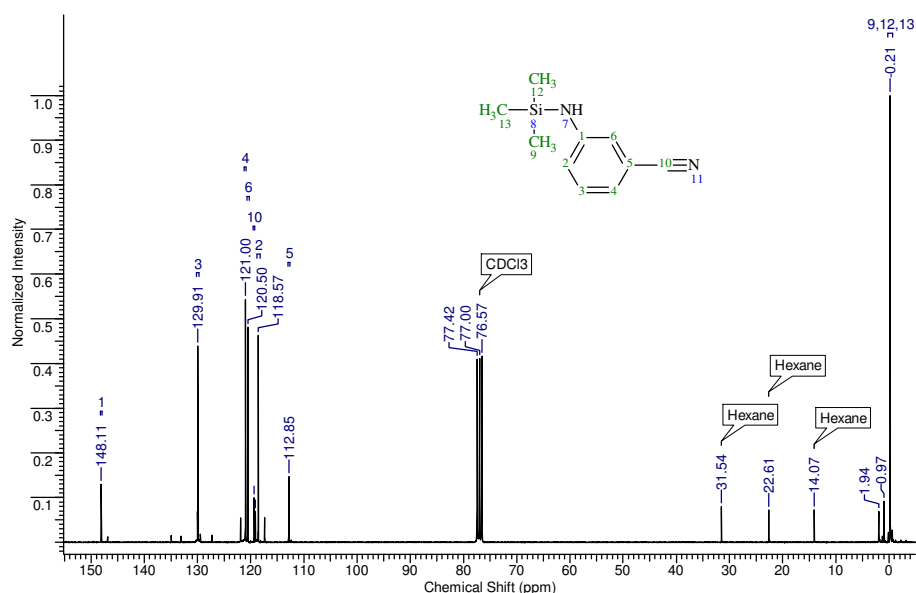


Figure 3.22: ¹³C-NMR spectrum of the silylated amine, [15]. Some impurities are observed in the spectrum corresponding to hexane. In addition, the small peaks in the aromatic region could correspond to the degradation of [15] to the unprotected nitrile due to the slight acidity of CDCl₃.

3.5.5) Reaction with 3'-trimethylsilaza-benzonitrile to form the dithiadiazolyl heterocycle

The reaction procedure followed to form the dithiadiazolyl heterocycle on [15] was the same as that to form the trimethylsiloxy derivatives. A solution of [15] in diethyl ether was reacted with a solution of LiHMDS, TMEDA and TMSCl. The solution turned orange in colour with some yellow precipitate forming.

Quenching the reaction with SCl_2 immediately precipitated a red-orange solid. The precipitate was worked up as before to yield a light orange powder which was analysed by mass spectrometry (Figure 3.23). The spectrum showed the desired dithiadiazolylum ion of 4-(3'-trimethylsilazaphenyl)-dithiadiazolylum chloride, **[16]**, as $(\text{M-H})^+$ at $m/z = 267$. Some further fragments and their corresponding m/z values are shown in the figure below. The base peak at $m/z = 159.8602$ corresponds to lithium bis(trimethylsilyl)amine (LiHMDS). In addition, the spectrum contains many unidentified peaks indicating that although the salt had formed, many side products had also formed.

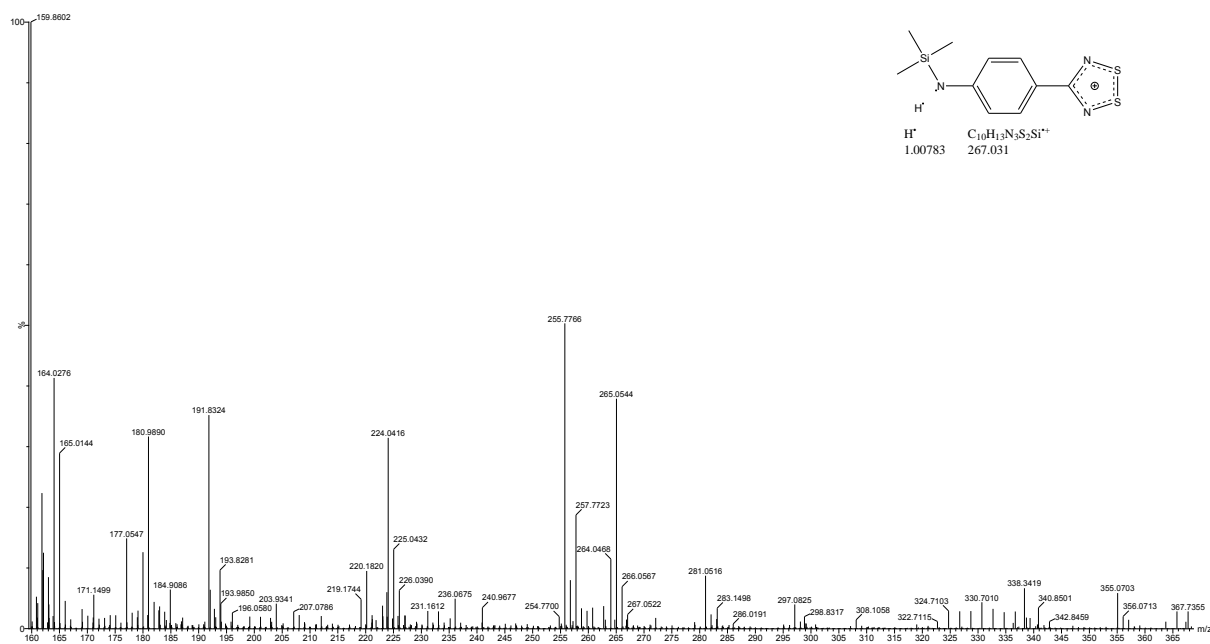


Figure 3.23: Mass spectrum of the crude powder resulting from the reaction to form the dithiadiazolyl heterocycle, [15]

A reduction reaction with Ph_3Sb was attempted with the crude salt, **[16]**. However, sublimation of the yellow residue yielded sulphur crystals. A repeat of the reduction and subsequent sublimation gave the same result.

Therefore, it appeared that the dithiadiazolyl heterocycle, **[16]**, could be formed in low yield by protecting the amine with a trimethylsilyl group. However, single protection was insufficient for the prevention of side reactions from occurring. Attempted reduction of the crude salt to the radical was unsuccessful.

3.5.6) Revision of amino protection

The method of protection for the amine group needed to be reconsidered as a result of the low yield of **[16]**. Amine protecting groups commonly used in the literature include

amides, imines and carbamates.²⁴ However, amides and imines require acid hydrolysis to remove the protecting groups which would probably react with the dithiadiazolyl heterocycle. However, for the *tert*-butylcarbonate protecting group, a paper by Jacquard *et al.* presented a convenient method to remove the protecting group under inert conditions by reaction with tetrabutylammonium fluoride (TBAF) in THF.³⁰

Thus, the 3'- and 4'-amino-benzonitrile starting materials were protected with *t*-Boc groups using *t*-Boc₂O, N,N-dimethyl-4-aminopyridine (DMAP) and Et₃N in DCM. After 48 hours, the reaction mixtures to protect the amines had both become yellow to orange in colour and TLC showed that the reactions had proceeded to completion. Workup yielded two orange oils that were analysed by ¹H-NMR confirming the formation of both of the doubly-protected 3'- and 4'-amino-benzonitriles, **[17]** and **[18]**, respectively. However, purification was necessary.

TLC of the crude mixtures showed three products in the 3'-amino-benzonitrile reaction whereas two were identified in the 4'-amino-benzonitrile reaction. The protected amines were purified by silica column flash chromatography using 10% (v/v) ethyl acetate in petroleum ether to separate the products. The fractions for each product were combined and dried *in vacuo*. Each product was then analysed by ¹H-NMR to determine the identity of the compound. ¹H-NMR spectra of the column fractions containing the desired products are shown: protected 3'-amino-benzonitrile, **[17]**, in Figure 3.24 and protected 4'-amino-benzonitrile, **[18]**, in Figure 3.25. The other two spots arising from the protection of 3'-amino-benzonitrile contained the unprotected and singly-protected 3'-amino-benzonitrile. The second spot on TLC from the protection reaction of 4'-amino-benzonitrile contained unreacted nitrile and *t*Boc₂O.

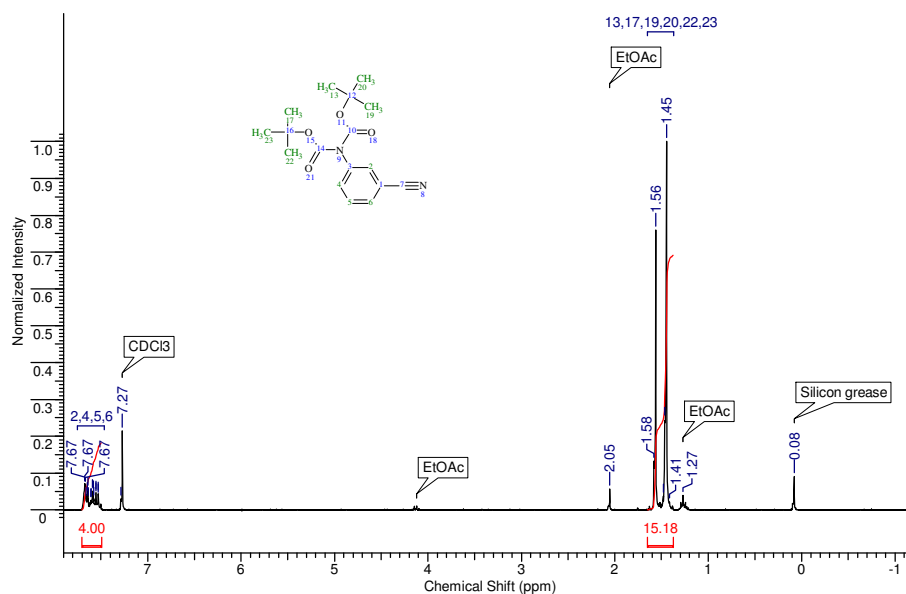


Figure 3.24: ¹H-NMR spectrum of the column fraction containing the protected 3'-aminobenzonitrile, [17]. The *t*Boc-groups appear to be chemically inequivalent resulting in a doublet at 1.45 ppm. Furthermore, this affects the aromatic protons: these could not be assigned to specific peaks in the aromatic region as they overlap forming a multiplet.

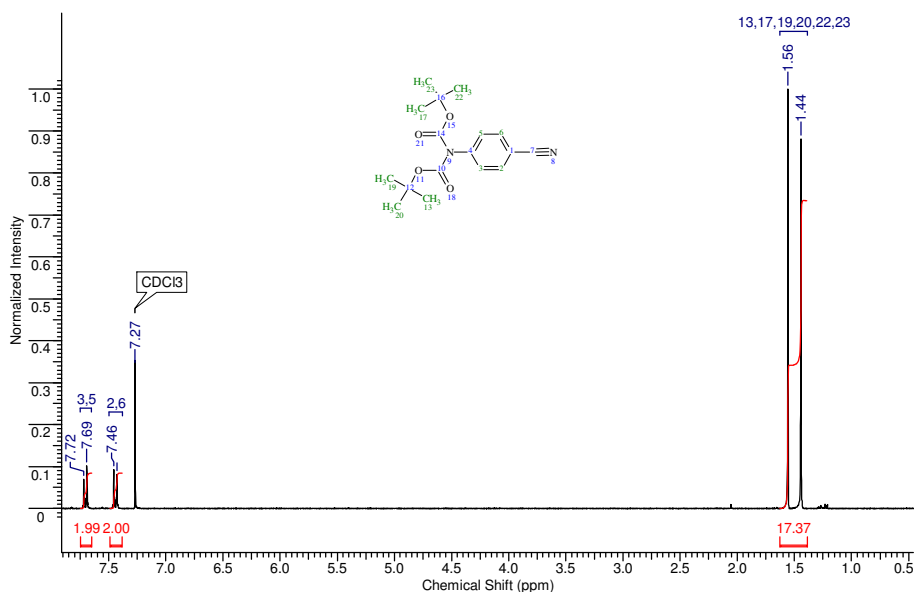


Figure 3.25: ¹H-NMR spectrum of the column fraction containing the protected 4'-aminobenzonitrile, [18]

3.5.7) Synthesis of 4-(3'-N,N-di-*tert*-butylcarbamato-phenyl)-1,2,3,5-dithiadiazolyl

The starting nitrile, [17], was added to a solution of LiHMDS and TMSCl in diethyl ether. The solution instantly became orange and was stirred overnight to ensure the complete reaction of the reagents. SCl₂ was added with the immediate precipitation of an orange solid. Workup of the reaction yielded a purple powder which was analysed by MS (Figure

3.26). In the mass spectrum, the molecular ion of 4-(3'-N,N-di-*tert*-butylcarbamatoxyphenyl)-1,2,3,5-dithiadiazolyl, [19], is not observed although many of the peaks correspond to conceivable fragments of [19]. It was theorised that reduction had occurred during the workup to a small extent presenting the purple colour. To support this, a dilute sample of the purple powder in solution was analysed by EPR, which showed the quintuplet indicative of the dithiadiazolyl radical (Figure 3.27).

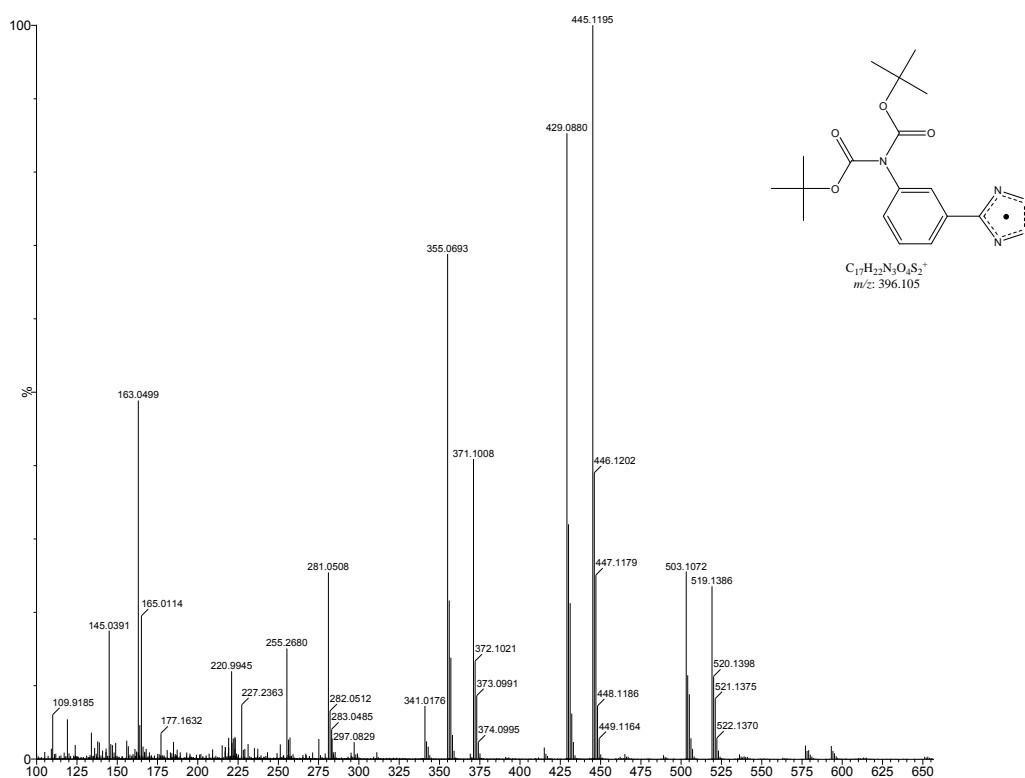


Figure 3.26: MS spectrum of the purple powder containing [19]

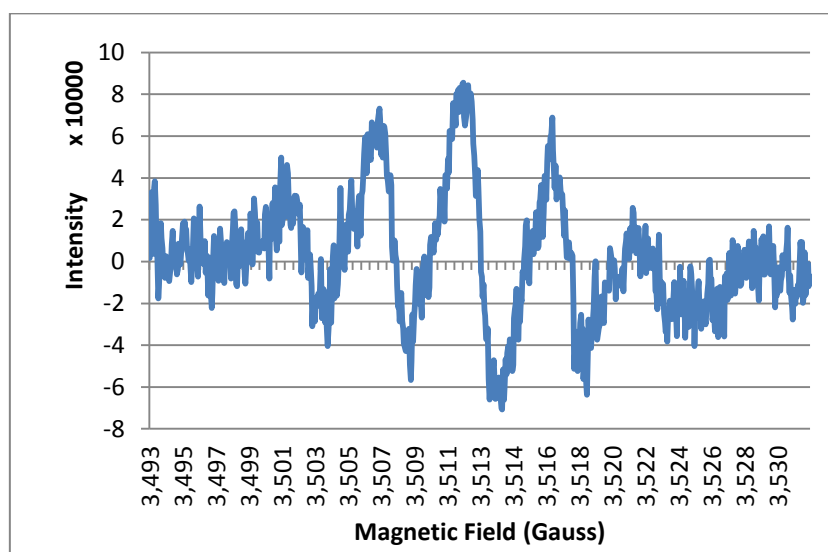


Figure 3.27: EPR spectrum of 4-(3'-N,N-di-*tert*-butylcarbamatoxyphenyl)-1,2,3,5-dithiadiazolyl, [19] (CH_2Cl_2 : $g = 2.010$, $a_N = 5.0$ G)

Sublimation of the powder yielded a red-purple film indicative of a dithiadiazolyl radical, however, no crystals were formed. Reduction reactions were also attempted with Ph_3Sb which produced a sticky purple residue. However, no crystals could be obtained.

3.5.8) Synthesis of 4-(4'-N,N-di-*tert*-butylcarbamato-phenyl)-1,2,3,5-dithiadiazolyl

The synthesis of this molecule followed the same procedure as the synthesis of [19]. Workup of the reaction yielded a pink-purple powder. Mass spectrometric analysis of the powder (Figure 3.28) did not show the molecular ion of the desired molecule, however, many peaks corresponding to conceivable fragments of [20] are observed. A dilute solution of the purple powder was analysed by EPR which showed the quintuplet indicative of the dithiadiazolyl radical (Figure 3.29).

The powder was sublimed yielding a red-purple film indicative of a dithiadiazolyl radical, however, no crystals were formed. Further reduction of the powder was attempted with Ph_3Sb . Sublimation of the purple residue yielded a purple film but no single crystals.

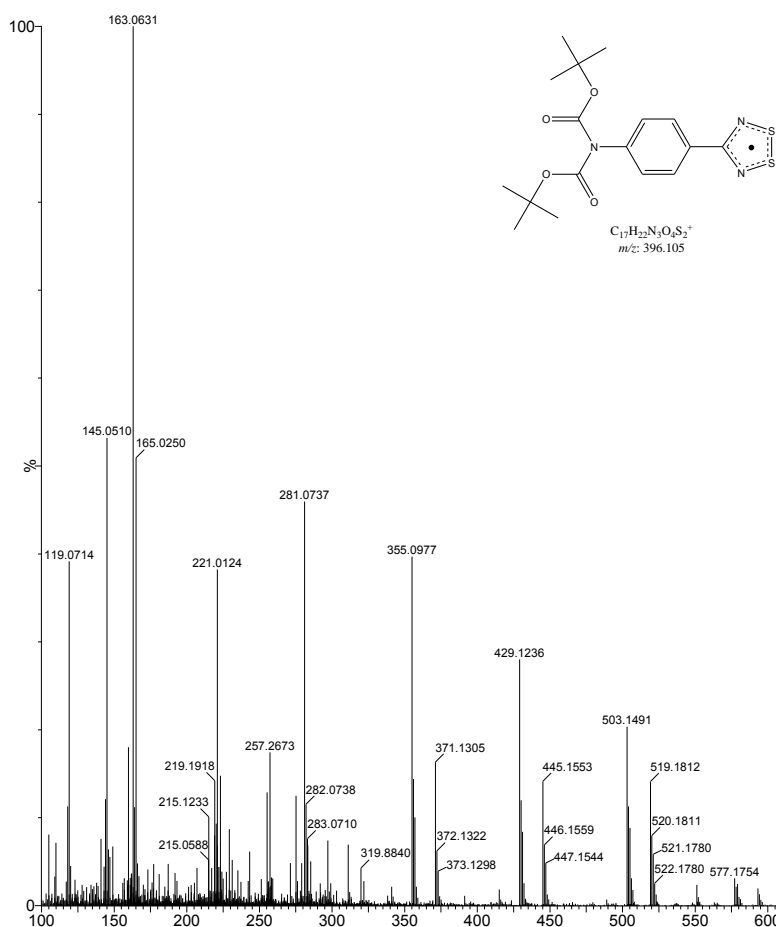


Figure 3.28: MS spectrum of the crude reaction mixture to form [20]

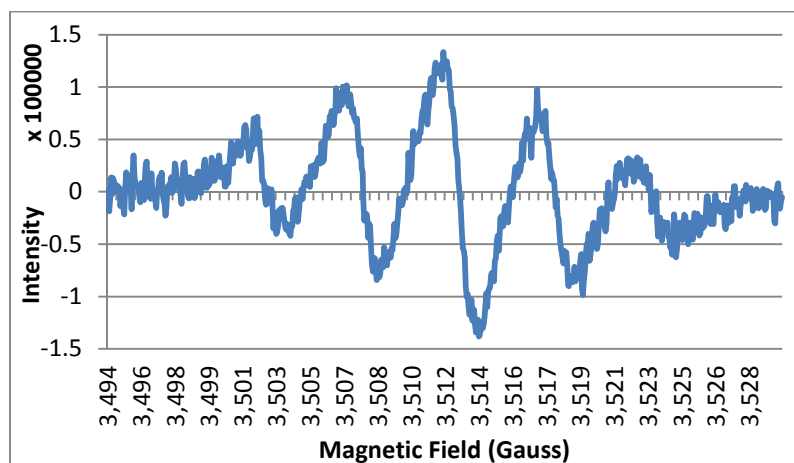


Figure 3.29: EPR spectrum of 4-(4'-N,N-di-*tert*-butylcarbamato)phenyl-1,2,3,5-dithiadiazolyl, [20] (CH_2Cl_2 : $g = 2.010$, $a_N = 5.1$ G)

3.6) Deprotection reactions

As mentioned in section 3.2), DiLauro *et al* showed a simple method to cleave oxygen-silicon bonds in an inert environment using a catalytic amount of cesium fluoride in a 100:1 mixture of DMSO and methanol.²⁵ However, experience has shown that the dithiadiazolyl heterocycles are unstable in the presence of DMSO and, furthermore, the acidic protons in methanol could react with the heterocycle. A literature survey revealed that deprotection reactions using cesium fluoride can be performed in a variety of solvents including THF and acetonitrile,³¹ and the attempts at deprotection were therefore carried out in THF.

The synthetic procedure to form the dithiadiazolyl radical offers two points at which deprotection can occur: before or after reduction of the dithiadiazolylum chloride salt to the radical. It was decided that deprotection would be performed after reduction as the solubility of the salt in THF is much lower than that of the radical, and experience has shown that the radical species are generally more stable than their corresponding salts.

The deprotection of 3'-trimethylsiloxy-[11] was attempted by reacting it with cesium fluoride and methanol in THF. No change was observed in the reaction mixture, however, after removing the solvent *in vacuo*, the remaining residue was golden in colour. Sublimation of the residue yielded no crystals. EPR analysis was negative for a radical species and it was concluded that deprotection of the radical had not been successful.

In order to test whether methanol caused the degradation of the dithiadiazolyl heterocycle, cesium fluoride was added to a solution of [11] in THF. After 5 hours, the

reaction was stopped and the solvent removed *in vacuo*. A sticky residue was obtained that was very similar in appearance to the unprotected silylated radical.

Cesium fluoride was also added to a solution of 4'-trimethylsiloxy-[14] in THF. The solid residue that remained after removing the THF *in vacuo* was golden in colour and it appeared that the radical had degraded.

It was concluded that deprotection of the siloxy derivatives was unsuccessful using this procedure.

3.7) Attempted synthesis of 4'-carboxyphenyl-1,2,3,5-dithiadiazolyl by lithium-halogen exchange

The possibility of functionalising the phenyl ring after the dithiadiazolyl heterocycle had been formed was mentioned in section 3.2. One of the methods highlighted was the lithium-halogen exchange followed by quenching the reaction with a suitable electrophile.

Because it proved difficult to form the dithiadiazolyl containing a carboxylic acid by other means, it was decided to attempt the lithium-halogen exchange. The 4'-bromophenyl-1,2,3,5-dithiadiazolyl radical was synthesised using standard procedures: reaction of the 4-bromo-benzonitrile with LiHMDS and quenching with SCl_2 to form the 4-(4'-bromophenyl)-1,2,3,5-dithiadiazolylium chloride salt, [21].

The salt, [21] was reduced with Zn-Cu in THF to afford the radical, [22]. The solution containing [22] was filtered to remove any impurities such as lithium chloride. *n*-Butyllithium was added to the solution of [22] in THF at $-78\text{ }^\circ\text{C}$ to effect the lithium-halogen exchange with the bromine atom on the radical. The solution remained black in colour. Carbon dioxide gas was then bubbled through the solution at room temperature for an hour, after which the THF was removed *in vacuo* yielding a solid residue of a red-purple colour. EPR analysis of the residue revealed that the dithiadiazolyl radical was unaffected by the reaction (Figure 3.30). MS analysis (Figure 3.31) revealed the residue to be the 4'-bromophenyl-1,2,3,5-dithiadiazolyl radical by the presence of its molecular ion at $m/z = 258.9$ and the peak at $m/z = 180.9$ corresponds to the loss of bromine. The molecular ion for the target molecule: 4'-carboxyphenyl-1,2,3,5-dithiadiazolyl ($m/z = 226$) is not observed in the spectrum.

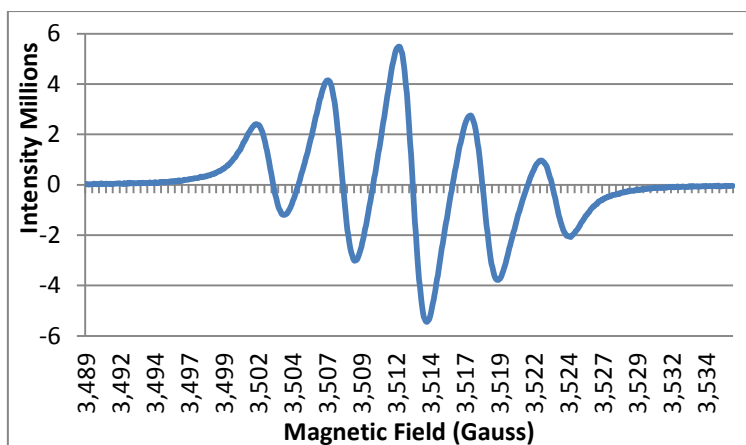


Figure 3.30: EPR spectrum of the residue after the attempted lithium-halogen exchange reaction and CO_2 quench. The pentet is indicative of a dithiadiazolyl radical. Thus, the radical species survived the lithium-halogen exchange and did not react with the *n*-BuLi. (298 K, CH_2Cl_2 : $g = 2.010$, $a_N = 5.2$)

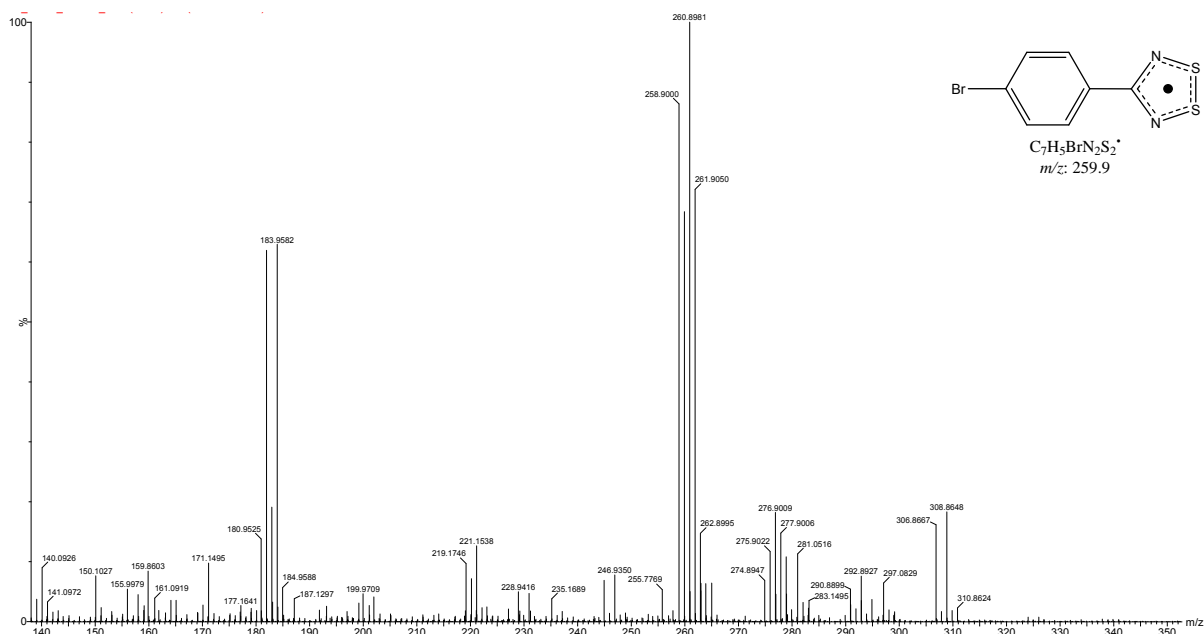


Figure 3.31: Mass spectrum of the product of the attempted lithium halogen exchange reaction with [22] and quench with CO_2 to form 4'-carboxyphenyl-1,2,3,5-dithiadiazolyl. The spectrum shows peaks corresponding to [22] and none corresponding to the desired product indicating that the reaction was unsuccessful.

3.8) Conclusions

This study into the viability of synthesising dithiadiazolyl radicals containing hydrogen-bonding functional groups for use in crystal engineering and co-crystallisation experiments has shown that this is not trivial. The common method to synthesise dithiadiazolyl radicals using LiHMDS cannot be used on nitriles which contain acidic hydrogen atoms. Although a small amount of the dithiadiazolylum chloride salt is formed, it is difficult to separate from

the products of the side reactions that occur. Thus, an alternate method needed to be employed to form the target compounds.

Reactions using NH_4Cl and SCl_2 in nitrobenzene yielded results that were difficult to interpret and intractable products were obtained.

Protection of the hydrogen-bonding groups before synthesis of the dithiadiazolyl heterocycle was then attempted. The 3'- and 4'-hydroxy-benzonitrile starting materials were successfully protected using TMSCl and the corresponding trimethylsiloxy-dithiadiazolyl radicals were formed. Deprotection reactions using cesium fluoride were attempted with little success. However, the use of cesium fluoride shows promise as a deprotecting agent and alternate reaction conditions should be investigated, such as using acetonitrile as a solvent instead of THF.

Interestingly, the protected trimethylsiloxy-dithiadiazolyl radicals are liquid at room temperature. Magnetic susceptibility studies should be performed to investigate whether the compound is a paramagnetic oil. EPR analysis conducted on the pure oils (instead of solutions) would be an initial experiment to determine whether the radicals are dissociated in the oil.

Protection of the 3- and 4-amino-benzonitrile starting materials proved to be a challenge. The use of trimethylsilyl chloride as a protecting agent provided the singly protected amine. However, formation of the dithiadiazolyl heterocycle from 3'-trimethylsilylaza-benzonitrile was unsuccessful. The manner of protection was reinvestigated and the amines were protected using *tert*-butylcarbonate protecting groups. Experiments to form the dithiadiazolyl heterocycle on these protected amines were performed using standard procedures. EPR analysis of the products of these reactions showed the presence of dithiadiazolyl radicals. However, the MS data did not show the desired molecular ion.

The use of lithium-halogen exchange reactions to functionalise dithiadiazolyl radicals shows promise as a synthetic route towards novel 1,2,3,5-dithiadiazolyl radicals containing functional groups that previously could not be synthesised, as the radical appears to be stable in the presence of *n*-butyllithium.

3.9) Future Work

In the case of the trimethylsiloxy-dithiadiazolyl radicals, future work should include the crystallisation of the protected radicals by freezing and the determination of their crystal structures. In addition, magnetic susceptibility studies should be done on these oils as 1,2,3,5-dithiadiazolyl radicals have been known to show paramagnetism in the melt.¹⁴ The deprotection of the protected radical species should also be investigated. As mentioned earlier, various reaction conditions should be tried in order to effect the removal of the trimethylsilyl groups. This includes the use of different solvents such as acetonitrile, heating and reflux, and longer reaction times. In addition, deprotection using different metal-halide salts may afford the deprotected dithiadiazolyl radicals.

The synthesis of the *t*-Boc-protected amino-dithiadiazolyl radicals should be optimised to yield greater quantities of the radical species and crystals should be grown. The crystal structures of these protected radicals should be solved as the bulky *t*-Boc groups may induce interesting and useful crystal packing arrangements. Deprotection of the *t*-Boc-protected amino-dithiadiazolyl radicals should be investigated. The procedure using TBAF in THF could be a good initial test reaction.

The potential of lithium-halogen exchange reactions to synthesise novel 1,2,3,5-dithiadiazolyl radicals should be investigated further considering that the radical species was shown to be stable in the presence of *n*-butyllithium. Longer reaction times may be required for the lithium-halogen exchange to take place before quenching with various electrophiles. Some interesting electrophiles to investigate could be SO₂, which could sulphonate the phenyl ring, or formaldehyde, which could result in a hydroxyl group situated one carbon away from the phenyl ring. The rotational flexibility afforded to the hydroxyl group may result in interesting and useful structure directing interactions in the solid state.

Co-crystallisation of the carboxy- and the deprotected hydroxy- and amino-dithiadiazolyl radicals should be investigated as interesting structure directing synthons could be formed in the solid state between these hydrogen-bonding groups. This could be done through sublimation or one of the other methods described in Chapter 2: from the melt or mixing in solution.

Finally, although it is a step away from pure organic magnets, complexation of these radical species with transition metals should be investigated. In the literature, the radicals

usually complex through one of the dithiadiazolyl heterocycle nitrogen atoms. However, the incorporation of hydrogen-bonding groups could allow the coordination of the dithiadiazolyl radical to the metal *via* the carboxy-, hydroxy- or amino-functional group attached to it. The coordination geometry of the transition metal used could yield interesting solid-state structures which, in turn, could provide interesting and useful properties. Furthermore, the use of a transition metal that exhibits magnetic properties may allow for the formation of a three-dimensional magnetic exchange pathway.

3.10) Experimental Procedures

Please consult Appendix A for Instrumentation and Chemicals used.

3.10.1) Boeré synthesis without protecting groups

The general reaction procedure used in these reactions is as follows:

The starting nitrile was added to a solution of LiHMDS in diethyl ether to form a milky white solution which was stirred overnight. The now off-white solution was quenched with S₂Cl₂ at 0°C yielding a light orange suspension. Filtration, washing with 2 x 10 ml diethyl ether and drying *in vacuo* revealed a cream to mustard coloured powder.

4-HYDROXY-BENZONITRILE TEST, [1]

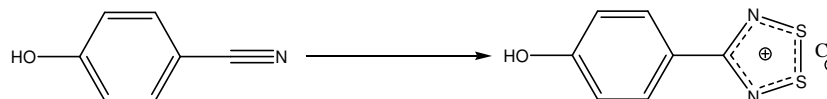
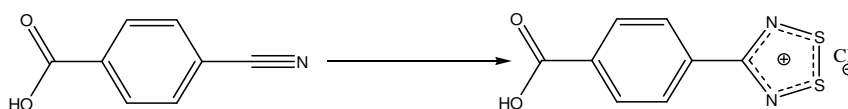


Table 3.1: Quantities of reagents used to form [1]

Reagent	Mass (g)	Volume (ml)	Number of moles (mmol)
LiHMDS	0.33	-	2.0
4'-Hydroxybenzonitrile	0.128	-	1.1
S ₂ Cl ₂	-	0.2	2.4
Et ₂ O	-	15	-
Et ₂ O wash	-	2 x 10	-

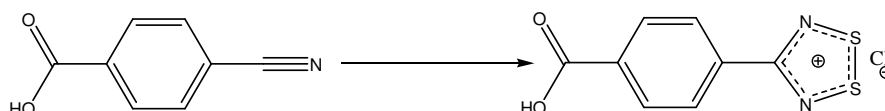
(+)-ESI-MS: *m/z* 197 (M⁺, 5%), 179 (4), 165 (7), 137 (88). (-)-ESI-MS: *m/z* 196 (M-H⁻, 13 %).

4-CARBOXY-BENZONITRILE TEST, [2]**Table 3.2: Quantities of reagents used to form [2]**

Reagent	Mass (g)	Volume (ml)	Number of moles (mmol)
LiHMDS	0.467	-	2.8
4'-Carboxybenzonitrile	0.214	-	1.5
S ₂ Cl ₂	-	0.2	2.4
Et ₂ O	-	15	-
Et ₂ O wash	-	2 x 10	-

Subsequent reduction reactions with Ph₃Sb were unsuccessful.

(+)-ESI-MS: *m/z* 225 (M⁺, 2%), 195 (1), 165 (100), (-)-ESI-MS: *m/z* 224 (M-H⁻, 1%), 178 (69), 146 (100).

4-CARBOXY-BENZONITRILE TEST WITH HMPA, [3]

In this reaction, HMPA was added to LiHMDS before the addition of the nitrile.

Table 3.3: Quantities of reagents used to form [3]

Reagent	Mass (g)	Volume (ml)	Number of moles (mmol)
LiHMDS	0.736	-	4.4
HMPA	-	1.6	9.0
4'-Carboxybenzonitrile	0.328	-	2.2
S ₂ Cl ₂	-	0.5	6.0
Et ₂ O	-	20	-
Et ₂ O wash	-	2 x 10	-

Filtration, washing with 2 x 10 ml diethyl ether and drying *in vacuo* revealed a sticky orange residue, [3]. Subsequent reduction reactions with Ph₃Sb were unsuccessful.

(+)-ESI-MS: *m/z* 225 (M⁺, 1%), 193 (30), 180 (100), 166 (2), 135 (2).

3.10.2) Alange synthesis

The general reaction procedure used in these reactions is as follows:

The nitrile was added to a suspension of NH_4Cl (0.524 g, 10 mmol) and SCl_2 (2.5 ml, 40 mmol) in nitrobenzene (5 ml). The red solution was heated to reflux in an oil bath at which point the solution became a bright orange colour. As described in the literature, the formation of crystals in the condenser corresponding to $[\text{S}_3\text{N}_2]\text{Cl}$ was observed. After refluxing for overnight, the flask was removed from the oil bath and was allowed to cool, precipitating a yellow solid. The mother liquor was filtered off and the yellow solid was dried *in vacuo*. The yellow powder, [4], was analysed by MS.

BENZONITRILE TEST, [4]

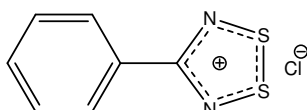


Table 3.4: Quantities of reagents used to form [4]

Reagent	Mass (g)	Volume (ml)	Number of moles (mmol)
NH_4Cl	0.524	-	10
SCl_2	-	2.5	40
Benzonitrile	-	1.0	10
Nitrobenzene	-	5	-

(+)-ESI-MS: m/z 182 (MH^+ , 100%)

4-CARBOXY-BENZONITRILE TEST, [5]

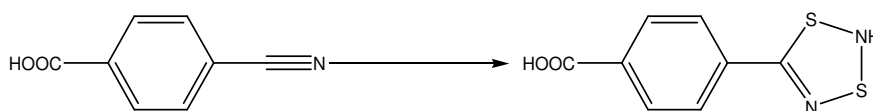


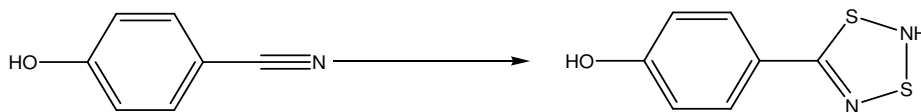
Table 3.5: Quantities of reagents used to form [5]

Reagent	Mass (g)	Volume (ml)	Number of moles (mmol)
NH_4Cl	0.740	-	13.8
SCl_2	-	4.0	63
4'-Carboxybenzotrile	1.997	-	13
Nitrobenzene	-	10	-

After washing with Et_2O , drying *in vacuo* yielded an orange solid, [5].

IR $\nu_{\text{max}}/\text{cm}^{-1}$: 3116s (CH), 3021br (OH), 2803s (CH), 1390vs (C=N).

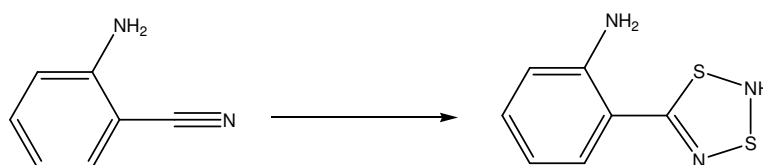
(+)-ESI-MS: m/z 224 (M-H^+ , 6%), 179 (2), 164 (14).

4-HYDROXY-BENZONITRILE TEST, [6]**Table 3.6: Quantities of reagents used to form [6]**

Reagent	Mass (g)	Volume (ml)	Number of moles (mmol)
NH_4Cl	0.225	-	4.2
SCl_2	-	1.1	16.8
4'-Hydroxybenzonitrile	0.500	-	4.2
Nitrobenzene	-	5	-
Et_2O wash		6 x 5	

The solution was a dark purple colour with a black-purple precipitate. After washing with Et_2O , drying *in vacuo* yielded a black-purple powder, [6].

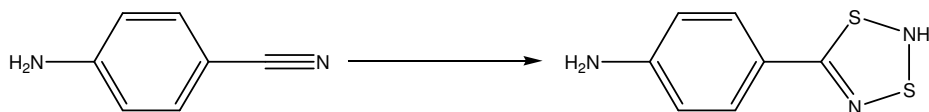
(+)-ESI-MS: m/z 198 (M^+ , 28).

2-AMINO-BENZONITRILE TEST, [7]**Table 3.7: Quantities of reagents used to form [7]**

Reagent	Mass (g)	Volume (ml)	Number of moles (mmol)
NH_4Cl	0.091	-	1.7
SCl_2	-	0.4	6.8
4'-Hydroxybenzonitrile	0.200	-	1.7
Nitrobenzene	-	4	-
Et_2O wash		6 x 5	

The solution was black with a black-purple precipitate. After washing with Et_2O , drying *in vacuo* yielded a black-purple powder, [7].

IR $\nu_{\text{max}}/\text{cm}^{-1}$: 3024br (NH), 1604m and 1477m (C=C), 1344s (C=N)

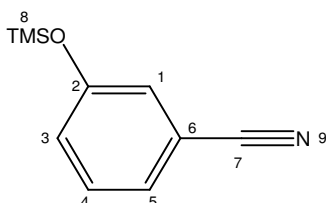
4-AMINO-BENZONITRILE TEST, [8]**Table 3.8: Quantities of reagents used to form [8]**

Reagent	Mass (g)	Volume (ml)	Number of moles (mmol)
NH ₄ Cl	0.226	-	4.2
SCl ₂	-	1.1	16.8
4'-Hydroxybenzonitrile	0.500	-	4.2
Nitrobenzene	-	10	-
Et ₂ O wash		6 x 5	

The solution was black in colour with a thick orange precipitate. After washing with Et₂O, drying *in vacuo* yielded a bright orange powder, [8].

IR $\nu_{\max}/\text{cm}^{-1}$: 3019m (NH), 2950m (CH), 2231m (C≡N), 1584m and 1493m (C=C), 1386s and 1345s (C=N).

(+)-ESI-MS: m/z 195 (M-H⁺, 6%), 178 (5), 164 (8), 133 (5).

3.10.3) Boeré synthesis with protecting groups**3-TRIMETHYLSILOXY-BENZONITRILE, [9]**

3-Cyanophenol (1.0 g, 8.4 mmol) was dissolved in dichloromethane (10 ml) in a 50 ml two-necked round-bottomed flask containing a magnetic stirrer bar and filled with nitrogen. Triethylamine (1.2 ml, 8.4 mmol) was added, followed by trimethylsilyl chloride (1.1 ml, 8.4 mmol) with the instantaneous formation of a white solid. A further 15 ml of dichloromethane was added to loosen the solid for the solution to stir. The temperature was increased to reflux and the milky solution was stirred overnight, resulting in a pale orange solution. The dichloromethane was removed *in vacuo* yielding a crude solid mixture containing both white and orange residues. The product was extracted from the crude with dry hexane. The hexane was removed *in vacuo* resulting in a colourless oil, [9] (1.062 g, 5.6 mmol). Subsequent reactions were performed where a stoichiometric amount of imidazole was used instead of triethylamine to yield similar results.

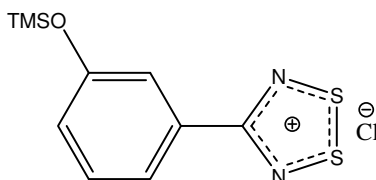
IR $\nu_{\max}/\text{cm}^{-1}$: 2960w (CH), 2229w (C≡N), 1596m and 1480m (C=C), 1281m and 1254m (C=N), 843s (SS), 964m (N-S).

(+)-ESI-MS: m/z 192 (MH⁺, 100%), 191 (M⁺, 28), 177 (12).

$^1\text{H-NMR}$ (300 MHz, CDCl_3) δ ppm 0.28 (9 H, s, 8-H) 7.05 (1 H, m, $^3J_{\text{H3-H4}}$ 8, 3-H), 7.09 (1 H, m, 1-H), 7.25 (1 H, m, 5-H), 7.31 (1 H, t, $^3J_{\text{H4-H5}}$ 8, 4-H).

$^{13}\text{C-NMR}$ (75 MHz, CDCl_3) δ ppm 0.12 (s, 8-C), 113.20 (s, 6-C), 118.61 (s, 7-C), 123.36 (s, 1-C), 125.06 (s, 3-C), 125.22 (s, 5-C), 130.43 (s, 4-C), 155.56 (s, 2-H).

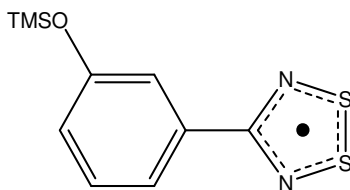
4-(3'-TRIMETHYLSILOXYPHENYL)-1,2,3,5-DITHIADIAZOLYLIUM CHLORIDE, [10]



A solution of LiHMDS was formed *in situ* by the reaction of HMDS (1.1 ml, 5.2 mmol) and *n*-butyllithium (3.4 ml, 5.2 mmol) in diethyl ether (30 ml) at -78°C . The solution was allowed to warm to room temperature after which TMEDA (0.8 ml, 5.2 mmol) was added to the solution. This solution was transferred via a cannula needle to a solution of [9] (0.993 g, 5.2 mmol) in diethyl ether (10 ml). Immediately, the mixing of the two clear solutions caused the resulting solution to become milky white. TMSCl (0.7 ml, 5.2 mmol) was added to improve solubility of the amidine in solution. The mixture was allowed to stir overnight after which it had become an off-white colour. Quenching the solution with SCl_2 (0.9 ml, 14.1 mmol) at 0°C caused the immediate precipitation of a bright orange solid. The solution was stirred for a further hour. Thereafter, the mother liquor was filtered off and the precipitate was washed with diethyl ether (2 x 15 ml) followed by drying *in vacuo* to yield a light orange powder, [10].

(+)-ESI-MS: m/z 270 (MH^+ , 100%), 269 (M^+ , 46), 255 (3), 235 (2), 205 (1), 192 (61), 177 (5).

4-(3'-TRIMETHYLSILOXYPHENYL)-1,2,3,5-DITHIADIAZOLYL, [11]

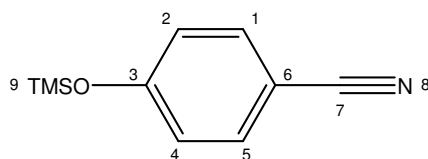


With Ph_3Sb : [10] (0.401 g, 1.3 mmol) and Ph_3Sb (0.227 g, 0.6 mmol) were placed together in a Schlenk filled with nitrogen. The mixture was heated to 60°C in an oil bath to melt the Ph_3Sb . As it melted, the solid powder changed from a light orange colour to a black-purple residue at the bottom of the Schlenk. Vacuum was applied allowing a red-purple film to sublime onto the cooler surfaces in the Schlenk. However, no crystals were formed.

With Zn-Cu/THF : [10] (0.623 g, 2.0 mmol) was placed in a Schlenk containing a magnetic stirrer bar and filled with nitrogen. THF (20 ml) was added to form an orange suspension, to which half an equivalent of Zn-Cu couple (0.069 g, 1.0 mmol) was added. The mixture was stirred overnight. The resulting red-purple solution contained a brown-green solid that was filtered off. The volume of the mother liquor was reduced and the resulting sticky red-purple residue was dried *in vacuo* to yield the product, [11].

(+)-ESI-MS: m/z 269 (M^+ , 100%), 192 (28), 176 (36), 165 (5), 119 (25).

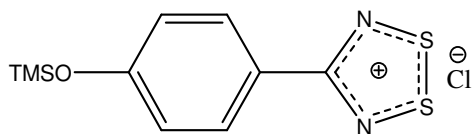
EPR (298 K, CH_2Cl_2): quintet ($g = 2.010$, $a_{\text{N}} = 5.1$ G).

4-CYANO-1-TRIMETHYLSILOXYBENZENE, [12]

4-Cyanophenol (1.000 g, 8.4 mmol) was dissolved in dichloromethane (20 ml) in a 50 ml two-necked round-bottomed flask containing a magnetic stirrer bar and filled with nitrogen. Imidazole (0.631 g 9.2 mmol) was added, followed by trimethylsilyl chloride (1.2 ml, 9.2 mmol) with the instantaneous formation of a white solid. The solution was heated to reflux and was allowed to react overnight. The volume of the resulting pale yellow solution was reduced by vacuum and the solid residue was dried *in vacuo*. The product was extracted from the crude mixture with dry hexane. The hexane was removed *in vacuo* yielding a colourless oil, [12] (0.986 g, 5.2 mmol).

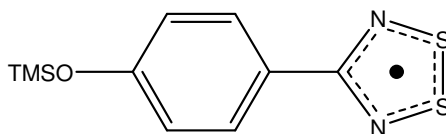
IR $\nu_{\max}/\text{cm}^{-1}$: 2225w (C≡N), 1602m and 1507m (C=C), 1273m and 1254m (C=N), 903m (N-S), 841s (S-S)

$^1\text{H-NMR}$ (300 MHz, CDCl_3) δ ppm 0.30 (9 H, s, 9-H), 6.87 (2 H, dt, $^3J_{\text{H1/5-H2/4}}$ 9, $^4J_{\text{H1-H5}}$ 2, 1-H and 5-H), 7.52 (2 H, dt, $^3J_{\text{H2/4-H1/5}}$ 9, $^4J_{\text{H2-H4}}$ 2, 2-H and 4-H).

4-(4'-TRIMETHYLSILOXYPHENYL)-1,2,3,5-DITHIADIAZOLYLIUM CHLORIDE, [13]

A solution of LiHMDS was formed *in situ* by the reaction of HMDS (1.0 ml, 4.8 mmol) and *n*-butyllithium (3.2 ml, 4.8 mmol) in diethyl ether (30 ml) at -78°C . The solution was allowed to warm to room temperature after which TMEDA (0.8 ml, 5.2 mmol) was added to the solution. This solution was transferred via a cannula needle to a solution of [12] (0.923 g, 4.8 mmol) in diethyl ether (10 ml). Immediately, the mixing of the two clear solutions caused the resulting solution to become milky white. TMSCl (0.6 ml, 4.8 mmol) was added to improve solubility of the amidine in solution. The mixture was allowed to stir overnight after which it had become an off-white colour. Quenching the solution with SCl_2 (0.8 ml, 12.6 mmol) at 0°C caused the immediate precipitation of a bright orange solid. The solution became very thick due to the precipitate, thus, 15 ml of diethyl ether was added and the solution was stirred for a further hour. Thereafter, the mother liquor was filtered off and the precipitate was washed with diethyl ether (2 x 15 ml) followed by drying *in vacuo* to yield a light orange powder, [13].

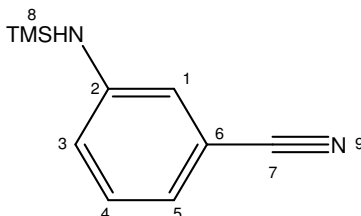
(+)-ESI-MS: m/z 270 (MH^+ , 18%), 269 (M^+ , 5), 192 (100), 176 (4)

4-(4'-TRIMETHYLSILOXYPHENYL)-1,2,3,5-DITHIADIAZOLYL, [14]

[13] (1.030 g, 3.4 mmol) was placed in a Schlenk containing a magnetic stirrer bar and filled with nitrogen. THF (30 ml) was added to form an orange suspension, to which half an equivalent of Zn-Cu couple (0.109 g, 1.7 mmol) was added. The mixture was stirred overnight. The resulting brown-yellow solution contained a dark coloured solid that was filtered off. The volume of the mother liquor was reduced and the resulting sticky red-purple residue was dried *in vacuo* to yield the product, [14].

(+)-ESI-MS: m/z 270 (M^+ , 2%), 192 (100)

EPR (298 K, CH_2Cl_2): quintet ($g = 2.010$, $a_N = 5.2$ G).

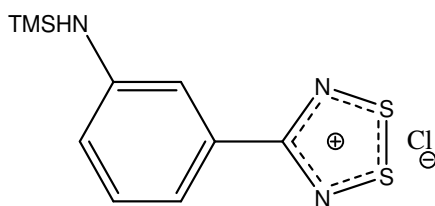
3-TRIMETHYLSILAZA-BENZONITRILE, [15]

3-Amino-benzonitrile (1.000 g, 8.5 mmol) was dissolved in dichloromethane (10 ml) in a 50 ml two-necked round-bottomed flask containing a magnetic stirrer bar and filled with nitrogen. Triethylamine (2.4 ml, 17.0 mmol) was added, followed by trimethylsilyl chloride (2.2 ml, 17.0 mmol) with the instantaneous formation of a white solid. A further 10 ml of dichloromethane was added to loosen the solid for the solution to stir. The temperature was increased to reflux and the milky solution was stirred overnight, resulting in a pale orange solution. The dichloromethane was removed *in vacuo* yielding a crude solid mixture containing an orange residue. The product was extracted from the crude with dry hexane. The hexane was removed *in vacuo* resulting in an orange oil, [15] (0.619 g, 3.3 mmol).

(+)-ESI-MS: m/z 191 (M^+ , 1%) 177 (1), 119 (100), 102 (1).

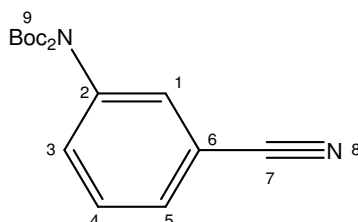
1H -NMR (300 MHz, $CDCl_3$) δ ppm 0.29 (8 H, s, 8-CH), 3.64 (br s, 8-NH), 6.82 (1 H, m, 3-H), 6.86 (1 H, m, 1-H), 6.96 (1 H, dt, $^3J_{H5-H4}$ 8, $^4J_{H5-H3/6}$ 1, 5-H), 7.17 (1 H, dt, $^3J_{H4-H3/5}$ 8, 4-H).

^{13}C -NMR (75 MHz, $CDCl_3$) δ ppm 0.21 (s, 8-C), 112.85 (s, 6-C), 118.57 (s, 3-H), 120.50 (s, 1-H) 121.00 (s, 5-H), 129.91 (4-H), 148.11 (s, 2-H)

4-(3'-TRIMETHYLSILAZAPHENYL)-1,2,3,5-DITHIADIAZOLYLIUM CHLORIDE, [16]

A solution of LiHMDS was formed *in situ* by the reaction of HMDS (0.55, 2.6 mmol) and *n*-butyllithium (1.7 ml, 2.6 mmol) in diethyl ether (20 ml) at -78°C . The solution was allowed to warm to room temperature after which TMEDA (0.4 ml, 2.6 mmol) was added to the solution. This solution was transferred via a cannula needle to a solution of [15] (0.487 g, 2.6 mmol) in diethyl ether (5 ml). Immediately, the mixing of the two solutions caused the resulting solution to become orange with a yellow precipitate. TMSCl (0.3 ml, 2.6 mmol) was added to improve solubility of the amidine in solution. The mixture was allowed to stir overnight after which it had become yellow in colour with an off-white precipitate. Quenching the solution with SCl_2 (0.5 ml, 7.9 mmol) at 0°C caused the immediate precipitation of a white solid. Stirring caused the precipitate to become brown in colour, ultimately settling on red-orange after stirring for a further hour. Thereafter, the mother liquor was filtered off and the precipitate was washed with diethyl ether (2 x 10 ml) followed by drying *in vacuo* to yield a light orange powder, [16].

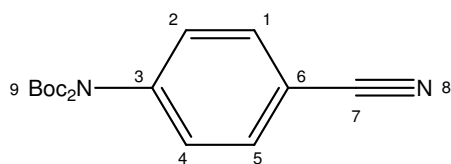
(+)-ESI-MS: m/z 267 ($\text{M}-\text{H}^+$, 4%), 255 (50), 254 (2), 236 (5), 204 (4), 193 (5), 180 (32), 164 (42)

3-CYANO-1-N,N'-BIS-T-BOC-AMINO BENZENE, [17]

3-Amino-benzonitrile (1.000 g, 8.5 mmol) was dissolved in dichloromethane (30 ml) in a 50 ml round-bottomed flask containing a magnetic stirrer bar and filled with nitrogen forming an orange solution. *t*-Boc₂O (4.618 g, 21.2 mmol), triethylamine (2.6 ml, 18.6 mmol) and DMAP (0.105 g, 0.85 mmol) were added to the solution which was stirred for 48 hours. The reaction was monitored with TLC. The resulting dark orange solution was diluted with 15 ml water and the layers separated. The aqueous layer was washed with 2 x 15 ml dichloromethane. The organic extracts were combined and dried over MgSO_4 . The MgSO_4 was filtered from the organic solution and was washed with dichloromethane (4 x 5 ml). The volume of the dichloromethane solution was reduced under reduced pressure and the resulting residue was dried *in vacuo* to yield the crude product as an orange oil. The product was purified by silica column flash chromatography to yield the product, [17], as a white solid (1.017 g, 3.2 mmol).

IR $\nu_{\text{max}}/\text{cm}^{-1}$: 2233w ($\text{C}\equiv\text{N}$), 1740m and 1715m ($\text{C}=\text{O}$), 1602w and 1482w ($\text{C}=\text{C}$), 1300m and 1243m ($\text{C}-\text{O}$).

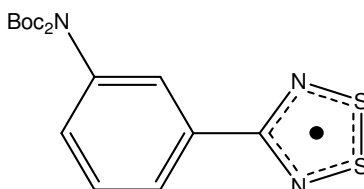
¹H-NMR (300 MHz, CDCl_3) δ ppm 1.45-1.56 (15 H, d, 9-H), 7.53 (4 H, m, 1-/3-/4-/5-H)

4-CYANO-1-N,N'-BIS-T-BOC-AMINO BENZENE, [18]

4-Amino-benzonitrile (1.000 g, 8.5 mmol) was dissolved in dichloromethane (30 ml) in a 50 ml round-bottomed flask containing a magnetic stirrer bar and filled with nitrogen forming an orange solution. *t*-Boc₂O (4.621 g, 21.2 mmol), triethylamine (2.6 ml, 18.6 mmol) and DMAP (0.108 g, 0.85 mmol) were added to the solution which was stirred for 48 hours. The reaction was monitored with TLC. The resulting dark orange solution was diluted with 15 ml water and the layers separated. The aqueous layer was washed with 2 x 15 ml dichloromethane. The organic extracts were combined and dried over MgSO₄. The MgSO₄ was filtered from the organic solution and was washed with dichloromethane (4 x 5 ml). The volume of the dichloromethane solution was reduced under reduced pressure and the resulting residue was dried *in vacuo* to yield the crude product as an orange oil. The product was purified by silica column flash chromatography to yield the product, [18], as a white solid (0.801 g, 2.5 mmol).

IR $\nu_{\text{max}}/\text{cm}^{-1}$: 2229w (C≡N), 1737m and 1724m (C=O), 1603w and 1502w (C=C), 1285m and 1247m (C-O).

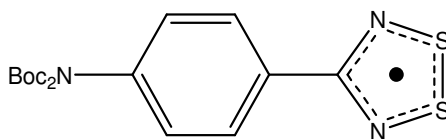
¹H-NMR (300 MHz, CDCl₃) δ ppm 1.44-1.56 (17 H, d, 9-H), 7.43 (2 H, dd, ³J_{H1/5-H2/4} 8, ⁴J_{H1-H5} 2, 1-/5-H), 7.69 (2 H, dd, ³J_{H2/4-H1/5} 9, ⁴J_{H2-H4} 2, 2-/4-H).

4-(3'-N,N'-BIS-T-BOC-AMINOPHENYL)-1,2,3,5-DITHIADIAZOLYL, [19]

A solution of LiHMDS was formed *in situ* by the reaction of HMDS (0.7 ml, 3.1 mmol) and *n*-butyllithium (2.1 ml, 3.1 mmol) in diethyl ether (30 ml) at -78°C. The solution was allowed to warm to room temperature forming a clear solution. [17] (1.0 g, 3.1 mmol) was dissolved and washed into the LiHMDS solution using 3 x 5 ml diethyl ether producing an instant orange solution which was stirred overnight. The resulting solution was clear yellow in colour with an orange brown precipitate. In order to aid the solubility of the amidine, TMSCl (0.5 ml, 3.8 mmol) was added to the solution. Thereafter, the reaction was quenched with SCl₂ (0.6 ml, 9.4 mmol) instantly forming an orange precipitate. The reaction was stirred for a further hour, after which the mother liquor was filtered off and the precipitate was washed with 2 x 15 ml diethyl ether. The solid residue was dried *in vacuo* yielding a purple powder. The purple powder was analysed by EPR which showed the presence of the characteristic pentet of a dithiadiazolyl radical. A portion of the purple powder, 4-(3'-N,N'-bis-*t*-Boc-aminophenyl)-1,2,3,5-dithiadiazolyl chloride (0.091 g, 0.2 mmol) was placed in a Schlenk filled with nitrogen. Vacuum was applied and the powder was heated to 80°C. A red-purple film formed on the cooler surfaces within the Schlenk. This was shown by EPR to be the radical.

(+)-ESI-MS: m/z 396 (M^+ , 0%), 371 (40), 355 (59), 341 (7), 281 (26), 255 (15), 227 (8), 177 (3), 145 (17), 163 (49). EPR (298 K, CH_2Cl_2): quintet ($g = 2.010$, $a_N = 5.0$ G).

4-(4'-N,N'-bis-t-Boc-aminophenyl)-1,2,3,5-dithiadiazolyl, [20]

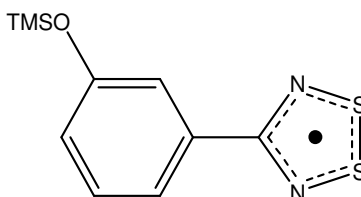


A solution of LiHMDS was formed *in situ* by the reaction of HMDS (0.6 ml, 2.6 mmol) and *n*-butyllithium (1.7 ml, 2.5 mmol) in diethyl ether (15 ml) at $-78^\circ C$. The solution was allowed to warm to room temperature forming a clear solution. [18] (0.783 g, 2.4 mmol) was dissolved and washed into the LiHMDS solution using 3 x 5 ml diethyl ether producing an instant bright cloudy yellow solution which was stirred overnight. The resulting solution was cloudy yellow in colour with a yellow precipitate. In order to aid the solubility of the amidine, TMSCl (0.4 ml, 3.0 mmol) was added to the solution. Thereafter, the reaction was quenched with SCl_2 (0.5 ml, 7.9 mmol) instantly forming an orange precipitate. The reaction was stirred for a further hour, after which the mother liquor was filtered off and the precipitate was washed with 2 x 15 ml diethyl ether. The solid residue was then dried *in vacuo* yielding a purple powder. The purple powder was analysed by EPR which showed the presence of the characteristic pentet of a dithiadiazolyl radical. A portion of the purple powder, 4-(4'-N,N'-bis-t-Boc-aminophenyl)-1,2,3,5-dithiadiazolium chloride (0.050 g, 0.1 mmol) was placed in a Schlenk filled with nitrogen. Vacuum was then applied and the powder was heated to $80^\circ C$. A red-purple film formed on the cooler surfaces within the Schlenk. This was shown by EPR to be the radical.

(+)-ESI-MS: m/z 396 (M^+ , 0%), 371 (16), 355 (40), 281 (56), 257 (18), 163 (100), 145 (53), 119 (39). EPR (298 K, CH_2Cl_2) quintet ($g = 2.010$, $a_N = 5.1$ G).

3.10.4) Deprotection reactions

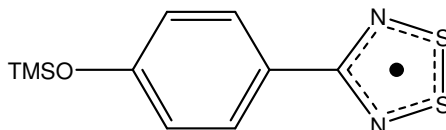
4-(3'-TRIMETHYLSILOXYPHENYL)-1,2,3,5-DITHIADIAZOLYL



- [11] (0.276 g, 1.0 mmol) was dissolved in THF (4 ml) forming a yellow solution. CsF (0.4 mmol) was added to the solution with no observable change. A stoichiometric amount of methanol (0.04 ml, 1.0 mmol) was added to the solution which was stirred for a further 10 minutes with no observable change. The THF was removed *in vacuo* yielding a solid golden coloured residue and a sticky red-purple residue. Sublimation of the solid yielded no product.
- This reaction was attempted after the reduction of the salt to the radical. Thus, 4-(3'-trimethylsilyloxyphenyl)-1,2,3,5-dithiadiazolium chloride (0.440 g, 1.4 mmol) was placed in a

Schlenk containing a magnetic stirrer bar and filled with nitrogen. A portion of THF (20 ml) was added to form an orange suspension. Half an equivalent of Zn-Cu couple (0.047 g, 0.7 mmol) was added and the reaction was stirred overnight. The yellow solution was filtered. CsF (0.205 g, 1.3 mmol) was added to the mother liquor and the reaction was stirred for 5 hours. No colour change was observed. The THF was removed *in vacuo* yielding a brown residue.

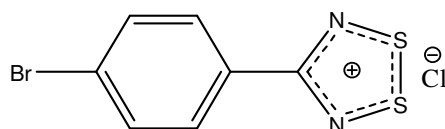
4-(4'-TRIMETHYLSILOXYPHENYL)-1,2,3,5-DITHIADIAZOLYL



1. This reaction was attempted after the reduction of the salt to the radical. Thus, 4-(4'-trimethylsilyloxyphenyl)-1,2,3,5-dithiadiazolylum chloride (0.658 g, 2.2 mmol) was placed in a Schlenk containing a magnetic stirrer bar and filled with nitrogen. A portion of THF (20 ml) was added to form an orange suspension. Half an equivalent of Zn-Cu couple (0.071 g, 1.1 mmol) was added and the reaction was stirred overnight. The resulting purple solution was filtered. CsF (0.322 g, 2.1 mmol) was added to the mother liquor and the reaction was stirred for 5 hours. No colour change was observed. The THF was removed *in vacuo* yielding a brown residue.

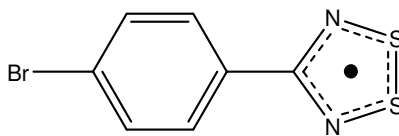
3.10.5) Synthesis of 4'-carboxyphenyl-1,2,3,5-dithiadiazolyl by lithium halogen exchange

4-(4'-BROMOPHENYL)-1,2,3,5-DITHIADIAZOLYL IUM CHLORIDE, [21]



Diethyl ether (35 ml) was added to a Schlenk tube filled with nitrogen and containing a magnetic stirrer bar and cooled to -78°C . 1,1,1,3,3,3-Hexamethyldisilazane (5.5 mmol, 1.0 ml) was added, followed by *n*-Butyllithium (5.5 mmol, 3.6 ml). The solution was allowed to warm to room temperature resulting in a clear solution. 4-Bromobenzonitrile (5.5 mmol, 1.003 g) was added to the mixture which was stirred overnight, resulting in a bright orange solution. The mixture was cooled to 0°C and a slight excess of SCl_2 (11.0 mmol, 0.9 ml) was added dropwise causing the immediate precipitation of the bright orange salt, **5**. The solution was allowed to warm to room temperature and stirred for a further hour. Thereafter, the mother liquor was filtered off and the bright orange residue was washed with diethyl ether (2 x 15 ml). Finally, the residue was dried *in vacuo* to yield the salt, **[21]**, as a bright orange powder.

(+)-ESI-MS: m/z 258.9 (M^+ , 78%), 180.9 (4)

4-(4'-BROMOPHENYL)-1,2,3,5-DITHIADIAZOLYLIUM CHLORIDE, [22]

[21] (0.540 g, 1.8 mmol) was added to THF (15 ml) in a Schlenk containing a magnetic stirrer bar and filled with nitrogen to form an orange suspension. Zn-Cu couple (59 mg, 0.9 mmol) was added and the mixture was stirred overnight. The resultant dark red solution was filtered and the solvent was reduced *in vacuo*. The dark red residue was dried *in vacuo*. Sublimation of the residue afforded red block crystals of [22].

(+)-ESI-MS: m/z 258.9 (M^+ , 45%)

EPR (298 K, CH_2Cl_2): quintet ($g = 2.010$, $a_N = 5.1$ G).

3.11) References

1. J.-M. Lehn, *Angewandte Chemie International Edition in English*, 1988, **27**, 89-112.
2. J.-M. Lehn, *Angewandte Chemie International Edition in English*, 1990, **29**, 1304-1319.
3. G. R. Desiraju, *Angewandte Chemie International Edition in English*, 1995, **34**, 2311-2327.
4. E. J. Corey, *Pure and Applied Chemistry*, 1967, **14**, 19-38.
5. R. Mondal, J. A. K. Howard, R. Banerjee and G. R. Desiraju, *Crystal Growth & Design*, 2006, **6**, 2507-2516.
6. T. S. Moore and T. F. Winmill, *Journal of the Chemical Society, Transactions*, 1912, **101**, 1635-1676.
7. L. Pauling, *Proceedings of the National Academy of Sciences*, 1928, **14**, 359-362.
8. L. Pauling, *The nature of the chemical bond and the structure of molecules and crystals: an introduction to modern structural chemistry*, Cornell University Press, Ithaca, NY, 1960.
9. G. C. Pimentel and A. L. McClellan, *The hydrogen bond*, W.H. Freeman, San Francisco, 1960.
10. T. Steiner, *Angewandte Chemie International Edition*, 2002, **41**, 48-76.
11. G. R. Desiraju, *Angewandte Chemie International Edition*, 2011, **50**, 52-59.
12. S. A. Fairhurst, K. M. Johnson, L. H. Sutcliffe, K. F. Preston, A. J. Banister, Z. V. Hauptman and J. Passmore, *Journal of the Chemical Society, Dalton Transactions*, 1986, 1465-1472.
13. C. B. Aakeroy, *Acta Crystallographica Section B-Structural Science*, 1997, **53**, 569-586.
14. J. M. Rawson, A. J. Banister and I. Lavender, *Advances in Heterocyclic Chemistry, Vol 62*, 1995, **62**, 137-247.
15. R. T. Boeré, R. T. Oakley and R. W. Reed, *Journal of Organometallic Chemistry*, 1987, **331**, 161-167.
16. R. R. Fraser and T. S. Mansour, *The Journal of Organic Chemistry*, 1984, **49**, 3442-3443.
17. R. R. Fraser, T. S. Mansour and S. Savard, *The Journal of Organic Chemistry*, 1985, **50**, 3232-3234.
18. J. McMurry, *Organic chemistry*, Thomson Brooks/Cole, 2008.
19. A. J. Banister, N. R. M. Smith and R. G. Hey, *Journal of the Chemical Society, Perkin Transactions 1*, 1983, 1181-1186.
20. G. G. Alange, A. J. Banister, B. Bell and P. W. Millen, *Journal of the Chemical Society, Perkin Transactions 1*, 1979, 1192-1194.
21. N. Burford, J. Passmore and M. J. Schriver, *Journal of the Chemical Society, Chemical Communications*, 1986, 140-142.

22. W. V. F. Brooks, N. Burford, J. Passmore, M. J. Schriver and L. H. Sutcliffe, *Journal of the Chemical Society, Chemical Communications*, 1987, 69-71.
23. C. Aherne, A. J. Banister, A. W. Luke, J. M. Rawson and R. J. Whitehead, *Journal of the Chemical Society, Dalton Transactions*, 1992, 1277-1282.
24. P. G. M. Wuts and T. W. Greene, *Greene's protective groups in organic synthesis*, Wiley-Interscience, Hoboken, NJ, 2007.
25. A. M. DiLauro, W. Seo and S. T. Phillips, *The Journal of Organic Chemistry*, 2011, **76**, 7352-7358.
26. G. van Look, G. Simchen and J. Heberle, *Silylating Agents*, Fluka Chemie AG, Buchs, 1995.
27. J. R. Pratt, W. D. Massey, F. H. Pinkerton and S. F. Thames, *The Journal of Organic Chemistry*, 1975, **40**, 1090-1094.
28. A. B. Smith III, M. Visnick, J. N. Haseltine and P. A. Sprengeler, *Tetrahedron*, 1986, **42**, 2957-2969.
29. T. P. Mawhinney and M. A. Madson, *The Journal of Organic Chemistry*, 1982, **47**, 3336-3339.
30. U. Jacquemard, V. Bénéteau, M. Lefoix, S. Routier, J.-Y. Mérour and G. Coudert, *Tetrahedron*, 2004, **60**, 10039-10047.
31. R. D. Crouch, *Tetrahedron*, 2004, **60**, 5833-5871.

Chapter 4: Novel Crystal Structures & Further Co-crystallisation Experiments

4.1) Introduction

It was mentioned in Chapter 2 that many different combinations of 1,2,3,5-dithiadiazolyl radicals have been sublimed together in order to attempt to form co-crystals with interesting and useful properties.¹ Nonetheless, the two co-crystals characterised in Chapter 2 remain the only two known to date. The first co-crystal comprises heterodimers of 4-phenyl- and 4-perfluorophenyl-1,2,3,5-dithiadiazolyl radicals and the second comprises heterodimers of 4-phenyl- and 4-(4'-perfluoropyridyl)-1,2,3,5-dithiadiazolyl radicals. This chapter is concerned with an investigation into synthesising new co-crystals. Two novel crystal structures of 1,2,3,5-dithiadiazolyl radicals were determined in the process.

4.2) A Supramolecular Strategy

4.2.1) The CN \cdots S-S Synthron

Considering the two co-crystals consisting of 1,2,3,5-dithiadiazolyl radicals, the success of their formation could be explained by a few similarities observed in their crystal structures. Firstly, the co-crystals are formed from dithiadiazolyl radicals whose molecular structures are very similar: the phenyl radical and its fluorinated counterpart differ only in that the hydrogen atoms in the phenyl radical are substituted for fluorine atoms. Similarly, the perfluoropyridyl radical differs from the phenyl radical in the substitution of the hydrogen atoms for fluorine atoms and, in addition, the carbon in the *para*- position relative to the dithiadiazolyl heterocycle is substituted for a nitrogen atom. Secondly, the incorporation of this nitrogen atom into the perfluoroaryl ring introduces a useful structure-directing synthron, N_{py} \cdots S-S, into the crystal structure causing chains of dimers to form.

From a crystal engineering perspective, chains of radicals which stack one on top of another in columns normal to the chain direction are desired as a starting point for the design of an organic magnetic material. This is observed² in the α -phase of the 3'-cyanophenyl-1,2,3,5-dithiadiazolyl radical, [1],* (Figure 4.1) which forms chains in the solid state through CN \cdots S-S interactions (Figure 4.2).

* The numbering of compounds synthesised in this chapter is independent of the other chapters. For a list of compounds and their numbers see Appendix B, Section B.3.

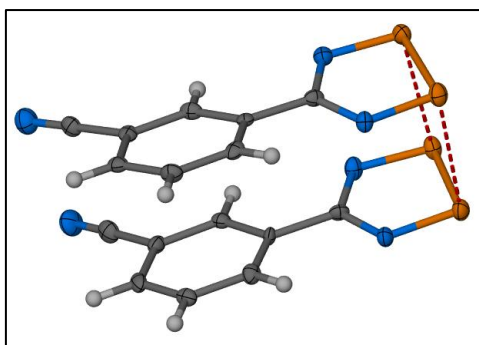


Figure 4.1: Diagram of the asymmetric unit of [1] in the solid state. Molecules dimerise in a *cis*-oid fashion through intermolecular S...S contacts. Non-hydrogen atoms in [1] are depicted as ellipsoids (50%).

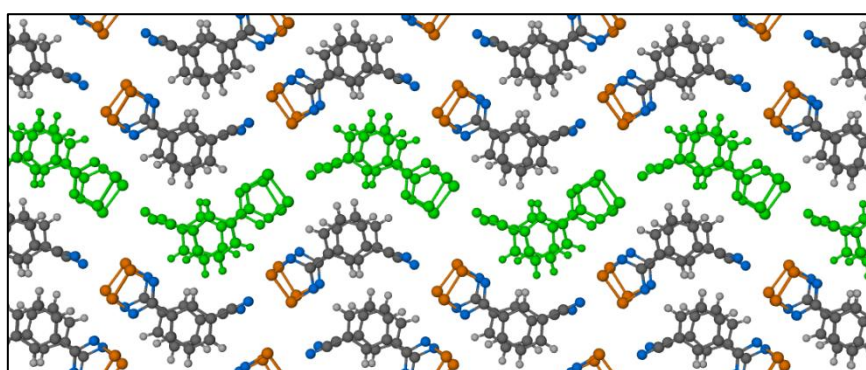


Figure 4.2: Crystal packing diagram of [1] viewed in the *b-c* plane. Dimers of radicals stack in columns normal to this plane. The radicals are shown to pack in antiparallel chains (shown in green for example) stabilised by CN...S-S interactions.

In addition to the CN...S-S interactions, the chains are stabilised by S...N contacts between dimers in adjacent chains. Because of the two-fold screw axis along which the chains are situated, it can be seen that these interactions alternate between the adjacent chains on either side of a given chain (Figure 4.3).

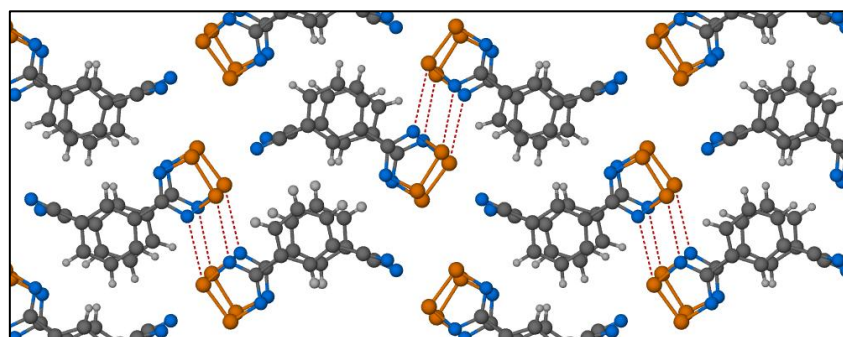


Figure 4.3: Crystal packing diagram of [1] showing interchain S...N contacts (red dashed lines).

This particular dithiadiazolyl radical, [1], is of interest because its β -phase (β -[1])² is isostructural^{3, 4} with its fluorinated derivative: 3'-cyanoperfluorophenyl-1,2,3,5-dithiadiazolyl,¹ [2] (Figure 4.4).[†] The radical [2] crystallises in the monoclinic space group $P2_1/n$ with a single molecule in the asymmetric unit that forms half of a *trans*-antarafacial $\pi^*-\pi^*$ dimer stabilised by $S\cdots S$ contacts of 3.115(1) Å (Figure 4.5).

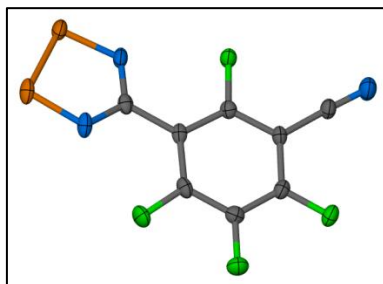


Figure 4.4: Asymmetric unit of [2]. Atoms are depicted as ellipsoids (50%).

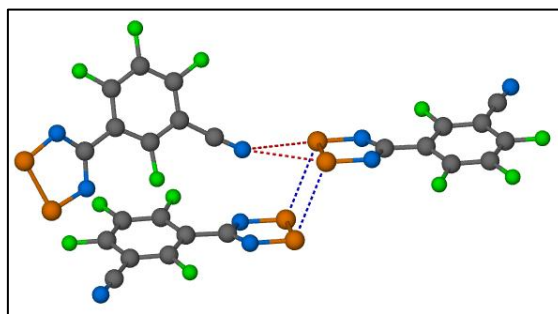


Figure 4.5: Crystal structure diagram showing intradimer $S\cdots S$ contacts in [2] (3.115(1) Å) as blue dashed lines and bifurcated interdimer $CN\cdots S-S$ contacts (3.037(3) – 3.101(2) Å) as red dashed lines.

To date, this is the only example of isostructurality between a 1,2,3,5-dithiadiazolyl radical and its fluorinated counterpart. Because β -[1] and [2] differ only in the exchange of the hydrogen atoms in β -[1] for fluorine atoms to give [2], these two radicals show promise as possible co-crystal formers as this could be likened to the phenyl-perfluorophenyl co-crystal (see Chapter 2). Furthermore, due to this isostructurality, a co-crystal between these two radicals may be more likely to form than between molecules with very different crystal structures making this combination of radicals worthy of investigation.

In addition, in both β -[1] and [2], the disulphide unit of the asymmetric unit forms a bifurcated interaction with the nitrile of an adjacent, crystallographically independent molecule ($CN\cdots S-S = 3.037(3) - 3.101(2)$ Å). Figure 4.6 shows a comparison between the

[†] The term isostructural describes two crystals that have the same crystal structure with small comparable variations in atomic coordinates permissible. Identical unit cell dimensions are not necessarily required.

crystal structures of β -[1] and [2]. The crystal structure of β -[1] forms similar *trans*-antarafacial dimers ($S\cdots S = 3.141 \text{ \AA}$) with bifurcated $CN\cdots S-S$ contacts of $2.979 - 3.102 \text{ \AA}$.⁵ A structural overlay of these two radicals (calculated in Mercury⁶⁻⁹) is shown in Figure 4.6c. Interestingly, the dithiadiazolyl heterocycle is co-planar with the phenyl ring in β -[1] whereas there is a 15° out-of-plane tilt angle in [2] due to the large fluorine atoms in the positions *ortho*- to the dithiadiazolyl heterocycle. This 15° out-of-plane tilt angle is much smaller than that seen in other fluorinated dithiadiazolyl radicals,¹⁰⁻¹³ suggesting a compromise in the torsion angle to maximise intermolecular contacts and minimise void space.

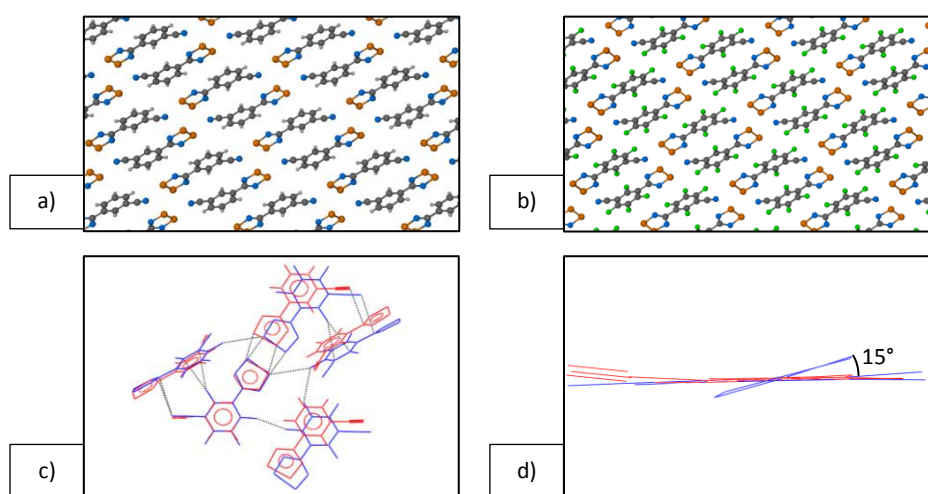


Figure 4.6: Comparison of the crystal structures of β -[1] and [2]: a) packing diagram of β -[1] viewed down the b axis, b) packing diagram of [2] viewed down the b axis, c) structural overlay of [1] (red) and [2] (blue) calculated in Mercury⁶⁻⁹ showing the isostructurality of [1] and [2] (intermolecular contacts are shown as black lines) and d) structural overlay of [1] and [2] showing the 15° out-of-plane tilt angle of the dithiadiazolyl heterocycle in [2] (blue) in comparison to the co-planar [1] (red).

The introduction of a supramolecular synthon such as $CN\cdots S-S$ into the known co-crystal consisting of phenyl- and perfluorophenyl-1,2,3,5-dithiadiazolyl radicals using [1] and [2] as co-crystal formers could form chains in the solid state such as those observed in α -[1]. In addition, co-crystallisation with [2] could minimise Peierls' distortion through the formation of uniform stacks due to the aryl-perfluoroaryl interaction.

4.2.2) The Nitro-Halogen Synthon

The nitro-halogen synthon was first identified during a study of the crystal structures of 4-chloro- and 4-bromo- β -nitrostyrene.^{14, 15} In 1996, Thalladi *et al.* showed that the nitro-iodo synthon is robust in the presence of a stronger synthon such as the carboxyl dimer.¹⁶

Furthermore, a computational study¹⁷ of the $X\cdots O_2N$ interaction ($X = Cl, Br, I$) showed the interaction energies of the $Cl\cdots O_2N$ and $Br\cdots O_2N$ interactions to be -5.74 and -6.54 kJ mol^{-1} , respectively, and from the trend observed the $I\cdots O_2N$ interaction was tentatively estimated at approximately -10 kJ mol^{-1} . Although these interactions are too weak to inhibit the dimerisation of radicals, they could induce interesting structural changes in the molecular crystal.

For this reason, the *para*-bromo-, *para*-iodo-, *meta*-nitro- and *para*-nitrophenyl-1,2,3,5-dithiadiazolyl radicals (Figure 4.7) were synthesised. The chloride salts of each of these derivatives have all previously been synthesised,^{18, 19} whereas only synthesis of the *para*-iodo-,²⁰ *meta*-nitro-,²¹ and *para*-nitrophenyl-radicals²² has previously been reported. Furthermore, only the crystal structure for [4] is known.²⁰

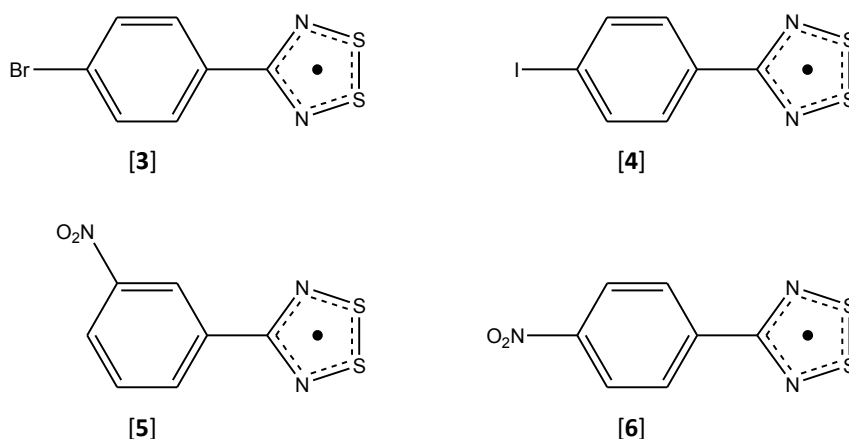


Figure 4.7: Molecular structures of the target molecules: [3] - *para*-bromophenyl-dithiadiazolyl, [4] - *para*-iodophenyl-dithiadiazolyl, [5] - *meta*-nitrophenyl-dithiadiazolyl and [6] - *para*-nitrophenyl-dithiadiazolyl

During this study, the crystal structures of the *para*-bromo- ([3]) and *meta*-nitro- ([5]) 1,2,3,5-dithiadiazolyl radicals were determined. Sublimation of the *para*-nitrophenyl-dithiadiazolyl radical after reduction experiments with Ph_3Sb or Zn-Cu couple in THF did not yield crystals of suitable quality for single crystal x-ray diffraction analysis. Before discussing the co-crystallisation experiments that were conducted, the two novel crystal structures will briefly be described.

4.3) Two Novel Crystal Structures

4.3.1) The Crystal Structure of 4-(4'-bromophenyl)-1,2,3,5-dithiadiazolyl, [3]

The asymmetric unit of the crystal structure of [3] is shown in Figure 4.8. Molecules of [3] dimerise in a *cis*-oid configuration stabilised by two intradimer S...S contacts (3.056(1) – 3.132(1) Å). Dimers pack in a herring-bone fashion in sheets in the *b*-*c* plane (Figure 4.9) stabilised by orthogonal Br...S-S (3.382(1) – 3.512(1) Å), Br...Ar (3.290(2) Å), Br...S (3.580(1) Å) and S-S...Ar (3.321(2) – 3.346(2) Å) interactions (Figure 4.9). These values were compared to the sum of the van der Waals radii²³ in each case: Br...S – 3.8 Å, Br...Ar_C – 3.65 Å and S...Ar_C – 3.55 Å. Each interaction is appreciably shorter than the sum of the van der Waals radii. In addition, the herring-bone sheets are stacked above one another and stabilised by close lateral S...N contacts (3.065(3) – 3.166(3) Å) which are slightly shorter than the sum of the van der Waals radii (3.2 Å)²⁴ (Figure 4.10). The small twist angles between the dithiadiazolyl heterocycle and the aryl ring (-5.46 – -8.40°) is comparable to other phenyl-substituted dithiadiazolyl radicals (0.8 – 17.3°).²⁵

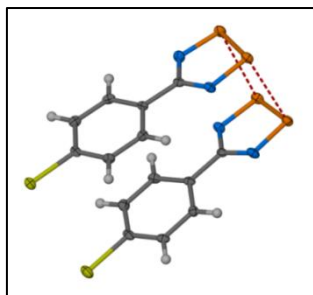


Figure 4.8: Asymmetric unit of the 4-(4'-bromophenyl)-1,2,3,5-dithiadiazolyl radical, [3]. *Cis*-oid dimers form in the solid state with intermolecular S...S contacts (3.056(1) and 3.132(1) Å) shown as red dashed lines. Non-hydrogen atoms are modelled as ellipsoids (50%).

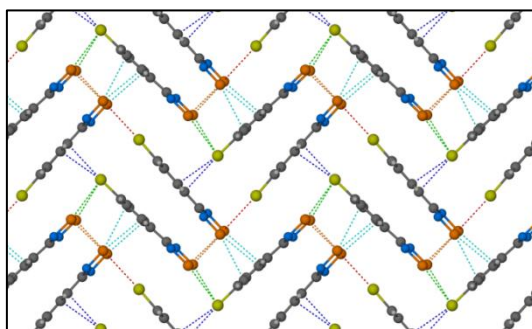


Figure 4.9: Crystal packing diagram of the *b*-*c* plane of [3] showing interdimer contacts as dashed lines: green - Br...S-S, dark blue - Br...Ar, red - Br...S and light blue - S-S...Ar. Intradimer S...S contacts are shown as dashed orange lines.

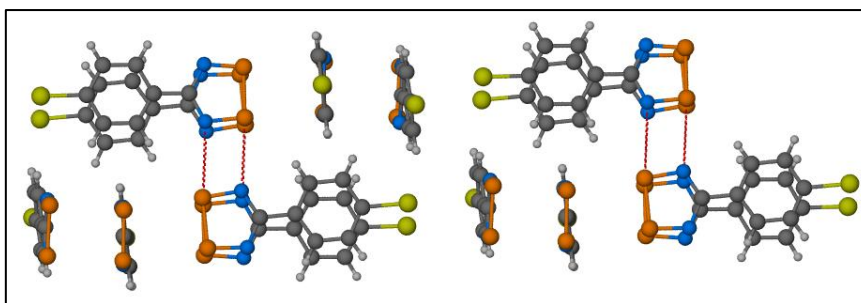


Figure 4.10: Crystal packing diagram [3] showing inter-dimer S...N contacts (3.065(3) – 3.166(3) Å) (red dashed lines) between herring-bone sheets of dimers.

4.3.2) The Crystal Structure of 4-(3'-nitrophenyl)-1,2,3,5-dithiadiazolyl, [5]

The 4-(3'-Nitrophenyl)-1,2,3,5-dithiadiazolyl radical crystallises as long, thin, red needles in the space group $P2_1/n$. In the solid state, molecules of [5] dimerise in a *cis*-oid fashion with intradimer S...S contacts (3.066(2) – 3.089(2) Å) (Figure 4.11) forming chains in the *b*-*c* plane (Figure 4.12). These chains are stabilised by interchain close lateral S...N contacts of 3.192(4) – 3.269(4) Å (Figure 4.12).

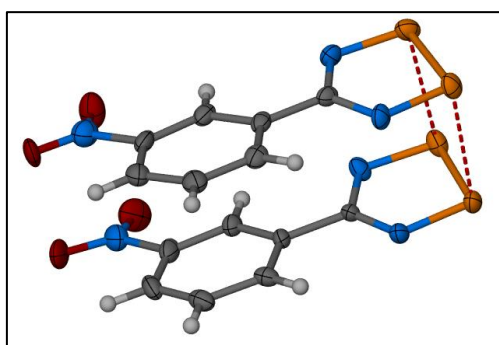


Figure 4.11: Asymmetric unit of 4-(3'-nitrophenyl)-1,2,3,5-dithiadiazolyl, [5], showing *cis*-oid dimerisation through strong intermolecular S...S contacts (3.066(2) – 3.089(2) Å). Non-hydrogen atoms are modelled as ellipsoids (50%).

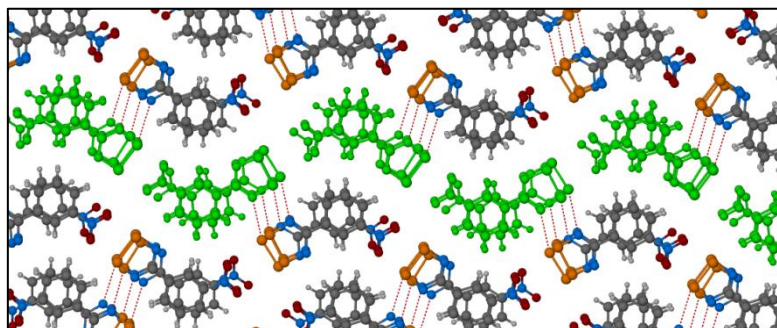


Figure 4.12: Crystal packing diagram of [5] viewing the *b*-*c* plane in which radical dimers form chains stabilised by interdimer NO₂...S-S (2.865(4) – 3.222(4) Å) interactions and interchain S...N contacts (3.192(4) – 3.269(4) Å).

Dimers in the chain are linked by close S \cdots O contacts of 2.865(4) – 3.222(4) Å, which are slightly shorter than the sum of the van der Waals radii²³ of 3.25 Å. In fact, the interdimer S \cdots O contacts involve staggered dimer pairs in the columns normal to the *b*-*c* plane (Figure 4.13). Dimer pairs are coloured differently to show their staggered conformation relative to adjacent columns. Furthermore, Figure 4.14 shows alternating layers of [5] in the columns (coloured blue and green). These two layers are distinguished from one another by the NO₂ \cdots S interactions formed between molecules in the chain. In the blue layers, the molecules in the chain are linked together by a NO₂ \cdots S-S interaction, or in other words, two O \cdots S interactions (3.030(4) – 3.222(4) Å). In contrast, green layers contain chains of molecules linked by only one O \cdots S interaction (2.865(4) Å).

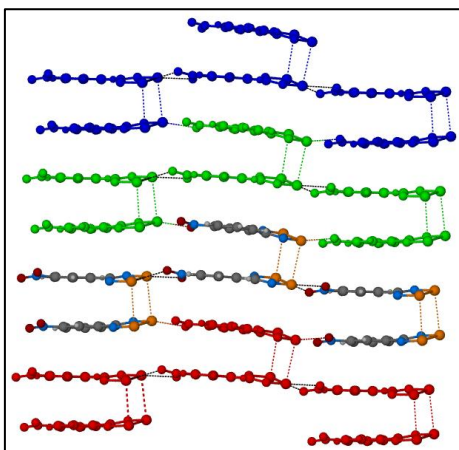


Figure 4.13: Crystal packing diagram showing layers of staggered dimers of [5] forming chains linked by NO₂ \cdots S interactions. Chains of dimers are coloured differently.

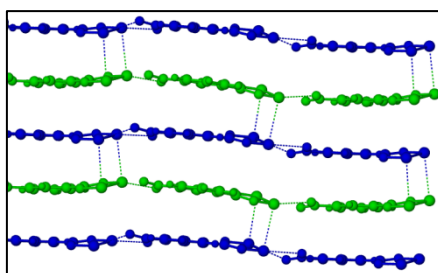


Figure 4.14: Crystal packing diagram showing different layers of [5] distinguished by their chain-forming interactions: the blue layers contain molecules of [5] in chains linked by a NO₂ \cdots S-S interaction (or two O \cdots S interactions) whereas the green layers contain molecules of [5] in chains linked by a single NO₂ \cdots S (or O \cdots S) interaction.

As a result of these interactions, a three-dimensional network of interactions is formed. This could act as a magnetic exchange pathway if spin-pairing through dimerisation could be overcome in the solid state. A good example of this is the 4-(4'-nitroperfluorophenyl)-1,2,3,5-dithiadiazolyl radical¹² which exhibits ferromagnetic ordering up to 1.6 K propagated

by a three-dimensional magnetic exchange pathway through $N_{\text{heterocycle}} \cdots N_{\text{nitro}}$ and $S \cdots O$ contacts. Spin-pairing of these radicals does not occur in the solid state as the radicals exist as monomers.

The heterocycle-aryl twist angle observed in [5] ranges between $8.49 - 11.07^\circ$ which is comparable to other phenyl-substituted dithiadiazolyl radicals.²⁵ In addition, the nitro group is also twisted out of the plane of the phenyl ring by $4.59 - 12.10^\circ$. The larger twist angle is observed for the nitro group which forms two $O \cdots S$ contacts whereas the smaller twist angle corresponds to the nitro group which only forms the single $O \cdots S$ contact in the solid state.

It was surprising to find that the crystal structure of [5] is, in fact, isostructural with the α -phase of 4-(3'-cyanophenyl)-1,2,3,5-dithiadiazolyl, α -[1]. A structure overlay of the two crystals structures was calculated in Mercury⁶⁻⁹ showing significant similarity between the two structures (Figure 4.15).

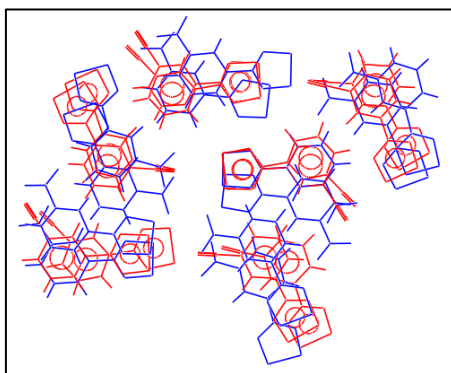


Figure 4.15: Structure overlay showing the isostructurality of [1] and [5] (calculated in Mercury⁶⁻⁹). Short contacts are omitted for clarity. A small difference in the out-of-plane twist angles, $1-5^\circ$, of the heterocycles with respect to the plane of the aryl rings is noticeable.

4.4) Co-crystallisation Experiments

4.4.1) [1] & [2] in THF

Considering that the powder patterns of 3'-cyanophenyl-[1] and 3'-cyanoperfluorophenyl-[2] are different (Figure 4.16), analysis by powder x-ray diffraction provides a suitable means to determine whether a co-crystal had formed. Furthermore, the work presented in Chapter 2 showed that the co-crystals could be formed by mixing the two co-crystal formers in THF and removing the solvent *in vacuo*. Therefore, an experiment to determine whether a co-crystal of [1] and [2] could be made by this simple method was

attempted. However, the purple residue obtained after removing the solvent *in vacuo* was shown to be amorphous by PXRD analysis.

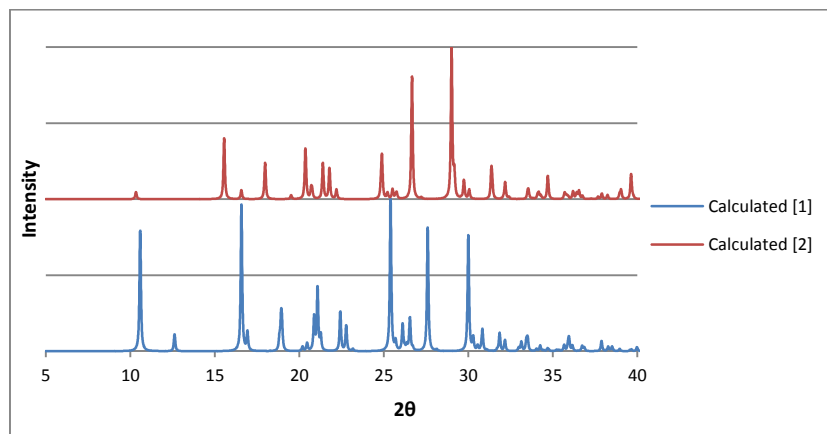


Figure 4.16: Powder patterns of [1] and [2] calculated from their crystal structures showing that PXRD would be able to show if a new phase had been formed between these two radicals.

Future work should investigate whether a co-crystal between [1] and [2] could be formed by melting the two radicals together.

4.4.2) [1] with other dithiadiazolyls

Maintaining the idea of using the aryl-perfluoroaryl interaction to cause stacking of the radicals in the solid state, [1] was sublimed with the pentafluorophenyl-1,2,3,5-dithiadiazolyl radical, [7] at 80°C under vacuum. However, due to the large difference in sublimation temperatures of the two radicals, red blocks corresponding to [7] formed on the side of the Schlenk while the dark needles of [1] remained intact at the bottom of the Schlenk. After scraping the crystals of [7] back down, the mixture was sublimed at 130°C yielding the same result.

In a similar experiment, [1] was sublimed with the perfluoropyridyl-1,2,3,5-dithiadiazolyl radical, [8] at 120°C. The sublimed material consisted of blue blocks similar in appearance to [8]. Unit cell determinations by SCXRD showed that these blue blocks were identical to [8] indicating that no co-crystal had formed.

Despite the fact that co-crystals did not grow by sublimation in these experiments, it is quite possible that a co-crystal could form from the melt or from mixing in THF. Future work should investigate these techniques further with various combinations of radicals.

4.4.3) Nitro-halogen synthon: co-reduction using Ph₃Sb

Mixtures of 4'-iodo-[4] and 3'-nitro-[5], and 4'-iodo-[4] and 4'-nitro-[6] were co-reduced by Ph₃Sb from the melt. Thereafter, the mixtures were sublimed at 100 °C in an attempt to form novel co-crystals.

In the case of the reduction mixture containing [4] and [5], two distinct morphologies of crystals were observed on the sides of the Schlenk: red blocks and long, thin, red needles. A unit cell determination of the red blocks showed they consisted of [4] whereas, a structure determination on the red needles showed they consisted of [5].

Sublimation of the reduction mixture containing [4] and [6] produced only red blocks on the sides of the Schlenk corresponding to [4] by unit cell determination. A yellow powder remained at the bottom of the Schlenk which could be the salt of [6] which was not reduced.

The combinations of 4'-bromo-[3] + [5] and [4] + [5] were mixed together in THF. In both cases, purple residues remained after removing the solvent *in vacuo*. PXRD analysis showed both mixtures to be amorphous. Combinations using [6] were not tried as sublimation to purify the radical after reduction did not yield sufficient quantities of [6].

The preparation of novel co-crystals using the nitro-halogen synthon has been unsuccessful to date.

4.4.4) [1] & [5]

Due to the isostructurality of 3'-cyano-[1] and 3'-nitro-[5], co-reduction and subsequent sublimation experiments were conducted between [1] and [5]. However, the sublimed material consisted mainly of [5] whereas [1] remained at the bottom of the Schlenk.

In a separate experiment, [1] and [5] were mixed together in THF. Thereafter, the solvent was removed *in vacuo* to yield a purple powder which was analysed by PXRD. The powder pattern showed an amorphous material.

Despite the use of different techniques including co-reduction, sublimation and solvent mixing to form co-crystals with 1,2,3,5-dithiadiazolyl radicals, no novel co-crystals were formed. Nonetheless, melt crystallisation could provide a means to prepare co-crystals. DSC analysis could help to screen possible combinations for melt crystallisation experiments.

4.5) Conclusions

In conclusion, the crystal structure was obtained for the dithiadiazolyl radical: 4-(3'-cyanoperfluorophenyl)-1,2,3,5-dithiadiazolyl, [2] which is isostructural with the β -phase of 3'-cyano-[1]. This interesting result led to the investigation into the possibility of co-crystallisation between [1] and [2]. However, the experiment to form a novel co-crystal with these two radicals by mixing in THF was unsuccessful. The co-crystallisation of [1] and [2] should be investigated further as their isostructurality could yield crystals with interesting structural features such as chains or stacks of radicals leading to interesting magnetic or conducting properties. The method of growing co-crystals from the melt should be investigated using [1] and [2]. A DSC analysis of a mixture of the two radicals may give an indication whether a co-crystal would form or not. In addition, co-crystallisation experiments using other dithiadiazolyl radicals in combination with [1] or [2] should be investigated, especially the isostructural dithiadiazolyl [5], although initial attempts at co-crystallisation between [1] and [5] have been unsuccessful.

Novel crystal structures were obtained for the 4-(4'-bromophenyl)- and 4-(3'-nitrophenyl)-1,2,3,5-dithiadiazolyl radicals, [3] and [5], respectively. The crystal structure of [3] shows *cis*-oid dimers stabilised by a number of interactions including Br \cdots S-S, Br \cdots S, Br \cdots Ar and S-S \cdots Ar interactions. In addition, close lateral S \cdots N contacts stabilise herring-bone layers of [3]. The crystal structure of [5] shows *cis*-oid dimers forming staggered stacks of chains stabilised by NO₂ \cdots S interactions. In addition, adjacent chains are stabilised by close lateral S \cdots N contacts. Consequently, a three-dimensional network of interactions exists in the crystal structure which could act as a magnetic exchange pathway if spin-pairing through dimerisation were to be overcome in the solid state. Co-crystallisation and crystal engineering may provide a means to overcome this dimerisation.

The 4-(4'-bromophenyl)-1,2,3,5-dithiadiazolyl radical should be analysed for polymorphism by thermal analysis and VT-PXRD. Similarly, the radical [5] should be analysed to determine whether any polymorphs exist. Due to its isostructurality with α -[1], it would be interesting if it had a β -phase which was isostructural with β -[1] and [2] as this could lead to interesting co-crystallisation experiments.

Although co-crystals were not formed between [4] and [5] or [6] after subliming a co-reduced mixture of their precursor salts, alternate methods of co-crystal formation between these radicals should be investigated such as growing the co-crystals from the melt. The

nitro-halogen synthon may be able to introduce interesting structural features into the co-crystal structure: possibly by aligning the radicals in a particular direction. A DSC analysis of various combinations of nitro- and halo-dithiadiazolyl radicals could provide an indication as to which combinations would favourably form co-crystals.

Co-crystallisation attempts were made between [3] + [5], and [4] + [5] by mixing in THF. Unfortunately, the resulting residues were amorphous. The use of co-crystallisation from the melt should be investigated.

Experiments to form co-crystals by sublimation using [1] + [7] and [1] + [8] were unsuccessful. This could be due to the sublimation temperature of [1] being higher than the sublimation temperatures of [7] and [8]. Alternate methods of co-crystal formation with these dithiadiazolyl radicals should be investigated.

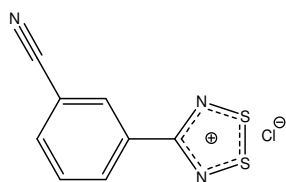
4.6) Experimental Procedures

Please consult Appendix A for Instrumentation and Chemicals used.

4.6.1) 1,2,3,5-Dithiadiazolyl Radicals

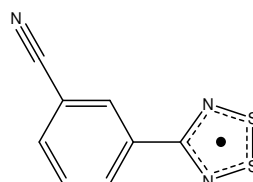
Salt formation: In a typical experiment, diethyl ether (50 ml) was added to a Schlenk tube filled with nitrogen and containing a magnetic stirrer bar and cooled to $-78\text{ }^{\circ}\text{C}$. 1,1,1,3,3,3-Hexamethyldisilazane (1.7 ml, 8.1 mmol) was added, followed by *n*-Butyllithium (5.5 ml, 8.1 mmol). The solution was allowed to warm to room temperature resulting in a clear solution. The corresponding nitrile (8.1 mmol) was added to the mixture which was stirred overnight, resulting in a pale yellow solution. The mixture was cooled to $0\text{ }^{\circ}\text{C}$ and a slight excess of SCl_2 (22.0 mmol, 1.4 ml) was added dropwise causing the immediate precipitation of a bright yellow or orange solid. The solution was allowed to warm to room temperature and stirred for a further hour. Thereafter, the mother liquor was filtered off and the bright yellow or orange solid was washed with diethyl ether (2 x 20 ml). The solid was dried *in vacuo* to yield the parent 1,2,3,5-dithiadiazolylium chloride salt as a bright yellow or orange powder.

Salt reduction: Zn-Cu couple/THF: A portion of the dithiadiazolylium chloride salt was added to a Schlenk tube filled with nitrogen and containing a magnetic stirrer bar. THF was added to the salt forming a bright yellow or orange suspension. Half an equivalent of Zn-Cu couple was added and the solution was stirred overnight. The resulting solution was filtered and the solvent was removed *in vacuo* to yield a residue. Colours of the solution and residue can vary between brown and purple. The radical was purified by sublimation under vacuum. *Ph₃Sb:* A portion of the parent salt was placed in a dry Schlenk tube filled with nitrogen. Half an equivalent of Ph_3Sb was added and the Schlenk was heated at $60\text{ }^{\circ}\text{C}$ in an oil bath until the bright yellow salt had changed colour from bright yellow to dark purple. Vacuum was applied to the Schlenk which was itself heated to sublime the radicals.

4-(3'-CYANOPHENYL)-1,2,3,5-DITHIADIAZOLYL, [1]**Table 4.1: Quantities of reagents used to form the salt of [1]**

Reagent	Mass (g)	Volume (ml)	Number of moles (mmol)
HMDS	-	1.65	7.8
<i>n</i> -BuLi	-	5.2	7.8
1,3-Dicyano-benzene	1.000	-	7.8
SCl ₂	-	1.3	20
Et ₂ O	-	50	-
Et ₂ O wash	-	2 x 15	-

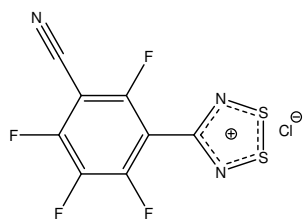
(+)-ESI-MS: *m/z* 206.9 (M⁺, 100%), 192.0 (4), 129.0 (6)

**Table 4.2: Quantities of reagents used to form the radical [1]**

Reagent	Mass (g)	Number of moles (mmol)
Salt	1.296	5.4
Ph ₃ Sb	0.900	2.5

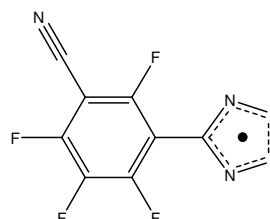
Ph₃Sb Reduction: The reduction mixture was heated at 120°C overnight affording purple needles of [1] on a cold-finger.

(+)-ESI-MS: *m/z* 206.9 (M⁺, 100%), 192.0 (4).
EPR (298 K, CH₂Cl₂): quintet (*g* = 2.007, *a_N* = 5.0 G).

4-(3'-CYANO-PERFLUOROPHENYL)-1,2,3,5-DITHIADIAZOLYL, [2]**Table 4.3: Quantities of reagents used to form the salt of [2]**

Reagent	Mass (g)	Volume (ml)	Number of moles (mmol)
HMDS	-	0.55	2.5
<i>n</i> -BuLi	-	1.7	2.5
Tetrafluoro-isophthalonitrile	0.500	-	2.5
SCl ₂	-	0.5	8
Et ₂ O	-	25	-
Et ₂ O wash	-	2 x 10	-

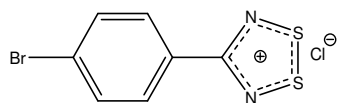
(+)-ESI-MS: *m/z* 277.9 (M⁺, 93%), 263.9 (6)

**Table 4.4: Quantities of reagents used to form the radical [2]**

Reagent	Mass (g)	Number of moles (mmol)
Salt	0.214	0.7
Ph ₃ Sb	0.110	0.31

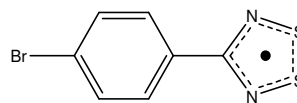
Ph₃Sb Reduction: The reduction mixture was heated at 120°C affording red-pink needles of [2] on the sides of the Schlenk.

(+)-ESI-MS: *m/z* 277.9 (M⁺, 100%), 263.9 (12)

4-(PARA-BROMOPHENYL)-1,2,3,5-DITHIADIAZOLYL, [3]**Table 4.5: Quantities of reagents used to form the salt of [3]**

Reagent	Mass (g)	Volume (ml)	Number of moles (mmol)
HMDS	-	1.2	5.5
<i>n</i> -BuLi	-	3.7	5.5
4-bromo-benzonitrile	1.000	-	5.5
SCl ₂	-	0.9	14
Et ₂ O	-	35	-
Et ₂ O wash	-	2 x 15	-

(+)-ESI-MS: *m/z* 258.9 (M⁺, 78%), 180.9 (4)

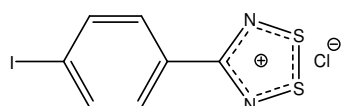
**Table 4.6: Quantities of reagents used to form the radical [3]**

Reagent	Mass (g)	Volume (ml)	Number of moles (mmol)
Salt	0.540	-	1.8
Zn-Cu	0.059	-	0.9
THF	-	15	-
Salt	0.170	-	0.58
Ph ₃ Sb	0.090	-	0.25

In both reduction experiments: The mixtures were heated at 100°C affording red blocks of [3] on the sides of the Schlenk.

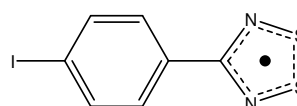
(+)-ESI-MS: *m/z* 258.9 (M⁺, 45%)

EPR (298 K, CH₂Cl₂): quintet (*g* = 2.010, *a_N* = 5.1 G).

4-(PARA-IODOPHENYL)-1,2,3,5-DITHIADIAZOLYL, [4]**Table 4.7: Quantities of reagents used to form the salt of [4]**

Reagent	Mass (g)	Volume (ml)	Number of moles (mmol)
HMDS	-	0.5	2.2
<i>n</i> -BuLi	-	1.5	2.2
4-iodo-benzonitrile	0.500	-	2.2
SCl ₂	-	0.4	6
Et ₂ O	-	25	-
Et ₂ O wash	-	2 x 10	-

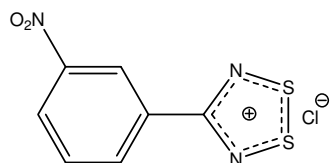
(+)-ESI-MS: *m/z* 307.9 (MH⁺, 100%), 306.9 (M⁺, 85), 292.9 (9), 260.9 (5), 229.9 (69)

**Table 4.8: Quantities of reagents used to form the radical [4]**

Reagent	Mass (g)	Number of moles (mmol)
Salt	0.196	0.6
Ph ₃ Sb	0.090	0.25

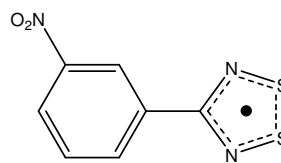
Ph₃Sb Reduction: The reduction mixture was heated at 100°C affording red blocks of [4] on the sides of the Schlenk.

(+)-ESI-MS: *m/z* 307.9 (MH⁺, 4%), 306.9 (M⁺, 5%), 229.9 (100)

4-(META-NITROPHENYL)-1,2,3,5-DITHIADIAZOLYL, [5]**Table 4.9: Quantities of reagents used to form the salt of [5]**

Reagent	Mass (g)	Volume (ml)	Number of moles (mmol)
HMDS	-	1.5	6.8
<i>n</i> -BuLi	-	4.5	6.8
3-Nitrobenzonitrile	1.000	-	6.8
SCl ₂	-	1.2	19
Et ₂ O	-	50	-
Et ₂ O wash	-	2 x 15	-

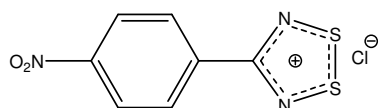
(+)-ESI-MS: *m/z* 225.9 (M⁺, 100%), 212.0 (13), 196.0 (5), 180.0 (3), 167.0 (5)

**Table 4.10: Quantities of reagents used to form the radical [5]**

Reagent	Mass (g)	Volume (ml)	Number of moles (mmol)
Salt	0.437	-	1.7
Zn-Cu	0.054	-	0.8
THF	-	15	-
Salt	0.146	-	0.6
Ph ₃ Sb	0.086	-	0.24

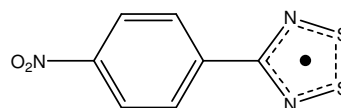
In both reduction experiments: The mixtures were at 100 °C affording red needle-shaped crystals of [5] on the sides of the Schlenk.

(+)-ESI-MS: *m/z* 225.9 (M⁺, 100%), 179.9 (4).
EPR (298 K, CH₂Cl₂): quintet (*g* = 2.010, *a_N* = 5.0 G).

4-(PARA-NITROPHENYL)-1,2,3,5-DITHIADIAZOLYL, [6]**Table 4.11: Quantities of reagents used to form the salt of [6]**

Reagent	Mass (g)	Volume (ml)	Number of moles (mmol)
HMDS	-	1.5	6.8
<i>n</i> -BuLi	-	4.5	6.8
4-Nitrobenzonitrile	1.000	-	6.8
SCl ₂	-	1.2	19
Et ₂ O	-	50	-
Et ₂ O wash	-	2 x 15	-

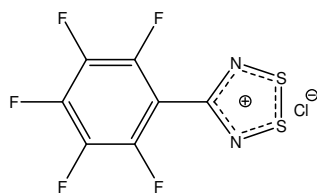
(+)-ESI-MS: *m/z* 225.9 (M⁺, 100%), 209.9 (9), 179.9 (3), 166.0 (7), 149.0 (4)

**Table 4.12: Quantities of reagents used to form the radical [6]**

Reagent	Mass (g)	Number of moles (mmol)
Salt	0.148	0.6
Ph ₃ Sb	0.090	0.25

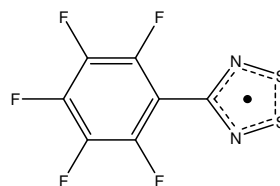
Reduction: The reduction mixture was heated at 100°C causing red-purple film of [6] to form on the sides of the Schlenk.

(+)-ESI-MS: *m/z* 225.9 (M⁺, 100%), 212.0 (6), 209.9 (4), 159.9 (3), 149.0 (3). EPR (298 K, CH₂Cl₂): quintet (*g* = 2.010, *a_N* = 5.1 G).

4-PERFLUOROPHENYL-1,2,3,5-DITHIADIAZOLYL, [7]**Table 4.13: Quantities of reagents used to form the salt of [7]**

Reagent	Volume (ml)	Number of moles (mmol)
HMDS	1.7	8.1
<i>n</i> -BuLi	5.5	8.1
Pentafluorobenzonitrile	1.0	8.1
SCl ₂	1.4	22
Et ₂ O	50	-
Et ₂ O wash	2 x 20	-

(+)-ESI-MS: *m/z* 270.9 (M⁺, 100%), 257.2 (5), 253.1 (2), 240.9 (3)

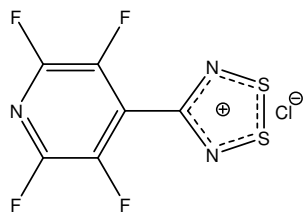
**Table 4.14: Quantities of reagents used to form the radical [7]**

Reagent	Mass (g)	Number of moles (mmol)
Salt	0.344	1.1
Ph ₃ Sb	0.158	0.45

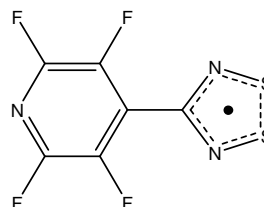
Reduction: The reduction mixture was heated at 40 °C affording red blocks of [7] on the sides of the Schlenk.

(+)-ESI-MS: *m/z* 270.9 (M⁺, 100%)

EPR (298 K, CH₂Cl₂): quintet (*g* = 2.010, *a_N* = 4.9 G).

4-PERFLUOROPYRIDYL-1,2,3,5-DITHIADIAZOLYL, [8]**Table 4.15: Quantities of reagents used to form the salt of [8]**

Reagent	Mass (g)	Volume (ml)	Number of moles (mmol)
HMDS	-	1.2	5.7
<i>n</i> -BuLi	-	3.8	5.7
Tetrafluoro-4-pyridine-carbonitrile	1.000	-	5.7
SCl ₂	-	1.0	16
Et ₂ O	-	40	-
Et ₂ O wash	-	2 x 20	-

**Table 4.16: Quantities of reagents used to form the radical [8]**

Reagent	Mass (g)	Number of moles (mmol)
Salt	0.149	0.5
Ph ₃ Sb	0.073	0.21

Reduction: The reduction mixture was heated at 100°C affording blue blocks of [8] on the sides of the Schlenk.

(+)-ESI-MS: *m/z* 253.9 (M⁺, 30%), 221.1 (16), 194.0 (100). EPR (298 K, CH₂Cl₂): quintet (*g* = 2.011, *a_N* = 5.0 G).

4.6.2) Co-crystallisation Experiments

MIXING [1] AND [2] IN THF

[1] (0.011 g, 0.05 mmol) and [2] (0.013 g, 0.05 mmol) were placed together in a dry Schlenk tube filled with nitrogen. Dry THF (3 ml) was added forming a yellow solution as the radicals dissolved. The solution was mixed for 10 minutes. Thereafter, the solvent was removed *in vacuo* and the resulting purple residue was dried. The bulk sample was scraped out of the Schlenk using a spatula and analysed by PXRD.

CO-SUBLIMATION OF [1] AND [7]

[1] (0.011 g, 0.05 mmol) and [7] (0.019 g, 0.07 mmol) were placed together in a dry Schlenk tube filled with nitrogen. Vacuum was applied and the Schlenk was placed in an oil bath at 80 °C. At this temperature, only red block-shaped crystals of [3] sublimed. Thus, these crystals were scraped back down to the bottom of the Schlenk with a spatula. The Schlenk was re-immersed in the oil bath now at 130 °C. Again, only red block-shaped crystals of [7] sublimed.

CO-SUBLIMATION OF [1] AND [8]

[1] (0.012 g, 0.06 mmol) and [8] (0.015 g, 0.06 mmol) were placed together in a dry Schlenk tube filled with nitrogen. Vacuum was applied and the Schlenk was placed in an oil bath at 120 °C. The sublimed material consisted of blue blocks that were shown by unit cell (Table 4.17) determination to be [8].

Table 4.17: Reduced cell parameters of the blue blocks obtained by sublimation shown to be [8] when compared the literature.

	Literature	Observed
<i>a</i>	9.654	9.68
<i>b</i>	10.151	10.24
<i>c</i>	10.715	10.86
α	66.30	66.01
β	63.22	63.55
γ	61.61	61.79

CO-REDUCTION AND SUBLIMATION OF [4] AND [5]

[4] (0.078 g, 0.25 mmol) and [5] (0.075 g, 0.33 mmol) were placed together in a dry Schlenk filled with nitrogen. Ph₃Sb (0.080 g, 0.23 mmol) was added and the mixture was heated at 60 °C to reduce the salts to their corresponding radicals from the melt of Ph₃Sb. Once the residue had changed colour completely from yellow-orange to dark purple, vacuum was applied to the Schlenk and the mixture was heated to 100 °C to sublime the radicals. Two distinct crystal habits were observed in the separate bands of the sublimed material: red blocks and fine red needles corresponding to [4] and [5], respectively.

Table 4.18: Unit cell parameters of the red blocks show them to consist of [4] when compared to the literature

	Literature	Observed
<i>a</i>	5.719	5.72
<i>b</i>	8.610	8.62
<i>c</i>	18.320	18.31
α	90	90
β	97.05	97.05
γ	90	90

CO-REDUCTION AND SUBLIMATION OF [4] AND [6]

[4] (0.112 g, 0.36 mmol) and [6] (0.116 g, 0.51 mmol) were placed together in a dry Schlenk filled with nitrogen. Ph₃Sb (0.115 g, 0.33 mmol) was added and the mixture was heated at 60 °C to reduce the salts to their corresponding radicals from the melt of Ph₃Sb. Once the residue had changed colour completely from yellow-orange to dark purple, vacuum was applied to the Schlenk and the mixture was heated to 100 °C to sublime the radicals. Only red block-shaped crystals corresponding to [4] were observed in the sublimed material.

Table 4.19: Unit cell parameters of the red blocks show them to consist of [4] when compared to the literature

	Literature	Observed
<i>a</i>	5.719	5.71
<i>b</i>	8.610	8.62
<i>c</i>	18.320	18.33
α	90	90
β	97.05	96.94
γ	90	90

MIXING [3] AND [5] IN THF

[3] (0.012 g, 0.05 mmol) and [5] (0.011 g, 0.05 mmol) were placed together in a dry Schlenk tube filled with nitrogen. Dry THF (3 ml) was added forming a brown solution as the radicals dissolved. The solution was mixed for 10 minutes. Thereafter, the solvent was removed *in vacuo* and the resulting purple residue was dried. The bulk sample was scraped out of the Schlenk using a spatula and analysed by PXRD.

MIXING [4] AND [5] IN THF

[4] (0.026 g, 0.08 mmol) and [5] (0.021 g, 0.08 mmol) were placed together in a dry Schlenk tube filled with nitrogen. Dry THF (3 ml) was added forming a yellow solution as the radicals dissolved. The solution was mixed for 10 minutes. Thereafter, the solvent was removed *in vacuo* and the resulting purple residue was dried. The bulk sample was scraped out of the Schlenk using a spatula and analysed by PXRD.

4.7) References

1. D. A. Haynes, *Unpublished results*, 2010.
2. A. W. Cordes, R. C. Haddon, R. G. Hicks, R. T. Oakley and T. T. M. Palstra, *Inorganic Chemistry*, 1992, **31**, 1802-1808.
3. A. Kálmán, L. Párkányi and G. Argay, *Acta Crystallographica Section B*, 1993, **49**, 1039-1049.
4. L. Fábrián and A. Kálmán, *Acta Crystallographica Section B*, 1999, **55**, 1099-1108.
5. A. W. Cordes, R. C. Haddon, R. G. Hicks, R. T. Oakley and T. T. M. Palstra, *Inorganic Chemistry*, 1992, **31**, 1802-1808.
6. R. Taylor and C. F. Macrae, *Acta Crystallographica Section B*, 2001, **57**, 815-827.
7. I. J. Bruno, J. C. Cole, P. R. Edgington, M. Kessler, C. F. Macrae, P. McCabe, J. Pearson and R. Taylor, *Acta Crystallographica Section B*, 2002, **58**, 389-397.
8. C. F. Macrae, P. R. Edgington, P. McCabe, E. Pidcock, G. P. Shields, R. Taylor, M. Towler and J. van de Streek, *Journal of Applied Crystallography*, 2006, **39**, 453-457.
9. C. F. Macrae, I. J. Bruno, J. A. Chisholm, P. R. Edgington, P. McCabe, E. Pidcock, L. Rodriguez-Monge, R. Taylor, J. van de Streek and P. A. Wood, *Journal of Applied Crystallography*, 2008, **41**, 466-470.
10. A. J. Banister, N. Bricklebank, I. Lavender, J. M. Rawson, C. I. Gregory, B. K. Tanner, W. Clegg, M. R. J. Elsegood and F. Palacio, *Angewandte Chemie International Edition in English*, 1996, **35**, 2533-2535.
11. G. Antorrena, J. E. Davies, M. Hartley, F. Palacio, J. M. Rawson, J. N. B. Smith and A. Steiner, *Chemical Communications*, 1999, 1393-1394.
12. A. Alberola, R. J. Less, C. M. Pask, J. M. Rawson, F. Palacio, P. Oliete, C. Paulsen, A. Yamaguchi, R. D. Farley and D. M. Murphy, *Angewandte Chemie International Edition in English*, 2003, **42**, 4782-4785.
13. A. Alberola, R. J. Less, F. Palacio, C. M. Pask and J. M. Rawson, *Molecules*, 2004, **9**, 771-781.
14. G. R. Desiraju and V. R. Pedireddi, *Journal of the Chemical Society, Chemical Communications*, 1989, 1112-1113.
15. V. R. Pedireddi, J. A. R. P. Sarma and G. R. Desiraju, *Journal of the Chemical Society, Perkin Transactions 2*, 1992, 311-320.
16. V. R. Thalladi, B. S. Goud, V. J. Hoy, F. H. Allen, J. A. K. Howard and G. R. Desiraju, *Chemical Communications*, 1996, 401-402.
17. F. H. Allen, J. P. M. Lommerse, V. J. Hoy, J. A. K. Howard and G. R. Desiraju, *Acta Crystallographica Section B*, 1997, **53**, 1006-1016.
18. C. M. Aherne, A. J. Banister, I. B. Gorrell, M. I. Hansford, Z. V. Hauptman, A. W. Luke and J. M. Rawson, *Journal of the Chemical Society, Dalton Transactions*, 1993, 967-972.
19. A. D. Bond, D. A. Haynes and J. M. Rawson, *Canadian Journal of Chemistry*, 2002, **80**, 1507-1517.
20. N. Bricklebank, S. Hargreaves and S. E. Spey, *Polyhedron*, 2000, **19**, 1163-1166.
21. G. Domschke, C. Walther, P. Tschöpe and A. Bartl, *Journal für Praktische Chemie/Chemiker-Zeitung*, 1994, **336**, 266-268.
22. R. T. Boere, K. Larsen, J. Fait, J. Yip and K. H. Mook, *Phosphorus Sulfur and Silicon and the Related Elements*, 1992, **64-5**, 321-324.
23. L. Pauling, *The nature of the chemical bond and the structure of molecules and crystals: an introduction to modern structural chemistry*, Cornell University Press, Ithaca, NY, 1960.
24. S. C. Nyburg and C. H. Faerman, *Acta Crystallographica Section B*, 1985, **41**, 274-279.
25. C. Allen, D. A. Haynes, C. M. Pask and J. M. Rawson, *CrystEngComm*, 2009, **11**, 2048-2050.

Chapter 5: Summary

5.1) Summary

This study aimed to characterise the two known dithiadiazolyl co-crystals and investigate alternative methods by which co-crystals with 1,2,3,5-dithiadiazolyl radicals could be formed. In addition, steps towards the synthesis of 1,2,3,5-dithiadiazolyl radicals that contain hydrogen-bonding were to be investigated. Finally, co-crystallisation experiments were to be conducted with combinations of 1,2,3,5-dithiadiazolyl radicals that have not yet been attempted.

The characterisation of the 4-phenyl-, 4-perfluorophenyl- and 4-perfluorophenyl-1,2,3,5-dithiadiazolyl radicals was carried out using thermogravimetric analysis (TGA) and differential scanning calorimetry (DSC). The sublimation temperatures of each of the radicals were determined by TGA, and DSC showed their respective melting and recrystallisation temperatures. In addition, DSC showed a phase change in 4-perfluoropyridyl-1,2,3,5-dithiadiazolyl radical at approximately 82 °C. Variable temperature powder X-ray diffraction (VT-PXRD) was used to confirm the phase transformation which was also observed by hot-stage microscopy. Future work should include the structural characterisation of this new phase.

The two known co-crystals formed between these radicals (phenyl- + perfluorophenyl-, and phenyl- + perfluoropyridyl-1,2,3,5-dithiadiazolyl radicals) were characterised thermally using DSC. The DSC thermograms show melting and crystallisation points for the co-crystals that are different from the pure co-crystal formers. Consequently, DSC could be used in the future to determine whether a co-crystal had formed between two radicals.

During the investigation, it was determined that the two known co-crystals form quantitatively when a mixture of the co-crystal formers is sublimed. Mechanochemical synthesis of co-crystals with 1,2,3,5-dithiadiazolyl radicals was investigated by dry grinding the co-crystal formers together however, the results show that a physical mixture was formed. The use of solvent-drop grinding, grinding in a glove box and longer grinding times should be investigated as a means to form co-crystals. However, because co-crystal formation with 1,2,3,5-dithiadiazolyl radicals requires the dissociation of the homodimers of the pure radical co-crystal formers before it can occur, mechanochemical synthesis may not be successful in synthesising co-crystals.

The method of melt co-crystallisation was investigated as a means to form the two known co-crystals. Mixtures of the co-crystal formers were melted and analysed by PXRD, showing positive results for the formation of both co-crystals. Melt experiments were also conducted *in situ* using a DSC instrument. The DSC plots showed the melting point of the lower melting co-crystal former and what could be the melting point of the co-crystal, although it is interesting that an event corresponding to crystallisation of the co-crystal is not first observed. In addition, events corresponding to the crystallisation of the co-crystals were observed on cooling, confirming that the co-crystals can be formed by melting. DSC analysis can thus be used as a screening method for the possible formation of co-crystals between different combinations of 1,2,3,5-dithiadiazolyl radicals.

The two known co-crystals could also be formed by co-reducing the parent salts of the co-crystal formers with Ph_3Sb and subliming the resulting mixture. In addition, the co-crystals could also be made by mixing the co-crystal formers in THF and removing the solvent *in vacuo*. The conversion to the co-crystal was shown to be quantitative in both cases.

In summary, it was shown that the two known co-crystals with 1,2,3,5-dithiadiazolyl radicals could be synthesised from the melt of the co-crystal formers, by subliming a co-reduced mixture of the radicals and by mixing the co-crystal formers in THF. These results are significant as they could provide a simple means by which to form co-crystals with 1,2,3,5-dithiadiazolyl radicals which were previously prepared by sublimation. Consequently, combinations of 1,2,3,5-dithiadiazolyl radicals that did not form co-crystals by sublimation could possibly be synthesised using one of these techniques.

The synthesis of novel dithiadiazolyl radicals containing hydrogen-bonding groups to be used in forming supramolecular synthons in the solid state was attempted. Results of the synthetic attempts indicated that the hydrogen-bonding groups required protection before the dithiadiazolyl heterocycle could be formed. This led to the synthesis of novel dithiadiazolyl radicals: 3'- and 4'-trimethylsiloxyphenyl- and 3'- and 4'-N,N'-bis-*t*-Boc-aminophenyl-1,2,3,5-dithiadiazolyl radicals. The trimethylsiloxy-derivatives are oils at room temperature. Their potential as paramagnetic liquids should be investigated. EPR could be used as an initial analytical method to determine whether or not the radicals are spin-paired in the liquid phase and thus, if they exhibit interesting magnetic properties.

Initial deprotection reactions of the trimethylsiloxyphenyl-derivatives with cesium fluoride were unsuccessful. Future work should investigate different reaction conditions such as solvent and the deprotection agent used.

Attempts were made to synthesise novel co-crystals with 1,2,3,5-dithiadiazolyl radicals using the CN \cdots S-S and nitro-halogen synthons. Co-crystallisation experiments were conducted using combinations of the following dithiadiazolyls: 3'-cyanophenyl-, 3'-cyanoperfluorophenyl-, 4'-bromophenyl-, 4'-iodophenyl-, 3'-nitrophenyl-, 4'-nitrophenyl-, perfluorophenyl- and perfluorophenyl-1,2,3,5-dithiadiazolyl radicals. In addition, co-crystallisation experiments were conducted using a variety of techniques (that were shown to be successful in forming the two known co-crystals in this study) including sublimation, co-reduction with Ph₃Sb and subsequent sublimation, and mixing in THF. However, these attempts were unsuccessful in producing novel co-crystals with 1,2,3,5-dithiadiazolyl radicals. Co-crystal formation from the melt between these radicals should be investigated.

During this study, novel crystal structures were determined for the 4'-bromophenyl- and 3'-nitrophenyl-1,2,3,5-dithiadiazolyl radicals. These crystal structures showed interesting supramolecular interactions including Br \cdots S-S (4'-bromophenyl-) and NO₂ \cdots S-S (3'-nitrophenyl-) contacts.

In conclusion, considering the aims of this study, the two known co-crystals were characterised using thermal analysis, which resulted in the identification of a polymorphic phase of the 4'-perfluorophenyl-1,2,3,5-dithiadiazolyl radical. In addition, investigation into alternative co-crystallisation techniques showed that co-crystals with 1,2,3,5-dithiadiazolyl radicals could be prepared from the melt, by mixing in solution and by subliming a co-reduced mixture of the radicals. Steps towards the synthesis of 1,2,3,5-dithiadiazolyl radicals that contain hydrogen-bonding groups were investigated showing that protection of the hydrogen-bonding moieties was required before the dithiadiazolyl radical could be formed. This led to the preparation of four novel dithiadiazolyl radicals, namely, the 3'- and 4'-trimethylsiloxyphenyl- and 3'- and 4'-N,N'-bis-*t*-Boc-aminophenyl-1,2,3,5-dithiadiazolyl radicals. Deprotection of the trimethylsiloxyphenyl-radicals to the target molecules containing hydrogen-bonding groups was unsuccessful under the conditions investigated. Finally, co-crystallisation experiments were conducted using combinations of 1,2,3,5-dithiadiazolyl radicals which had not been attempted before. However, no novel co-crystals were synthesised. Although, as a result of these experiments, two novel crystal structures

were determined of the 4'-bromophenyl- and 3'-nitrophenyl-1,2,3,5-dithiadiazolyl radicals by single-crystal X-ray diffraction.

Appendix A

A.1.) Instrumentation and Chemicals

A.1.1.) Chemicals & Glassware

Chemicals used in these experiments were purchased from Aldrich. Tetrahydrofuran and diethyl ether were distilled under nitrogen from sodium wire using benzophenone as an indicator. DCM was distilled under nitrogen from calcium hydride.

Glassware was dried for at least an hour at 120 °C, thereafter it was placed under vacuum of 10^{-1} Torr and cyclically flushed with nitrogen and evacuated. Standard Schlenk techniques were employed. All reactions were performed under a positive pressure of 2.8 kPa of 5.0 grade nitrogen (Air Products).

A.1.2.) Single-Crystal & Powder X-Ray Diffraction

Intensity data for single-crystal structure analysis were collected on a Bruker-Nonius SMART Apex I diffractometer equipped with a Mo fine-focus sealed tube ($K\alpha$ 0.71Å) and a 0.5 mm MonoCap collimator and Oxford Cryogenics Cryostat (700 Series Cryostream Plus) or Bruker Apex DUO CCD diffractometer with a multilayer monochromator was used. Mo- $K\alpha$ radiation ($\lambda = 0.71073$ Å) was selected for the experiments using the DUO. The temperature of the crystal was controlled using an Oxford Cryostream Cooler. Data reduction was done by means of the standard procedure using the Bruker software package SAINT¹ and the absorption corrections and the correction of other systematic errors were performed using SADABS.² The structures were solved by direct methods using SHELXS-97 and refined using SHELXL-97.³ X-Seed⁴ was used as the graphical interface for the SHELX program suite. Hydrogen atoms were placed in calculated positions using riding models.

Powder X-ray diffraction experiments were carried out on a PANalytical X'Pert PRO instrument with Bragg-Brentano geometry. Intensity data were collected using an X'Celerator detector and 2 θ scans in the range of 4-50° were performed. During the experiment the powdered sample was exposed to Cu- $K\alpha$ radiation ($\lambda = 1.5418$ Å). All powder patterns except those collected during the variable temperature experiment were obtained using the flat-stage reflection-transmission spinner. Samples were mounted on a zero background holder. For the variable temperature experiment, the sample was sealed within a glass capillary and the capillary spinner configuration (with focusing mirror) of the instrument was used since this setup allows for very accurate temperature control using an Oxford Cryostream Cooler.

A.1.3.) Electron Paramagnetic Resonance

EPR spectra were recorded at 298 K with a Bruker EMXplus X-band EPR spectrometer (8-inch ER 072 magnet, 2.7 kW power supply, EMX-m40X microwave bridge operating from 9.3 to 9.9 GHz), and

a high sensitivity continuous-wave resonator. Samples were polycrystalline solids and dilute solutions of arbitrary concentration in dry dichloromethane in an otherwise ambient atmosphere.

A.1.4.) Nuclear Magnetic Resonance

All ^1H and ^{13}C nuclear magnetic resonance spectra were recorded using a 300 MHz Varian VNMRs (75 MHz for ^{13}C) NMR spectrometer using deuterated solvents. Residual solvent peak or external reference were used to record the chemical shifts (δ) which are all reported in ppm. All spectra were recorded at 25°C. Data was processed using ACD/SpecManager product version 10.08.

A.1.5.) Mass Spectrometry

Mass spectrometric analysis was performed by the Central Analytical Facility (CAF) of the University of Stellenbosch. Spectra were collected using a Waters Synapt G2 instrument or Waters API Q-TOF Ultima. For the Waters Synapt G2 instrument, the sample was introduced using the ASAP probe while the Waters UPLC was used for the Waters API Q-TOF Ultima. The instrument was operated in APCI positive mode using a Capillary voltage of 3 kV and a Cone Voltage 15 V. The mass spectrum for the 4-phenyl-1,2,3,5-dithiadiazolyl radical in Chapter 2 was collected using a Waters GCT Premier instrument. The sample was injected into the GC column using an injector temperature of 260 °C and a split ratio of 1:10. Helium was used as the carrier gas with a flow rate of 1 ml min⁻¹. The sample was ionised and analysed using EI in the positive mode using an electron energy of 70 eV.

A.1.6.) Infrared Spectroscopy

Infrared spectra were acquired using a Nexus Thermo-Nicolet FT-IR instrument using a single bounce ATR.

A.1.7.) Isolation and Purification of the *t*-Boc-protected amines in Chapter 3

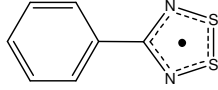
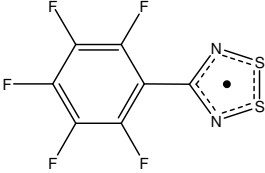
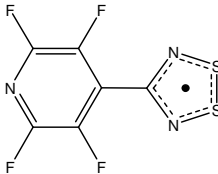
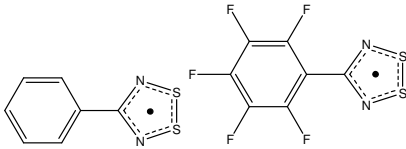
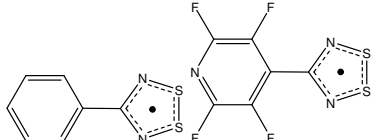
Products were isolated from dirty reaction mixtures by column chromatography using Merck silica gel 60 (particle size 0.040-0.063 mm) using a mixture of ethyl acetate and petroleum ether as solvent. Thin layer chromatography (TLC) was used to monitor the progress of the experiments and was carried out on Aluminium backed Merck silica gel 60 F254 plates

1. *SAINT Data Reduction Software*, Version 6.45; Bruker AXS Inc., Madison, WI, **2003**.
2. (a) *SADABS*, Version 2.05; Bruker AXS Inc., Madison, WI, **2002**; (b) R. H. Blessing, *Acta Crystallographica Section A: Foundational Crystallography* **1995**, *51*, 33-38.
3. G. M. Sheldrick, *Acta Crystallographica Section A: Foundational Crystallography* **2008**, *64*, 112-122.
4. L. J. Barbour, *Journal of Supramolecular Chemistry* **2001**, *1*, 189-191.
5. (a) A. L. Spek P. van der Sluis, *Acta Crystallographica Section A: Foundational Crystallography* **1990**, *46*, 194-201; (b) A. L. Spek, *Journal of Applied Crystallography* **2003**, *36*, 7-13.

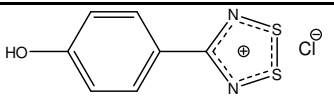
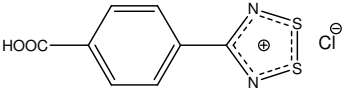
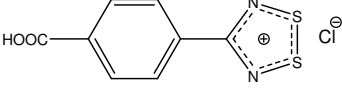
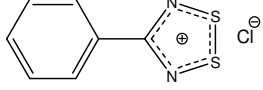
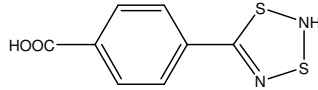
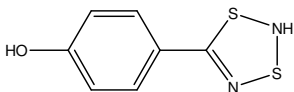
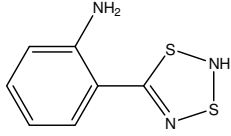
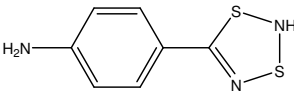
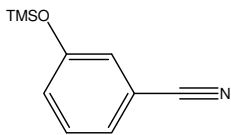
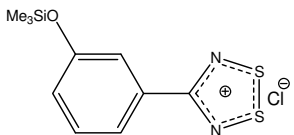
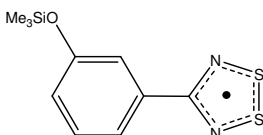
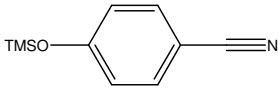
Appendix B

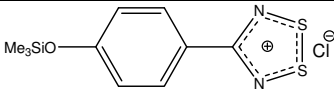
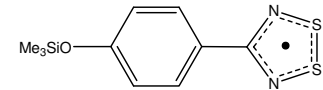
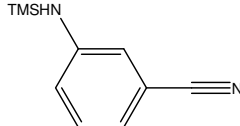
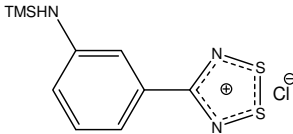
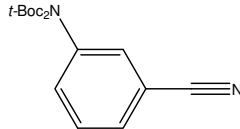
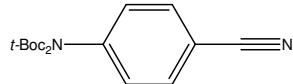
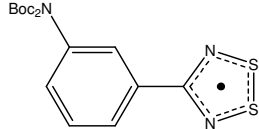
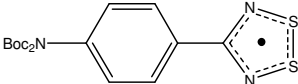
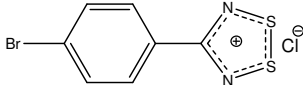
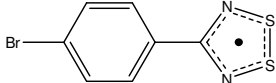
B.1.) Molecular Numbering

B.1.1) Chapter 2

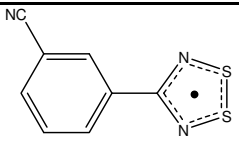
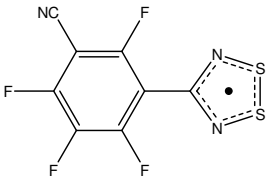
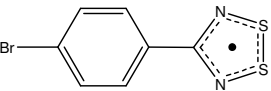
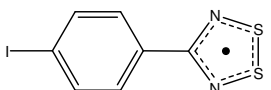
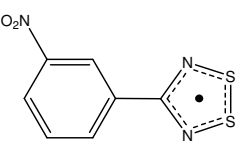
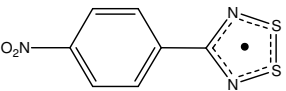
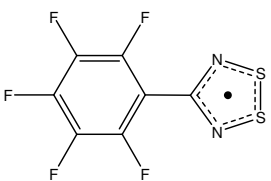
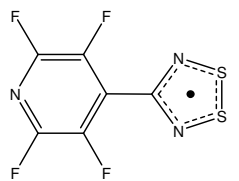
Number	Name	Molecular Structure
[1]	4-phenyl-1,2,3,5-dithiadiazolyl	
[2]	4-perfluorophenyl-1,2,3,5-dithiadiazolyl	
[3]	4-(4'-perfluoropyridyl)-1,2,3,5-dithiadiazolyl	
[1-2]	4-phenyl-1,2,3,5-dithiadiazolyl-4-perfluorophenyl-1,2,3,5-dithiadiazolyl co-crystal	
[1-3]	4-phenyl-1,2,3,5-dithiadiazolyl-4-(4'-perfluoropyridyl)-1,2,3,5-dithiadiazolyl co-crystal	

B.1.2) Chapter 3

Number	Name	Molecular Structure
[1]	4-(4'-hydroxyphenyl)-1,2,3,5-dithiadiazolylium chloride	
[2]	4-(4'-carboxyphenyl)-1,2,3,5-dithiadiazolylium chloride	
[3]	4-(4'-carboxyphenyl)-1,2,3,5-dithiadiazolylium chloride	
[4]	4-phenyl-1,2,3,5-dithiadiazolylium chloride	
[5]	5-(4'-carboxyphenyl)-1,3,2,4-dithiadiazole	
[6]	5-(4'-hydroxyphenyl)-1,3,2,4-dithiadiazole	
[7]	5-(2'-aminophenyl)-1,3,2,4-dithiadiazole	
[8]	5-(4'-aminophenyl)-1,3,2,4-dithiadiazole	
[9]	3-trimethylsiloxy-benzonitrile	
[10]	4-(3'-trimethylsiloxyphenyl)-1,2,3,5-dithiadiazolylium chloride	
[11]	4-(3'-trimethylsiloxyphenyl)-1,2,3,5-dithiadiazolyl	
[12]	4-cyano-1-trimethylsiloxybenzene	

Number	Name	Molecular Structure
[13]	4-(4'-trimethylsiloxyphenyl)-1,2,3,5-dithiadiazolium chloride	
[14]	4-(4'-trimethylsiloxyphenyl)-1,2,3,5-dithiadiazolyl	
[15]	3-trimethylsilaza-benzonitrile	
[16]	4-(3'-trimethylsilazaphenyl)-1,2,3,5-dithiadiazolium chloride	
[17]	3-cyano-1-N,N'-bis-t-Boc-aminobenzene	
[18]	4-cyano-1-N,N'-bis-t-Boc-aminobenzene	
[19]	4-(3'-N,N'-bis-t-Boc-aminophenyl)-1,2,3,5-dithiadiazolyl	
[20]	4-(4'-N,N'-bis-t-Boc-aminophenyl)-1,2,3,5-dithiadiazolyl	
[21]	4-(4'-bromophenyl)-1,2,3,5-dithiadiazolium chloride	
[22]	4-(4'-perfluoropyridyl)-1,2,3,5-dithiadiazolyl	

B.1.3) Chapter 4

Number	Name	Molecular Structure
[1]	4-(3'-cyanophenyl)-1,2,3,5-dithiadiazolyl	
[2]	4-(3'-cyanoperfluorophenyl)-1,2,3,5-dithiadiazolyl	
[3]	4-(4'-bromophenyl)-1,2,3,5-dithiadiazolyl	
[4]	4-(4'-iodophenyl)-1,2,3,5-dithiadiazolyl	
[5]	4-(3'-nitrophenyl)-1,2,3,5-dithiadiazolyl	
[6]	4-(4'-nitrophenyl)-1,2,3,5-dithiadiazolyl	
[7]	4-perfluorophenyl-1,2,3,5-dithiadiazolyl	
[8]	4-(4'-perfluoropyridyl)-1,2,3,5-dithiadiazolyl	

CD Appendix

The attached CD contains:

Structural data relating to the final refinement of all single-crystal structures determined in this study including '.RES' and the Crystallographic Information File, '.CIF'. The '.RES' and '.CIF' files have been given the following file names for the respective 1,2,3,5-dithiadiazolyl radical:

1,2,3,5-Dithiadiazolyl Radical	'RES' and 'CIF' File name
3'-cyanophenyl-	3cyano
3'-cyanoperfluorophenyl-	3cyanoperfluoro
3'-nitrophenyl-	3nitro
4'-bromophenyl-	4bromo